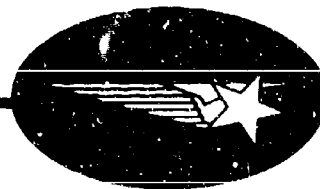


AD 654055

3-27-67-1 • VOL. 2

3-27-67-1 • VOL. 2 • MAY 1967



214
DASA 1971-2

THERMAL RADIATION PHENOMENA

VOL. 2

THE EQUILIBRIUM RADIATIVE PROPERTIES OF AIR – THEORY

This document has been approved
for public release and sale; its
distribution is unlimited.

497

DASA 1971-2
3-27-67-1 Vol 2
May 1967

THERMAL RADIATION PHENOMENA
The Equilibrium Radiative Properties
of Air: Theory
by
B. H. Armstrong and R. W. Nicholls

Edited by
John L. Magee and Henry Aroeste

Open Publication was approved by the Department of Defense on 7 April 1967

Distribution of this document is unlimited

FOREWORD

"Thermal radiation" is electromagnetic radiation emitted by matter in a state of thermal excitation. The energy density of such radiation in an enclosure at constant temperature is given by the well known Planck formula. The importance of thermal radiation in physical problems increases as the temperature is raised; at moderate temperatures (say, thousands of degrees Kelvin) its role is primarily one of transmitting energy, whereas at high temperatures (say, millions of degrees Kelvin) the energy density of the radiation field itself becomes important as well. If thermal radiation must be considered explicitly in a problem, the radiative properties of the matter must be known. In the simplest order of approximation, it can be assumed that the matter is in thermodynamic equilibrium "locally" (a condition called local thermodynamic equilibrium, or LTE), and all of the necessary radiative properties can be defined, at least in principle. Of course whenever thermal radiation must be considered, the medium which contains it inevitably has pressure and density gradients and the treatment requires the use of hydrodynamics. Hydrodynamics with explicit consideration of thermal radiation is called "radiation hydrodynamics".

In the past twenty years or so, many radiation hydrodynamic problems involving air have been studied. In this work a great deal of effort has gone into calculations of the equilibrium properties of air. Both thermodynamic and radiative properties have been calculated. It has been generally believed that the basic theory is well enough understood that such calculations yield valid results, and the limited experimental checks which are possible seem to support this hypothesis. The advantage of having sets of tables which are entirely calculated is evident: the calculated quantities are self-consistent on the basis of some set of assumptions, and they can later be improved if calculational techniques are improved, or if better assumptions can be made.

The origin of this set of books was in the desire of a number of persons interested in the radiation hydrodynamics of air to have a good source of reliable information on basic air properties. A series of books dealing with both theoretical and practical aspects was envisaged. As the series materialized, it was thought appropriate to devote the first three volumes to the equilibrium properties of air. They are:

The Equilibrium Thermodynamic Properties of Air,
by F. R. Gilmore

The Radiative Properties of Heated Air,
by B. H. Armstrong and R. W. Nicholls

Tables of Radiative Properties of Air,
by Lockheed Staff

The first volume contains a set of tables along with a detailed discussion of the basic models and techniques used for their computation. Because of the size of the related radiative tables and text, two volumes were considered necessary. The first contains the text, and the second the tables. It is hoped that these volumes will be widely useful, but because of the emphasis on very high temperatures it is clear that they will be most attractive to those concerned with nuclear weapons phenomenology, reentry vehicles, etc.

Our understanding of kinetic phenomena, long known to be important and at present in a state of rapid growth, is not as easy to assess as are equilibrium properties. Severe limitations had to be placed on choice of material. One volume is offered at this time:

Excitation and Non Equilibrium Phenomena in Air,
by Landshoff, et al.

It provides material on the more important processes involved in the excitation of air, criteria for the validity of LTE and special radiative effects.

A discussion of radiation hydrodynamics was felt to be necessary and another volume was planned to deal with this topic:

Radiation Hydrodynamics of High Temperature Air,
by Landshoff, Hillendahl, et al.

It is not ready for publication at this time. It will review the basic theory of radiation hydrodynamics and discuss the application to fireballs in the atmosphere.

The choice of material for these last two volumes was made with an eye to the needs of the principal users of the other three volumes.

Most of the work on which these volumes are based was supported by the United States Government through various agencies of the Defense Department and the Atomic Energy Commission. The actual preparation of the volumes was largely supported by the Defense Atomic Support Agency.

We are indebted to many authors and organizations for assistance and we gratefully acknowledge their cooperation. We are particularly grateful to the RAND Corporation for permission to use works of F. R. Gilmore and H. L. Brode and to the IBM Corporation for permission to use some of the work of B. H. Armstrong. Most of the other authors are employed by the Lockheed Missiles and Space Company, in some cases as consultants.

Finally we would like to acknowledge the key role of Dr. R. E. Meyerott of LMSC in all of this effort, from the initial conception to its realization. We are particularly grateful to him for his constant advice and encouragement.

Criticism and constructive suggestions are invited from all readers of these books. We understand that much remains to be done in this field, and we hope that the efforts represented by this work will be a stimulus to its development.

The Editors

J. L. Magee

H. Aroeste

Preface

This volume is concerned with all theoretical aspects of the transmission of thermal radiation in equilibrium air. It was prepared by Dr. B. H. Armstrong and Professor Ralph Nicholls with some assistance from the Lockheed staff.

The principal objective of this work is the description in detail of models and approximations which have been made in calculations of absorption coefficients for air and its constituents. It cannot always be assumed that the basic theory is well-known, and some effort is made to present key derivations and discuss points which have frequently been allowed to remain obscure in treatments of this sort. In contrast with the situation in thermodynamic properties, we can expect very significant developments in both theory and models in the future, and the presentation here is to be considered as a status report. However, the authors have prepared a very scholarly work which should be widely useful.

The reader is expected to have some knowledge of quantum mechanics and a certain amount of familiarity with atomic and molecular structure. Such a reader will be able to understand current work in thermal radiation after mastery of the material presented here.

In a companion volume we have presented an extensive compilation of tables of radiative properties of air. Nevertheless, we have felt that the inclusion of some tables and figures summarizing the most important of these properties in the present volume would substantially increase its usefulness. Such material is presented in Appendix A.

We would like to thank Dr. Armstrong and Professor Nicholls for their splendid cooperation. Thanks are also due the IBM Corporation for allowing Dr. Armstrong's work to be included in our series on "Thermal Radiation."

J. L. Magee

H. Aroeste

Contents

Part A: Theory of Radiation in Hot Gases

Chapter		Page
1	Introduction (B. H. Armstrong, R. W. Nicholls)	1
2	Elementary Radiative Transfer (B. H. Armstrong)	9
	2.1 The equation of radiative transfer (without scattering)	10
	2.2 Local thermodynamic equilibrium	16
	2.3 Scattering	24
	2.4 Emission from a gas sample in the optically thin limit	28
	2.5 Emission from a gas sample in the optically thick limit	35
	2.6 Emission from a gas sample of intermediate optical depth	42
3	Theory of Radiation (B. H. Armstrong)	68
	3.1 Classical Lorentz formulation	68
	3.2 Quantum formulation of radiation theory	78
	3.2.1 Formal theory	
	3.2.2 Reduction of the general formula to formulas for specific processes	
	3.2.3 Reduction of formulas for many-electron atoms	143
	3.2.4 Free-free radiative transitions	172
	3.3 Line broadening	209
4	Theory of Molecular Absorption (R. W. Nicholls)	217
	4.1 The Born-Oppenheimer approximation and its consequences	218
	4.2 The Heit-London factors	231
	4.3 Franck-Condon factors and r-centroids, vibrational wave functions and molecular potentials	232
	4.4 The electronic transition moment and band strength	245

Part B: Spectral and Mean Absorption Coefficients of Heated Air

Chapter		Page
5	Historical Review: Research on Hot Gas Absorption Coefficients since 1900 (B. H. Armstrong)	253
6	General Features of Air Absorption Coefficients (B. H. Armstrong)	267
	6.1 Spectral absorption coefficients	267
	6.2 Mean absorption coefficients	271
	6.3 Inequalities and bounds on mean absorption coefficients	288
7	Molecular Absorption Coefficients (R. W. Nicholls)	305
	7.1 Molecular species and transitions of importance	306
	7.2 Less important molecular species and transitions	316
	7.3 Review of calculations of the molecular contribution to the absorption coefficient of air	319
	7.3.1 Early work of the 1940's	322
	7.3.2 Approximate methods of the 1950's	323
	7.3.3 Calculation with the SACHA code in the 1960's	332
8	Atomic Absorption Coefficients (B. H. Armstrong)	355
	8.1 Survey of atomic models	356
	8.2 Hydrogenic and simple-Coulomb-force models	362
	8.2.1 Photoelectric cross sections	364
	8.2.2 Hydrogenic free-free absorption	377
	8.2.3 Hydrogenic bound-bound transitions and oscillator strengths	382
	8.2.4 Coherent scattering from bound systems	391
	8.2.5 Compton scattering cross sections	397
	8.3 Analytic formulas and approximations to hydrogenic absorption coefficients	401
	8.3.1 The Rosseland-Menzel-Pekeris formula	401
	8.3.2 The Strömngren function	403
	8.3.3 High-temperature limiting values of the opacity	411
	8.4 Non-hydrogenic absorption-coefficient calculations	415
	8.4.1 Deficiencies of the hydrogenic approximation	415
	8.4.2 The methods used by Armstrong, Johnston, and Kelly (1965)	422
	8.5 Review of major calculations made to date	428
Appendix	A Spectroscopic Properties of Six Important Band Systems Which Contribute to the Opacity of Heated Air (R. W. Nicholls)	471

PART A

THEORY OF RADIATION IN HOT GASES

BLANK PAGE

Chapter 1. INTRODUCTION

This volume is one of a set which is concerned with all aspects of thermal radiation phenomena in heated air, over a wide range of temperature and density. Thermal radiation phenomena are meant to be those which arise due to or are related to, the passage of electromagnetic energy through an atmosphere of some type when significant interaction occurs between the radiation stream and the atmosphere. It is usually implied that some type of partial thermal equilibrium is produced by this interaction, although not a complete one, of course. In the case of complete thermal equilibrium, there can be only an uninteresting homogeneous system with no net transport of radiation at all. Radiation is a significant mode of energy transfer in all gases at sufficiently high temperatures, and in many situations at low temperatures as well. Since radiative energy transfer is controlled by the absorption coefficient which is, in turn determined by the microscopic atomic and molecular, and the statistical/thermodynamic properties of the medium, much of these volumes are concerned with these underlying properties. In particular, after a brief introduction to the theory of radiative transfer limited to conditions of local thermodynamic equilibrium, the present volume is mainly concerned with the detailed application of the basic quantum theory of radiation to real atomic and molecular systems. The transfer problem only reappears occasionally to guide this application into the practical channels which constitute the raison d'etre of the book.

Although radiation transport is now of wide interdisciplinary application, most of its basic developments were made in an astrophysical milieu. Some of its contemporary applications are in stellar, solar and planetary atmospheres and aeronomy, in meteor, missile and rocket re-entry phenomena, in

combustion physics and chemistry, and in plasma and weapons physics. Towards very high temperatures there are fewer contributing effects and therefore the situation is conceptually somewhat simpler. Fig. 1.1 illustrates some significant subdivisions and interrelations towards the high-temperature limit of our considerations. As one progresses downwards in temperature, the effects and interactions proliferate and become, at our present state of knowledge, more fragmented and diverse, so that we will not attempt an illustration in this case.

A large fraction of the work dating from World War II on specific problems in the above fields of application has been motivated by defense needs and financed by government contracts. As a result, much of the literature on the subject is comprised of unpublished and therefore unrefereed contract reports which are not universally available to the scientific community. Much of the work described in this "grey" literature (Goody, 1964) is important, but some obscurities and errors in an already complex field have propagated through these reports. Other problems due to the particular history of this field have also occurred. For example, a perusal of the reports concerned with opacity calculations shows a considerable repetition of some of the formal arguments involved in justifying the calculations (although not in the calculations themselves), and a lack of assignments of priority, or acknowledgements. There has also been a substantial lack of cross referencing. This has all been due in part, of course, to the classified nature of some of the projects, particularly the earlier ones, and the fact that even the unclassified reports were often not readily available to some of the authors, who then found it necessary to repeat some of the derivations. However, once such a situation has been created it is generally self stimulating even in the absence of the original causes, due to

the large amount of effort which must be expended to ameliorate it. We hope the present volume will help to exorcise these ghosts; however, all the relevant material has still not been declassified so that this goal cannot be completely reached even at the present time.

The initiation, not long ago, by Prof. S.S. Penner of the Journal of Quantitative Spectroscopy and Radiative Transfer has done much to provide an appropriate vehicle for the open publication of this work, and the reader is referred to that journal for recent research papers on topics discussed in this volume.

Formidable experimental difficulties associated with the controlled laboratory study of really hot gases have limited most experimental work in the field to temperatures below $20,000^{\circ}\text{K}$. Thus, much reliance has had to be placed on theoretical research involving models of increasing realism, complexity and sophistication. As implied above, the basic theory employed has its roots in (a) astrophysical discussions of the transfer of radiation through stellar envelopes, and (b) in the applied quantum mechanics of the radiative properties of atoms and molecules. The bulk transport of radiation through hot gases is usually discussed in terms of the radiation absorption coefficient, which is a phenomenological parameter of the material through which the radiation passes. This absorption coefficient in turn, can be specified as a function of wavelength and absorber gas properties by recourse to quantum theory and statistical mechanics. From a detailed knowledge of the "spectral" absorption coefficient of the gas, realistic mean absorption coefficients can be derived in terms of which radiation transport may more conveniently be discussed. In addition, if conditions of local thermodynamic equilibrium prevail, absorption coefficients

are related by Kirchoff's law to the emission coefficients of the gas.

The macroscopic absorption coefficient is comprised of two factors. These are (a) the populations of the absorbing species and (b) the cross section per particle, or the microscopic "absorption coefficient". The first of these factors is obtainable from statistical mechanics, and a full discussion as well as tables are given, in the volume of this series, *The Equilibrium Thermodynamic Properties of High Temperature Air* by Gilmore. In order that the statistical mechanics treatment be realistic, accurate information must be available on the thermochemical properties of the absorbers, and on equilibrium constants, when chemical processes (dissociation, etc.) that can occur are also temperature dependent. The second of these factors requires a quantum mechanical description of atomic/molecular structure to determine radiative transition probabilities and is discussed in detail in subsequent chapters of the present volume. Realistic atomic and molecular models are needed for adequate calculations of this second factor. Careful experimental measurements of atomic and molecular properties are also needed in order to assess or verify the quality of the models selected. Much progress has been made during the past two decades in the approximate, yet realistic quantum mechanical analyses of complex atomic systems.

It should be emphasized here that both the above-mentioned aspects of the problem of the theoretical calculation of absorption coefficients require the strong support of experimental programs that can provide the basic atomic and molecular data on which the calculations often depend. Thus, experimental work in this field (among others, of course) occupies a dual role, since it must provide some of the basic input information as well as serve its traditional role in verifying the outcome of calculations.

It has come as a surprise to many that all such basic measurements were not made long ago. The growth of research institutes in "Laboratory Astrophysics" is indicative of the large amount of atomic and molecular physics left to be done.

The study of absorption coefficients of air may be further subdivided quite naturally into two parts as a function of temperature. At low temperatures, say below $12,000^{\circ}\text{K}$, most of the absorbing species in air are molecular, and both the statistical mechanics of absorber populations, and the quantum theory of absorbing transitions must be couched in molecular terms. At higher temperatures, air becomes a multispecies ionic gas. Theory (both statistical and quantum mechanics) is far more developed for atomic than for molecular species, and realistic calculations can be more readily carried out on both aspects of the absorption coefficient, as is shown in later chapters.

The realistic and comprehensive theoretical studies that can now be carried out or have been performed in the past decade have only become possible due to a number of circumstances. The availability of large-scale, high-speed digital computers, the experimental provision of relatively good critical experimental data, and the development of detailed and cogent theoretical models and methods, have all been necessary conditions which had to be established before such work as is discussed herein could be seriously undertaken. It is interesting to note that the accurate calculation of opacities covers a remarkably wide range of physical phenomena and theories. While crude opacity values are relatively easy to obtain, accurate values are very difficult to calculate. Even though, for most aspects of the calculations, the basic physical processes are reasonably well understood, the carrying out of the necessary calculations is a tedious and complicated task, and long-term efforts are required.

As a commentary on the recent development of a relatively modest scientific field, it is worth observing how much the need for air opacity values (in view of the character of these quantities) has stimulated research on such a wide and otherwise diverse variety of topics.

The plan of this volume, in detail, is as follows: the volume is divided into two parts, the first of which (Part A, Chapters 1-4) contains the basic theory of radiation transport, and the quantum theory of radiation as applied to individual atomic and molecular species. The second part (Part B, Chapters 5-8) discusses the calculation of the opacity of heated air based on the theory presented in Part A. Chapter 2 reviews the elementary theory of radiative transfer to establish definitions used later in the book, and to present the overall scope of the problem. Chapter 3 reviews and discusses that part of the quantum theory of radiation by atoms which is needed for the applications discussed in Chapter 8. The formal results of the theory are reduced to the formulas for specific radiative processes, and some clarifying and comparative comments are made on the equivalent formulae derived by a number of authors. Chapter 4 extends the theory of Chapter 3 to take account of radiative transitions by molecular species. Chapter 5 is a brief historical review of research over the last few decades on absorption coefficients and opacity, and is included to place the discussion of later chapters in correct perspective. Chapter 6 discusses the general features of the spectral and mean absorption coefficients introduced in Chapter 2, as applied to a real multicomponent gas such as air. Some inequalities and bounds for the mean absorption coefficients are derived.

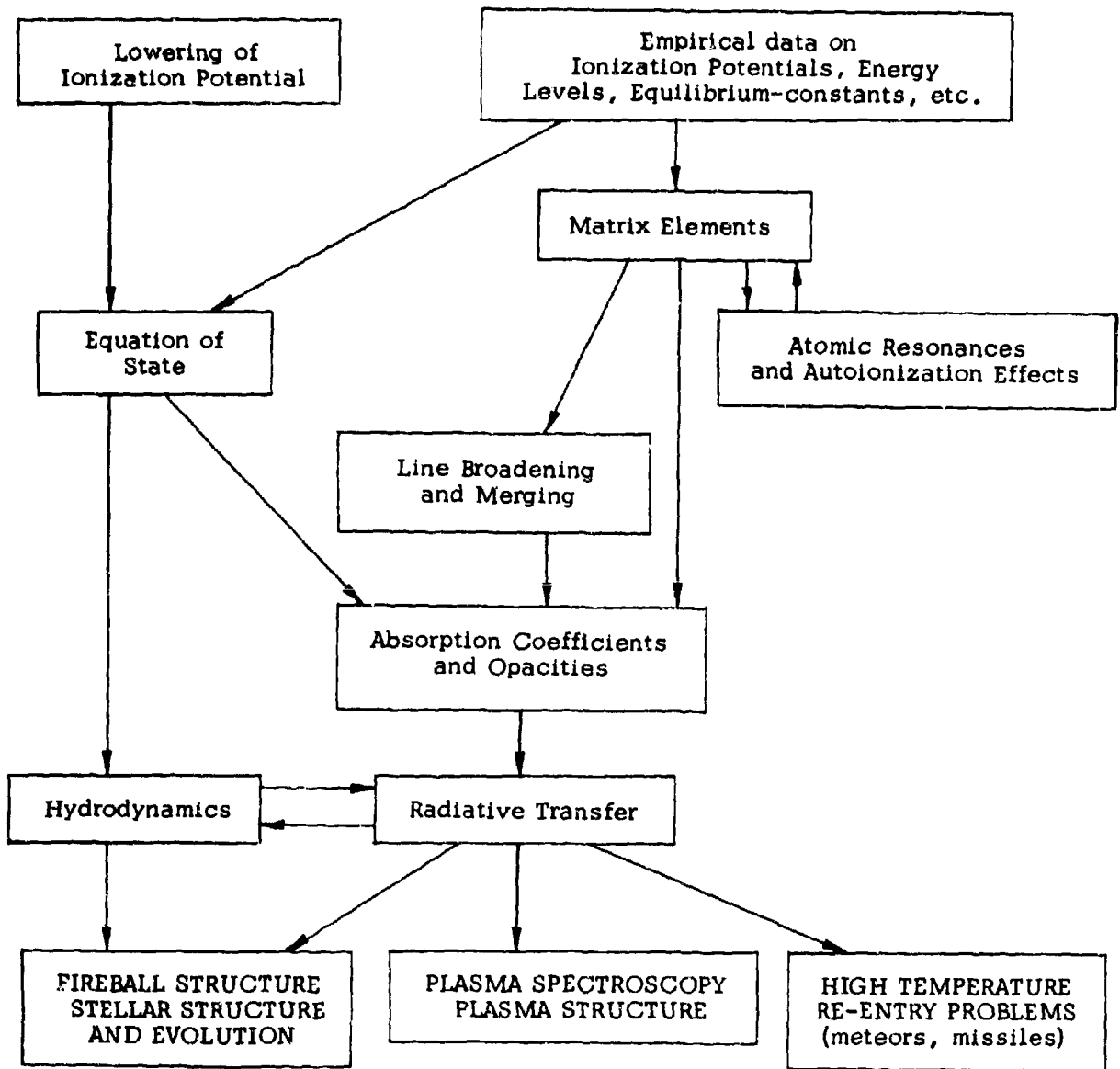
After the historical discussion of Chapter 5 and the review of the general features of air absorption coefficients of Chapter 6, the remaining discussion is arranged in order of ascending temperature. Thus, Chapter 7 reviews

opacity calculations on air up to temperatures of about $20,000^{\circ}\text{K}$, i.e., the region where molecular contributions dominate the system or cannot be neglected. Strong reliance is placed in this region on experimental knowledge of molecular spectra. Chapter 8 covers opacity calculations in the high-temperature (above $20,000^{\circ}\text{K}$) region where atomic species dominate. The atomic models needed for such calculations are briefly reviewed first, and then the more important contributing processes. Finally some of the recent large-scale air-opacity calculations are reviewed. In contrast to the character of Chapter 7, an entirely ab initio approach to the calculations can be taken; however, in practice, most calculations still make use of empirical atomic energy level information.

An appendix is included to show how the detailed molecular properties of O_2 , N_2 , NO , and their ions are taken into account in the calculations of Chapter 7.

Fig. 1.1

SOME SIGNIFICANT SUBDIVISIONS AND INTERCONNECTIONS
OF HIGH-TEMPERATURE RADIATION PHYSICS



Chapter 2. ELEMENTARY RADIATIVE TRANSFER

In this chapter, a non-rigorous review of the theory of radiative transfer indicates how the subject is dominated by the concept of spectral absorption coefficient. An attempt is made to provide some physical insight into the requirements which the applications of transfer theory impose on the calculation of absorption coefficients, and to demonstrate the physical significance of the Planck and Rosseland mean absorption coefficients. For this reason, certain elementary solutions to the transfer equation have been emphasized. An excellent and more comprehensive discussion of radiative transfer, which also emphasizes the physical aspects, has recently been given by Goody (1964) (see also Morse and Feshbach, 1953, 2.2). The formal theory is more extensively developed by Chandrasekhar (1939, 1950) and Kourganoff (1952). A good reference for the present purpose, although unavailable in the open literature, is the report by H. Mayer (1947). Aller (1963) gives an excellent account of approximate solutions.

We first undertake in Sec. 2.1 a brief discussion of the formulation of the transfer equation and the definitions involved. In this initial discussion, we neglect scattering; however, a few remarks on this subject are given later, in Sec. 2.3. In Sec. 2.2 we consider the definition of local thermodynamic equilibrium in some detail, in order to clarify the roles of induced and spontaneous emission in radiative transfer.

In many problems the spectral distribution of the radiation is not of primary concern. For these cases an appropriately defined mean value of the absorption coefficient is useful. The manner in which the mean value

is calculated depends on the characteristics of the problem under consideration. A limiting case of physical interest is that of an optically thin sample of gas, i.e., a sample whose dimensions are small compared with the mean free path of radiation in the gas. Consideration of this leads to the definition of the Planck mean absorption coefficient. Conversely the equally important optically thick case is conveniently described in terms of the Rosseland mean absorption coefficient. These two limiting cases are discussed in detail and the respective mean absorption coefficients are derived.

Finally, we present a short discussion of the problem of radiation transfer for intermediate optical depths. In view of the complications involved, we limit our considerations to isothermal, uniform-density conditions.

2.1 The equation of radiative transfer (without scattering)

Consider a collimated beam of radiation of frequency ν incident on an extended volume of gas which absorbs the radiation, but does not emit. If F_ν is the flux of radiant energy per unit frequency interval, that is, energy per ($\text{cm}^2 \times \text{sec} \times \text{unit frequency interval}$) this flux is assumed to be attenuated by each thin slab of gas of thickness δx in proportion to the product of the magnitude F_ν and the thickness δx . This is illustrated in Fig. (2-1). Thus, we can write

$$\delta F_\nu = -\alpha_\nu F_\nu \delta x \quad (2.1-1)$$

which defines the constant of proportionality μ_v , the linear or volume absorption coefficient, as

$$\mu_v = \lim_{\delta x \rightarrow 0} \left\{ -\frac{\delta F_v}{F_v \delta x} \right\} .$$

This phenomenological rule, known as Lambert's, Bouguer's, or Beer's law, leads, when integrated, to the exponential decay law:

$$F_v = F_{v0} e^{-\mu_v x} \quad (2.1-2a)$$

which is borne out in many experimental circumstances. From the usual interpretation of transport parameters, $l_v \equiv \mu_v^{-1}$ is thought of as a mean free path for absorption. Thus, Eq. (2.1-2a) can be rewritten

$$F_v = F_{v0} e^{-x/l_v} \quad (2.1-2b)$$

Experimentally, re-emission follows absorption, so that δF_v as given in Eq. (2.1-1) must be augmented by the radiation emitted in the slab δx and the result is the equation of transfer, Eq. (2.1-4). Furthermore, the emitted flux will in general not be so well collimated as our ideal parallel incident beam, so the definition of F_v must be generalized to energy per unit solid angle across unit surface normal to a specified direction θ, ϕ with a unit vector \vec{n} . This is illustrated in Fig. 2-2 which shows an infinitesimal pencil of beams within an element of solid angle $d\Omega$ about

the direction \vec{n} traversing a slab of gas of thickness L which extends to infinity in directions perpendicular to x . The relationship between the flux $F_{\nu 0}$ of the collimated (or parallel) beam of radiation and the general intensity function $I_{\nu}(\theta, \phi)$ which allows for an angular distribution is established through the Dirac δ -function (Chandrasekhar, 1950, p. 22):

$$I_{\nu}(\theta, \phi) = F_{\nu 0} \delta(\cos \theta_0 - \cos \theta) \delta(\phi - \phi_0) \quad (2.1-3a)$$

where θ_0, ϕ_0 is the direction of the parallel beam, and the δ -functions satisfy

$$\int_{4\pi} \delta(\cos \theta_0 - \cos \theta) \delta(\phi - \phi_0) d\vec{n} = 1 \quad (d\vec{n} = \sin \theta d\theta d\phi) \quad (2.1-3b)$$

$I_{\nu}(\theta, \phi) \equiv I_{\nu}(\vec{n})$ is called the specific intensity and has dimensions of energy per unit time per unit frequency interval per unit solid angle per unit area normal to \vec{n} . The resulting equation of radiative transfer which takes account of absorption and emission in the slab can then be written as

$$\frac{dI_{\nu}(\vec{n})}{ds} = j_{\nu}(\vec{n}) \rho - \mu_{\nu} I_{\nu}(\vec{n}) \quad (2.1-4)$$

where s denotes length measured in the direction \vec{n} . The energy per unit time radiated in the direction \vec{n} by a unit mass of gas per unit frequency per unit solid angle has been denoted by $j_{\nu}(\vec{n})$, the emission coefficient, and ρ is the mass density. For convenience, the emission coefficient is

often replaced by the source function defined as

$$J_{\nu}(\vec{n}) = \rho j_{\nu}(\vec{n}) / \mu_{\nu} \quad (2.1-5a)$$

The equation of radiative transfer becomes

$$\frac{1}{\mu_{\nu}} \frac{dI_{\nu}(\vec{n})}{ds} = J_{\nu}(\vec{n}) - I_{\nu}(\vec{n}) \quad (2.1-5b)$$

The decrease in beam intensity $(-\delta I_{\nu})$ can be expressed in a number of equivalent ways, each of which defines a different absorption coefficient. All of the resulting equations are derived from Eq. (2.1-1) which invokes simple proportionality to beam intensity I_{ν} (by virtue of Eq. (2.1-3a)) and the increment of path length δx . Eq. (2.1-1) thereby defines the linear (or volume for unit cross section) absorption coefficient μ_{ν} whose dimensions are $(\text{length})^{-1}$.

The effect of mass density ρ or number density N_{ν} of absorbing particles is seen in Eqs. (2.1-6a) and (2.1-6b) below which define, respectively, the mass absorption coefficient κ_{ν} and atomic absorption coefficient α_{ν} . κ_{ν} has dimensions of $(\text{length})^2 (\text{mass})^{-1}$. α_{ν} has dimensions $(\text{length})^2$. It is thus often treated as an absorption cross-section which interpretation is pursued further in the next section.

$$\delta I_{\nu} = -\kappa_{\nu} I_{\nu} (\rho \delta x) \quad (2.1-6a)$$

$$\delta I_{\nu} = -\alpha_{\nu} I_{\nu} (N_{\nu} \delta x) \quad (2.1-6b)$$

We note that $\rho \delta x$ is the mass increment δm per unit area, and similarly $N_{\nu} \delta x$ is the number increment δN_{ν} per unit area. Comparison between Eqs. (2.1-1), (2.1-6a), and (2.1-6b) lead to

$$\mu_{\nu} = \kappa_{\nu}^0 = \alpha_{\nu} N_{\nu} = \frac{1}{\ell_{\nu}} \quad (2.1-6c)$$

which relates most of the absorption coefficient parameters in common use.

One absorption coefficient parameter not previously discussed is the dimensionless quantity, the optical depth τ_{ν} . Its infinitesimal increment is defined by

$$d\tau_{\nu} = \mu_{\nu} ds \quad (2.1-7)$$

and, therefore, the total optical depth between points s' and s is

$$\tau_{\nu}(s', s) \equiv \int_{s'}^s \mu_{\nu} ds \quad (2.1-8a)$$

(One should note that it is customary in astrophysics to measure optical depth backwards along the line ss' . This would require a minus sign in the above definitions.) The foregoing definitions of radiative transfer quantities along with others which we do not consider here, have been conveniently summarized by Aller (1963).

The equation of transfer (2.1-5b) may now be written

$$\frac{dI_{\nu}}{dr_{\nu}} = J_{\nu}(\bar{\Omega}) - I_{\nu}(\bar{\Omega}) \quad (2.1-8b)$$

Eq. (2.1-8b), which governs the transport of electromagnetic energy through an atmosphere, is often difficult to solve. An extensive literature pertaining to it has accrued over the years, principally in the fields of astrophysics and meteorology (Goody, 1964; Kourganoff, 1952; Chandrasekhar, 1939, 1950; Mayer, 1947; Aller, 1963; Elsasser, 1942; Milne, 1930; Bond, Watson and Welch, 1965). Exact solutions can be obtained for only a very limited number of model problems so that approximate methods of solution are of paramount importance. As stated by Goody (1964), the physical content of the equation of transfer is very meager. Under the conditions of local thermodynamic equilibrium, most of the physics of the situation is in fact contained in the absorption coefficient κ_ν , the discussion of which constitutes the primary subject of this book.

A general solution to Eq. (2.1-8b) can be obtained formally as follows (Goody, 1964). Consider a beam along the direction $\vec{\Omega}$ as indicated in Fig. 2-2. Multiply Eq. (2.1-8b) by $e^{-\tau_\nu(s', s'')}$ to obtain

$$\frac{d}{d\tau_\nu} \left[e^{-\tau_\nu(s', s'')} I(s'', \vec{\Omega}) \right] = e^{-\tau_\nu(s', s'')} J_\nu(s'', \vec{\Omega}) \quad (2.1-9)$$

Integrating this equation along the direction $\vec{\Omega}$ from $s'' = s'$ to $s'' = s$, we obtain

$$e^{-\tau_\nu(s', s)} I_\nu(s, \vec{\Omega}) = I_\nu(s', \vec{\Omega}) + \int_{s'}^s e^{-\tau_\nu(s', s'')} J_\nu(s'', \vec{\Omega}) d\tau_\nu$$

Thus using Eq. (2.1-8a)

$$I_{\nu}(s, \vec{\Omega}) = e^{-\tau_{\nu}(s', s)} I_{\nu}(s', \vec{\Omega}) + \int_{s'}^s e^{-\tau_{\nu}(s'', s)} J_{\nu}(s'', \vec{\Omega}) d\tau_{\nu} \quad (2.1-10)$$

Thus the intensity $I_{\nu}(s, \vec{\Omega})$ at s is equal to the intensity $I_{\nu}(s', \vec{\Omega})$ incident at some previous point (s') exponentially diminished by absorption, plus the integrated intensity emitted between s'' and s' , each element again diminished by the absorption which takes place ahead of s'' . In the limiting case of an optically-deep medium, we can take s' at $-\infty$ and set the incident intensity term equal to zero. Eq. (2.1-10) then becomes

$$I_{\nu}(s, \vec{\Omega}) = \int_{-\infty}^s e^{-\tau_{\nu}(s'', s)} J_{\nu}(s'', \vec{\Omega}) d\tau_{\nu} \quad (2.1-11)$$

which shows how the radiation emerging from an emitting gas is limited by absorption in the gas.

2.2 Local thermodynamic equilibrium

One of the most common situations in which a solution to the equation of radiative transfer is sought is that in which local thermodynamic equilibrium (LTE) is assumed. This assumption is often introduced through the assertion that Kirchoff's law

$$J_{\nu} = \kappa_{\nu} B_{\nu}(T) \quad (2.2-1)$$

holds point-wise. This implies that at each point in the system a local temperature T is defined. However, it may vary from point to point over the system (Kornganoff, 1952; Chandrasekhar, 1939, 1950; Aller, 1963). In this formula I_ν is the radiant energy emitted per unit mass per unit time per unit solid angle per unit frequency interval and κ_ν is the similarly defined mass absorption coefficient. We recall from Section 2.1 that $\kappa_\nu \rho$ is defined such that

$$dI_\nu = -\kappa_\nu \rho I_\nu ds \quad (2.2-2)$$

is the change in the emerging radiation intensity after traversal of a distance ds in the medium to which κ_ν pertains, assuming there is no emission. $B_\nu(T)$ is the usual Planck function $2h\nu^3 e^{-h\nu/kT} / c^2 (1 - e^{-h\nu/kT})$, ν the frequency, and T is the absolute temperature.

Complications arise through the neglect of induced emission effects (which cause I_ν to depend somewhat on incident intensities) in these equations. Chandrasekhar (1939, Chap. 5, section 3) points out that incorrect results are obtained if I_ν of Eq. (2.2-1) is substituted directly into the transfer equation (2.1-4). Ad-hoc corrections are then necessary to compensate for the neglect of induced emission effects.

These problems may be avoided and natural allowance be made for the effect of induced emission if a local temperature (and thus LTE) is defined through a Boltzmann equation relating the occupation numbers N_n and N_m of two quantum states involved* in absorption or emission (Chandrasekhar, 1939, Eq. 108ff and discussion following Eq. 118, Mayer, 1947)

$$\frac{N_m}{N_n} = \exp(h\nu_{nm}/kT) \quad (2.2-3)$$

* In any real physical situation there will usually be many absorbing and emitting states, and often many different atomic and molecular species. Since the transitions and species can be treated one at a time and then added, we limit ourselves to single events and single species in this chapter. This is conceptually much simpler, and involves no loss of generality if the reader bears in mind that the appropriate sums must ultimately be carried out.

where $h\nu_{nm} = E_n - E_m$ is the energy separation between the states. For simplicity statistical weights have been assumed to be unity in this discussion. LTE so defined makes no assumption about the radiation field which need not be in equilibrium with matter. In practice it is often not in equilibrium except at the center of strong spectral features. Eq. (2.2-1) implicitly includes the radiation field but Eq. (2.2-3) does not.

To follow the consequences of this definition it is necessary to introduce the Einstein coefficients A_{nm} and B_{nm}^* for spontaneous and induced emission, respectively. We define these coefficients as follows. $A_{nm} b(\nu)/4\pi$ is the probability per unit time, per unit frequency interval, per unit solid angle that an atomic or molecule in excited state n emits a photon with energy centered about $h\nu_{nm} = E_n - E_m$. The line-shape factor $b(\nu)$ has been included so that our results can be expressed per unit frequency interval. The $b(\nu)$ shape is the probability distribution in frequency for the photon, and represents the probability per unit frequency interval that the photon produced in the transition $n \rightarrow m$ has the frequency ν .

The usual definitions of the Einstein coefficients (see, e.g. Chandrasekhar, 1939; also Sec. 3.1 of the sequel) which assume infinitesimally sharp lines do not incorporate this factor and consequently require cumbersome double definitions of emission and absorption coefficients and of intensities. The normalization condition $\int_0^\infty b(\nu) d\nu = 1$ is satisfied by $b(\nu)$, and it will be further discussed in the next section (2.3). By using this factor in our definitions at this point, all quantities can be expressed as functions of frequency, rather than some appearing integrated over the line profile.

From the foregoing definitions we see that the energy emitted spontaneously

* The Einstein B-coefficient B_{nm} and the Planck function $B_\nu(T)$ should not be confused.

in a time dt into the solid angle $d\Omega$ and the frequency interval $d\nu$ by the excited atom or molecule is

$$dE_S(\nu) = \frac{h\nu A_{nm} b(\nu)}{4\pi} dt d\Omega d\nu \quad (2.2-4a)$$

Since the spontaneous emission is isotropic, the total number of photons spontaneously emitted per second per unit frequency interval per atom into all angles is $A_{nm} b(\nu)$. Now it turns out that the probability of the emission of a photon $h\nu_{nm}$ is augmented by stimulated emission if the atom is immersed in a field of radiation containing a distribution of frequencies about ν_{nm} . Thus, B_{nm} is defined so that $c^{-1} B_{nm} I_\nu(\vec{\Omega}) d\Omega d\nu dt$ is the probability that an excited atom or molecule in state n is stimulated by an external intensity of radiation $I_\nu(\vec{\Omega})$ to emit a photon with energy centered about $h\nu_{nm}$ in the direction $\vec{\Omega}$, the frequency interval $d\nu$ and time dt . Thus the stimulated or induced energy emitted by the single system into the various differential intervals is

$$dE_I(\nu) = (h\nu) c^{-1} B_{nm} b(\nu) I_\nu(\vec{\Omega}) d\Omega d\nu dt \quad (2.2-4b)$$

The coefficients A_{nm} and B_{nm} are properties of the individual atomic or molecular systems, and their evaluation is a problem in the quantum theory of radiation which will be discussed in Chapter 3. We assume, while discussing radiation transport, that they are known quantities. Eqs. (2.2-4a) and (2.2-4b) are respectively the spontaneous and stimulated radiant energy contributions emitted per atom or molecule. The total radiant

energy emitted by an element of volume dv (with mass $dm = \rho dv$) will then be obtained by adding these two terms and multiplying by the number of particles within the element dv that are in the quantum state n . Thus, if n_n is the number density of particles in the state n ,

$$b(\nu)n_n dv [A_{nm}/4\pi + c^{-1} B_{nm} I_\nu(\Omega)] h\nu d\Omega dv dt \quad (2.2-5)$$

is the energy emitted by the volume element dv in time dt into the element of solid angle $d\Omega$ and frequency interval $d\nu$ about ν_{nm} . The energy emitted per unit mass of material will be this quantity divided by the mass ρdv of the element. The energy per unit mass per unit solid angle, frequency interval and time is called the emission coefficient j_ν .

Thus

$$j_\nu = \frac{n_n}{\rho} \left[\frac{A_{nm}}{4\pi} + c^{-1} B_{nm} I_\nu(\Omega) \right] h\nu b(\nu) \quad (2.2-6)$$

It is shown in Chapter 3 that if A_{nm} , B_{nm} and B_{mn} are the Einstein coefficients for spontaneous emission, stimulated emission and (stimulated) absorption for transitions between levels n (upper) and m (lower), each assumed for simplicity to be of unit statistical weight, then

$$\frac{A_{nm}}{B_{nm}} = \frac{8\pi h\nu^3}{c^3} \quad (2.2-7a)$$

$$B_{nm} = B_{mn} \quad (2.2-7b)$$

The B-coefficients are defined here relative to radiation energy density rather than to radiation intensity (Aller, 1963; Allen, 1963). We may further relate the absorption coefficients μ_ν and κ_ν to B_{mn} by appeal to Eqs. (2.1-1), (2.1-3a), and (2.1-6a). Thus

$$-\delta I_\nu = \mu_\nu I_\nu \delta x = \rho \kappa_\nu I_\nu \delta x = n_m I_\nu \delta x B_{mn} h\nu b(\nu) c^{-1}$$

or

$$\mu_\nu = \rho \kappa_\nu = n_m B_{mn} h\nu b(\nu) c^{-1} \quad (2.2-7c)$$

From Eqs. (2.2-6) and (2.2-7a, b, c)

$$A_{nm} = \frac{8\pi h\nu^3}{c^3} \frac{\mu_\nu}{n_m (h\nu) b(\nu)}$$

and

$$j_\nu = \frac{n_n}{\rho} \left[\frac{2\nu^2}{c^2} \frac{\mu_\nu}{n_m} + \frac{\mu_\nu}{n_m h\nu} I_\nu(\Omega) \right] h\nu \quad (2.2-8)$$

This may be rewritten in a more compact form using the definitions of LTE (Eq. (2.2-3)) and the Planck function:

$$B_\nu(T) = \frac{2h\nu^3}{c^2} \frac{1}{e^{\frac{h\nu}{kT}} - 1} \quad (2.2-9)$$

Thus

$$j_\nu = \frac{e^{-\frac{h\nu}{kT}}}{\rho} \left[\mu_\nu B_\nu(T) (e^{\frac{h\nu}{kT}} - 1) + \mu_\nu I_\nu(\Omega) \right]$$

which reduces to

$$\rho j_{\nu} = \mu_{\nu}' B_{\nu}(T) + e^{-\frac{h\nu}{kT}} \mu_{\nu} I_{\nu}(\Omega) \quad (2.2-10)$$

where

$$\mu_{\nu}' = \mu_{\nu} (1 - e^{-h\nu/kT}) \quad (2.2-11a)$$

κ'_{ν} may similarly be defined by

$$\kappa'_{\nu} = \kappa_{\nu} (1 - e^{-h\nu/kT}) \quad (2.2-11b)$$

Thus

$$j_{\nu} = \kappa'_{\nu} B_{\nu}(T) + e^{-h\nu/kT} \kappa_{\nu} I_{\nu}(\Omega) \quad (2.2-11c)$$

Eq. (2.2-11c) explicitly shows how the augmented emission coefficient j_{ν} depends on I_{ν} as a result of stimulated emission. In this the expression for j_{ν} , which should be used when a change of quantum state occurs, the first term is the contribution to the emission coefficient from spontaneous emission and the second term is the contribution from stimulated emission.

That is

$$j_{\nu}^{(\text{spontaneous})} = \kappa'_{\nu} B_{\nu}(T) \quad (2.2-12a)$$

and

$$j_{\nu}^{(\text{stimulated})} = \kappa_{\nu} e^{-h\nu/kT} I_{\nu}(\Omega) \quad (2.2-12b)$$

There are therefore two equivalent ^{*} ways of formulating the principle of local thermodynamic equilibrium, viz.,

$$\frac{N_m}{N_n} = \exp\left(\frac{h\nu}{kT}\right) \quad (2.2-13a)$$

$$j_\nu \text{ (spontaneous)} = \kappa'_\nu B_\nu(T) \quad (2.2-13b)$$

Eq. (2.2-13b) is more useful here since it allows the transfer equation without allowance for scattering to be written in similar form to Eq. (2.1-4).

Thus

$$\frac{1}{\rho} \frac{dI_\nu}{ds} = j_\nu \text{ (spontaneous)} + j_\nu \text{ (induced)} - \kappa_\nu I_\nu \quad (2.2-14)$$

Eqs. (2.2-11b), (2.2-12a,b) and (2.2-14) lead to the following form for the transfer equation which also implies existence of LTE:

$$\frac{1}{\rho} \frac{dI_\nu}{ds} = \kappa'_\nu (B_\nu - I_\nu) \quad (2.2-15a)$$

or

$$\frac{dI_\nu}{ds} = \mu'_\nu (B_\nu - I_\nu) \quad (2.2-15b)$$

* Note that we have not included scattering in this definition; this is sometimes done in Astrophysics by means of a generalization of Eq. (2.2-13b).

Eq. (2.2-15b) is very similar to Eq. (2.1-5b) and its formal solution may thus be written down from inspection of Eq. (2.1-10) replacing I_{ν} by B_{ν} and μ_{ν} by μ'_{ν} respectively. The formal general solution of Eq. (2.2-15b) is therefore

$$I_{\nu}(s, \vec{\Omega}) = e^{-\tau'_{\nu}(s', s)} I_{\nu}(s', \vec{\Omega}) + \int_{s'}^s e^{-\tau'_{\nu}(s'', s)} B_{\nu}(T(\tau'_{\nu})) d\tau'_{\nu} \quad (2.2-16)$$

where

$$\tau'_{\nu}(s'', s) \equiv \int_{s''}^s \mu'_{\nu} ds \quad (2.2-17)$$

2.3 Scattering

The type of scattering of primary interest in the study of high-temperature plasmas is coherent scattering from the ground and low-lying states of atoms and/or molecules and their ions. (By coherent scattering is meant scattering that occurs without a change in frequency of the photon involved, and without a change of state of the atomic system involved.) Therefore, we will confine ourselves here to a few remarks concerning coherent, non-relativistic scattering which are intended to point out the difference between transfer by (coherent) scattering and transfer by absorption/emission. For more extensive discussions of the general subject of scattering, see, e.g., Chandrasekhar, (1950), and Van de Hulst (1957). Explicit forms of the cross sections involved for coherent scattering from hydrogen, and for Compton

scattering, will be considered in the next chapter, along with mention of the relativistic corrections required for Compton scattering at sufficiently high temperatures.

Once the assumption of LTE is made, and the emission and absorption terms in the transfer equation appropriately simplified, these terms will differ from the scattering terms which appear in the transfer equation. The reason is that emission into a beam by scattering is not accompanied by a transition of the atom or molecule and is thus not directly affected by excited states of the system other than the one which the system is in at the moment of scattering. That is to say, absorption and emission occur with a change of state of the system, whereas scattering does not. The two types of processes, i.e., scattering and absorption/emission will be related and pass one into the other for short-lived excited states. For such states, scattering cannot be distinguished from a real absorption followed almost simultaneously by a real emission with the emitting system reverting to its initial state (Heitler, 1954). This happens near a resonance line and is further complicated by the fact that a photon with energy near enough to a real excitation energy can produce the real excitation, or transition, with the help of a transfer of energy from or to a nearby electron or ion. (cf. Baranger, 1962; "The One-Electron Approximation".) Thus, if we compute all real absorption and emission transitions, including those which need an outside interaction of energy 0 to ΔE to occur, we will have included the scattering produced by virtual states which fail to conserve energy by an amount between 0 and ΔE .

Mayer (1947) has shown that there is no correction of the form $1 - e^{-u}$ to be applied to non-relativistic scattering. Actually, one should not expect it, since the atom does not change state and hence, there is no upper state to re-emit back into the beam, but it can be demonstrated rigorously. Mayer does this by showing that the induced scattering into the beam is exactly cancelled by induced scattering out of the beam. Pictorially what he demonstrates is as shown in Fig. 2-3. Emission into the direction Ω' depends on an integral of the form

$$\int_{\Omega} \frac{d\sigma_s(\Omega-\Omega')}{d\Omega} I(\Omega) d\Omega \quad (2.3-1)$$

over all other directions Ω , which is the ordinary scattering term, and an induced scattering term proportional to

$$\int_{\Omega} \frac{d\sigma(\Omega-\Omega')}{d\Omega} I(\Omega) I(\Omega') d\Omega \quad (2.3-2)$$

That is to say, this second term depends on the beam intensity in the scattered direction, which is why it is called induced scattering. However, the scattering out of the beam contains a term

$$\int \frac{d\sigma(\Omega'-\Omega)}{d\Omega'} I(\Omega') I(\Omega) d\Omega' \quad (2.3-3)$$

which, with the proper proportionality factors exactly cancels the previous term. The implication apparently is that since induced scattering does occur, one might expect a correction analogous to the $1 - e^{-u}$ correction obtained in the case of absorption and emission to appear. However, it is not just induced emission that leads to this correction (if this were the case we would need only to correct the absorption term in the transfer equation and no distinct emission term correction would appear (since both absorption and induced emission are proportional to the intensity I , they can always be lumped together).

The existence of spontaneous emission is also required - - an emission term independent of the incident intensity. This is what is lacking in the case of scattering. There is no spontaneous scattering. As Mayer (1947) points out, the scattering terms in the transfer equation are proportional to $n_b(1 + n_b)$ (n_b = number of "radiation oscillators"). Thus, there is no term independent of n_b as there is in the case of emission (which is proportional to $1 + n_b$).

The diminution of the beam $I_\nu(\vec{n})$ due to scattering within the element of distance ds can thus be written

$$\delta I_\nu^{(sc)}(\vec{n}) = - N_\nu \sigma_{sc} I_\nu(\vec{n}) ds \quad (2.3-4)$$

where σ_{sc} is the total cross section for scattering by the particles with number density N_ν . In addition to this depletion, the beam will be augmented by the amount

$$\delta I_\nu^{(sc)}(\vec{n}) = N_\nu \int_{\Omega'} I_\nu(\vec{n}') \frac{d\sigma(\vec{n}' \rightarrow \vec{n})}{d\Omega'} d\Omega' \quad (2.3-5)$$

where $\frac{d\sigma(\Omega'-\Omega)}{d\Omega'}$ is the differential cross section for scattering from the direction Ω' into the direction Ω . If we add the above terms to the transfer equation, Eq. (2.2-15b), we obtain

$$\frac{dI_\nu}{ds} = \mu_\nu'(B_\nu - I_\nu) + N_\nu \int \frac{d\sigma(\Omega'-\Omega)}{d\Omega'} I_\nu(\Omega') d\Omega' - \mu_\nu^{(sc)} I_\nu \quad (2.3-6)$$

where we have defined $\mu_\nu^{(sc)}$ by:

$$\mu_\nu^{(sc)} \equiv N_\nu \sigma_{sc} \quad (2.3-7)$$

2.4 Emission from a gas sample in the optically thin limit

The Planck or "Emission Mean" Absorption Coefficient

Before defining the Planck mean absorption coefficient, let us investigate the flux emitted by a plane-parallel slab of gas in order to define the optically thin limit in several more or less equivalent ways. Consider the radiation from an isolated slab of gas at temperature T , as in Fig. 2-2. The total monochromatic radiation flux per unit area leaving one face of the slab within the solid angle $\Delta\Omega$ is

$$F_{\nu+} = \int_{\Delta\Omega} I_\nu \cos \theta d\Omega \quad (2.4-1)$$

where θ is measured from the x-direction normal to the slab. Multiplying the transfer equation, Eq. (2.2-15), on both sides by $d\Omega$ using $dx = ds \cos \theta$, and integrating over the hemisphere of outward directions, yields the equation

$$\int_{\Delta\Omega} \frac{dI_\nu}{dx} \cos \theta d\Omega = \Delta\Omega \mu_\nu' B_\nu - \mu_\nu' \int_{\Delta\Omega} I_\nu d\Omega \quad (2.4-2)$$

From Eq. (2.4-1) and the definition of the mean (partial) outward intensity

$\bar{I}_{\nu+}$,

$$\bar{I}_{\nu+} \equiv \frac{1}{\Delta\Omega} \int_{\Delta\Omega} I_{\nu} d\Omega \quad (2.4-3)$$

we can rewrite Eq. (2.4-2) as

$$\frac{dF_{\nu+}}{dx} = \Delta\Omega \mu'_{\nu} (B_{\nu} - \bar{I}_{\nu+}) \quad (2.4-4)$$

The optically thin approximation now consists in neglecting* $\bar{I}_{\nu+}$ relative to B_{ν} , and taking the derivative $dF_{\nu+}/dx$ as the ratio of finite increments of emitted flux δF_{ν} and slab thickness δx . With these approximations we obtain from Eq. (2.4-4) the integrated flux or total radiant energy emitted within the solid angle $\Delta\Omega$,

$$\delta F_{+} \cong \Delta\Omega \cdot \delta x \int \mu'_{\nu} B_{\nu}(T) d\nu \quad (2.4-5)$$

The same result could be obtained by integrating Eq. (2.2-10) for the emission coefficient upon neglect of (a) self-absorption, and (b) induced emission.

The flux from a volume element $\delta V = \delta A \delta s$ cut out by the walls of an infinitesimal slab is (see Fig 2-4)

$$\delta F_{+} \cong \int_{\nu} \int_{\Omega} j_{\nu} \rho \delta V \cos \theta d\nu d\Omega / \delta A \quad (2.4-6)$$

But $\delta s = \delta x / \cos \theta$ and $\rho j'_{\nu} \cong \mu'_{\nu} B_{\nu}(T)$. Thus

$$\delta F_{+} \cong \delta x \int_{\nu} \int_{\Omega} \mu'_{\nu} B_{\nu}(T) d\nu d\Omega = \Delta\Omega \delta x \int \mu'_{\nu} B_{\nu}(T) d\nu$$

* Recall that we are considering an isolated slab; hence, there is no incident intensity at the boundary.

If $\Delta\Omega$ is the entire hemisphere, then Eq. (2.4-6) becomes

$\delta F_{+} = [2\pi \int \mu'_{\nu} B_{\nu}(T) d\nu] \delta x$. The result can also be obtained as follows from the general solution to the transfer equation, Eq. (2.2-16), using the approximation $\mu'_{\nu} \delta x \ll 1$. With the additional assumption that the incident intensity vanishes, Eq. (2.2-16) yields the total outward flux from one side of an isothermal slab as

$$F = 2\pi \int d\nu B_{\nu}(T) \int_{\theta} \left(1 - e^{-\frac{\mu'_{\nu} \delta x}{\cos \theta}}\right) \cos \theta \sin \theta d\theta \quad (2.4-7)$$

We wish to show that the correct result - to first order in $\mu'_{\nu} \delta x$ - is obtained by expanding the exponential in spite of the fact that $\cos \theta \rightarrow 0$ within the range of the integration. With a change of variables Eq. (2.4-7) becomes

$$F = 2\pi \int d\nu B_{\nu}(T) \left[\frac{1}{2} - E_3(\mu'_{\nu} \delta x) \right] \quad (2.4-8)$$

where

$$E_n(y) = \int_1^{\infty} \frac{dx}{x^n} e^{-xy} \quad (2.4-9)$$

are the usual exponential integrals (Chandrasekhar, 1950). By use of the relations

$$\left. \begin{aligned} nE_{n+1}(y) &= e^{-y} - yE_n(y) \\ E_1(y) &= -\gamma - \log y + \sum_{n=1}^{\infty} (-1)^{n-1} \frac{y^n}{n \cdot n!} \end{aligned} \right\} \quad (2.4-10)$$

as given by Chandrasekhar (1950) ($\gamma = \text{Euler's constant}$), we find

$$F = 2\pi \int d\nu B_\nu(T) \left\{ \mu'_\nu \delta x + O \left[(\mu'_\nu \delta x)^2 \log \mu'_\nu \delta x \right] + O \left[(\mu'_\nu \delta x)^2 \right] \right\} \quad (2.4-11)$$

which agrees with Eq. (2.4-5) to first order in $\mu'_\nu \delta x$ (with $\Delta\Omega = 2\pi$). This result shows that radiation in the angles near $\theta = \pi/2$, which are not involved in many practical cases, does not contribute to F in first order. There is contribution in first order to \bar{I}_ν where the result corresponding to Eq. (2.4-11) is

$$\bar{I}_\nu = (1 + \gamma) \mu'_\nu \delta x + (\mu'_\nu \delta x) \log \mu'_\nu \delta x + O \left[(\mu'_\nu \delta x)^2 \right]$$

The radiative energy emitted by one face of a slab of perfect radiator in thermal equilibrium at temperature T can be obtained from Eq. (2.4-7) by letting $\delta x \rightarrow \infty$. The result is, for the energy emitted per unit area,

$$\int_\nu \int_{2\pi} B_\nu(T) \cos \theta \, d\Omega \, d\nu = \int_{2\pi} B(T) \cos \theta \, d\Omega = \frac{\sigma T^4}{\pi} \int_{2\pi} \cos \theta \, d\Omega = \sigma T^4 \quad (2.4-12)$$

where

$$B(T) \equiv \int B_\nu(T) \, d\nu = \sigma T^4 / \pi \quad (2.4-13)$$

We can define the (flux) emissivity ϵ of a slab relative to this standard as the ratio of the total radiant energy one face of the slab emits to that emitted by one face of a blackbody slab at the same temperature. Thus for a thin slab, ϵ is given by the ratio

$$\epsilon = \frac{\delta F_+}{\sigma T^4} = \frac{2\pi \delta x \int \mu_\nu^i B_\nu(T) d\nu}{\sigma T^4} \quad (2.4-14)$$

Since this quantity depends on the slab thickness, it is somewhat more satisfactory to define $\epsilon/\delta x$ as the emissivity per unit length. If we define the Planck mean absorption coefficient (or emission mean) $\bar{\mu}_P(T)$ as

$$\bar{\mu}_P(T) = \frac{\int \mu_\nu^i B_\nu(T) d\nu}{\int B_\nu(T) d\nu} = \frac{\pi \int \mu_\nu^i B_\nu(T) d\nu}{\sigma T^4} \quad (2.4-15)$$

then the emissivity per unit length of an optically thin slab becomes

$$\epsilon/\delta x = 2\bar{\mu}_P(T) \quad (2.4-16)$$

A similar quantity, the "hemispherical emissivity" ϵ_h is sometimes used (Penner, 1959). It is defined as the ratio of the radiant flux emitted by a hemispherical volume (with radius δR) of gas into a "point" collector at the center of its base. We will show that $\epsilon_h/\delta R$ is one-half the thin-slab emissivity per unit length;

$$\epsilon_h/\delta R = \bar{\mu}_P(T) \quad (2.4-17)$$

In general, the relation between the emissivity and the mean absorption coefficient depends on the geometry of the emitting sample through a numerical factor (Bond, Watson, and Welch, 1965). We can illustrate this directly in the thin-slab limit with reference to Fig. 2-5. The radiation arriving at 0 from the shaded volume H within the hemispherical shell contributes to the hemispherical emissivity. The radiation arriving at 0 from the remainder of the slab, S, is the additional contribution which arises in the thin-slab definition. We shall show that these two contributions are equal in the limit of small optical depth.

Consider the isothermal solution to the transfer equation (Eq. (2.1-11)) divided into the contributions from regions H and S:

$$\begin{aligned}
 I_{\nu} &= \int_0^{\tau_{\nu}} B_{\nu}(T) e^{-\tau'_{\nu}} d\tau'_{\nu} = \int_0^{\tau_{\nu 1}} B_{\nu}(T) e^{-\tau'_{\nu}} d\tau'_{\nu} + \int_{\tau_{\nu 1}}^{\tau_{\nu 2}} B_{\nu}(T) e^{-\tau'_{\nu}} d\tau'_{\nu} \\
 &= B_{\nu}(T) \left[1 - e^{-\tau_{\nu 1}} \right] + B_{\nu}(T) \left[e^{-\tau_{\nu 1}} - e^{-\tau_{\nu 2}} \right]
 \end{aligned}
 \tag{2.4-18}$$

where

$$\begin{aligned}
 \tau_{\nu 1} &= \mu'_{\nu} R \\
 \tau_{\nu 2} &= \mu'_{\nu} R / \cos \theta
 \end{aligned}
 \tag{2.4-19}$$

We obtain the flux crossing the surface at 0 by multiplying I_ν of Eq. (2.4-18) by $\cos \theta \, d\Omega \, d\nu$, and integrating over $d\Omega$ and $d\nu$. The result is

$$F = F_1 + F_2 \quad (2.4-20)$$

where

$$F_1 = \pi \int B_\nu(T) \left(1 - e^{-\mu'_\nu R}\right) d\nu \quad (2.4-21)$$

is the contribution from the hemispherical region H and

$$F_2 = \int_\nu \int_{2\pi} B_\nu(T) \left(e^{-\tau_{\nu 1}} - e^{-\tau_{\nu 2}}\right) \cos \theta \, d\Omega \, d\nu \quad (2.4-22)$$

is the contribution from the remainder of the slab, region S.

We make the approximation of small optical depth, viz., $\tau_\nu \ll 1$, and expand the exponentials. The justification of this expansion has been given in Eq. (2.4-11).

This leads to

$$F_1 = \pi R \int B_\nu(T) \mu'_\nu d\nu \quad (2.4-23)$$

and

$$F_2 = \int_\nu \int_{2\pi} B_\nu(T) [-\mu'_\nu R + \mu'_\nu R / \cos \theta] \cos \theta \, d\Omega \, d\nu \quad (2.4-24)$$

$$= \pi R \int B_\nu(T) \mu'_\nu d\nu$$

From Eqs. (2.4-23) and (2.4-24)

$$F_1 = F_2$$

From the definition of the Planck mean absorption coefficient, (Eq. (2.4-15)) the thin-slab emissivity is

$$\frac{F}{\sigma T^4} = 2\bar{\mu}_p(T) \quad (2.4-25)$$

while the hemispherical emissivity is

$$\frac{F_1}{\sigma T^4} = \bar{\mu}_p(T) \quad (2.4-26)$$

2.5 Emission from a gas sample in the optically thick limit

The Rosseland or "Diffusion Mean" Absorption Coefficient

Whereas the Planck mean is of interest when the intensity $I_\nu \ll B_\nu$, another mean becomes of importance in the "opposite" limit, namely,

$$I_\nu \cong B_\nu \quad (2.5-1)$$

We have previously noted that when $I_\nu \ll B_\nu$ and LTE prevails, the radiation is far from being in equilibrium with the matter. On the other hand, Eq. (2.5-1) will be satisfied when the radiation is nearly in equilibrium with the matter.

Inserting Eq. (2.5-1) as a zeroth-order approximation into the transfer equation, Eq. (2.2-15) we obtain

$$I_{\nu} \approx B_{\nu} - \frac{1}{\mu_{\nu}'} \frac{dB_{\nu}}{ds} \quad (2.5-2)$$

for a first order approximation. With Eq. (2.4-1) the integrated net flux* in the x-direction can be given, as illustrated in Fig. 2-6, by

$$F_x = - \int \frac{1}{\mu_{\nu}'} \frac{dB_{\nu}}{ds} \cos \theta \, d\Omega \, d\nu \quad (2.5-3)$$

since the first term of Eq. (2.5-2) is isotropic and thus does not contribute to the net flux. Substituting $s = x/\cos \theta$,

$$F_x = - \int \frac{1}{\mu_{\nu}'} \frac{dB_{\nu}}{dx} \cos^2 \theta \, d\Omega \, d\nu = - \frac{4\pi}{3} \int \frac{1}{\mu_{\nu}'} \frac{dB_{\nu}}{dx} \, d\nu \quad (2.5-4)$$

with similar expressions for F_y and F_z . Thus,

$$\vec{F} = - \frac{4\pi}{3} \int \frac{1}{\mu_{\nu}'} \vec{\nabla} B_{\nu}(T) \, d\nu = - \left(\frac{4\pi}{3} \int \frac{1}{\mu_{\nu}'} \frac{dB_{\nu}}{dT} \, d\nu \right) \vec{\nabla} T \quad (2.5-5)$$

If the Rosseland mean absorption coefficient is now defined as

$$\frac{1}{\mu_R} \equiv \int \frac{1}{\mu_{\nu}'} \frac{dB_{\nu}(T)}{dT} \, d\nu \Bigg/ \int \frac{dB_{\nu}(T)}{dT} \, d\nu \quad (2.5-6)$$

* We are here considering angular integrations over the complete sphere.

Eq. (2.5-5) becomes

$$\vec{F} = -\frac{4\pi}{3} \frac{1}{\bar{\mu}_R} \left(\int \frac{dB_\nu}{dT} d\nu \right) \vec{\nabla} T = -\frac{4\pi}{3} \frac{1}{\bar{\mu}_R} \vec{\nabla} B(T) \quad (2.5-7)$$

In terms of the Rosseland mean free path $\Lambda_R = \bar{\mu}_R^{-1}$, and the radiation density $u = \frac{4\pi}{c} \int B_\nu(T) d\nu$, Eq. (2.5-7) can be written

$$\vec{F} = -\frac{c\Lambda_R}{3} \vec{\nabla} u \quad (2.5-8)$$

This equation is the basis of the definition of the Rosseland mean free path Λ_R , the Rosseland mean absorption coefficient $\bar{\mu}_R$, and the Rosseland mean opacity $\bar{\kappa}_R$ where

$$\bar{\kappa}_R = \bar{\mu}_R / \rho \quad (2.5-9)$$

Note that in contrast to the Planck mean, the Rosseland mean is an inverse mean and thus emphasizes small values of the absorption coefficient. The Planck mean emphasizes large values of absorption coefficient.

Eq. (2.5-8) is analogous to that of the diffusion equation (Kennard, 1938)

$$\vec{j} = D\vec{\nabla} n \quad (2.5-10)$$

where \vec{j} is a current, n is a particle density and D is the diffusion coefficient. Thus Λ_R is an effective diffusion length and $c\Lambda_R/3$ is the

diffusion coefficient. Eq. (2.5-7) describes the diffusion of the photons through the gas.

The limits of validity of Eq. (2.5-7) can be obtained by examining the approximations implicit in Eqs. (2.5-1) and (2.5-2) as follows. The transfer equation (Eq. (2.2-15)) may be written

$$I_{\nu} = B_{\nu} - \frac{1}{\mu'_{\nu}} \frac{dI_{\nu}}{ds} \quad (2.5-11)$$

Also

$$\frac{dI_{\nu}}{ds} = \frac{dI_{\nu}}{dT} \frac{dT}{ds}$$

If $I_{\nu} \cong B_{\nu}$, (Eq. (2.5-1)) then $1/\mu'_{\nu} dI_{\nu}/ds$ must be small compared to B_{ν} , thus from Eqs. (2.5-1) and (2.5-11)

$$\frac{1}{\mu'_{\nu}} \frac{dI_{\nu}}{dT} \frac{dT}{ds} \ll B_{\nu}(T) \quad (2.5-12)$$

which is the basic requirement of the approximation. But as $I_{\nu} \cong B_{\nu}$

$$\frac{1}{\mu'_{\nu}} \frac{dT}{ds} \ll B_{\nu}(T) / \frac{dB_{\nu}(T)}{dT} \quad (2.5-13)$$

But the Planck function $B_{\nu}(T)$ is given by

$$B_{\nu}(T) = \frac{2h\nu^3}{c^2} / e^{h\nu/kT} - 1$$

thus

$$B_\nu(T) / \frac{dB_\nu(T)}{dT} = \frac{(1 - e^{-h\nu/kT}) kT^2}{h\nu} \quad (2.5-14)$$

Therefore from Eqs. (2.5-13) and (2.5-14),

$$\frac{1}{\mu'_\nu} \frac{\left| \frac{dT_\nu}{dS} \right|}{T} \ll \frac{1 - e^{-h\nu/kT}}{h\nu/kT} \quad (2.5-15)$$

which expresses the limit of validity of the diffusion approximation.

A derivation of the Rosseland diffusion theory can also be given by analogy to simple kinetic diffusion theory (Kennard, 1938, p. 188 ff) if one notes that the specific intensity I_ν has the nature of an energy distribution function (cf 2.4 of Morse and Feshbach, 1953), or that $I_\nu/h\nu$ has the nature of a particle distribution function. With reference to Fig. 2-7, let n be the density of particles (in this case photons) at the surface S . We assume that the density varies only with x so that the density at dr is $n + \Delta x \frac{dn}{dx}$. It is well known from elementary kinetic theory that the particle flux Γ across a given surface within a gas is given by

$$\Gamma = \frac{1}{4} n \bar{v} \quad (2.5-16)$$

where \bar{v} is the average velocity of the particles (Kennard, 1938, p. 62). If one retraces this derivation giving all the particles the same velocity c the same result is obtained. In view of the change in density along x , the rate at which particles collide within $d\tau$ and thereafter cross S [i.e., photons are absorbed and re-emitted to cross S] will be increased by the amount $\frac{1}{4} \Delta x \frac{dn}{dx} c$. Thus, the flow of photons towards $-x$ will be

$$\Gamma_- = \frac{1}{4} nc + \frac{1}{4} (\Delta \bar{x}_-) c \frac{dn}{dx} \quad (2.5-17)$$

where $\Delta \bar{x}_-$ is the average value of Δx at the last point of collision for each particle. With a similar expression for Γ_+ , and by use of $\Delta \bar{x}_- = \frac{2}{3} l$, $\Delta \bar{x}_+ = -\frac{2}{3} l$, where l is the mean free path between collisions (Kennard, 1938, p. 140), we obtain the net particle flow across the surface S :

$$\Gamma = \Gamma_+ + \Gamma_- = \frac{1}{3} cl \frac{dn}{dx} \quad (2.5-18)$$

Generalizing this expression to three dimensions and setting the mean free path l for photons of frequency ν equal to $1/\mu'_\nu$, we obtain the photon number flux per unit frequency interval:

$$\bar{\Gamma}_\nu = \frac{c}{3\mu'_\nu} \bar{\nabla} n_\nu \quad (2.5-19)$$

This result can be compared directly with the standard form of the diffusion equation Eq. (2.5-10), to yield $c/3\mu'_\nu$ as the effective photon diffusion coefficient.

For photons in equilibrium [or approximate equilibrium according to Eq. (2.5-1)] the particle density per unit frequency interval n_ν is given by

$$n_\nu = \left(\frac{1}{h\nu}\right) \frac{4\pi}{c} B_\nu(T) \quad (2.5-20)$$

with the result that the photon energy flux $h\nu \vec{\Gamma}_\nu = \vec{F}_\nu$ becomes

$$\vec{F}_\nu = \frac{4\pi}{3\mu_\nu} \vec{\nabla} B_\nu(T) \quad (2.5-21)$$

in agreement with Eq. (2.5-5). Performing the frequency integration leads again to the definition of the Rosseland mean free path of Eq. (2.5-6).

The foregoing derivations of the Rosseland diffusion theory have been given for the physical insight which they convey. The more rigorous standard derivation (Goody, 1964; Chandrasekhar, 1939) is to set the source function $I_\nu(s^*, \vec{\Omega})$ ($\equiv I_\nu(\tau_\nu(s^*, s))$) in Eq. (2.1-11) equal to $B_\nu[\tau_\nu(s^*, s)]$ and expand $B_\nu(\tau_\nu)$ in the Taylor series

$$B_\nu[\tau_\nu(s'', s)] = B_\nu(s) + \left. \frac{dB_\nu}{d\tau_\nu} \right|_s \tau_\nu(s'', s) + \left. \frac{d^2 B_\nu}{d\tau_\nu^2} \right|_s \frac{\tau_\nu^2(s'', s)}{2} + \dots \quad (2.5-22)$$

The integration indicated in Eq. (2.1-11) can now be carried out and the flux computed to obtain the result given in Eq. (2.5-7).

2.6 Emission from a gas sample of intermediate optical depth

Radiative transfer in the realistic general case of intermediate, or finite, optical depth, where one cannot make the approximation that the radiating gas sample is optically thin or optically thick, is quite difficult to handle mathematically. Resort is usually made to numerical integrations of the transfer equation (Hillendahl, 1964) involving elaborate approximation techniques or to alternative methods as the Invariant Imbedding techniques of Ambartsumian and Chandrasekhar (Goody, 1964; Chandrasekhar, 1950). Mean absorption coefficients are no longer so useful in expressions for the net radiative flux, since the coefficients become dependent on path length and on the geometrical configuration of the sample. Intensities and fluxes are thus computed directly.

A formal simplicity can be given to certain of the intensity and flux expressions however, by defining mean absorption coefficients, which are of convenience in calculation. The mathematics for the general case of intermediate optical depth is sufficiently complex that the only situations for which closed analytic solutions exist are those for gas samples with extremely simple geometric configurations at constant density and temperature. We will therefore, consider explicitly only these conditions and configurations. Consideration of more general cases can be facilitated by means of "transmission functions" which we will also define and discuss briefly.

Consider an isothermal, plane-parallel slab of gas of uniform density, of thickness L , and of infinite extent perpendicular to the x -axis (Fig. 2-2). Now select an infinitesimal pencil of radiation through the slab at an angle θ to the x -axis. The outward intensity $I_{\nu+}$ along such a pencil can readily be obtained from first principles. (See, for example, Penner, 1959, pp. 13-15.)

We make use of the general solution, Eq. (2.2-16), with the incident intensity $I_{\nu}(s', \bar{\Omega})$ set equal to zero, and the lower limit s' taken as zero. For $x \leq L$, since the density and temperature are assumed to be constant, and there is azimuthal symmetry in $\bar{\Omega}$, we can write Eq. (2.2-16) as

$$I_{\nu}(L, \theta) = B_{\nu}(T) \int_0^{\mu_{\nu}' L / \cos \theta} e^{-\mu_{\nu}' s'} d(\mu_{\nu}' s') \quad (2.6-1)$$

The integration can be performed immediately, leading to the result

$$I_{\nu}(L, \theta) = B_{\nu}(T) (1 - e^{-\mu_{\nu}' L / \cos \theta}) \quad (2.6-2)$$

In terms of the normal optical depth $\tau_{\nu}^n \equiv \int_0^x \mu_{\nu}' dx$, where x , as in Fig 2-2, is measured normal to the slab, or in terms of our original path-length variable s , this result has the equivalent forms:

$$I_{\nu}(\tau_{\nu}^n, \theta) = B_{\nu}(T) \left[1 - e^{-\tau_{\nu}^n / \cos \theta} \right] \quad (2.6-3)$$

$$I_{\nu}(s, \bar{\Omega}) = B_{\nu}(T) \left[1 - e^{-\mu_{\nu}' s} \right]$$

Penner (1959, p. 14) calls the last of these expressions the "basic law for uniformly distributed radiators". We note that for $s = R$ the last of these expressions is also appropriate for the intensity observed at the center of the base of a hemisphere of radius R .

If we multiply the intensity as given by Eq. (2.6-3) by $\cos \theta$ and integrate over solid angle in order to compute the flux from one face of the slab we find

$$F_{\nu} = 2\pi B_{\nu}(T) \int_0^{\pi/2} \left(1 - e^{-\mu'_{\nu} x / \cos \theta} \right) \cos \theta \sin \theta d\theta \quad (2.6-4)$$

This is usually expressed in terms of the exponential integrals $E_n(y) \equiv \int_1^{\infty} \frac{e^{-yt}}{t^n} dt$ previously introduced in Section 2.4, by use of the transformation $t = 1/\cos \theta$. With these substitutions Eq. (2.6-4) becomes (cf., Eq. (2.4-8))

$$F_{\nu} = \pi B_{\nu}(T) \left[1 - 2E_3(\mu'_{\nu} x) \right] \quad (2.6-5)$$

The total flux over all frequencies is obtained from this expression by integration over ν :

$$F = \sigma T^4 \left[1 - \frac{2\pi}{\sigma T^4} \int B_{\nu}(T) E_3(\mu'_{\nu} x) d\nu \right] \quad (2.6-6)$$

This expression has been used with the assumption of a constant absorption coefficient to obtain a simple estimate of the effects of finite optical thickness (Davis, 1964). If μ'_{ν} is assumed to be a constant $\bar{\mu}'$ independent of ν , Eq. (2.6-6) becomes

$$F = \sigma T^4 \left[1 - 2E_3(\bar{\mu}' x) \right] \quad (2.6-7)$$

Computations of \bar{F}/F by Strack (1962) using $\bar{\mu}' = \bar{\mu}_p$, the Planck mean, indicate that this is a useful approximation only under certain rather limited circumstances. For further calculations of \bar{F} see Davis (1964). The correct value of $\bar{\mu}'$ that makes this expression exact is

$$\bar{\mu}' = -\frac{\cos \theta}{x} \ln \int_0^{\infty} \frac{B_{\nu}(T)}{B(T)} e^{-\mu_{\nu}' x / \cos \theta} d\nu \quad (2.6-7a)$$

as can be readily verified by substitution in Eq. (2.6-7) (where $B(T)$ is defined as in Eq. (2.4-13)).

Because of the frequent appearance of the exponential function $e^{-\mu_{\nu}s}$ involving the absorption coefficient and path length, it is convenient to define and name it as an independent quantity. The customary name* applied is intensity transmission function (Elsasser, 1942; Chandrasekhar, 1950) since it is the ratio of the diminished intensity to the original intensity under isothermal, homogeneous conditions, i.e.,

$$e^{-\mu_{\nu}s} = \frac{I_{\nu}(s)}{I_{\nu}(0)} \equiv \text{Tr}(\mu_{\nu}s) \quad (2.6-8)$$

(cf. Eq. (2.1-2)) in the presence of pure absorption alone. Although, strictly speaking, one can have pure absorption alone only under non-equilibrium circumstances, under more general circumstances this exponential function still constitutes an integrating factor for the transfer equation (cf. Eqs. (2.1-9 and 2.1-10)) as long as induced emission can be neglected. From Eqs. (2.2-11 and 2.2-12), one sees that this is possible as long as $h\nu/kT \gg 1$. This is generally true for optical or infrared radiation at atmospheric temperatures, so that the transmission function $e^{-\mu_{\nu}s}$ is customarily used in such low-temperature applications (cf., e.g., Goody, 1964). At higher temperatures

* We define and use herein only this intensity transmission function. A flux transmission function is often also defined and used; cf., e.g., Elsasser (1942).

one cannot generally neglect induced re-emission into the beam, so that Eq. (2.6-8) no longer constitutes the most useful definition of a function from which radiative intensities and fluxes can be more or less directly obtained.

Under conditions of LTE, the function which most effectively replaces $e^{-\mu_\nu s}$ as an integrating factor for the transfer equation is $e^{-\mu'_\nu s}$ where μ'_ν (as before) is the modified absorption coefficient $\mu_\nu (1 - e^{-h\nu/kT})$. It is also called a transmission function even though, strictly speaking, it is not the simple ratio of two intensities. For gases in LTE, a direct connection of $e^{-\mu'_\nu s}$ with observation is afforded by the definition of emissivity for a non-thin slab. Let us define the spectral emissivity of an isothermal gas sample as the ratio of the flux it emits per unit frequency interval to the flux per unit frequency interval which a blackbody emits. Then from Eq. (2.6-3) we find for the spectral emissivity $\epsilon_{\nu c}$ of an infinitesimal pencil of gas of length s the result

$$\begin{aligned} \epsilon_{\nu c} &\equiv \frac{I_\nu(s, \vec{\Omega})}{B_\nu(T)} = 1 - e^{-\mu'_\nu s} \\ &\equiv 1 - \text{Tr}(\mu'_\nu s) \end{aligned} \tag{2.6-9a}$$

For such an infinitesimal pencil the intensity will all be in the direction of the pencil; hence, the flux and intensity are the same. Approximately the same result would be obtained for a long, narrow cylinder or column of gas. Hence, the emissivity given by Eq. (2.6-9a) is also known as the beam or column (spectral) emissivity and has been given a subscript c . It can also be called the hemispherical* emissivity, since by holding s constant and integrating F_ν and $B_\nu \cos \theta$ over a hemisphere we obtain the emissivity that would be observed at the center of the base of a hemisphere

* All these names are somewhat confusing, but we mention them since they are in the literature. In view of the defining equation, Eq. (2.6-9a), it would probably be most straight forward to call this quantity the intensity emissivity.

as at 0 in Fig. 2-5. Of course, this "high-temperature" definition $e^{-\mu_\nu s}$ can still be used at low temperatures as long as LTE prevails or $h\nu \gg kT$, whereas the reverse is not true, viz., $e^{-\mu_\nu s}$ is no longer appropriate at high temperatures. The definition of emissivity given by Eq. (2.6-9) is very similar to the definition of absorption function $A(\mu_\nu s)$ often employed in low-temperature radiation studies. If there is negligible re-emission into the beam, the fraction of the original beam intensity $I_\nu(0)$ which is absorbed (under isothermal, homogeneous conditions) is given by

$$A(\mu_\nu s) = (I_\nu(0) - I_\nu(s)) / I_\nu(0) = 1 - \exp(-\mu_\nu s)$$

or,

$$A(\mu_\nu s) = 1 - \text{Tr}(\mu_\nu s) \tag{2.6-9b}$$

Although this definition is formally almost identical to that given in Eq. (2.6-9a), the difference in interpretation and validity should be noted. If there is appreciable re-emission into the beam, Eq. (2.6-9b) loses its direct significance.

To define a total emissivity, we need to take the ratio of the total (frequency-integrated) intensity to the integrated Planck function as in Section 2.4. Thus the total (isothermal) column emissivity can be written as

$$\begin{aligned} \epsilon_c &= \frac{\int d\nu (1 - e^{-\mu_\nu s}) B_\nu(T)}{\int B_\nu(T) d\nu} \\ &= \frac{\int d\nu [1 - \text{Tr}(\mu_\nu s)] B_\nu(T)}{B(T)} \end{aligned} \tag{2.6-10}$$

Experimentally, one would expect to observe intensities that are effectively averages over small frequency intervals, such as line or band emissivities. The frequency intervals of concern here for defining and computing such emissivities are those which contain from a fraction of a spectrum line to perhaps a few lines. Under most conditions the Planck functions will normally not vary substantially over such an interval and the average of the intensity over $\Delta\nu_i$ can be written as

$$\bar{I}_{\nu_i}^{\Delta\nu} = \bar{\epsilon}_{ci} B_{\nu_i}(T) = [1 - \overline{\text{Tr}_i(\mu_{\nu}^t s)}] B_{\nu_i}(T) \quad (2.6-11)$$

where
$$\bar{\epsilon}_{ci} = 1 - \overline{\text{Tr}_i(\mu_{\nu}^t s)} \quad (2.6-12a)$$

and
$$\overline{\text{Tr}_i(\mu_{\nu}^t s)} = \frac{1}{\Delta\nu_i} \int_{\Delta\nu_i} e^{-\mu_{\nu}^t s} d\nu \quad (2.6-12b)$$

with the result that the total column emissivity becomes (cf. Goody, 1964), if we choose equal intervals $\Delta\nu_i$,

$$\epsilon_c = \frac{\sum_i \bar{\epsilon}_{ci} B_i(T)}{\sum_i B_i(T)} \quad (2.6-13)$$

where i rather than ν_i is used to label the frequency intervals and $B_i(T) = \int_{\Delta\nu_i} \frac{B_{\nu}(T) d\nu}{\Delta\nu_i}$. The column (or intensity) emissivity can be converted to

a slab (or flux) emissivity ϵ_s by integration of I_ν and B_ν over a hemisphere of outward directions as in the preceding Eq. (2.6-4). Thus, we can write

$$\epsilon_s = \frac{\int d\Omega \int d\nu \left(1 - e^{-\mu'_\nu x / \cos \theta} \right) B_\nu(T) \cos \theta}{2\pi \int B_\nu(\bar{\nu}) d\nu} \quad (2.6-14)$$

$$= 1 - \frac{2\pi}{\sigma T^4} \int d\nu B_\nu(T) \left[E_3(\mu'_\nu x) \right]$$

which is, of course, just the ratio $F/\sigma T^4$ as given by Eq. (2.6-6).

Although, as mentioned previously, mean absorption coefficients are not as significant for finite optical depth as in the limiting cases, it is still instructive to define them. This amounts merely to a re-expression of the formulas for flux and intensity that one obtains directly from the transfer equation, but it provides a certain amount of conceptual continuity between the limiting cases. Also, because of the rapid, violently-fluctuating frequency dependence of the spectral absorption, it is often essential to define mean absorption coefficients to make a given calculation tractable, as well as physically meaningful.

The frequency integrated intensity of Eq. (2.6-3) which is

$$I(\theta, x) = \int \left(1 - e^{-\mu'_\nu x / \cos \theta} \right) B_\nu(T) d\nu \quad (2.6-15)$$

can be expressed in the same form as the spectral intensity by the proper definition of a mean absorption coefficient which we will call $\bar{\mu}_T$. Thus, we can write

$$I(\theta, x) = \left(1 - e^{-\bar{\mu}_T x / \cos \theta} \right) B(T) \quad (2.6-16)$$

if we define $\bar{\mu}_T$ as in Eq. (2.6-7a) (Mayer, 1964)

$$\bar{\mu}_T(x, \theta) = - \frac{\cos \theta}{x} \ln \int_0^{\infty} \frac{B_\nu}{B(T)} e^{-\mu'_\nu x / \cos \theta} d\nu \quad (2.6-17)$$

$$= - \frac{\cos \theta}{x} \ln \int \frac{B_\nu}{B(T)} \text{Tr}(\mu'_\nu x / \cos \theta) d\nu \quad (2.6-18)$$

Analogously, the (frequency) average transmission function $\overline{\text{Tr}(\mu'_\nu s)}$ can be re-expressed as an average absorption coefficient by means of the definition

$$\bar{\mu}(s) = - \frac{1}{s} \ln \left\{ \overline{\text{Tr}(\mu'_\nu s)} \right\} \quad (2.6-19)$$

The total emissivities can then be expressed simply in terms of $\bar{\mu}_T$, which, in turn, can then be expressed in terms of the $\bar{\mu}$. The hemispherical, or column (intensity) emissivity becomes

$$\epsilon_c = \frac{I(s, \vec{n})}{B(T)} = 1 - e^{-\bar{\mu}_T s} \quad (2.6-20)$$

while the slab ("flux") emissivity takes the form

$$\epsilon_s = \frac{\int I(\theta, x) \cos \theta d\Omega}{\pi B(T)} = \frac{1}{\pi} \int (1 - e^{-\bar{\mu}_T x / \cos \theta}) \cos \theta d\Omega \quad (2.6-21)$$

Although this is an exact expression, it is not of great practical value because of the labor involved in obtaining $\bar{\mu}_T(x, \theta)$.

The connection between $\bar{\mu}(s)$ and $\bar{\mu}_T(x, \theta)$ can be seen by considering averages over limited spectral regions across which B_ν does not vary appreciably (viz., regions over which the transmission function may be averaged as in Eq. (2.6-11)). For such a region $\Delta\nu$, which we label with the index i we have:

$$\begin{aligned} \bar{\mu}_T(x, \theta) &= -\frac{\cos \theta}{x} \ln \left[\sum_i \frac{B_i}{B(T)} \int_{\Delta\nu_i} e^{-\mu'_\nu x / \cos \theta} d\nu \right] \\ &= -\frac{\cos \theta}{x} \ln \left[\sum_i \frac{B_i \Delta\nu_i}{B(T)} \left[\text{Tr}_i(\mu'_\nu x / \cos \theta) \right] \right] \quad (2.6-22) \\ &= -\frac{\cos \theta}{x} \ln \left[\sum_i \frac{B_i \Delta\nu_i}{B(T)} e^{-\bar{\mu}(x / \cos \theta)_i x / \cos \theta} \right] \end{aligned}$$

Rearranging and taking the exponential of both sides yields

$$e^{-\bar{\mu}_T(x, \theta) x / \cos \theta} = \sum_i \frac{B_i \Delta\nu_i}{B(T)} e^{-\bar{\mu}'(x, \theta)_i (x / \cos \theta)} \quad (2.6-23)$$

For the hemispherical or column emissivity, one obtains from Eq. (2.6-20) and Eq. (2.6-23)

$$\epsilon_c = 1 - \frac{1}{B(T)} \sum_i B_i \Delta \nu_i e^{-\bar{\mu}'(s)_i s} \quad (2.6-24)$$

Eqs. (2.6-16) - (2.6-24) are primarily of computational interest. In this respect they are not trivial since they (together with Eqs. (2.6-11) and (2.6-12) for the transmission function average) assist in determining the type of spectral average one should use in order to avoid specifying any more spectral detail than is essential for a given calculation. They provide criteria for ascertaining which spectral features of the absorption coefficient are most important under a given set of circumstances. Thus, we can see that the spectral average needed for a geometry which is neither optically thin nor optically thick is that of the absorption coefficient in the exponential $e^{-\mu'_\nu s}$. Spectral regions within $\Delta \nu$ for which

$$\mu'_\nu s \gg 1 \quad (2.6-25)$$

will contribute zeros to the average

$$\frac{1}{\Delta \nu} \int e^{-\mu'_\nu s} d\nu$$

and to an emissivity such as given by Eq. (2.6-10) or Eq. (2.6-20). Thus, one only needs to know accurately the width of such regions. Much less

accuracy is needed for the strength of u_ν since one only has to ascertain that $u_\nu' s \gg 1$. On the other hand, for very weak regions where

$$u_\nu' s \ll 1 \quad (2.6-26)$$

the integrand $e^{-u_\nu' s}$ is near unity. In this case one can expand the exponential and the contribution to an emissivity such as Eq. (2.6-24) is proportional to $u_\nu' s$; therefore, the strengths of these regions are of greatest importance and their widths are relatively unimportant.

The relative importance of the widths and strengths of small spectral regions (particularly lines), show up even more distinctly in the calculation of Rosseland and Planck mean absorption coefficients and will be discussed in more detail when we consider the calculation of these quantities later (see Part B). The geometric parameter or length s does not enter their calculation so that the relative importance of different spectral features is fixed once and for all by the basic assumptions. For the intermediate optical depths now being considered, the appearance of the parameter s provides another variable which affects the importance of a given spectral feature in the absorption coefficient as a function of optical depth. Similar considerations are applicable to the gross contributions

$\frac{B_1 e^{-\mu_1(x)x}}{B}$ to the emissivity as given by Eq. (2.6-24) for different l .

The only difference is that the gross contributions given by Eq. (2.6-24) have the Planck function B_l as an additional weighting factor compared to the fine contributions (for which B_ν is constant)

which make up

$$\frac{1}{\Delta\nu} \int e^{-\tau_{\nu}^0} d\nu$$

Thus, if one is calculating an integrated flux or total emissivity away from the Planck function maximum, where B_{λ} is small, much less accuracy is required in the specification of μ_{ν} than for regions near the Planck maximum.

Spectrum lines usually constitute a large fraction of the detail which must be accounted for in a radiation transport or absorption coefficient calculation. Since they often exhibit common features and regularities which can be used to simplify their treatment, it is worthwhile to consider briefly the transport of radiation within the profile of an individual spectrum line. Furthermore, since lines, as opposed to more continuous spectral features (such as ionization and dissociation) occur in virtually infinite number and with a wide variety of shapes and features, it is preferable to group such lines whenever possible into classes which can be treated as units. For this reason, we will also touch upon the subject of band models. By this is meant a relatively simple analytic or stochastic representation of a large number of actual lines.

Before considering band models per se, we give a brief exposition of absorption or emission for a single line designated by the index α . The absorption coefficient for a line can be written as

$$\mu'_{\nu\alpha} = S_{\alpha} b_{\alpha}(\nu - \nu_0) \quad (2.6-27)$$

where S_{α} is the intensity of the line and $b_{\alpha}(\nu - \nu_0)$ is a shape factor.

The line shape factor is to be normalized to unity:

$$\int_{-\infty}^{+\infty} h(\nu - \nu_0) d(\nu - \nu_0) = 1 \quad (2.6-28)$$

over the profile of a line, so that the frequency integral of the absorption coefficient is equal to S_α

$$\int_{-\infty}^{+\infty} \mu'_{\nu\alpha} d(\nu - \nu_0) = S_\alpha \quad (2.6-29)$$

We can apply the definition of the absorption function $A(\mu_\nu s)$ or the column emissivity $\epsilon_{\nu c\alpha}$ to a single line using Eqs. (2.6-9a, b). These definitions for the line α , become

$$\begin{aligned} \epsilon_{\nu c\alpha}(s) &= 1 - \text{Tr}_\alpha(\mu'_\nu s) \\ A_\alpha(\mu_\nu s) &\doteq 1 - \text{Tr}_\alpha(\mu'_\nu s) = \epsilon_{\nu c\alpha}(s) \end{aligned} \quad (2.6-30)$$

The approximate equality symbol \doteq has been used for the absorption function to remind us that this quantity represents an observable net attenuation only approximately, and this notation will be retained in the sequel where this latter interpretation is implied. The approximation is, of course, very good at low temperatures where the re-emission into the incident beam is negligible.

Another useful definition is that of average absorption \bar{A} , of a single line, which is for the line α that is a member of a group of lines,

$$\bar{A}_\alpha \doteq \frac{1}{\Delta} \int_{-\infty}^{+\infty} \{1 - \exp(-\mu_{\nu\alpha} s)\} d\nu \quad (2.6-31)$$

where Δ is the average spacing between lines. This is related to the so-called equivalent width $W_\alpha(s)$ by

$$W_\alpha(s) = \bar{\lambda}_\alpha \Delta \quad (2.6-32)$$

where the basic definition of $W_\alpha(s)$ is given by

$$W_\alpha(s) = \int_{-\infty}^{+\infty} [1 - \exp(-\mu_{\nu\alpha} s)] d\nu \quad (2.6-33)$$

$$= \int_{-\infty}^{+\infty} A_\alpha(\mu_\nu s) d\nu$$

By use of Eq. (2.6-30), the equivalent width is seen to satisfy the exact relation

$$W_\alpha(s) = \int_{-\infty}^{+\infty} \epsilon_{\nu\alpha}(s) d\nu \quad (2.6-34)$$

The origin of the name "equivalent width" lies in the fact that $W_\alpha(s)$ is the width of a totally absorbing line ($\mu_{\nu\alpha} = \infty$) having the same integrated absorption function, viz., the same value of $\int A_\alpha(\mu_\nu s) d\nu$ as the given line. The relation between $W(s)$ and s is known, for historical reasons in astrophysics, as the "curve of growth." As stated in Eq. (2.6-34), $W(s)$ is also equal to the frequency integral of the column emissivity. We note, however, that this

is not the total column emissivity as we defined this latter quantity in Eq. (2.6-10), since the Planck function appears as a weighting factor in the total emissivity definition.

Experimental observations of the intensity of a line profile as a function of absorbing thickness (in a cold gas) are often reduced to curves of growth for comparison with theory. The theoretical prediction for such a curve for lines with a Lorentz shape:

$$b(\nu - \nu_0) = \frac{1}{\pi} \frac{w_L}{(\nu - \nu_0)^2 + w_L^2} \quad (2.6-35)$$

(w_L is the Lorentz half-width)

can be obtained by inserting Eq. (2.6-35) into the definition of $W_\alpha(s)$ as given in Eq. (2.6-33) and performing the integration. The result one obtains (due originally to Ladenburg and Reiche, 1913) is

$$W(u) = 2\pi w_L u e^{-u} \{I_0(u) + I_1(u)\} \quad (2.6-36)$$

where $u = S_\alpha s / 2\pi w_L$, and I_0 and I_1 are Bessel functions, for imaginary argument, of the zeroth and first order, respectively (Whittaker and Watson, 1952). These considerations of a single line are applicable to a band of isolated lines of equal intensity either by summation over the band or by reduction of the band to a single average line. For bands of isolated lines of unequal intensities, a generalization can readily be made to N lines if a distribution function can be specified for the N line strengths.

The average equivalent width of the lines is

$$\bar{W}(s) = \frac{1}{N} \sum_{\alpha=1}^N W_{\alpha}(s) \quad (2.6-37)$$

In order to compute \bar{W} , some assumption must be made regarding the distribution of line intensities. For example, for exponential and inverse-first-power distributions of the line strength S it can be shown (Goody, 1964) that, for the Lorentz line shape,

$$\bar{W}(\text{exp}) = \frac{2\pi w_L u}{(2u + 1)^{1/2}} \quad (2.6-38)$$

and

$$\bar{W}(\text{inverse}) = 2\pi w_L \left[e^{-u} I_0(u) + 2ue^{-u} \{I_0(u) + I_1(u)\} - 1 \right] \quad (2.6-39)$$

respectively. The definition of u as given following Eq. (2.6-36) must be modified in each case by replacing S by the average line strength \bar{S} for the exponential distribution, and by the maximum line strength S for the inverse first power distribution.

Although the above models may be modified to include overlapping lines, more elegant and powerful techniques are available through the formulation of regular and random models based on a statistical approach. Both regular and random models depend on an assumed "multiplication property" of transmission functions. That is to say, suppose there are two non-reacting

components (1) and (2) of a mixture so that

$$\text{Tr}_\nu(1, 2) = \text{Tr}_\nu(1) \times \text{Tr}_\nu(2) \quad (2.6-40)$$

Then if the interval $\Delta\nu$ over which averaging takes place is sufficiently large, we can also write

$$\bar{\text{Tr}}_\nu(1, 2) = \bar{\text{Tr}}_\nu(1) \times \bar{\text{Tr}}_\nu(2) \quad (2.6-41)$$

if the transmission for component (1) and component (2) are uncorrelated. The conditions under which this is valid are discussed by Goody (1964).

The regular model was first developed by Elsasser (1942). The model consists of an infinite number of lines of equal intensity with equal spacing between lines, which may be allowed to overlap. The absorption coefficient for Lorentz lines may then be written as

$$\mu'_\nu = \sum_{i=-\infty}^{i=+\infty} \left(\frac{S}{\pi}\right) \frac{w_L}{(\nu - i\delta)^2 + w_L^2} \quad (2.6-42)$$

where δ is the frequency spacing between lines and the average absorption can then be shown to be

$$\bar{A} = 1 - E(y, u) \quad (2.6-43)$$

where $y = w_L/S$ and

$$E(y, u) = \int_{-1/2}^{+1/2} \exp\left(-2\pi uy \frac{\sinh 2\pi y}{\cosh 2\pi y - \cos 2\pi x}\right) dx \quad (2.6-44)$$

The function $E(y, u)$ cannot be written explicitly in terms of known functions and must be numerically integrated or treated in limiting cases.

The random model was first considered by Mayer (1947) and Goody (1952). In its most general form, it refers to N overlapping lines of unequal intensity randomly spaced in an interval $\Delta\nu = N\delta$ for which it can be shown that

$$\bar{T}_1 = \frac{1}{\Delta\nu_1} \int_{\Delta\nu_1} \exp \left\{ - \left[\sum_{i=1}^N \mu_{\nu_i}^i \right] s \right\} d\nu \quad (2.6-45)$$

Eq. (2.6-45) has recently been applied by Churchill, Hagstrom, and Landshoff (1964) to a computation for heated air. The integral is approximated by evaluating the argument at many points in $\Delta\nu_1$ and utilizing a trapezoidal integration scheme. The final results show that an average \bar{T} over $\Delta\nu_1$ may be fitted to the following simple empirical form

$$\bar{T}_1(s) = \frac{1}{2} \left[\exp(-\mu_1^i s) + \exp(-\mu_2^i s) \right] \quad (2.6-46)$$

where μ_1^i and μ_2^i are mean absorption coefficients for two groupings of lines. Tables of μ_1^i and μ_2^i as well as graphs of the behavior of \bar{T}_1 are given for temperatures between 1000°K and 12,000°K and densities from atmospheric normal to 10^{-4} normal.

In considering lines superimposed upon a background continuum, it is of interest to inquire into the degree of separability that exists between the two types of emission. What we can show* is that the total energy

* The method is due to S. A. Hagstrom.

radiated by an atmosphere equals the energy of the continuum emission plus the energy of the line emission diminished by the factor $\exp(-\mu_c s)$, where μ_c is the continuum absorption coefficient which is assumed to be essentially constant over some frequency interval $\Delta\nu$. The intensity $I_\nu(s, \vec{n})$ in the direction \vec{n} due to an emitting column of gas of length s is given by

$$I_\nu(s, \vec{n}) = B_\nu(T) (1 - e^{-(\mu_c' + \mu_L')s}) \quad (2.6-47)$$

where μ_c' and μ_L' are the continuum and line contributions to the absorption coefficient, respectively. Integrating Eq. (2.6-47) over the interval $\Delta\nu$ we get

$$\begin{aligned} I_{\Delta\nu}(s, \vec{n}) &= \int_{\Delta\nu} d\nu B_\nu(T) (1 - e^{-(\mu_c' + \mu_L')s}) \\ &= \int_{\Delta\nu} d\nu B_\nu(T) - e^{-\mu_c' s} \int_{\Delta\nu} B_\nu(T) e^{-\mu_L' s} d\nu \end{aligned} \quad (2.6-48)$$

where we have assumed μ_c' is constant over $\Delta\nu$.

The intensity due to lines alone is

$$\begin{aligned} I_{\Delta\nu}^L(s, \vec{n}) &= \int_{\Delta\nu} d\nu B_\nu(T) (1 - e^{-\mu_L' s}) \\ &= \int_{\Delta\nu} d\nu B_\nu(T) - \int_{\Delta\nu} d\nu B_\nu(T) e^{-\mu_L' s} \end{aligned} \quad (2.6-49)$$

or, rearranging,

$$\int_{\Delta\nu} d\nu B_\nu(T) e^{-\mu'_L s} = \int_{\Delta\nu} d\nu B_\nu(T) - I_{\Delta\nu}^L \quad (2.6-50)$$

Substituting Eq. (2.6-50) into Eq. (2.6-48), we get

$$\begin{aligned} I_{\Delta\nu} &= \int_{\Delta\nu} d\nu B_\nu(T) - e^{-\mu'_C s} \int_{\Delta\nu} d\nu B_\nu(T) + I_{\Delta\nu}^L(s, \vec{n}) e^{-\mu'_C s} \\ &= I_{\Delta\nu}^C + I_{\Delta\nu}^L e^{-\mu'_C s} \end{aligned} \quad (2.6-51)$$

where the continuum intensity $I_{\Delta\nu}^C$ is given by

$$I_{\Delta\nu}^C(s, \vec{n}) = \int_{\Delta\nu} d\nu B_\nu(T) (1 - e^{-\mu'_C s}) \quad (2.6-52)$$

Note that Eq. (2.6-51) holds regardless of whether the lines overlap or not.

The importance of Eq. (2.6-51) is that it gives us a ready idea as to the relative importance of continuum versus line effects. Thus, if, for example,

$$\mu'_C s > 0.1$$

the continuum spectrum will cause an apparent reduction in the line contribution, and in regions where

$$\mu'_C s \gg 1$$

the lines may be disregarded entirely, for most practical purposes.

The relation (Eq. (2.6-51)) may be put into an equivalent form in terms of partial (intensity) emissivities:

$$\begin{aligned} \epsilon_{\Delta\nu} &= \frac{I_{\Delta\nu}^C}{\int_{\Delta\nu} dv B_\nu(T)} + \frac{I_{\Delta\nu}^L e^{-\mu'_C s}}{\int_{\Delta\nu} dv B_\nu(T)} \\ &= 1 - (1 - \epsilon_{\Delta\nu}^L) e^{-\mu'_C s} \end{aligned} \quad (2.6-53)$$

or

$$\epsilon_{\Delta\nu} = \epsilon_{\Delta\nu}^L + \epsilon_{\Delta\nu}^C - \epsilon_{\Delta\nu}^L \epsilon_{\Delta\nu}^C \quad (2.6-54)$$

where

$$\epsilon_{\Delta\nu}^L = \frac{I_{\Delta\nu}^L}{\int_{\Delta\nu} B_\nu(T) dv}$$

and

$$\epsilon_{\Delta\nu}^C = \frac{I_{\Delta\nu}^C}{\int_{\Delta\nu} B_\nu(T) dv} = 1 - e^{-\mu'_C s}$$

are the line and continuum partial emissivities, respectively.

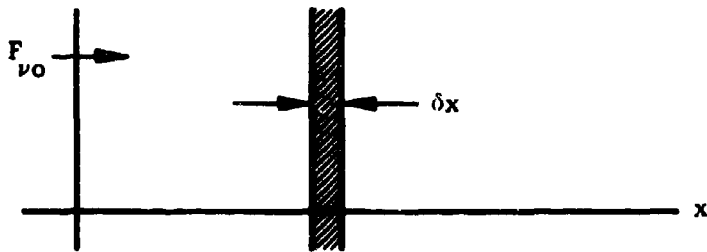


FIG. 2-1 ILLUSTRATION OF A COLLIMATED BEAM OF RADIATION $F_{\nu 0}$ INCIDENT ON A PLANE-PARALLEL SLAB OF GAS (SHADED SECTION).

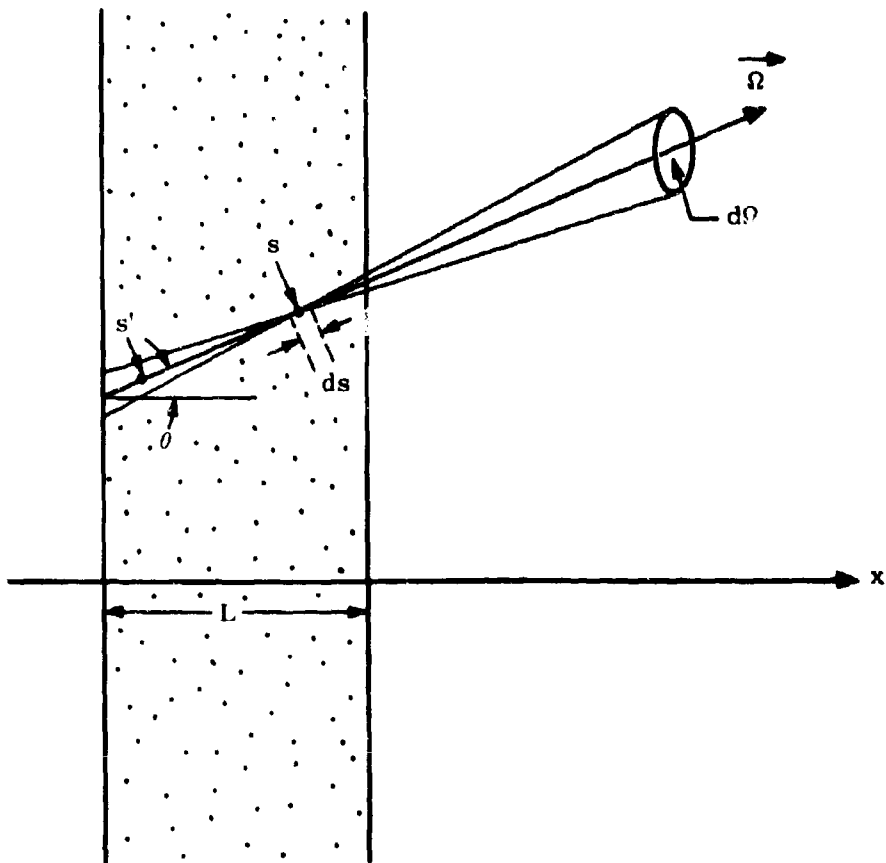


FIG. 2-2 ILLUSTRATION OF AN
INFINITESIMAL CONE OF RADIATION
IN A SLAB OF GAS OF THICKNESS L .

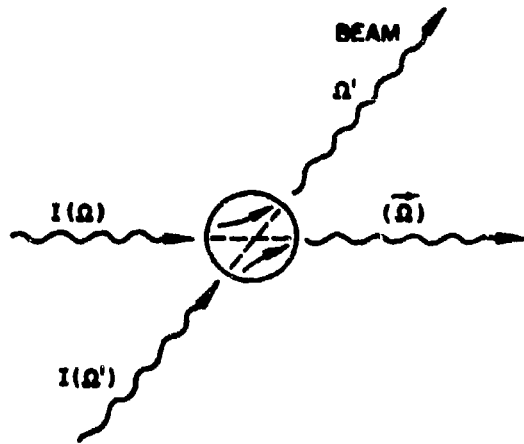
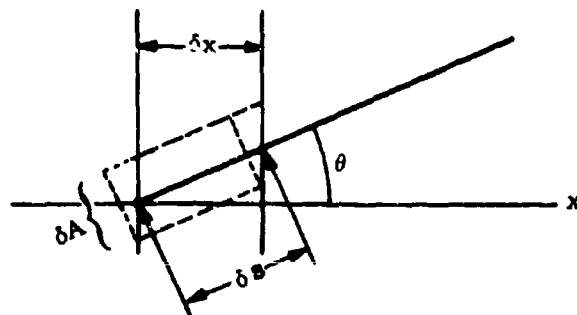


FIG. 2-3 ILLUSTRATION OF INDUCED SCATTERING. $I(\Omega')$ REPRESENTS THE BEAM INTENSITY IN THE PARTICULAR DIRECTION Ω' ; SCATTERING INDUCED BY THE INTENSITY $I(\Omega)$ DIVERTS PART OF THIS BEAM INTO THE DIRECTION Ω . THE EFFECT IS SYMMETRIC BETWEEN THE DIRECTIONS Ω AND Ω' .



(ΔA IS MEASURED NORMAL TO THE DIRECTION OF THE BEAM)

FIG. 2-4 FLUX EMISSION FROM AN ELEMENT OF VOLUME IN A SLAB OF THICKNESS Δx .

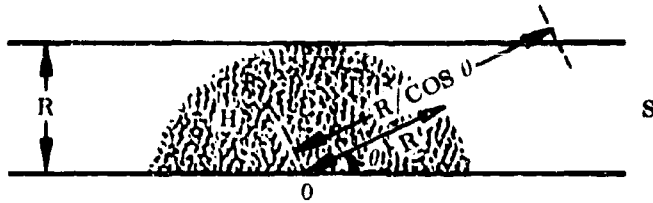


FIG. 2-5 THIN-SLAB AND HEMISPHERICAL GEOMETRIES

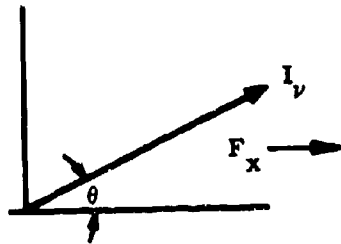


FIG. 2-6 INTENSITY I_v AND x -COMPONENT OF FLUX F_x .

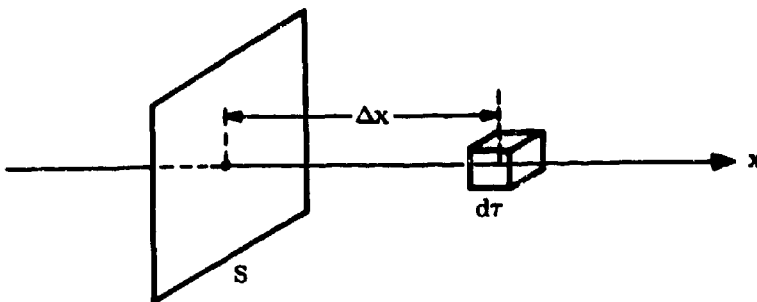


FIG. 2-7 TRANSPORT ACROSS A SURFACE AREA , S .

Chapter 3. THEORY OF RADIATION

In Chapter 2 we reviewed the influence of absorption coefficients and related experimentally measurable quantities on the transport of radiation through gases. The absorption coefficients and related quantities were introduced as atomic constants, and no discussion was made of the factors which determine them. In this chapter we therefore review the classical and quantum models of radiation theory which are used to determine the absorption coefficients and other transition parameters of atoms and molecules.

3.1 Classical Lorentz formulation

The Lorentz theory (an excellent discussion is given in Stone, 1963) based on the classical model of interaction between electromagnetic radiation and matter is well known. It involves the examination of the behavior of an ensemble of damped linear, simple harmonic electron oscillators (called "atoms") driven by the electric vector of the electromagnetic wave. The theory has been spectacularly successful in discussing dispersion, and many other phenomena of physical optics. In spite of its limitations, and the apparently arbitrary assumptions which have to be applied to overcome them, much physical insight can be obtained by study of the Lorentz model.

In the discussion of the anomalous dispersion, the equation of motion of a typical damped, driven, oscillating electron is

$$m\ddot{x} + b\dot{x} + kx = eE \exp(i\omega t) \quad (3.1-1)$$

where

$$\gamma = b/m \quad (3.1-2)$$

is called the damping constant. The characteristic angular frequency of the electron is

$$\omega_0 = (k/m)^{1/2} \quad (3.1-3a)$$

$$\omega_0 = 2\pi \nu_0 \quad (3.1-3b)$$

and the angular frequency of the driving E-vector is $\omega = 2\pi\nu$. Straightforward and well-known analysis leads to the following expression for the frequency dependence of the absorption coefficients

$$\alpha_\nu = \frac{e^2}{mc} \frac{\left(\frac{\gamma}{4\pi}\right)}{\left(\nu - \nu_0\right)^2 + \left(\frac{\gamma}{4\pi}\right)^2} \quad (\text{cm}^2) \quad (3.1-4a)$$

$$\mu_\nu = \frac{Ne^2}{mc} \frac{\left(\frac{\gamma}{4\pi}\right)}{\left(\nu - \nu_0\right)^2 + \left(\frac{\gamma}{4\pi}\right)^2} = N \alpha_\nu \quad (\text{cm}^{-1}) \quad (3.1-4b)$$

$$K_\nu = \frac{Ne^2}{mcp} \frac{\left(\frac{\gamma}{4\pi}\right)}{\left(\nu - \nu_0\right)^2 + \left(\frac{\gamma}{4\pi}\right)^2} = \frac{N \alpha_\nu}{\rho} \quad (\text{cm}^2/\text{gm}) \quad (3.1-4c)$$

where N is the number of absorbing atoms per cm^3 .

These equations represent the 'Lorentz' radiation-damping natural line profile and, apart from a redefinition of γ in the quantum formulation, retain the same form of a tuned, damped oscillator in this case as a typical Lorentz line is illustrated in Fig. 3-1, where the width W at 'half power point' is seen to be the distance between the two frequencies at which the two terms in the denominator of Eqs. (3.1-4a, b, c) are equal. Thus we have

$$W = \frac{\gamma}{2\pi} \quad (3.1-5)$$

From a consideration of the decay of the oscillation due to classical dipole radiation, it is easy to show that when the driving field is removed, if t is the time for the power to decay to $1/e$ of its initial value, the damping constant has the value

$$\gamma = \frac{1}{t} = \frac{8\pi^2 \nu^2 e^2}{3 mc^2} = \frac{0.233}{\lambda^2} \text{ sec}^{-1} \quad (\lambda \text{ in cm}) \quad (3.1-6a)$$

or

$$t = 4.50 \lambda^2 \text{ (sec)} \quad (3.1-6b)$$

Integration by elementary methods of Eq. (3.1-4a) with respect to ν over a spectral line leads to the important result (see Aller, 1963)

$$\int \alpha_\nu d\nu = \frac{\pi e^2}{mc} \quad (3.1-7a)$$

In order to compare such an equation with experiment the model has to be refined somewhat. Atoms exhibit more than one spectrum line and it is thus assumed that the electron is so bound that it can oscillate at one of a number of characteristic frequencies ν_0 . The 'fraction' of the electron associated with any one characteristic frequency is designated f and is called the classical oscillator strength at that frequency. This requires that the right hand side of Eq. (3.1-7a) be multiplied by f , and thus

$$\int \alpha_\nu d\nu = \frac{\pi e^2}{mc} \cdot f \quad (3.1-7b)$$

The similar expressions for the other integrated absorption coefficients become

$$\int \mu_\nu d\nu = \frac{\pi e^2}{mc} Nf \quad (3.1-7c)$$

$$\int K_\nu d\nu = \frac{\pi e^2}{mc} \frac{Nf}{\rho} \quad (3.1-7d)$$

When $\bar{\nu}$ is measured in cm^{-1} rather than sec^{-1} Eq. (3.1-7b) takes the form

$$\int \alpha_{\nu} d\bar{\nu} = \frac{\pi e^2}{mc^2} f \quad (3.1-7e)$$

and a similar change occurs in the denominator of Eq. (3.1-7c and d).

The equivalent width W (Section 2.5) of an optically thin line may be written as

$$W = \int \tau_{\nu} d\nu = Nx \int \alpha_{\nu} d\nu = \frac{\pi e^2}{mc} Nfx \quad (3.1-8)$$

Thus for optically thin lines, W can be used to measure N , f or x .

The application of Eq. (3.1-8) to the optically thick case involves a discussion of the curve of growth (see Aller, 1963 and Section 2.5).

A few properties of classical oscillator strengths are noted briefly.

a) The 'sum rule'

$$\sum f = 1 \quad (3.1-9)$$

is obeyed.

b) For continuous spectra Eq. (3.1-7b) is written

$$\alpha_{\nu} d\nu = \frac{\pi e^2}{mc} \frac{df}{d\nu} d\nu \quad (3.1-10)$$

where df is the element of oscillator strength associated with the frequency increment $d\nu$.

c) In the classical formulation, the oscillator strength of a line is a good parameter with which to specify the integrated absorption coefficient of the line.

Finally we make brief mention from a classical standpoint of scattering processes and of the Einstein A and B coefficients.

Light Scattering. Suppose a classical oscillator with frequency ν_0 is hit by a photon of frequency ν . It can then be shown (Heitler, 1954) that the total cross section is

$$\varphi = \frac{8\pi}{3} r_0^2 \frac{\nu^4}{(\nu_0^2 - \nu^2)^2 + \nu^2 \gamma^2} \quad (3.1-11)$$

where

$$r_0 = e^2/mc^2 \quad (3.1-12)$$

is the classical electron radius, and γ is the natural line breadth, given as

$$\gamma = \frac{2}{3} \frac{\nu_0^2}{c} r_0 \quad (3.1-13)$$

From Eq. (3.1-11) one can discuss three cases of interest:

- 1) for $\nu_0 \ll \nu$ and $\gamma \ll \nu$, we obtain Thomson scattering cross section

$$\varphi = \frac{8\pi}{3} r_0^2 \quad (3.1-14)$$

- 2) when $\nu_0 \gg \nu$, we have Rayleigh scattering cross section

$$\varphi = \frac{8\pi}{3} r_0^2 \frac{\nu^4}{\nu_0^4} \quad (3.1-15)$$

3) with $\nu \sim \nu_0$, one has the Lorentz cross section

$$\varphi = \frac{2\pi}{3} r_0^2 \frac{\nu^2}{(\nu_0 - \nu)^2 + \gamma^2/4} \quad (3.1-16)$$

When $\nu \sim \nu_0$ in case 3) we have the phenomenon of coherent scattering at resonance or resonance fluorescence, which from a quantum viewpoint can also be considered as a single process equivalent to absorption and emission of a photon.

Einstein A & B Coefficients. In a transition of spontaneous emission from U(pper) to L(ower) states, the number of radiative transitions per second is $N_U A_{UL}$, where A_{UL} is the Einstein A-coefficient or transition probability per atom per second for spontaneous emission. Thus the energy $E_S^{(UL)}$ radiated per second from unit volume into all 4π of solid angle is (cf, Eq. (2.2-4a), integrated over Ω and ν):

$$E_S^{(UL)} = N_U A_{UL} h\nu_{UL} \quad (3.1-17)$$

where N_U is the number density of excited atoms in the state U.

Similarly, in the L-U absorption transition stimulated by a beam of radiation with specific intensity I_ν , and hence, energy density per unit solid angle I_ν/c , the number of absorption transitions per second is*

$$N_L B_{LU} \frac{I_\nu}{c} d\Omega \quad (3.1-18)$$

The coefficient B_{LU} is called the Einstein B-coefficient for absorption or for stimulated (induced) emission. Thus, the energy per unit area per unit time absorbed out of the beam I_ν within a path length dx is

$$dE_A^{(UL)} = dx N_L \int B_{LU} I_\nu \frac{h\nu_{LU}}{c} d\Omega \quad (3.1-19)$$

However, from the definition of the absorption coefficient α_ν , we know that this absorbed energy should be

$$dE_A^{(UL)} = N_L dx \int \int \alpha_\nu I_\nu d\nu d\Omega \quad (3.1-20)$$

where the frequency integration is carried out over the width of the line U-L.

By comparing these two formulas for the case of a line over whose width I_ν does not vary appreciably, we find the relationship between α_ν , B_{LU} , and the line oscillator strength:

$$\int \alpha_\nu d\nu = B_{LU} \frac{h\nu_{LU}}{c} = \frac{\pi e^2}{mc} f_{LU} \quad (3.1-21)$$

* The B-coefficient is sometimes defined relative to the intensity alone, rather than relative to the energy density. In this event, no factor c appears in this expression.

The last equality follows from Eq. (3.1-7b).

We can therefore write

$$f_{LU} = \frac{m}{\pi e^2} h\nu_{LU} B_{LU} \quad (3.1-22)$$

When U is g_U -fold degenerate and L is g_L -fold degenerate, the B-coefficients of the component transitions may be summed to give an overall B-coefficient which will apply when the levels all lie at the same energy (Davidson, 1962).

$$\sum_{U_1 L_1} B_{U_1 L_1}(\nu) = g_U B_{UL} = g_L B_{LU} \quad (3.1-23)$$

Similarly, by a detailed balancing argument the following relation can be shown to exist between the A- and B-coefficients in the general case of degeneracy (Davidson, 1962):

$$g_U A_{UL} = g_L B_{LU} \frac{8\pi h\nu^3}{c^3} = g_U B_{UL} \frac{8\pi h\nu^3}{c^3} \quad (3.1-24)$$

The intensities are however, still controlled by Eqs. (3.1-17) and (3.1-20).

The energy absorbed per unit time, E_{cl} , by a (single) classical electron oscillator (corresponding to Eq. (3.1-19)) is given by

$$E_{cl} = \frac{\pi e^2}{mc} \int I_{\nu} d\Omega \quad (3.1-25)$$

(cf. Heitler, 1954, p. 38, Eq. 19.)

in terms of the specific intensity I_{ν} . The quantum-mechanical result (which we will derive in the next section*) is

$$E_{Q.M.} = \frac{4\pi^2 e^2}{3\hbar c} \nu |\vec{r}_{\beta\alpha}|^2 \int I_{\nu}(\vec{n}) d\Omega \quad (3.1-26)$$

in terms of the matrix element $\vec{r}_{\beta\alpha}$.

The two results can be connected by the definition of the quantum-mechanical f-number:

$$f_{\alpha\beta} = \frac{4\pi m}{3\hbar} \nu_{\alpha\beta} |\vec{r}_{\alpha\beta}|^2 \quad (3.1-27)$$

(see Eq. (3.2-62), following.)

With this definition, Eq. (3.1-26) yields

$$E_{Q.M.} = \frac{\pi e^2}{mc} f_{\alpha\beta} \int I_{\nu} d\Omega \quad (3.1-28)$$

in analogy to Eq. (3.1-25). That is to say, we obtain

$$E_{Q.M.} = f_{\alpha\beta} E_{cl} \quad (3.1-29)$$

* See Eq. (3.2-43). By multiplying $w_{\beta\alpha}$ of this equation by $\hbar w$, the result used here can be obtained.

Thus, the oscillator strength, which in classical terms is associated with the fraction of the electron responsible for the radiative transition, may also be thought of as the fraction or factor which converts the classical energy absorbed or radiated per unit time to the correct quantal value.

A classical derivation of photoelectric absorption has been given by Thompson and an improved semiclassical derivation has been given by Kramers. These are described by Compton (1926) in Chapters 6 and 12, respectively.

3.2 Quantum formulation of radiation theory

3.2.1 Formal theory

We will not attempt to expound or review the basic principles of the quantum theory of radiation. Rather, in the spirit of the applied investigator, we shall derive the working formulas needed for applications of the theory from its basic formal results. In this spirit we will also tabulate some of the parameters needed for applications to the radiative properties of heated air. We will also attempt, where it appears useful, to correlate the results of several more or less standard texts or references (Bates and Damgaard, 1949; Bethe and Salpeter, 1957; Dirac, P.A.M., 1947; Griem, H.R., 1964; Heitler, W., 1954; Mayer, H., 1947; Schiff, L.I., 1955; Slater, 1960) where their authors employ different conventions, and to include some of the details of the reduction of the general formulas that are normally glossed over or left to the reader in these texts.

The basic formulas that we need, called "Golden Rules" by Fermi (1950), are

$$w_{ij} = \frac{2\pi}{\hbar} |H'_{ij}|^2 \frac{dn}{dE} \quad (3.2-1)$$

and

$$w_{ij} = \frac{2\pi}{\hbar} \left| \sum_k \frac{H'_{jk} H'_{ki}}{E_j - E_k} \right|^2 \frac{dn}{dE} \quad (3.2-2)$$

These formulas give the transition probability per unit time for a transition from state i to state j induced by a perturbation with matrix element

H'_{ij} (first-order perturbation, Eq. (3.2-1)) or $\sum_k \frac{H'_{ik} H'_{kj}}{E_j - E_k}$ (second-order perturbation, Eq. (3.2-2)).

The indices i and j are symbolic for all the quantum numbers needed to define the system (atom + radiation) before and after the transition, respectively. The factor $\frac{dn}{dE}$ is the number density of final states in the cases where there is a continuous range of final states (e.g., spontaneous emission, photoelectric absorption), or the density of initial states in the cases where there is a single final state but a continuous range of initial states* (e.g., line absorption). These formulas are derived by Schiff (1955) and are derived and justified in detail by Heitler (1954). Although they can be derived heuristically for radiative transitions within the framework of ordinary quantum mechanics and semi-classical radiation theory, they cannot be rigorously justified except by appeal to quantum field theory.**

Although in principle one is interested in all processes which result in the absorption or emission of a photon from or into an incident beam, in practice one usually confines oneself to the processes which dominate the absorption and emission in the temperature-density regime of interest. In this spirit, we will limit our attention to discrete atomic transitions, photoelectric and free-free transitions, and simple scattering processes. We will not concern ourselves with radiative corrections or relativistic effects.

The first three of these processes, viz., discrete atomic transitions, photoelectric, and free-free transitions, termed "simple absorption" by Mayer (1947), are usually the most important and we will emphasize them

* For the existence of a transition probability per unit time, a continuous range of states must exist in either the initial or final state. For a discussion of this point see Heitler (1954), or Schiff (1955).

** Or to the rules of Quantum Electrodynamics, see Feynman (1962), p. 4.

accordingly. We will first reduce Eqs. (3.2-1) and (3.2-2) to the specific transitions listed above that we wish to treat. This can be done without reference to the type of atomic system because the nature of the atomic system is concealed in the wave functions used to compute the matrix elements H'_{ij} . After deriving the formulas specific to the various transitions, we will proceed to specify the atomic systems. In applying Eqs. (3.2-1) and (3.2-2) for the transition probability to different situations, one usually must deal with degenerate states (i.e., states with the same energy, but differing in some other quantum number or numbers). In view of the principle of equal a priori probabilities in phase space one should, in the absence of additional information, average over degenerate initial states and sum over degenerate final states (Tolman, R.C., 1938, Sections 98 and 99). This degeneracy must arise from different spatial orientations or from degeneracy on quantum numbers other than the energy, as the sum over the energy states lying in a small region ΔE allowed by the uncertainty principle (and therefore effectively degenerate) has already been carried out in the derivation of Eq. (3.2-1). It is this sum that leads to the appearance of the "number density of states" dn/dE . With this prescription, the transition probability per unit time becomes

$$w_{ij} = \frac{2\pi}{\hbar} \frac{1}{g_i} \sum_{\alpha(i)} \sum_{\beta(j)} |H'_{\alpha\beta}|^2 \frac{dn}{dE} \quad (3.2-3)$$

for first-order processes, where the index $\alpha(i)$ labels the degenerate family of g_i states (i) and the index $\beta(j)$ labels the family of g_j states (j). That is to say, i and j uniquely specify the energy of two degenerate states and α and

β run over the remaining quantum numbers. For simplicity in the derivations which we now undertake, we will compute transition probabilities, cross sections, etc. for a pair of distinct, non-degenerate substates α and β of a single atomic electron, and after doing this return to the general situation.

3.2.2 Reduction of the general formula to formulae for specific processes

For radiative processes, the perturbation term that enters the Hamiltonian for the interaction between the radiation field and an atomic electron is*

$$H' = -\frac{e}{mc} \vec{p} \cdot \vec{A} \quad (3.2-4)$$

where \vec{p} is the momentum operator of the atomic electron and \vec{A} is the electromagnetic vector potential. The normalization of \vec{A} and the density of states of the radiation field $\frac{dn_R}{dE}$ are related so that a consistent choice of the two must be made when $\frac{dn_R}{dE}$ is the appropriate density of states to use. For emission of a photon by an atomic system which makes a transition between two bound states, the necessary continuous range of states is provided by the radiation field which is produced in the final state. Similarly for absorption accompanied by a transition between two bound states, the continuous range of states is provided by the presence of the radiation field in the initial state. A consistent choice of $\frac{dn_R}{dE}$ and the matrix element of the interaction term given by Eq. (3.2-4) is given

* This arises, of course, from expanding the term $\frac{1}{2m} (\vec{p} - \frac{e}{c} \vec{A})^2$ in the Hamiltonian. See Schiff (1955), Sec. 35. It also can be interpreted as the interaction energy $-\frac{1}{c} \vec{j} \cdot \vec{A}$ between the atomic electron current $\vec{j} = e\vec{v}$ and the vector potential \vec{A} . See also Power, E.A. (1964), p. 101.

by Heitler (1954) as

$$\frac{dn_R}{dE} = \frac{\omega^2 d\bar{\Omega}}{(2\pi c)^3 \hbar} \quad (3.2-5)$$

$$M'_{\beta\alpha} = M_{\alpha\beta}^* = -\frac{e}{m} \left(\frac{2\pi\hbar}{\omega}\right)^{1/2} (n_\omega + 1)^{1/2} \int \psi_\beta^* \vec{p} \cdot \vec{\epsilon} e^{-i\vec{k}_\gamma \cdot \vec{r}} \psi_\alpha dv \quad (3.2-6)$$

In these equations dn_R is the number of photon states per unit volume of a given polarization in the energy range E to $E + dE$ and in the solid angle element $d\bar{\Omega}$ about the propagation vector \vec{k}_γ . The polarization is specified by the unit vector $\vec{\epsilon}$ and there are two independent directions of polarization. The matrix element given in Eq. (3.2-6) is appropriate for the state α to contain n_ω photons per radiation oscillator (cell in the phase space of the radiation field) and the state β to contain $n_\omega + 1$ photons per oscillator. Hence, we can use α and β as initial and final states, respectively, for emission, or β and α as initial and final states, respectively, for absorption. In this latter instance, however, it will be necessary to replace n_ω by $n_\omega - 1$ and $n_\omega + 1$ by n_ω .

The matrix element of Eq. (3.2-6) depends on a particular radiation oscillator within the infinitesimal range $dn_R = \omega^2 d\bar{\Omega} dE / (2\pi c)^3 \hbar$ only through the "occupation number" of the cell, n_ω . Since, as stated previously, the square of the matrix element appearing in Eq. (3.2-1) (or Eq. (3.2-3) has been summed over this infinitesimal volume of phase space, when we make use of Eq. (3.2-5) as the density of final states and Eq. (3.2-6) as the matrix element in Eq. (3.2-1), n_ω should be replaced by \bar{n}_ω , the

average number of photons per radiation oscillator in the range dn_R .

3.2.2.1 Bound-State Emission

We now insert Eqs. (3.2-5) and (3.2-6) into

Eq. (3.2-1) ($\alpha \equiv i, \beta \equiv j$) to obtain

$$dw_{\alpha\beta} = \frac{e^2 \omega_{\alpha\beta}}{2\pi \hbar^2 m^2 c^3} \left| \vec{p} \cdot \vec{\epsilon} e^{-i\vec{k} \cdot \vec{r}} \right|_{\alpha\beta}^2 (\bar{n}_\omega + 1) d\Omega \quad (3.2-7)$$

for the transition probability per unit time for emission into the solid angle element $d\Omega$. The matrix element of $\vec{p} \cdot \vec{\epsilon} e^{-i\vec{k} \cdot \vec{r}}$ indicated by the subscripts α, β after the absolute value brackets is defined by the integral appearing in Eq. (3.2-6).

We now need to relate the occupation number n_ω of the radiation oscillators to the intensity of a beam of photons. Since the number of radiation oscillators (cells in phase space) per unit volume in an energy range dE is given by Eq. (3.2-5), we can from this equation compute the intensity of radiation corresponding to the presence of some average number \bar{n}_ω , of photons per radiation oscillator. The physical properties of photons within the infinitesimal range $dn_R = \frac{\omega^2 d\vec{\Omega} dE}{(2\pi c)^3 \hbar}$ of oscillator states are the same; hence, a measurement of the intensity would not discriminate among them and would therefore constitute a measure of the average occupation of these dn_R states. Since $\frac{1}{\hbar \omega c} I_\omega(\bar{n}) d\vec{\Omega} d\omega$ is the number of photons per cm^3 in the (angular) frequency range $d\omega$ and in the element of solid angle $d\Omega$, it must be equal to \bar{n}_ω times the number of radiation oscillators per cm^3 in the same differential ranges $d\vec{\Omega}$ and $d\omega$.

Hence, we have

$$\frac{1}{\hbar \omega c} I_{\omega}(\vec{\Omega}) d\omega d\Omega = \bar{n}_{\omega} \left\{ \frac{\omega^2 d\vec{\Omega}}{(2\pi c)^3 \hbar} \right\} \hbar d\omega \quad (3.2-8)$$

which can be solved for $I_{\omega}(\vec{\Omega})$ in terms of \bar{n}_{ω} :

$$I_{\omega}(\vec{\Omega}) = \bar{n}_{\omega} \left\{ \frac{\hbar \omega^3}{(2\pi)^3 c^2} \right\} \quad (3.2-9)$$

or vice versa. The intensity function $I_{\omega}(\vec{\Omega})$ has been defined previously in Sec. .2.1.

We will generally make use of the dipole-length approximation wherein the exponential in the matrix element is taken to be unity and the electron momentum operator \vec{p} is replaced by the coordinate operator \vec{r} through use of the relation (Schiff, 1955, p. 253)

$$\vec{p}_{\alpha\beta} = i m \omega_{\alpha\beta} \vec{r}_{\alpha\beta} \quad (3.2-10)$$

Making use of Eq. (3.2-10) , we obtain from Eq. (3.2-7)

$$\frac{d\omega_{\alpha\beta}}{d\Omega} = \frac{e^2 \omega_{\alpha\beta}^3}{2\pi \hbar c^3} |\vec{\epsilon} \cdot \vec{r}_{\alpha\beta}|^2 (\bar{n}_{\omega} + 1) \quad (3.2-11)$$

which by use of Eq. (3.2-9) becomes:

$$\frac{d\omega_{\alpha\beta}}{d\Omega} = \frac{e^2 \omega_{\alpha\beta}^3}{2\pi \hbar c^3} |\vec{\epsilon} \cdot \vec{r}_{\alpha\beta}|^2 \left(1 + \frac{I_{\omega}(\Omega) 8\pi^3 c^2}{\hbar \omega^3} \right) \quad (3.2-12)$$

The first term in this expression is the spontaneous transition probability and the second is the induced transition probability. The total transition probability (with emission into any solid angle element $d\Omega$), is of course, obtained by integrating Eq. (3.2-12) over all angles. However, except for isotropic radiation, this is not interesting as an atomic parameter, as it will depend on the intensity I_ω . The total spontaneous transition probability is an atomic parameter in any event, and can be obtained from Eq. (3.2-12) by integrating the first term over all angles. This parameter is also known as the Einstein A-coefficient:

$$w_{\alpha\beta}(\text{spont}) = A_{\alpha\beta} = \int \frac{dw(\text{spont})}{d\Omega} d\Omega = \frac{e^2 \omega_{\alpha\beta}^3}{2\pi \hbar c^3} \sum_{\ell} \int |\hat{\epsilon}_{\ell} \cdot \vec{r}_{\alpha\beta}|^2 d\Omega \quad (3.2-13)$$

The indicated summation (ℓ) over the two independent polarization directions must be carried out before following the usual procedure of taking an average over the random orientations of the dipole moment of the atom, since the contribution of a given polarization depends on the dipole-moment orientation which is specified by the vector $\vec{r}_{\alpha\beta} = x_{\alpha\beta} \vec{i} + y_{\alpha\beta} \vec{j} + z_{\alpha\beta} \vec{k}$. The summation can be carried out with reference to Fig. 3-2 by taking $\vec{r}_{\alpha\beta}$ as the direction of the Z-axis.

With this convention, and taking $\vec{\epsilon}_1$ and $\vec{\epsilon}_2$ as two mutually perpendicular but otherwise arbitrary polarization vectors, we obtain,* since $d\Omega$ is an element of solid angle about the direction \vec{k}_Y , and since

$$\int_0^\pi \sin^2 \theta d\Omega = 2\pi \int_0^\pi \sin^3 \theta d\theta = \frac{8\pi}{3},$$

the result (valid for a fixed direction $\vec{r}_{\alpha\beta}$):

$$\begin{aligned} \Lambda_{\alpha\beta} &= \frac{e^2 \omega_{\alpha\beta}^3}{2\pi \hbar c^3} \int |\vec{r}_{\alpha\beta}|^2 \sin^2 \theta [\cos^2 \psi' + \sin^2 \psi'] d\Omega \\ &= \frac{4}{3} \frac{e^2 \omega_{\alpha\beta}^3}{\hbar c^3} |\vec{r}_{\alpha\beta}|^2 \quad (\text{a}), \text{ or,} \quad (3.2-14) \\ &= \frac{64\pi^4 e^2}{3 \hbar \lambda_{\alpha\beta}^3} |\vec{r}_{\alpha\beta}|^2 \quad (\text{b}) \end{aligned}$$

It is not necessary now to average over orientations of the dipole moment, as no directional dependence on $\vec{r}_{\alpha\beta}$ remains, due to the integration over solid angle. Eq.(3.2-14a) is in the form given by Bethe and Salpeter (1957), Eq. 59.11, and Eq. (3.2-14b) is in the form given by Bates and Damgaard (1949), with the added provision that $|\vec{r}_{\alpha\beta}|^2$ be summed and averaged over final and initial states.

Because of the isotropic nature** of the emission given by Eq. (3.2-14), the emission per unit solid angle is just $\Lambda_{\alpha\beta}/4\pi$. We now compute the transition probability for induced emission from the second term of Eq. (3.2-12).

* Note that we might as well have taken a single unit polarization vector lying in the plane of $\vec{r}_{\alpha\beta}$ and \vec{k} , since the components perpendicular to this plane do not contribute.

** On account of our dipole approximation, $|\vec{r}_{\alpha\beta}|$ does not depend on the propagation vector \vec{k}_Y .

Thus

$$\frac{dw_{\alpha\beta}}{d\Omega} (\text{ind}) = \frac{e^2_{\omega\alpha\beta}}{2\pi \hbar c^3} \times \frac{8\pi^3 c^2}{\hbar \omega^3} \left\{ |\vec{\epsilon}_1 \cdot \vec{r}_{\alpha\beta}|^2 I_{\omega}^{(1)}(\vec{n}) \right. \\ \left. + |\vec{\epsilon}_2 \cdot \vec{r}_{\alpha\beta}|^2 I_{\omega}^{(2)}(\vec{n}) \right\} \quad (3.2-15)$$

where the superscripts on the two $I_{\omega}(\vec{n})$ factors indicate the polarization.

We assume that the radiation is unpolarized so that $I_{\omega}^{(1)}(\vec{n}) = I_{\omega}^{(2)}(\vec{n}) = \frac{1}{2} I_{\omega}(\vec{n})$ and obtain

$$\frac{dw_{\alpha\beta}}{d\Omega} (\text{ind}) = \frac{2\pi^2 e^2}{\hbar^2 c} |\vec{r}_{\alpha\beta}|^2 I_{\omega}(\vec{n}) \sin^2 \theta \quad (3.2-16)$$

Now θ is the angle between the propagation vector \vec{k}_{γ} and the atom dipole moment vector $\vec{r}_{\alpha\beta}$. Thus, we can simplify Eq. (3.2-16) by now averaging over random orientations of the dipole moment. To do this we multiply Eq. (3.2-16) by $\frac{d\Omega'}{4\pi}$ where $d\Omega'$ is an element of solid angle about $\vec{r}_{\alpha\beta}$. Since $\frac{1}{4\pi} \int \sin^2 \theta d\Omega' = \frac{2}{3}$, we obtain

$$\frac{dw_{\alpha\beta}}{d\Omega} (\text{ind}) = \frac{4\pi^2 e^2}{3 \hbar^2 c} |\vec{r}_{\alpha\beta}|^2 I_{\omega}(\vec{n}) \quad (3.2-17)$$

The total induced or stimulated emission can now be calculated from

this result by integration over all angles of emission:

$$w_{\alpha\beta}(\text{ind}) = \frac{4\pi^2 e^2}{3\hbar^2 c} |\vec{r}_{\alpha\beta}|^2 \int I_{\omega}(\vec{\Omega}) d\vec{\Omega} \quad (3.2-18)$$

The induced or stimulated transition probability given by Eq. (3.2-18) is related to the Einstein B-coefficient. The B-coefficient is defined here so that

$$\frac{dw_{\alpha\beta}}{d\Omega}(\text{ind}) = B_{\alpha\beta} \left(\frac{1}{c} \rho_{\nu}(\vec{\Omega}) \right) \quad (3.2-19)$$

which is the radiation density (ρ_{ν}) rather than radiation flux (I_{ν}) definition as $\rho_{\nu} = I_{\nu}/c$. (Compare with Eqs. (2.2-4b) and (2.2-7a,b,c))

Comparing this with Eq. (3.2-17) and noting that

$$I_{\nu}(\vec{\Omega}) = I_{\omega}(\vec{\Omega}) \frac{d\omega}{d\nu} = 2\pi I_{\omega}(\vec{\Omega})$$

we obtain

$$\begin{aligned} \frac{2\pi}{c} B_{\alpha\beta} &= \frac{4\pi^2 e^2}{3\hbar^2 c} |\vec{r}_{\alpha\beta}|^2, \text{ or,} \\ B_{\alpha\beta} &= \frac{\pi e^2}{3\hbar^2} |\vec{r}_{\alpha\beta}|^2 = \frac{8\pi^3 e^2}{3\hbar^2} |\vec{r}_{\alpha\beta}|^2 \end{aligned} \quad (3.2-20)$$

The last form agrees with the result given by Slater (1960a, p. 142), whereas Eq. (3.2-18) is the form given by Schiff (1955, p. 253). Griem (1964, p. 28) employs a quantity $B_{\alpha\beta}$ defined such that the total transition probability $\bar{w}_{\alpha\beta}$ is expressed in terms of the average intensity $\bar{I}_{\omega} = \frac{1}{4\pi} \int I_{\omega}(\vec{\Omega}) d\vec{\Omega}$:

$$w_{\alpha\beta} = A_{\alpha\beta} + B_{\alpha\beta} \frac{2\pi}{c} \int I_w d\Omega = A_{\alpha\beta} + \frac{8\pi^2 B_{\alpha\beta}}{c} I_w$$

Thus, his formula for $A_{\alpha\beta}$ is the same as ours (recalling that for the time being we are assuming our states to be non-degenerate, so that the statistical weights are all unity) but his formula for $B_{\alpha\beta}$ differs from ours by the factor $\frac{8\pi^2}{c}$.

It is perhaps appropriate to observe at this point that the ratio $A_{\alpha\beta}/B_{\alpha\beta}$ as given by Eqs. (3.2-14) and (3.2-20) has the value

$$\frac{A_{\alpha\beta}}{B_{\alpha\beta}} = \frac{8\pi h\nu_{\alpha\beta}^3}{c^3} \quad (3.2-21)$$

which, as stated in Eq. (3.1-24) of Section 3.1, is required by general considerations of detailed balance (see, e.g., Slater, 1960, p. 21).

Although the more or less heuristic method of "averaging over atom orientations", (performing an average over the angle between $\vec{r}_{\alpha\beta}$ and \vec{k}_ν) is the simplest method of eliminating the direct dependence of the transition probability on the coordinate system chosen, it is not necessarily the most perspicuous, and is in fact somewhat redundant.** The final result will still have to be summed and averaged over the magnetic quantum numbers of the final and initial states, respectively. This redundancy can be removed, at the expense of somewhat more algebra, in the following fashion.

* Griem uses MKS units; hence, to convert to cgs units the factor $4\pi\epsilon_0$ should be removed from his formulas (specifically his Eqs. 2-48 and 2-54).

** In the absence of an external field, different orientations of the atom correspond to different superpositions over degenerate sublevels, which are to be summed over and/or averaged, anyway.

By use of the spherical harmonics addition theorem (Rose, 1957; Eq. 4.28), we can write $\vec{r} \cdot \vec{e} = r \sum_{m'} Y_{1m'}^+(\theta, \phi) Y_{1m'}(\theta, \phi) \times \left(\frac{4\pi}{3}\right)$, where \vec{e} is a unit vector, as

$$\vec{r} \cdot \vec{e} = r \sum_{m'} Y_{1m'}^+(\theta, \phi) Y_{1m'}(\theta, \phi) \times \left(\frac{4\pi}{3}\right)$$

where $\theta, \phi, \theta', \phi'$ specify the orientation of \vec{r} and \vec{e} , respectively with respect to some fixed axis. We can then write for the relevant matrix element

$$\int \psi_{\beta}^+ \vec{r} \cdot \vec{e} \psi_{\alpha} dv = \left(\frac{4\pi}{3}\right) \int R_{\beta} r R_{\alpha} Y_{\beta}^+(\theta, \phi) \times \sum_{m'} Y_{1m'}^+(\theta, \phi) Y_{1m'}(\theta, \phi) Y_{\alpha}(\theta, \phi) dv \quad (3.2-22)$$

Now the integral over the product of three spherical harmonics has the value (Rose, 1957, pp. 61-62)

$$\int d\Omega Y_{l_3 m_3}^+ Y_{l_2 m_2} Y_{l_1 m_1} = \left[\frac{(2l_1+1)(2l_2+1)}{4\pi(2l_3+1)} \right]^{1/2} C(l_1 l_2 l_3; m_1 m_2 m_3) \times C(l_1 l_2 l_3; 000) \quad (3.2-23)$$

where the $C(l_1 l_2 l_3; m_1 m_2 m_3)$ are Clebsch-Gordan coefficients (we follow Rose's notation). Using this result and the fact that $m_3 = m_1 + m_2$, we obtain for the matrix element (Eq. (3.2-22))

* For the definition of these quantities, see Section 3.2.3.

$$\begin{aligned}
\int \psi_{\beta}^{\dagger} \vec{r} \cdot \vec{e} \psi_{\alpha} dv &= \vec{r}_{\beta\alpha} \cdot \vec{e} = \left(\frac{4\pi}{3}\right)^{1/2} \int R_{\beta} r R_{\alpha} r^2 dr \left[\frac{(2\ell_{\alpha}+1)}{(2\ell_{\beta}+1)}\right]^{1/2} C(\ell_{\alpha} \ell_{\beta}, m_{\alpha}, m_{\beta}-m_{\alpha}, m_{\beta}) \\
&\quad \times C(\ell_{\alpha} \ell_{\beta}, 000) Y_{1m_{\beta}-m_{\alpha}}(\theta, \varphi) \\
&= \left(\frac{4\pi}{3}\right)^{1/2} R_{\alpha\beta} \left(\frac{2\ell_{\alpha}+1}{2\ell_{\beta}+1}\right)^{1/2} C(\ell_{\alpha} \ell_{\beta}, m_{\alpha}, m_{\beta}-m_{\alpha}, m_{\beta}) C(\ell_{\alpha} \ell_{\beta}, 000) \\
&\quad \times Y_{1, m_{\beta}-m_{\alpha}}(\theta, \varphi)
\end{aligned} \tag{3.2-24}$$

where we have defined $R_{\alpha\beta} = \int R_{\beta} R_{\alpha} r^3 dr$. We now wish to sum this expression over final states (β) and average it over initial states (α).

First we carry out sum over final states by summing over m_{β} and noting that $m_{\beta}-m_{\alpha}$ can take on only the values $0, \pm 1$. Denoting the matrix element $\int \psi_{\beta}^{\dagger} \vec{r} \cdot \vec{e} \psi_{\alpha} dv$ by $M_{\beta\alpha}$, we can now write

$$\begin{aligned}
\sum_{m_{\beta}} |M_{\beta\alpha}|^2 &= \left(\frac{4\pi}{3}\right)^2 R_{\alpha\beta}^2 \left(\frac{2\ell_{\alpha}+1}{2\ell_{\beta}+1}\right) C^2(\ell_{\alpha} \ell_{\beta}; 000) \left[C^2(\ell_{\alpha} \ell_{\beta}; m_{\alpha}, 0, m_{\alpha}) Y_{1,0}^2 \right. \\
&\quad \left. + C^2(\ell_{\alpha} \ell_{\beta}; m_{\alpha}, 1, m_{\alpha}+1) Y_{1,1}^2 + C^2(\ell_{\alpha} \ell_{\beta}; m_{\alpha}, -1, m_{\alpha}-1) Y_{1,-1}^2 \right].
\end{aligned} \tag{3.2-25}$$

In order to perform the average over m_{α} , we make use of Eq. 3.16c of Rose (1957):

$$C^2(\ell_1 \ell_2 \ell_3; m_1 m_2 m_3) = \left(\frac{2j_3+1}{2j_2+1}\right) C^2(\ell_1 \ell_3 \ell_2; m_1, -m_3, -m_2) \tag{3.2-26}$$

By interchanging the indices according to this relation, the sum and average needed becomes

$$\frac{1}{2l_\alpha + 1} \sum_{m_\alpha} \sum_{m_\beta} |M_{\beta\alpha}|^2 = \left(\frac{4\pi}{3}\right) R_{\alpha\beta}^2 \left(\frac{1}{2l_\beta + 1}\right) C^2(l_\alpha, l_\beta; 000) \times \quad (3.2-27)$$

$$\sum_{m_\alpha} \left[\frac{2l_\beta + 1}{3} C^2(l_\alpha, l_\beta, 1; m_\alpha, -m_\alpha, 0) Y_{1,0}^2 + \frac{2l_\beta + 1}{3} C^2(l_\alpha, l_\beta, 1; m_\alpha, -1 - m_\alpha, -1) \right. \\ \left. \times Y_{1,1}^2 + \frac{2l_\beta + 1}{3} C^2(l_\alpha, l_\beta, 1; m_\alpha, 1 - m_\alpha, 1) Y_{1,-1}^2 \right]$$

Each of the sums over the squares of the C-coefficients can now be carried out by means of the orthonormality relations satisfied by these coefficients (Rose, 1957, Eq. 3.7), with the result that each sum is unity. Eq. (3.2-27) thus becomes

$$\frac{1}{2l_\alpha + 1} \sum_{m_\alpha} \sum_{m_\beta} |M_{\beta\alpha}|^2 = \frac{4\pi}{9} R_{\alpha\beta}^2 C^2(l_\alpha, l_\beta; 000) \left(\sum_m Y_{1m}^2(\theta, \varphi) \right) \quad (3.2-28)$$

By use of the formula (Bethe and Salpeter, 1957, Eq. A.42)

$$\sum |Y_{lm}(\theta, \varphi)|^2 = \frac{2l+1}{4\pi} .$$

we can finally write this result for one polarization vector $\vec{\epsilon}_1$ as

$$\frac{1}{2l_\alpha + 1} \sum_{m_\alpha} \sum_{m_\beta} |M_{\beta\alpha}|^2 = \frac{1}{3} R^2_{\alpha\beta} C^2(l_\alpha, l_\beta; 000) \quad (3.2-29)$$

Since this result no longer depends on the polarization vector we need only multiply by 2 to account for the two independent polarization vectors.

For spontaneous emission, we found previously

$$w_{\alpha\beta}(\text{spont.}) = \frac{e^2 \omega^3}{2\pi \hbar c^3} \int \left\{ \left| \vec{r}_{\alpha\beta} \cdot \vec{\epsilon}_1 \right|^2 + \left| \vec{r}_{\alpha\beta} \cdot \vec{\epsilon}_2 \right|^2 \right\} d\Omega$$

If we make use of the sum and average we have just found, we can evaluate this as

$$\begin{aligned} w(\text{spont}) &= \frac{1}{2l_\alpha + 1} \sum_{m_\alpha} \sum_{m_\beta} w_{\alpha\beta}(\text{spont}) \\ &= \frac{e^2 \omega^3}{3\pi \hbar c^3} R^2(l_\alpha, l_\beta) C^2(l_\alpha, l_\beta; 000) \int d\Omega \\ &= \frac{4e^2 \omega^3}{3\hbar c^3} R^2(l_\alpha, l_\beta) C^2(l_\alpha, l_\beta; 000) \end{aligned} \quad (3.2-30)$$

with an analogous result for induced emission. We have changed notation on R from: $R_{\alpha\beta}$ to $R(l_\alpha, l_\beta)$ since this quantity does not depend on m_α or m_β . From the properties of the Clebsch-Gordan coefficients

we know that $C(l_\alpha l_\beta; 000)$ vanishes unless $l_\beta = l_\alpha \pm 1$. The values of the particular Clebsch-Gordan coefficients $C(l, 1, l+1; 000)$ may be found in a number of places. Condon and Shortly (1935, Table 2³), e.g., give

$$C^2(l, 1, l+1; 000) = \frac{(l+1)}{2l+1} \quad (3.2-31)$$

$$C^2(l, 1, l-1; 000) = \frac{l}{2l+1}$$

These are the coefficients (for the single, non-equivalent electron case) called C_{l+1} , and C_{l-1} by Bates (1946, see Table I for s^2S and p^2P electron), and called $C(l \rightarrow l+1)$ and $C(l \rightarrow l-1)$ by Burgess and Seaton (1960). With these values of the C-coefficients we now obtain for the spontaneous-emission transition probability

$$w_{l, l+1}(\text{spont}) = \frac{4e^2 \omega^3}{3\hbar c^3} \frac{l+1}{2l+1} R^2(l, l+1) \quad (3.2-32)$$

$$w_{l, l-1}(\text{spont}) = \frac{4e^2 \omega^3}{3\hbar c^3} \frac{l}{2l+1} R^2(l, l-1)$$

In order to demonstrate that this result is indeed the same as the result obtained by averaging over "atom orientations" and then averaging and summing over initial and final states, we must show that

$$\frac{1}{2l_\alpha + 1} \sum_{m_\alpha} \sum_{m_\beta} |\vec{r}_{\alpha\beta}|^2 = C^2(l_\alpha l_\beta; 000) R^2(l_\alpha l_\beta) \quad (3.2-33)$$

since if this is true, Eq. (3.2-30) and Eq. (2.2-14) will agree. To show this, first we note that (cf, e.g., Rose, 1957, Eq. III.22)

$$\begin{aligned}
 x &= \left(\frac{4\pi}{6}\right)^{1/2} r \left[Y_{1,-1} - Y_{1,1} \right] \\
 y &= -\left(\frac{4\pi}{6}\right)^{1/2} r \left[Y_{1,-1} + Y_{1,1} \right] \\
 z &= \left(\frac{4\pi}{3}\right)^{1/2} r Y_{1,0}
 \end{aligned}
 \tag{3.2-34}$$

With these relations and over previous definition of $R_{\beta\alpha} \equiv \int R_{\beta}^* R_{\alpha} r^3 dr$ we can write the matrix elements of x , y , and z as

$$\begin{aligned}
 x_{\beta\alpha} &\equiv \int \psi_{\beta}^* x \psi_{\alpha} dv \\
 &= \left(\frac{2\pi}{3}\right)^{1/2} R_{\beta\alpha} \int Y_{\beta}^* (Y_{1,-1} - Y_{1,1}) Y_{\alpha} d\Omega \\
 y_{\beta\alpha} &= -\left(\frac{2\pi}{3}\right)^{1/2} R_{\beta\alpha} \int Y_{\beta}^* (Y_{1,1} + Y_{1,-1}) Y_{\alpha} d\Omega \\
 z_{\beta\alpha} &= \left(\frac{4\pi}{3}\right)^{1/2} R_{\beta\alpha} \int Y_{\beta}^* Y_{10} Y_{\alpha} d\Omega
 \end{aligned}
 \tag{3.2-35}$$

By Eq.(3.2-23), the angular integration over the three spherical harmonics can be performed, yielding,

$$\begin{aligned}
x_{\beta\alpha} &= \left(\frac{2\pi}{3}\right)^{1/2} R_{\beta\alpha} \left[\frac{3(2l_\alpha+1)}{4\pi(2l_\beta+1)}\right]^{1/2} C(l_\alpha l_\beta; 000) \left[C(l_\alpha l_\beta; m_\alpha, -1, m_\beta) - C(l_\alpha l_\beta; m_\alpha, 1, m_\beta) \right] \\
y_{\beta\alpha} &= \left(\frac{2\pi}{3}\right)^{1/2} R_{\beta\alpha} \left[\frac{3(2l_\alpha+1)}{4\pi(2l_\beta+1)}\right]^{1/2} C(l_\alpha l_\beta; 000) \left[C(l_\alpha l_\beta; m_\alpha, -1, m_\beta) + C(l_\alpha l_\beta; m_\alpha, 1, m_\beta) \right] \\
z_{\beta\alpha} &= \left(\frac{4\pi}{3}\right)^{1/2} R_{\beta\alpha} \left[\frac{3(2l_\alpha+1)}{4\pi(2l_\beta+1)}\right]^{1/2} C(l_\alpha l_\beta; 000) C(l_\alpha l_\beta; m_\alpha, 0, m_\beta) \tag{3.2-36}
\end{aligned}$$

If now we square and add these components, the cross terms in $|x_{\beta\alpha}|^2$ and $|y_{\beta\alpha}|^2$ cancel yielding

$$\begin{aligned}
|\vec{r}_{\beta\alpha}|^2 &= |x_{\beta\alpha}|^2 + |y_{\beta\alpha}|^2 + |z_{\beta\alpha}|^2 \tag{3.2-37} \\
&= R_{\beta\alpha}^2 \left(\frac{2l_\alpha+1}{2l_\beta+1}\right) C^2(l_\alpha l_\beta; 000) \left[C^2(l_\alpha l_\beta; m_\alpha, -1, m_\beta) + C^2(l_\alpha l_\beta; m_\alpha, 1, m_\beta) \right. \\
&\quad \left. + C^2(l_\alpha l_\beta; m_\alpha, 0, m_\beta) \right]
\end{aligned}$$

But we have that (Rose, 1957, Eq. 3.16b)

$C^2(j_1 j_2 j_3; m_1 m_2 m_3) = C^2(j_2 j_1 j_3; m_2 m_1 m_3)$; hence, we obtain from Eq. (3.2-37)

$$\begin{aligned}
|\vec{r}_{\beta\alpha}|^2 &= \left(\frac{2l_\alpha+1}{2l_\beta+1}\right) R_{\beta\alpha}^2 C^2(l_\alpha l_\beta; 000) \left[C^2(l_\alpha l_\beta; -1, m_\alpha, m_\beta) + C^2(l_\alpha l_\beta; 1, m_\alpha, m_\beta) \right. \\
&\quad \left. + C^2(l_\alpha l_\beta; 0, m_\alpha, m_\beta) \right] \tag{3.2-38}
\end{aligned}$$

The term in brackets is now the orthonormal sum on the first m -index and hence, equals unity (Rose, 1957, Eq. 3.7). Thus, we finally arrive at

$$\frac{1}{2l_{\alpha}+1} \sum_{m_{\alpha}} \sum_{m_{\beta}} |\vec{r}_{\beta\alpha}|^2 = R_{\beta\alpha}^2 C^2(l_{\alpha} l_{\beta}; 000)$$

which was to be demonstrated (Eq. (3.2-33)). In what follows, we will continue the tradition of averaging over "atom orientations" because of its simplicity, with the understanding, however, that it can be replaced by the foregoing more detailed considerations if necessary.

3.2.2.2 Bound-State Absorption

To obtain the transition probability per unit time for absorption we want the initial state β to contain \bar{n}_ω photons per radiation oscillator (to correspond to the intensity $I_\omega(\bar{n})$ through the relation, Eq. (3.2-9), and the final state α to contain $\bar{n}_\omega - 1$ photons per oscillator. In addition, we need to specify that the density of states given by Eq. (3.2-5) now pertains to the initial state. The matrix element given by Eq. (3.2-6) becomes

$$|H'_{\beta\alpha}| = -\frac{e}{m} \sqrt{\frac{2\pi\hbar\bar{n}_\omega}{\omega}} |\vec{p} \cdot \vec{\epsilon} e^{-i\vec{k} \cdot \vec{r}}|_{\beta\alpha} \quad (3.2-39)$$

With $\frac{dn_R}{dE}$ as given by Eq. (3.2-5), the transition probability per unit time (Eq. (3.2-1)) for absorption of radiation from an element of solid angle $d\Omega$ becomes, using Eq. (3.2-10)

$$dw_{\beta\alpha} = \frac{e^2 \omega^3}{2\pi c^3 \hbar} |\vec{\epsilon} \cdot \vec{r}_{\alpha\beta}|^2 n_\omega^{(\epsilon)} d\Omega ,$$

for a given polarization $\vec{\epsilon}$. By use of Eq. (3.2-9) this can also be expressed as

$$dw_{\beta\alpha} = \frac{4\pi^2 e^2}{\hbar^2 c} |\vec{\epsilon} \cdot \vec{r}_{\alpha\beta}|^2 I_\omega^{(\epsilon)}(\bar{n}) d\Omega . \quad (3.2-40)$$

If now we average this over polarizations we obtain in the same manner

as before

$$dw_{\beta\alpha} = \frac{2\pi^2 e^2}{\hbar^2 c} |\vec{r}_{\alpha\beta}|^2 I_{\omega}(\vec{n}) \sin^2 \theta d\Omega \quad (3.2-41)$$

Again we average over atom dipole-moment orientations $\left(\int \frac{d\Omega}{4\pi}\right)$ and this produces a factor 2/3. The net result is

$$dw_{\beta\alpha} = \frac{4\pi^2 e^2}{3\hbar^2 c} |\vec{r}_{\alpha\beta}|^2 I_{\omega}(\vec{n}) d\Omega \quad , \quad (3.2-42)$$

or, the total transition probability per unit time for absorption becomes,

$$w_{\beta\alpha} = \frac{4\pi^2 e^2}{3\hbar^2 c} |\vec{r}_{\alpha\beta}|^2 \int I_{\omega}(\vec{n}) d\Omega \quad (3.2-43)$$

These results (Eqs. (3.2-42) and (3.2-43)) are seen to be identical with the differential and total transition probabilities for induced or stimulated emission, Eqs. (3.2-17) and (3.2-18), respectively. These results can be correlated with those of Schiff (Eq. 35.23, 1955) by noting that the intensity $I(\omega)$ as defined by Schiff is the total intensity integrated over all angles, viz, our $\int I_{\omega}(\vec{n}) d\Omega$.

As in the case of induced emission the total transition probability per unit time given by Eq. (3.2-43) is not solely a atomic parameter except in the case of isotropic radiation. Since we do not, in general, wish to be restricted to isotropic radiation it is convenient for us to define a purely atomic parameter which can be called an absorption coefficient per atom which is a cross section. In order to define such a parameter, we first must take into account the fact that a line is not infinitesimally sharp. In any actual physical system this is

true, as the absorption will cover a finite (even if small) range of frequencies (Heitler, 1954, pp. 181-186; Mayer, 1947, p. 8) about the resonance frequency $\omega_{\alpha\beta} = (E_{\beta} - E_{\alpha})/\hbar$. We can define the transition probability per unit frequency interval w_{ω} by the relation

$$w_{\omega} = \lim_{\Delta\omega \rightarrow 0} \frac{\Delta W}{\Delta\omega}$$

where ΔW is that contribution to the total transition probability which occurs in the angular frequency range $\Delta\omega$. Then we must have

$$W = \int w_{\omega} d\omega \quad (3.2-44)$$

where the integration is taken over the entire profile of the line in order that the total transition probability be equal to the sum of its parts. In view of Eq. (3.2-44) it is convenient to account for the line shape phenomenologically by assigning a line shape factor $b(\omega)$ to the line such that

$$w_{\omega} = W b(\omega) \quad (3.2-45)$$

Eq. (3.2-45) will be valid if we normalize $b(\omega)$ according to

$$\int_{-\infty}^{\infty} b(\omega) d\omega = 1. \quad (3.2-46)$$

Thus, w_{ω} as given by Eq. (3.2-45) is the number of transitions per unit time per unit frequency interval. For the idealized infinitely sharp

transition, we have

$$b(\omega) = \delta(\omega - \omega_{\alpha\beta}) \quad (3.2-47)$$

whereas, for real transitions, $b(\omega)$ will be a finite (but usually still sharp) function.

We now recall that $I_{\omega}(\vec{n}) d\Omega$ refers to the incident beam intensity in the direction \vec{n} . A cross section for absorption can be defined by reducing this angularly distributed beam intensity to a plane-parallel incident beam through

$$d\Omega I_{\omega}(\vec{n}) = I_0(\omega) \delta(\vec{n}) d\Omega \quad (3.2-48)$$

where I_0 (photons per cm^2/sec per unit frequency interval) is the parallel incident beam intensity. Since $\int \delta(\vec{n}) d\Omega = 1$, we can substitute Eq. (3.2-48) into Eq. (3.2-43) together with Eqs. (3.2-44) and (3.2-45). The result after carrying out the integration over \vec{n} is

$$w_{B\alpha} = \frac{4\pi^2 e^2}{3\hbar^2 c} |\vec{r}_{\alpha\beta}|^2 \int_{\omega} I_0(\omega) b(\omega) d\omega \quad (3.2-49)$$

for the total transition probability per unit time, and by dropping the ω -integration, we obtain

$$w_{B\alpha}(\omega) = \frac{4\pi^2 e^2}{3\hbar^2 c} |\vec{r}_{\alpha\beta}|^2 I_0(\omega) b(\omega) \quad (3.2-50)$$

for the transition probability per unit time per unit frequency interval.

A cross section can now be defined by

$$\sigma_{\beta\alpha}(\omega) = \frac{w_{\beta\alpha}(\omega) \hbar\omega}{I_0(\omega)} \quad (3.2-51)$$

which, according to Eq. (3.2-50), will have the value

$$\sigma_{\beta\alpha}(\omega) = \frac{4\pi^2 e^2 \omega}{3\hbar c} |\vec{r}_{\alpha\beta}|^2 b(\omega) \quad (3.2-52)$$

The frequency integral of this quantity

$$\int \sigma_{\beta\alpha}(\omega) d\omega = \frac{4\pi^2 e^2 \omega}{3\hbar c} |\vec{r}_{\alpha\beta}|^2 \quad (3.2-53)$$

is just the ratio $S/I_0(\omega)$ as given by Heitler (1954, p. 180, Eq. 19) where S is the energy absorbed per unit time as he defines it. Since (as noted after Eq. (3.2-43)) the transition probabilities per unit time for absorption and induced emission are identical, it can be seen that the cross sections for these two processes are also equal. This requires that the shape of an absorption line be the same as an emission line* which must be true from general equilibrium considerations (Heitler, 1954, p. 186).

Just as in the discussion by Bethe and Salpeter (1957, p. 296) of photoelectric absorption, the cross section we have defined here has the physical interpretation that $\int \sigma(\omega) \frac{I_0(\omega)}{\hbar\omega} d\omega = w$ is the probability per

* When emitted or absorbed at the atom -- not after transfer through a medium.

second that an atom upon which the flux $I_0(\omega)$ is incident will be excited.

Also,

$$\tau = N_V \sigma(\omega) \quad (3.2-54)$$

is the probability per centimeter that a photon of angular frequency ω will be absorbed in a medium consisting of N_V absorbing atoms per cm^3 .

Thus, we can interpret the product $\sigma N_V I_0 dx$ as :

$$\begin{aligned} (\sigma N_V dx) I_0(\omega) &= \text{(probability of photon absorption in } dx) \\ &\quad \times \frac{\text{Number of photons} \times h\omega}{\text{cm}^2\text{-sec-frequency interval}} \\ &= \text{energy absorbed in } dx \text{ per cm}^2 \text{ per sec} \\ &\quad \text{per unit frequency interval.} \\ &= dI_0(\omega) . \end{aligned} \quad (3.2-55)$$

Alternatively, we can interpret this product as:

$$\begin{aligned} \frac{\sigma(\omega) I_0(\omega)}{h\omega} (N_V dx) h\omega &= \frac{\text{Probability of excitation per atom}}{\text{second} \times \text{frequency interval}} \\ &\quad \times (\text{number of atoms/cm}^2) \times \text{energy of excitation} \\ &= \text{energy absorbed in } dx \text{ per cm}^2 \\ &\quad \text{per unit frequency interval} \\ &= dI_0(\omega) . \end{aligned} \quad (3.2-56)$$

As far as the transfer equation (Sec. 2.1) is concerned, it is not really necessary to define a cross section. This was done in Sec. 2.1 for convenience of interpretation, but all that is needed is the energy that is absorbed (and/or emitted) from the beam. The absorption can be obtained directly from the transition probability (per unit frequency interval) since

$$dI_{\omega}(\vec{r}) = - N_V \hbar \omega d\bar{w}_{\alpha\beta}(\omega) ds \quad (3.2-57)$$

for the beam intensity decrement $dI_{\omega}(\vec{r})$ in a distance ds . The phenomenological definition of the absorption coefficient is (Sec. 2.1)

$$\mu(\omega) = - \frac{dI_{\omega}(\vec{r})}{ds} \frac{1}{I_{\omega}(\vec{r})} \quad (3.2-58)$$

Inserting Eq. (3.2-42) into Eq. (3.2-57) with the definitions Eq. (3.2-44) and Eq. (3.2-45) now leads to*

$$\mu(\omega) = - \frac{dI_{\omega}(\vec{r})}{ds} \cdot \frac{1}{I_{\omega}(\vec{r})} = N_V \cdot \frac{4\pi^2 e^2 \omega}{3\hbar c} |\vec{r}_{\alpha\beta}|^2 b(\omega) \quad (3.2-59)$$

Thus, the quantity $\frac{4\pi^2 e^2 \omega}{3\hbar c} |\vec{r}_{\alpha\beta}|^2 b(\omega)$ can also be referred to as the absorption coefficient per atom $(\mu(\omega)/N_V)$.

* This result implicitly assumes that the absorption is due entirely to the single transition $\alpha - \beta$. This has been done for simplicity, to avoid cumbersome summation signs.

Dirac (1947, p. 245) gives

$$\frac{8\pi^3 \nu}{hc} |\vec{r}_{\alpha\beta} \cdot \vec{\epsilon}|^2 \quad (3.2-60)$$

as an absorption coefficient. Referring to p. 245 of his book, however, we see that this is the "probability per unit time of an absorption taking place with an incident beam of one particle per unit area per unit time per unit frequency range". Hence, it is obtainable from our Eq. (3.2-40). First we set $I_{\omega}(\vec{\Omega}) = \hbar \omega N_{\alpha}^{(\epsilon)}(\omega) \delta(\vec{\Omega})$ where $N_{\alpha}^{(\epsilon)}(\omega) d\omega$ is the number of photons of a given polarization ϵ in the angular frequency interval $d\omega$ crossing unit area per second, and then integrate over $\vec{\Omega}$. We obtain

$$w_{\alpha\beta}^{(\epsilon)} (\text{sec}^{-1}) = \frac{4\pi^2 e^2 \omega}{\hbar c} |\vec{\epsilon} \cdot \vec{r}_{\alpha\beta}|^2 N_{\alpha}^{(\epsilon)}(\omega) \quad (3.2-61)$$

Now we convert to frequency ν rather than angular frequency ω by $N_{\alpha}(\omega) d\omega = n_{\alpha}(\nu) d\nu$, or $N_{\alpha}(\omega) = \frac{n_{\alpha}(\nu)}{2\pi}$. Dirac's absorption coefficient, Eq. (3.2-60), is then equal to $w_{\alpha\beta}^{(\epsilon)}$ for $n_{\alpha}(\nu) = 1$.

Another quantity commonly defined is the oscillator strength or f-number (Bethe and Salpeter, 1957, p. 256; Condon and Shortley, 1935, p. 108) for a transition from a (single) state β to a (single) state α :

$$f_{\alpha\beta} = \frac{2m}{3\hbar} \omega_{\alpha\beta} |\vec{r}_{\alpha\beta}|^2 \quad (3.2-62)$$

In terms of this quantity our cross section $\sigma_{\alpha\beta}(\omega)$ (Eq. (3.2-52)) becomes

$$\sigma_{\alpha\beta}(\omega) = \frac{2\pi^2 e^2}{mc} f_{\alpha\beta} b(\omega) \quad (3.2-63)$$

or, in terms of $b(\omega) d\omega = b(2\pi\nu) \times 2\pi d\nu = b'(\nu) d\nu$ and $\sigma(\omega) d\omega = \sigma(\nu) d\nu$, this can be written,

$$\sigma(\nu) = \frac{\pi e^2}{mc} f b'(\nu) \quad (3.2-64)$$

where we drop the subscripts for simplicity.

The f-number definition is made, of course, because of the classical correspondences noted in Sec. 3.1. That is to say, if we integrate the definition (Eq. (3.2-64)) over frequency ν :

$$\int \sigma(\nu) d\nu = \frac{\pi e^2}{mc} f$$

we recover the classical expression, Eq. (3.1-7b) of Section 3.1.

3.2.2.3 Photoelectric Absorption and Radiative Recombination

In the case of photoelectric absorption and emission we must deal with a free electron in the presence of a residual ion. Hence, we must specify the type of wave function (and its normalization) that is to be used to describe the free electron. The simplest description, if applicable, is to use a plane-wave momentum eigenfunction normalized to the volume L^3 . This is the method illustrated by Schiff (1955) and by Heitler (1954), and is an appropriate approximation for high-energy absorption, and is mathematically and conceptually convenient as well.*

* For the limitations of this approximation and improvements thereon, see Bethe and Salpeter, 1957, Section 70; Mott and Massey, 1949, p. 356.

However, at low energies the effect of the potential in the final state is important, the dipole approximation is usually valid, and one is usually interested in a final state that is an angular momentum eigenfunction rather than a linear momentum eigenfunction. Since the questions involved in passing from a free-state eigenfunction of one type to one of another type as well as the free-state normalization methods are not trivial, we shall attempt to give a fairly complete discussion of these aspects in order to facilitate the use and understanding of the fundamental formulas.

Differential Cross Section for Linear Momentum Final Eigenstate

Although in the calculation of the photoelectric transition probability our basic equation is still Eq. (3.2-1), the calculation is somewhat more subtle on account of the free electron which appears in the final state. In order to obtain a transition probability per unit time in the case of bound-bound absorption, it was necessary to sum over the continuous range of initial (photon) states. Hence in that case, the density of states $\frac{dn}{dE}$ was taken to be the density of initial photon states per unit volume, and was expressed in terms of the incident intensity through Eq. (3.2-9). For photoelectric transitions, there is a continuous range of states in the final state of the system provided by the free electron, so that the derivation employed in the case of bound-bound transitions is no longer appropriate. The final state sum employed in arriving at Eq. (3.2-1) should now be over a differential element of the free electron phase space, and dn/dE taken as the density of final free electron momentum eigenstates in this phase space which is

$$\frac{dn_e}{dE} = \frac{d^3 \vec{p}_e L^3}{(2\pi\hbar)^3 dE} = \frac{mp d\vec{\Omega}_e L^3}{(2\pi\hbar)^3} \quad (3.2-65)$$

since $dE = (p/m) dp$. The normalization volume for the free electron has been denoted by L^3 , and the result is for electrons of a given spin, not both spins. We will discuss the sums and averages over degenerate states later. The matrix elements obtained from Eq. (3.2-6) just as for bound-bound absorption except that n_{ω} is not now required to be the average value \bar{n}_{ω} (we are not summing over radiation oscillators) but we could take it to be \bar{n}_{ω} if convenient, since the rest of the matrix element and $\frac{dn_e}{dE}$ is independent of the radiation oscillator (within the infinitesimal element dn_p).

As in the case of Eq. (3.2-39), for an absorption transition we want the occupation numbers to go from n_{ω} to $n_{\omega} - 1$ so that our matrix element for photoelectric absorption becomes

$$|H'|_{\beta\alpha} = \frac{1}{\sqrt{L^3}} \frac{e}{m} \sqrt{\frac{2\pi\hbar n_{\omega}}{\omega}} |\vec{p} \cdot \vec{\epsilon} e^{-i\vec{k} \cdot \vec{r}}|_{\beta\alpha} \quad (3.2-66)$$

and we must bear in mind that we have assumed, in specifying $\frac{dn_e}{dE}$ by Eq. (3.2-65), that the free electron is normalized within a volume L^3 . We will return to this point later. We have also explicitly inserted the photon normalization volume V . This was set equal to unity previously since dn_R/dE was expressed as the number density per unit volume, and the two factors if included explicitly would cancel against each other (see Heitler, 1954, p. 57).

Since $\frac{dn_R}{dE}$ was not used as before, it seems advisable to display it explicitly now. Heitler (1954) evaluates a transition probability and cross section in the following manner. He assumes an initial system of just the atom plus one photon*. Then n_{ω} in Eq. (3.2-66) is unity

* That this procedure is not possible in the case of discrete absorption follows from the requirement of a continuous range of initial photon states in order for a transition probability per unit time to exist for discrete absorption.

for some one radiation oscillator (in the initial state) and vanishes for all others. In the final state all $n_{\omega} = 0$. Thus, with no photons in the final state, the density of final states per unit energy interval (of the free electron) is just that given by Eq. (3.2-65). Inserting Eqs. (3.2-65) and (3.2-66) (with $n_{\omega} = 1$) into Eq. (3.2-1), we obtain (initial state β , final state α):

$$dw_{\beta\alpha} = \frac{1}{2\pi} \frac{e^2}{V\omega_{\beta\alpha}} \left| \vec{p} \cdot \vec{\epsilon} e^{-i\vec{k} \cdot \vec{r}} \right|_{\alpha\beta}^2 \times \frac{v d\vec{\Omega}_e L^3}{\hbar^3} \quad (3.2-67)$$

for the transition probability per unit time for the absorption of a photon of angular frequency ω with emission of an electron of velocity v into the element of solid angle $d\vec{\Omega}_e$. If again, we make use of the dipole approximation and Eq. (3.2-10), this result can be written as

$$dw_{\beta\alpha} = \frac{m^2 e^2 \omega_{\beta\alpha}}{2\pi \hbar^3 V} \left| \vec{r} \cdot \vec{e} \right|_{\alpha\beta}^2 v d\vec{\Omega}_e \Sigma^3 \quad (3.2-68)$$

We can obtain a cross section from this result by noting that the intensity corresponding to one photon in the volume V is

$$I_0 = \frac{\hbar\omega c}{V} \quad (3.2-69)$$

(not per unit frequency interval)

With this value of the intensity, the formula

$$d\sigma_{\beta\alpha} = dw_{\beta\alpha} \hbar\omega/I_0 \quad (3.2-70)$$

for the cross section (cf. Eq. (3.2-51)) becomes,

$$d\sigma_{\beta\alpha} = \frac{dw_{\beta\alpha} V}{c} \quad (3.2-71)$$

so that, from Eq. (3.2-68)

$$d\sigma_{\beta\alpha} = \frac{m^2 e^2 \omega_{\beta\alpha}^2}{2\pi \hbar^3 c} |\vec{r} \cdot \vec{e}|_{\alpha\beta}^2 vL^3 d\vec{\Omega}_e \quad (3.2-72)$$

For unpolarized light, with reference to Fig. 3-2, we can now average over the two independent polarization directions:

$$\begin{aligned} d\sigma_{\beta\alpha} &= \frac{m^2 e^2 \omega_{\beta\alpha}^2}{2\pi \hbar^3 c} vL^3 d\vec{\Omega}_e \left\{ \frac{1}{2} \left(|\vec{r} \cdot \vec{e}_1|_{\alpha\beta}^2 + |\vec{r} \cdot \vec{e}_2|_{\alpha\beta}^2 \right) \right\} \quad (3.2-73) \\ &= \frac{m^2 e^2 \omega_{\beta\alpha}^2}{4\pi \hbar^3 c} vL^3 d\vec{\Omega}_e \left\{ |\vec{r}_{\alpha\beta}|^2 \sin^2 \theta \right\} \end{aligned}$$

where θ , as noted in Fig. 3-2 is the angle between the photon propagation direction \vec{k} and the vector $\vec{r}_{\alpha\beta}$.

Before proceeding to obtain the total cross section, it is interesting to re-derive the above result without making the assumption $n_\omega = 1$.

If we wish to use the matrix element Eq. (3.2-66) as it stands with $n_\omega \neq 1$, then there will be $n_\omega - 1$ photons present in the final state.

For each free electron state there will now be (cf. Eq. (3.2-5))

$$dn_R = V\omega^2 d\vec{\Omega}_R d\omega / (2\pi c)^3$$

photon states (containing photons with the same physical properties).

Therefore, we must average the (square of the) matrix element Eq. (3.2-66)

over the initial photon states which requires setting $n_{\omega} = n_{\omega'}$, and using the factor $dn_R \times \frac{dn_e}{dE}$ for the final state density. The transition probability now becomes

$$\delta w_{\beta\alpha} = \frac{e^2 \bar{n}_{\omega}}{2\pi V \omega_{\beta\alpha}} \left| \vec{p} \cdot \vec{\epsilon} e^{-i\vec{k} \cdot \vec{r}} \right|_{\alpha\beta}^2 \frac{v d\vec{\Omega}_e L^3}{\hbar^3} \times \frac{V \omega^2 d\vec{\Omega}_r dw}{(2\pi c)^3} \quad (3.2-74)$$

But, by Eq. (3.2-8),

$$\frac{\bar{n}_{\omega} \times \omega^2 d\vec{\Omega}_R dw}{(2\pi c)^3} = \frac{I_{\omega}(\vec{\Omega}) dw d\vec{\Omega}_P}{\hbar \omega c}$$

whereby we obtain from Eq. (3.2-74)

$$\delta w_{\beta\alpha} = \frac{e^2}{2\pi \omega_{\beta\alpha}} \left| \vec{p} \cdot \vec{\epsilon} e^{-i\vec{k} \cdot \vec{r}} \right|_{\alpha\beta}^2 \frac{v d\vec{\Omega}_e L^3}{\hbar^3} \times \frac{I_{\omega}(\vec{\Omega}) dw d\vec{\Omega}_P}{\hbar \omega c}$$

From this result, which can be written

$$\delta w_{\beta\alpha} = \left\{ \frac{e^2 m^2 \omega_{\beta\alpha}}{2\pi \hbar^3} \left| \vec{r} \cdot \vec{\epsilon} \right|_{\alpha\beta}^2 v L^3 d\vec{\Omega} \right\} \frac{I_{\omega}(\vec{\Omega}) dw d\vec{\Omega}_P}{\hbar \omega c} \quad (3.2-75)$$

It is easy to see the greater flexibility of the initial state description in the case of photoelectric absorption as opposed to the case of discrete absorption. For a plane-parallel, monochromatic beam

$$I_{\omega}(\vec{\Omega}) = I_0 \delta(\vec{\Omega}) \delta(\omega - \omega_{\beta\alpha})$$

Eq. (3.2-74) reduces to

$$\begin{aligned}
 dw_{\beta\alpha} &= \iint \delta w_{\beta\alpha} d\omega d\Omega \\
 &= \frac{e^2 m^2 \omega_{\beta\alpha}}{2\pi \hbar^3} |\vec{r} \cdot \vec{\epsilon}|_{\alpha\beta}^2 vL^3 d\Omega \frac{I_0}{\hbar\omega_{\beta\alpha} c}
 \end{aligned}
 \tag{3.2-76}$$

A differential cross section is usually defined on the basis of these definitions and is (cf. Eq. (3.2-70))

$$\frac{d\sigma_{\beta\alpha}}{d\Omega_e} = \frac{dw/d\Omega_e \times \hbar\omega_{\beta\alpha}}{I_0}
 \tag{3.2-77}$$

which yields, using Eq. (3.2-76)

$$\frac{d\sigma_{\beta\alpha}}{d\Omega_e} = \frac{e^2 m^2 \omega_{\beta\alpha}}{2\pi \hbar^3 c} |\vec{r} \cdot \vec{\epsilon}|_{\alpha\beta}^2 vL^3 .$$

This is, of course, identical to Eq. (3.2-72). However, it can also be defined directly from Eq. (3.2-75) by means of

$$\frac{d\sigma}{d\Omega_e} = \frac{\delta w \times \hbar\omega}{I_w(\vec{\Omega}) d\omega d\vec{\Omega}_p d\Omega_e}
 \tag{3.2-78}$$

This leads to the same result, of course, but is explicitly independent of the nature of the incident beam. We can also derive (heuristically) the photoionization cross section semiclassically* -- that is, without the

* This can also be done, of course, for bound-bound transitions (Schiff, 1955). We choose to do it in the photoelectric case, instead.

use of the field-theoretic-matrix element Eq. (3.2-6). We follow the treatment of Sec. 35 of Schiff (1955). In this case, we have the perturbation as given by Eq. (3.2-4), but the radiation is not quantized. Thus, the final state density does not include photon states and is just as given by Eq. (3.2-65):

$$\frac{dn_e}{dE} = \frac{mp \, d\vec{\Omega}_e \, L^3}{(2\pi\hbar)^3}$$

The transition probability is still

$$w = \frac{2\pi}{\hbar} |H'|^2 \frac{dn}{dE}$$

Since this formula comes from ordinary quantum mechanics if the radiation field is not quantized. Thus for a transition with emission of an electron into $d\vec{\Omega}_e$ we obtain

$$dw = \frac{2\pi}{\hbar} \frac{e^2}{m^2 c^2} |\vec{p} \cdot \vec{A}|^2 \frac{mp L^3 d\vec{\Omega}_e}{(2\pi\hbar)^3} \quad (3.2-79)$$

Now classically we can take*

$$\vec{A} = \vec{e} A_0 e^{-i(\vec{k} \cdot \vec{r} - \omega t)} \quad (3.2-80)$$

* The conditions under which this is valid and the matrix element Eq. (3.2-4) is the only required perturbing term are discussed by Schiff (1955) in Sec. 35.

for the vector potential. The Poynting vector $\frac{c}{4\pi} (\vec{E} \times \vec{H})$ averaged over a period $2\pi/\omega$ of the oscillation has the magnitude $\frac{\omega^2}{2\pi c} |A_0|^2$.

This is the intensity I_0 of the classical wave given by Eq. (3.2-80).

(I_0 not per unit frequency interval.)

The cross section is again given by

$$d\sigma = \frac{dW_{\alpha\beta}}{I_0}$$

With the above expression for the intensity and Eq. (3.2-80) we obtain from Eq. (3.2-79) (using $p_{\alpha\beta} = im\omega_{\alpha\beta} \vec{r}_{\alpha\beta}$)

$$d\sigma = \frac{1}{2\pi} \frac{e^2 m^2 \omega}{\hbar^3 c} |\vec{r} \cdot \vec{\epsilon}|^2 vL^3 d\vec{\Omega}_e$$

in agreement with our previous result (Eq. (3.2-72)).

Unfortunately this simple form of the differential cross section (or the more explicit form averaged over polarizations, Eq. (3.2-73)) is not a particularly useful formula, except at high energies where a plane wave final state is a good approximation. Except in this latter approximation the angle θ which appears in Eq. (3.2-73) is not the angle of physical interest. In radiation absorption studies of the type we are concerned with here, this is not a disadvantage, as one is not usually concerned with the differential cross section per se*, but rather with the total cross section obtainable from it by a suitable integration over angles.

* An extensive discussion of the differential cross section and the angular distribution of the photoejected electrons is given by Bethe and Salpeter (1957). See especially Secs. 69, 70, and 72.

Recombination and Photoelectric Total Cross Sections by Integration of Differential Cross Sections

It is evident from the form of Eq. (3.2-73) that it would be conceptually simpler to integrate this equation over photon propagation directions (for a fixed $|\vec{r}_{\alpha\beta}|$) than over photoelectron directions. We would thereby avoid having to determine directly the dependence of $|\vec{r}_{\alpha\beta}|$ on the direction of the photoelectron in the final state. We can perform the integration of Eq. (3.2-73) over photon propagation directions in lieu of photoelectron directions by relating the basic photoelectric cross section of Eq. (3.2-72) to the cross section for the inverse process of radiative recombination. In this latter process, a free electron is incident, in the initial state, on an atom or ion. It is captured with the emission of a photon in the transition to the final state, which therefore contains a photon and an atom or ion of charge one unit less than that of the initial bound system.

If we equate the squared matrix elements for the photoelectric process and for the radiative recombination process by means of Eq. (3.2-1)

we obtain, in an obvious notation,

$$\frac{dw_{\alpha\beta}(\text{P.E.})}{\frac{m^2 c^3 d\Omega_e}{(2\pi\hbar)^3}} = \frac{dw_{\beta\alpha}(\text{R})}{\frac{m^2 c^3 d\Omega_\nu}{(2\pi c)^3}} \quad (3.2-81)$$

where the denominators are the final state densities for photons (right hand side) and for electrons (left hand side), discussed previously. (cf. Eqs. (3.2-5) and (3.2-6)). For the photoelectric process, Eq. (3.2-71) relates the transition probability dw (P.E.) to the differential cross section. For recombination, we have from the definition of cross section

$$d\sigma = \frac{dw}{|\vec{S}|} \quad (3.2-82)$$

Where \vec{S} (particles per cm^2 per sec) is the electron flux. In the photoelectric case we have previously specified that the free electron is normalized to a volume L^3 ; since \vec{S} is given by

$$\vec{S} = \frac{\hbar}{2im} (\psi^* \nabla \psi - \psi \nabla \psi^*) \quad (3.2-83)$$

we can use a plane wave $\psi_e(\vec{r}) = e^{i\vec{k}_e \cdot \vec{r}} / L^{3/2}$ so normalized to keep track of the proper normalization factors. Eq. (3.2-83) yields, for the plane wave,

$$\vec{S} = \frac{\vec{v}_e}{L^3} \quad (3.2-84)$$

so that we can write Eq. (3.2-82) as

$$d\sigma_R = \frac{L^3 dw_R}{v_e} \quad (3.2-85)$$

From this result and from Eqs. (3.2-71) and (3.2-81) we obtain the relation

$$\frac{d\sigma_{\alpha\beta}(\text{P.E.})}{d\Omega_e} = \frac{m^2 v_c^2}{\hbar^2 \omega_{\alpha\beta}^2} \frac{d\sigma_{\beta\alpha}(R)}{d\Omega_Y} \quad (3.2-86)$$

If now we refer both differential cross sections to the angle* between \vec{p} and \vec{k}_Y , Eq. (3.2-86) can be multiplied by an element of solid angle $d\Omega$ taken about \vec{p} and referred to an axis along \vec{k}_Y on the left hand side of Eq. (3.2-86), and taken about \vec{k}_Y and referred to an axis along \vec{p} on the right hand side of Eq. (3.2-86). Both sides can then be integrated over the full solid angle to yield

$$\tau_{\alpha\beta}(\text{P.E.}) = \frac{m^2 v_c^2}{\hbar^2 \omega_{\alpha\beta}^2} \tau_{\beta\alpha}(R) \quad (3.2-87)$$

* Since both cross sections can be defined physically only in terms of this angle.

Since the cross sections in this expression in general represent transitions between degenerate sublevels, they are not the physically observed quantities. The latter, which we will call $\sigma(\text{P.E.})$ and $\sigma(\text{R})$ can be obtained by averaging and summing the above relation over initial and final states. That is to say, by definition we have

$$\sigma(\text{P.E.}) = \frac{1}{g_{i'}} \sum_{\alpha(i')} \sum_{\beta(j')} \sigma_{\alpha\beta}(\text{P.E.}) ,$$

and

(3.2-88)

$$\sigma(\text{R}) = \frac{1}{g_{i'}} \sum_{\alpha(i')} \sum_{\beta(j')} \sigma_{\alpha\beta}(\text{R})$$

where we have used i' to denote the collection of degenerate states of the bound system (ion plus active bound electron) and the photon. The collection of degenerate states of the residual ion (minus a bound electron) and the free electron has been denoted by j' . The appropriate statistical weights are, of course, $g(i')$ and $g(j')$, respectively. If we now sum Eq. (3.2-87) according to Eqs. (3.2-88), we obtain

$$\sigma(\text{P.E.}) = \frac{g_{j'}}{g_{i'}} \frac{m^2 v^2 c^2}{\lambda^2 \omega^2} \sigma(\text{R}) \quad (3.2-89)$$

(We have primed the state index in order to be able to conveniently differentiate between the composite systems of atom/ion plus photon/electron, and the bound systems--atom or ion alone. Thus, g_j and g_i will be used to represent the statistical weights of the ion and atom alone.)

This is usually called the "Milne Relation" after E.A. Milne (1924) who first derived it (from more general considerations than we have used here). To return to our original argument, Eq. (3.2-86) can be written, by use of Eq. (3.2-72), as

$$\frac{m^2 v_e^2 c^2}{\hbar^2 \omega^2} \frac{d\sigma_{\alpha\beta}(R)}{d\Omega_Y} = \frac{d\sigma_{\alpha\beta}(P.E.)}{d\Omega_e} = \frac{m^2 e^2 \omega_{\alpha\beta}}{2\pi \hbar^2 c} v_e L^3 |\vec{r}_{\alpha\beta} \cdot \vec{\epsilon}|^2 \quad (3.2-90)$$

To obtain the physically observed photoelectric cross section in terms of the matrix element we must now average Eq. (3.2-90) over initial states and sum it over final states. We can explicitly perform the sum over the two independent polarization directions as in Eq. (3.2-73) (but without the factor 1/2 since we now want a sum, not an average). We obtain the result

$$\frac{m^2 v_e^2 c^2}{\hbar^2 \omega^2} \frac{d\sigma(R)}{d\Omega_Y} = \frac{m^2 e^2 \omega v_e L^3}{2\pi \hbar^3 c g_j} \sum_{\alpha(i)} \sum_{\beta(j')} |\vec{r}_{\alpha\beta}|^2 \sin^2 \theta \quad (3.2-91)$$

(The prime on the i has been dropped, since we have now explicitly included the sum over polarization directions.)

For a fixed direction $\vec{r}_{\alpha\beta}$, this result can be immediately integrated over all photon propagation directions \vec{k}_Y (viz., θ) by use of

$\int \sin^2 \theta d\Omega = 8\pi/3$. Calling $\int \frac{d\sigma(R)}{d\Omega_Y} d\Omega_Y = \tau_R$, and setting $g_{j'} = 2g_j$ to account explicitly for the sum over initial electron spins (j now refers to

the degenerate states of the ion only), we obtain

$$\sigma_R = \frac{2e^2 \omega^3 L^3}{3\hbar c^3 v_e g_j} \sum_{\alpha(i)} \sum_{\beta(i)} |\vec{r}_{\alpha\beta}|^2 \quad (3.2-92)$$

for the recombination cross section.

For the photoelectric cross section, this yields by use of Eq. (3.2-89) , the result

$$\sigma(\text{P.E.}) = \frac{2m^2 e^2 \omega v L^3}{3\hbar^3 c g_i} \sum_{\alpha(i)} \sum_{\beta(i)} |\vec{r}_{\alpha\beta}|^2 \quad (3.2-93)$$

Analogous to the electron-spin-weight case, we must set $g_i = 2g_1$, since we are explicitly accounting for the two polarization directions as is customarily done; g_1 is then, as stated previously, the weight of the atomic bound state. It is now evident that $|\vec{r}_{\alpha\beta}|^2$ cannot actually depend on the direction of the photoejected electron.

In the recombination process, the direction of the incoming electron is, for the differential cross section, a preferred direction as is the direction of the outgoing photon. However, once one integrates over all outgoing photon directions to obtain the total cross section, and sums over the (degenerate) m-sublevels of the electron in the final bound state, the "preferred" nature of the incoming electron direction disappears. This is so, since there are no longer any other preferred directions to relate it to, and a change in the

incoming electron direction would merely correspond to rotating the laboratory apparatus. This is the reason one can take as the wave function for the total cross section for recombination, a free-electron function of the form

$$\psi(\vec{r}) = \sum_{\ell=1}^{\infty} (2\ell + 1) i^{\ell} e^{-i\sigma_{\ell}} R_{E\ell}(r) P_{\ell}(\cos \theta) ,$$

even though this form implies that the z-direction coincides with the beam direction. Then our result above, based on detailed balance, implies that this same form is valid for the photoelectric process.

Another way to view this is as follows. Let us pick some "absolute" coordinate system unconnected with the atom and unconnected with the photoelectron direction, \vec{p}_e . Then our photoelectric or recombination process determines 4 vectors: \vec{k}_γ , \vec{p}_e , $\vec{r}_{\alpha\beta}$, and \vec{a} , where we denote by \vec{a} the atom orientation, and where \vec{a} and \vec{p}_e completely determine $\vec{r}_{\alpha\beta}$. We can draw a diagram as shown in Fig. 3-3. Now $|\vec{r}_{\alpha\beta}|^2$ cannot depend on the absolute orientation of any of these vectors (i.e. their orientation relative to the arbitrary system we have chosen), because this can be changed at will by merely rotating the axis. Furthermore, $\vec{r}_{\alpha\beta}$ does not depend on \vec{k}_γ at all (recall that the use of $\vec{r}_{\alpha\beta}$ means that we are taking the dipole approximation) so that the angle between \vec{p}_e and $\vec{r}_{\alpha\beta}$ does not depend on \vec{k}_γ , either, nor on the coordinate system chosen. It is fixed once and for all by the magnitude of \vec{p}_e and the nature of the interaction between the electron and the ion. Because of this fixed relationship between \vec{p}_e and

$\vec{r}_{\alpha\beta}$ one can obtain the correct total cross section from Eq. (3.2-73) by replacing $d\Omega_e$ by $d\Omega_{\vec{r}}$, the element of solid angle about $\vec{r}_{\alpha\beta}$ and integrating over θ (which is the angle between \vec{k}_γ and $\vec{r}_{\alpha\beta}$). Once the integration is carried out over all angles θ the result is equivalent to having integrated over Ω (the angle between \vec{k}_γ and \vec{p}_e) in spite of the fact that the differential cross section expressed in terms of θ is not the physically appropriate one.

In order to obtain the differential cross section accurately, considerable pains must be taken in the specification of the final state wave function. This is not a trivial problem and we do not wish to discuss it here, since our only interest is in the total cross section. For a discussion of this problem, and references to the literature, see Schiff (1955) Sec. 37 and Bethe and Salpeter (1957) Secs. 69, and 70. Bethe and Salpeter also give a discussion of the angular distribution of photoejected electrons in Section 72.

The quantity $\vec{r}_{\alpha\beta}$ in the present case, wherein one of the states α, β is asymptotically a plane wave, viz., asymptotically the momentum has a definite direction, is an essentially different quantity than in the case of two bound states. In the case of two bound states, we could consider $\vec{r}_{\alpha\beta}$ connected in a one-to-one correspondence with the orientation of the atom (viz., a system of coordinates fixed in the atom in some prescribed fashion). In the present case, however, the free wave function makes $\vec{r}_{\alpha\beta}$ depend on a quantity--the free electron momentum direction--which is disconnected from the atom, and which asymptotically has a definite directional dependence.

(If we were considering an angular momentum eigenstate for the free electron, the situation would remain analogous to the bound case. But we would then pass directly to a total cross section rather than through the intermediary of a differential cross section as in the present case. We will take this situation up presently.)

Thus, we cannot now strictly average over orientations of the atom, or employ the integral over the three spherical harmonics inside the matrix element integration in just the same way as we did in Eqs. (3.2-22) to (3.2-30). However, the angle between $\vec{r}_{\alpha R}$ and \vec{k}_γ as we have seen is in a one-to-one correspondence with the angle between the free electron momentum \vec{p}_e and the photon vector \vec{k}_γ . Therefore, we can also average $\frac{d\sigma_{\alpha\beta}}{d\Omega_e}$ as given in Eq. (3.2-73) over the angle α between $\vec{r}_{\alpha R}$ and \vec{k}_γ , in analogy to the "average over atom orientations" carried out in the discrete transition case. The resulting average differential cross section is then independent of α as well as θ and equals $\frac{d\sigma_{\alpha\beta}}{d\Omega_e}$ averaged over outgoing momentum directions. Although this isotropic average is no longer of any value as a differential cross section, the total cross section follows from it by simply multiplying by 4π .^{*} The result, of course, is the same as the results obtained by the other methods described above. We append one further observation to this discussion.

In a plane wave approximation for the final state (which is not very accurate at low energies) the angle between $\vec{r}_{\alpha R}$ and \vec{k}_γ is equal to the angle between \vec{p}_e and \vec{k}_γ . We can see this as follows. If either

* This was the procedure followed by Armstrong, Holland and Meyerott (1958).

state α or β in Eq. (3.2-10) is a plane wave (momentum eigenfunction) the momentum operator eigenvalue can be taken from under the integral sign.

If α , say, is the state to be approximated by a plane wave, we can write Eq. (3.2-10) as

$$\vec{p}_\alpha = \left\{ (im\omega_{\alpha\beta}) / \int \psi_\beta^* \psi_\alpha dv \right\} \vec{r}_{\alpha\beta}$$

Since the quantities in the brackets are scalars, this result shows that the momentum vector \vec{p}_α in the final state lies in the same direction as $\vec{r}_{\alpha\beta}$.

Hence the angle θ in Eq. (3.2-73) is approximately equal to the angle between the momentum vector of the ejected photoelectron and the photon propagation vector \vec{k} . Also, in this approximation, it is clear that

$$|\vec{r}_{\alpha\beta}|^2 \propto p_\alpha^2 \text{ does not depend on the direction of } \vec{p}_\alpha.$$

The result we have obtained so far (Eq. 3.2-93) for the total photoelectric cross section is valid for a linear-momentum-eigenfunction final state (viz., a final state which is asymptotically a linear momentum eigenfunction). Since this is not the most generally useful form, we will illustrate the passage from the linear momentum form to a form with angular momentum eigenfunctions in the final state.

The general solution for a positive-energy electron in any central potential that has the proper asymptotic behavior appropriate to the definition of the differential cross section can be written (Mott and Massey, 1949, p. 46)

as

$$u(r, \theta, \varphi) = \frac{1}{L^{3/2}} \sum_{\ell=0}^{\infty} \sqrt{4\pi} (2\ell+1)^{1/2} i^{\ell} e^{-i\delta_{\ell}} R_{E\ell}(r) Y_{\ell 0}(\theta, \varphi) \quad (3.2-94)$$

This is an expansion in angular momentum eigenfunctions of a wave which asymptotically has a definite direction. In the case of a Coulomb potential $\frac{ze}{r}$, the phase shift $\delta_{\ell}(\text{Coul.})$ is given by

$$\delta_{\ell}(\text{Coul.}) = \arg \Gamma(\ell + 1 + i z/k)$$

$R_{E\ell}(r)$ is the radial wave function computed in the appropriate potential and has the asymptotic behavior

$$R_{E\ell}(r) \sim \frac{\sin(kr - \pi\ell/2 - \delta_{\ell})}{kr} \quad (3.2-95)$$

For phase shifts $\delta_{\ell} = 0$ this becomes a plane wave in the z-direction normalized to a volume L^3 , and $R_{E\ell}(r)$ becomes $j_{\ell+1/2}(kr)$. The distorting effects of a non-vanishing potential enter asymptotically through the phase shifts δ_{ℓ} . For the above wave function $u(r, \theta, \varphi)$, Eq. (3.2-93) for the photoelectric cross section becomes

$$\sigma(\text{P.E.}) = \frac{2m^2 e^2 \omega^2}{3\hbar^3 c g_i} \sum_{m_0} \left| \sum_{\ell} \int R_{\alpha}(r) Y_{\ell m_0}(\theta, \varphi) \sqrt{4\pi} (2\ell+1)^{1/2} i^{\ell} e^{-i\delta_{\ell}} R_{E\ell}(r) Y_{\ell 0}(\theta, \varphi) r^2 dr d\Omega \right|^2 \quad (3.2-96)$$

We have dropped the final state summation over β indicated previously as the final state represented by $u(r, \beta)$ has no further degenerate sub-levels.

We can carry out the angular integrations required in Eq. (3.2-96) by means of our previous Eqs. (3.2-36). If we set $\ell_\alpha = \ell$, then non-vanishing terms occur only for $\ell_\beta = \ell \pm 1$. Eq. (3.2-96) becomes

$$\begin{aligned} \sigma(\text{P.E.}) = \frac{2m^2 e^2 \omega^2}{3h^3 c g_1} \sum_{m_\alpha} 2\pi(2\ell+1) & \left\{ R_{\ell-1, \ell} C(\ell, 1, \ell-1; 0, 0) [C(\ell, 1, \ell-1; m_\alpha, -1, 0) \right. \\ & - C(\ell, 1, \ell-1; m_\alpha, 1, 0)] + R_{\ell+1, \ell} C(\ell, 1, \ell+1; 0, 0) [C(\ell, 1, \ell+1; m_\alpha, -1, 0) \\ & - C(\ell, 1, \ell+1; m_\alpha, 1, 0)] \left. \right\}^2 \\ & + \left\{ R_{\ell-1, \ell} C(\ell, 1, \ell-1; 0, 0) [C(\ell, 1, \ell-1; m_\alpha, -1, 0) + C(\ell, 1, \ell-1; m_\alpha, 1, 0)] \right. \\ & + R_{\ell+1, \ell} C(\ell, 1, \ell+1; 0, 0) [C(\ell, 1, \ell+1; m_\alpha, -1, 0) + C(\ell, 1, \ell+1; m_\alpha, 1, 0)] \left. \right\}^2 \\ & + 2 \left\{ R_{\ell-1, \ell} C(\ell, 1, \ell-1; 0, 0) C(\ell, 1, \ell-1; m_\alpha, 0, 0) \right. \\ & \left. + R_{\ell+1, \ell} C(\ell, 1, \ell+1; 0, 0) C(\ell, 1, \ell+1; m_\alpha, 0, 0) \right\}^2 \end{aligned} \quad (3.2-97)$$

where $R_{\ell \pm 1, \ell} = \int_0^\infty R_\ell(r) R_{E, \ell \pm 1}(r) r^3 dr$.

We now note that in the sum over m_α only one component contributes for a given projection quantum number of the free electron in the final state. Since we have taken the free electron m -value to be zero, the particular value of m_α selected out is determined by $m_\alpha = 0 - m_2$ where m_2 is 0 or ± 1 . For reasons to be discussed later, we do not ascribe this numerical value to m_α , but we designate the one m_α value which yields a non-vanishing term in the sum over m_α as m_α , m_α' , or m_α'' , depending on m_2 , and drop the \sum_{m_α} . If one now expands the brackets in this expression, some of the terms cancel. One then obtains by collecting the remaining terms the result

$$\begin{aligned}
 \sigma(\text{P.E.}) = \frac{2m^2 e^2 \omega \nu}{3\hbar^3 c g_1} (2\ell+1) 4\pi \left\{ R_{\ell-1,\ell}^2 C^2(\ell, 1, \ell-1; 000) \left[C^2(\ell, 1, \ell-1; m_\alpha, -1, 0) \right. \right. \\
 \left. \left. + C^2(\ell, 1, \ell-1; m_\alpha', 1, 0) + C^2(\ell, 1, \ell-1; m_\alpha'', 0, 0) \right] \right. \\
 \left. + R_{\ell+1,\ell}^2 C^2(\ell, 1, \ell+1; 000) \left[C^2(\ell, 1, \ell+1; m_\alpha, -1, 0) + C^2(\ell, 1, \ell+1; m_\alpha', 1, 0) \right. \right. \\
 \left. \left. + C^2(\ell, 1, \ell+1; m_\alpha'', 0, 0) \right] \right. \\
 \left. + 2R_{\ell-1,\ell} R_{\ell+1,\ell} C(\ell, 1, \ell-1; 000) C(\ell, 1, \ell+1; 000) \right. \\
 \left. \left[C(\ell, 1, \ell-1; m_\alpha, -1, 0) C(\ell, 1, \ell+1; m_\alpha, -1, 0) \right. \right. \\
 \left. \left. + C(\ell, 1, \ell-1; m_\alpha', 1, 0) C(\ell, 1, \ell+1; m_\alpha', 1, 0) \right. \right. \\
 \left. \left. + C(\ell, 1, \ell-1; m_\alpha'', 0, 0) C(\ell, 1, \ell+1; m_\alpha'', 0, 0) \right] \right\} \quad (3.2-98)
 \end{aligned}$$

The orthogonality relation (Rose, 1957, Eq. 3.7)

$$\sum_{m_1} C(j_1 j_2 j; m_1 m - m_1, m) C(j_1 j_2 j'; m_1 m - m_1, m) = \delta_{jj'}$$

along with the relation (Rose, 1957, Eq. 3.16b)

$$C(j_1 j_2 j_3; m_1 m_2 m_3) = (-1)^{j_1 + j_2 - j_3} C(j_2 j_1 j_3; m_2 m_1 m_3)$$

can be employed to simplify this complicated expression. The transposition of the first two indices along with the second of the two C-equations above shows that the first two terms in square brackets are again orthonormal sums over the first m -index (cf. Eq.(3.2-38)) and, hence, equal unity. The third expression in square brackets corresponds to the orthonormality relation above for $j \neq j'$ and, hence, vanishes. Since $g_1 = 2\ell + 1$, we obtain from Eq. (3.2-98) ,

$$\tau(\text{P.E.}) = \frac{2m^2 e^2 \mu v}{3\hbar^3 c} \left\{ 4\pi C^2(\ell, 1, \ell - 1; 000) R_{\ell-1, \ell}^2 + 4\pi C^2(\ell, 1, \ell + 1; 000) R_{\ell+1, \ell}^2 \right\} \quad (3.2-99)$$

This agrees with the result first given in this form by Bates* (1946), when account is taken (cf. Eq.(3.2-31)) of the values of the C^2 -factors, and the

* Monthly Notices Roy. Astro. Soc. 106, 432 (1946).

energy quantum numbers which we have suppressed in our definition of $R_{\ell\pm 1, \ell}$. Because of our transposition of the first and second projection quantum numbers in the C-coefficients in the square brackets of Eq. (3.2-98), the foregoing derivation does not actually depend on the m-value of the free electron which we took to be zero (the derivation would have been a little simpler had we allowed it to so depend). Because of this, our result is independent of which direction we choose as our z-axis which is the implied momentum direction for the wave function of Eq. (3.2-94). We will not demonstrate this in the detail of the preceding derivation, but by noting the following situation. Our result, Eq. (3.2-99) shows that we could have taken the ℓ -sum in Eq. (3.2-96) out of the absolute value-squared brackets, as all the cross terms vanish. The reason must lie in the fact that Eq. (3.2-94) represents a superposition of degenerate ℓ -sublevels, and we could have considered transitions into them individually and summed the resulting individual transition probabilities in the usual fashion after the rule of "averaging over initial states and summing over final states". Had we done this, we would not have had to examine the cross terms at all. Now from the spherical harmonics addition theorem (Rose, 1957, Eq. 4.27)

$$Y_{\ell 0}(\theta, 0) = \left(\frac{4\pi}{2\ell+1} \right)^{1/2} \sum_m Y_{\ell m}^*(\theta, \varphi_1) Y_{\ell m}(\theta_2, \varphi_2) \quad (3.2-100)$$

we can de-couple the electron coordinate vector direction θ_e, φ_e and the z-axis (or momentum) direction θ_p, φ_p . To consider a transition into a single l, m sublevel we would use one term of

$$u(r, \theta, \varphi) = \frac{1}{L^{3/2}} \sum_{l=0}^{\infty} \sqrt{4\pi(2l+1)}^{1/2} i^l e^{-\delta l} R_{El}(r) \times \left\{ \left(\frac{4\pi}{2l+1} \right)^{1/2} \sum_M Y_{lM}^*(\theta_p, \varphi_p) Y_{lM}(\theta_e, \varphi_e) \right\} \quad (3.2-101)$$

in the formula for the cross section. Summing over all these sublevels as final degenerate states, we would have

$$\sigma(\text{P.E.}) = \frac{2\pi^2 e^2 \omega \nu}{3h^3 c} \left\{ 4\pi R_{l-1,l}^2 C^2(l, 1, l-1; 000) \left[\sum_M \frac{4\pi}{2l-1} \left| Y_{l-1,M}(\theta_p, \varphi_p) \right|^2 \right] + 4\pi R_{l+1,l}^2 C^2(l, 1, l+1; 000) \left[\sum_M \frac{4\pi}{2l+3} \left| Y_{l+1,M}(\theta_p, \varphi_p) \right|^2 \right] \right\}$$

since the formulas are just the same as we used before except for the added factor $Y_{lM}^*(\theta_p, \varphi_p) \times \left(\frac{4\pi}{2l+1} \right)^{1/2}$ and the non-zero value of M . If we now make use of the formula (Bethe and Salpeter, 1957, Eq. A.42)

$$\sum_M \left| Y_{lM}(\theta, \varphi) \right|^2 = \frac{2l+1}{4\pi} \quad (3.2-102)$$

the equation above reduces back to the result Eq. (3.2-99) , and we see explicitly that our result is independent of the direction that the wave function Eq. (3.2-94) implies for the asymptotic momentum direction. If this were not so, we would, of course, be in trouble, for we have already integrated over the outgoing momentum directions! The foregoing considerations, however, afford an explicit substantiation of our statement, made previously (see Fig. 3-3 , e.g.) that $|\vec{r}_{\alpha\beta}|^2$ is independent of the direction of the electron momentum* .

Total Photoelectric Cross Section -- Angular Momentum Final Eigenstate

It is interesting now to back up and rederive the photoelectric cross section making direct use of an angular momentum eigenfunction for the free electron state, and of spherical-box normalization for the radial function. The wave function for a free particle with a specific angular momentum l and confined to a sphere of radius R is** (Goldberger and Watson, 1964, pp. 18-20)

$$\psi_{k_e l m}(\vec{r}) = \left(\frac{2}{R}\right)^{1/2} k_e j_l(k_e r) Y_{lm}(\theta, \varphi) \quad (3.2-103)$$

* when β designates the asymptotic linear momentum eigenstate, not one of the sublevels M defined above. When these are considered, they must be summed over as above to get all the components of $x_{\alpha\beta}$, $y_{\alpha\beta}$, etc., in the "rotated" coordinate system.

** The normalization factor $\left(\frac{2}{R}\right)^{1/2} k_e$ can be obtained from the properties of the spherical Bessel functions as given, e.g., by Schiff, 1955, or more simply, from the asymptotic sinusoidal form of $j_l(kr)$.

The spherical Bessel functions have the asymptotic behavior

$$j_\ell(kr) \sim \frac{\sin(kr - \ell\pi/2)}{kr}$$

If a short-range potential exists near the origin, the radial wave function has the asymptotic form above except that the phase shift is no longer $\ell\pi/2$. In general, we can write the asymptotic form of the radial wave function as in Eq. (3.2-95), recalling that in the case of a Coulomb potential contribution, the phase shift δ_ℓ will be a slowly varying function of r .

For spherical-box normalization, we want the wave function to vanish at the radius R . In order for this to occur, we must have

$$k_e R - \ell/2 - \delta_\ell = n\pi, \quad (3.2-104)$$

in view of the asymptotic behavior, Eq. (3.2-95), of the radial wave function.

Differentiating this relation with respect to n we find (denoting the value of k_e which satisfies (3.2-104) as k_n)

$$dn = \frac{R}{\pi} dk_n, \quad (3.2-105)$$

or, since $k = \left(\frac{2mE}{\hbar^2}\right)^{1/2}$, we can write this as

$$\frac{dn}{dE_n} = \frac{R}{\pi} \left(\frac{m}{\hbar^2 k_n} \right) \quad (3.2-106)$$

this gives us the number density of radial eigenstates over the wave-number range dk_n or the energy range dE_n . The sum over states in the present

case can be indicated by $\sum_{n=0}^{\infty} \sum_{l=0}^{\infty} \sum_{m=-l}^{m=l}$. The asymptotic form of the radial wave function Eq. (3.2-95) can now be used along with Eq. (3.2-103) (which provides the normalization) to obtain the result

$$\left| \psi_{klm}(r) \right|^2 \frac{dn}{dE} \sim \frac{2m}{\pi \hbar^2 k_e} \frac{\sin^2(k_e r - \pi l/2 - \delta_l)}{r^2} \left| Y_{lm} \right|^2 \quad (3.2-107)$$

which is independent of R , just as the corresponding quantity is independent of L^3 in the rectangular-box normalization. For this reason, we can assume that the limit $R \rightarrow \infty$ will ultimately be taken so that the index n on k_e and E need not be explicitly acknowledged. The matrix element for photoelectric absorption is again as given by Eq. (3.2-66), and as usual we convert from $|\vec{p}|_{\alpha\beta}$ to $|\vec{r}|_{\alpha\beta}$ by means of Eq. (3.2-10). For simplicity we take n_w in the matrix element equal to 1, which implies that the cross section is given by (cf. Eq. (3.2-71))

$$\sigma_{\alpha\beta} = \frac{w_{\alpha\beta} V}{c} \quad (3.2-108)$$

where V is the photon normalization volume. Combining Eqs. (3.2-1), (3.2-10), (3.2-106), and (3.2-108)), we obtain

$$\sigma_{\alpha\beta} = \frac{4\pi m e^2 w_{\alpha\beta} R}{\hbar^2 k_e c} \left| \vec{r}_{\alpha\beta} \cdot \vec{e} \right|^2 \quad (3.2-109)$$

In this result, the matrix element $\vec{r}_{\alpha\beta}$ is defined as

$$\vec{r}_{\alpha\beta} = \int \psi_{nlm}(\vec{r}) \vec{r} \psi_{k_e l' m'}^*(\vec{r}) d^3 \vec{r} .$$

Using Eq. (3.2-103) we see that this is approximately equal to

$$\vec{r}_{\alpha\beta} = \left(\frac{2}{R}\right)^{1/2} k_e \int (j_l(k_e r) Y_{l'm'}) \vec{r} \psi_{nlm} d^3 \vec{r} . \quad (3.2-110)$$

Since $j_l(k_e r)$ has the asymptotic behavior $\frac{\sin kr}{kr}$, we can use this result to pass to other equations for \vec{r} involving different asymptotic normalization conventions. For example, we would have

$$\vec{r}_{\alpha\beta} = \left(\frac{\pi k_e \hbar^2}{R m}\right)^{1/2} \int u_w \vec{r} \psi_b d^3 \vec{r} \quad (3.2-111)$$

where

$$u_w \sim \sqrt{\frac{2m}{\pi \hbar^2 k_e}} \left(\frac{\sin k_e r}{r}\right) Y_{l'm'} \quad (3.2-112)$$

and if we insert Eq. (3.2-111) into Eq. (3.2-109) we obtain

$$\sigma_{\alpha\beta}^{(w)} = \frac{4\pi^2 e^2 u}{c} \left| \int u_w \vec{r} \cdot \vec{\epsilon} \psi_b d^3 \vec{r} \right|^2 \quad (3.2-113)$$

This is the formula given by Bethe and Salpeter (1957) in their Eq. 71.1.

The normalization of u_w has been chosen so that $\int u_w(r) u_w(r) r^2 dr = \delta(E-E')$ where $E = \frac{\hbar^2 k^2}{2m}$, as will be discussed later. With the usual average*

$|\vec{r}_{\alpha\beta} \cdot \vec{e}|^2 = |\vec{r}_{\alpha\beta}|^2 \cos^2\theta = \frac{1}{3} |\vec{r}_{\alpha\beta}|^2$ over atom orientations and the formal designation of the sum and average over initial and final states

Eq. (3.2-113) can also be written as

$$\sigma = \frac{8\pi^3 e^2 v}{3c \omega_l} \sum \sum \int u_w \vec{r} \psi_b d^3 \vec{r} \Big|^2 \quad (3.2-114)$$

in agreement with Eq. 1 of Burgess and Seaton (1960).

Let us now define a matrix element $\vec{r}_{nlm}^{El'm'}$ by the relation

$$\vec{r}_{nlm}^{El'm'} = \int \left[R_{nlm}(r) Y_{lm}(\theta, \varphi) \right]^* \vec{r} \left[R_{El'm'}(r) Y_{l'm'}(\theta, \varphi) \right] d^3 \vec{r} \quad (3.2-115)$$

where $R_{El'm'}(r)$ is normalized according to Eq. (3.2-95). By comparing this form with Eq. (3.2-110), it is easy to see that Eq. (3.2-109) can now be written as

$$\sigma_{\alpha\beta} = \frac{8\pi^2 m^2 e^2 v}{3\hbar^3 c} \left| \vec{r}_{nlm}^{El'm'} \right|^2 \quad (3.2-116)$$

* It is fair to do this now, as in the discrete case, because of our choice of eigenfunctions.

where the factor $1/3$ appears again if we average over atom orientations, and where k_e has been replaced according to $k_e = mv/\hbar$. If we now insert the explicit sum and average over final and initial states,

$\frac{1}{2\ell+1} \sum_m \sum_{m'}$ we obtain from Eq. (3.2-116)

$$\sigma_{\ell, \ell \pm 1} = \frac{2m^2 e^2 \omega v}{3\hbar^3 c} \cdot \frac{4\pi}{2\ell+1} \sum_m \sum_{m'} \left\{ \left| r_{n\ell m}^{E, \ell-1, m'} \right|^2 + \left| r_{n\ell m}^{E, \ell+1, m'} \right|^2 \right\} \quad (3.2-117)$$

Using the relation (Bethe and Salpeter, 1957, Eqs. 60.12 and 60.13)

$$\sum_{m'} \left| r_{n\ell m}^{E, \ell \pm 1, m'} \right|^2 = \frac{(\ell + \frac{1}{2}) \pm \frac{1}{2}}{2\ell+1} \left(R_{n\ell}^{E, \ell \pm 1} \right)^2 \quad (3.2-118)$$

and noting that the sum over m yields simply a factor $2\ell+1$ after carrying out the sum over m' above, we obtain

$$\sigma_{\ell, \ell \pm 1} = \frac{2m^2 e^2 \omega v}{3\hbar^3 c} \left\{ \frac{4\pi\ell}{2\ell+1} \left(R_{n\ell}^{E, \ell-1} \right)^2 + \frac{4\pi(\ell+1)}{2\ell+1} \left(R_{n\ell}^{E, \ell+1} \right)^2 \right\}$$

in agreement* with Eq. (3.2-99). Note that in obtaining this result using an angular momentum final state function we did not need to pass through the intermediate step of computing a differential cross section. The specification of the final state as an angular momentum eigenstate allows us to proceed directly to a total absorption cross section.

* The energy quantum numbers suppressed in Eq. (3.2-99) have been restored to the R-factors here.

Normalization of Free-electron Radial Wave Functions

Since the transition probability depends on the square of the final state wave function multiplied by the density of final states $\frac{dn}{dE}$, we can inquire as to what normalization of the radial wave function will permit us to set $\frac{dn}{dE} = 1$. In the case of angular momentum final eigenstates, since the angular states are discrete they do not contribute to dn/dE . Therefore, we need only to incorporate the factor $\sqrt{\frac{dn}{dE}}$ into $R_{E\ell}(r)$ is the radial eigenfunction*. From Eq. (3.2-107) we see that the radial eigenfunction normalized in this fashion will have the asymptotic form

$$\sqrt{\frac{dn}{dE}} R_{E\ell}(r) \sim \left(\frac{2}{\pi}\right)^{1/2} \left(\frac{m}{\hbar^2}\right)^{1/2} \cdot \frac{\sin(kr + \delta_\ell)}{\sqrt{kr}} \quad (3.2-119)$$

One further question is of interest: the above normalization permits us to take a unit density of final states, but what does it yield for the quadratic integral of the wave function itself? In other words, what is the relationship of the asymptotic normalization of the free-state wave function, and the square integral normalization of the same function? To obtain this relationship, we can compute the value of the integral

$$\int \left[\left(\frac{dn}{dE}\right)^{1/2} R_{E,\ell}(r) \right]^* \left[\left(\frac{dn}{dE'}\right)^{1/2} R_{E',\ell}(r) \right] r^2 dr = I_\ell(E, E') \quad (3.2-120)$$

137

* For the free-state eigenfunction of Eq. (3.2-103) this is just

$$R_{E\ell}(r) = \left(\frac{2}{R}\right)^{1/2} k_e J_\ell(k_e r) .$$

In order to do this, we consider the radial Schrödinger equation obeyed by

$$\frac{f(E, \ell; r)}{r} = R_{E, \ell}(r) \left(\frac{dR}{dE} \right)^{1/2} \quad (3.2-121)$$

This equation is

$$\left[\frac{d^2}{dr^2} - \frac{\ell(\ell+1)}{r^2} - \frac{2m}{\hbar^2} V(r) + k^2 \right] f(E, \ell; r) = 0 \quad (3.2-122)$$

If we consider this equation for two values of E , E and E' , say, multiply it in each case by the function belonging to the other eigenvalue, integrate both resulting equations from zero to R and subtract them, we obtain

$$\int_0^R dr \left[f D^2 f' - f' D^2 f \right] + (k'^2 - k^2) \int f f' dr = 0 \quad (3.2-123)$$

The terms in $V(r)$ and ℓ cancel, and we have set $f(E, \ell; r) \equiv f$, $f(E', \ell; r) \equiv f'$, and $\frac{d}{dr} \equiv D$. If we integrate by parts twice, we can show that

$$\int_0^R dr (f D^2 f') = (f D f' - f' D f)_R + \int_0^R dr f' D^2 f \quad (3.2-124)$$

With this result, we obtain from Eq. (3.2-123) the result

$$\int_0^{\infty} f f' dr = \frac{1}{k^2 - (k')^2} \lim_{R \rightarrow \infty} \left[f D f' - f' D f \right]_R \quad (3.2-125)$$

We can now evaluate $I_{\ell}(E, E')$ as defined by Eq. (3.2-120).

That is to say, we can now write

$$I_{\ell}(E, E') = \frac{1}{k^2 - (k')^2} \lim_{R \rightarrow \infty} \left[f D f' - f' D f \right]_R \quad (3.2-126)$$

where the asymptotic form of f is given by Eqs. (3.2-110) and (3.2-121)

$$f \sim \left(\frac{2m}{\pi \hbar^2} \right)^{1/2} \frac{\sin(kr + \delta_{\ell})}{\sqrt{k}} \quad (3.2-127)$$

Inserting Eq. (3.2-127) into Eq. (3.2-126), we obtain

$$\left(\frac{\pi \hbar^2}{2m} \right) I(E, E') = \lim_{R \rightarrow \infty} \frac{1}{k^2 - (k')^2} \left[\frac{\sin kR (k')^{1/2} \cos k'R}{k^{1/2}} - \frac{\sin k'R (k)^{1/2} \cos kR}{(k')^{1/2}} \right] \quad (3.2-128)$$

where we have neglected δ_{ℓ} for simplicity. Using the identity $2 \sin \alpha \cos \beta = \sin(\alpha + \beta) + \sin(\alpha - \beta)$, this becomes

$$\left(\frac{\pi \hbar^2}{2m} \right) I(E, E') = \lim_{R \rightarrow \infty} \frac{1}{2/kk'} \left[- \frac{\sin(k + k')R}{(k + k')} + \frac{\sin(k - k')R}{(k - k')} \right] \quad (3.2-129)$$

Now the δ -function can be represented by (Schiff, 1955)

$$\pi \delta(k) = \lim_{R \rightarrow \infty} \frac{\sin kR}{k} \quad (3.2-130)$$

With this representation, we obtain from Eq. (3.2-129),

$$I(E, E') = \left(\frac{2m}{\pi \hbar^2} \right) \times \frac{\pi}{2k} \delta(k - k') \quad (3.2-131)$$

since the first term in Eq. (3.2-129) does not contribute if we limit ourselves to $k, k' > 0$. Since $\delta(k - k') = 2k \delta(k^2 - (k')^2)$ this result can also be written as

$$I(E, E') = \left(\frac{2m}{\hbar^2} \right) \delta(k^2 - (k')^2) \quad (3.2-132)$$

or, since

$$\delta(k^2) = \delta(E) \frac{dE}{d(k^2)} = \delta(E) \left(\frac{\hbar^2}{2m} \right), \quad (3.2-133)$$

we can finally write our result as

$$I(E, E') = \int \left[\frac{dn}{dE} \right]^{1/2} R_{E; \ell}(r) \left[\left(\frac{dn}{dE'} \right)^{1/2} R_{E'; \ell}(r) \right] r^2 dr = \delta(E - E') \quad (3.2-134)$$

The asymptotic behavior of the wave function so normalized is given by Eq. (3.2-119).

Therefore, as stated previously, with the use of a wave function having this asymptotic form we can set $\frac{dn}{dE} = 1$ in the equation for the transition probability (Eq.(3.2-1)) , as the final state density will have been included in the matrix element. We can now correlate our results with a formula given by Bethe and Salpeter (1957). The matrix element for photoelectric absorption, Eq. (3.2-66) can be written as

$$|H'|_{m'l; m'l'} = \frac{1}{v^{1/2}} \frac{e\hbar}{m} \left(\frac{2\pi\hbar}{\omega}\right)^{1/2} |\bar{D}_{m'l; m'l'}^{(e)}|^2 \quad (3.2-135)$$

where

$$\bar{D}_{m'l; m'l'}^{(e)} = \int \psi_{m'l}^*(r) \bar{\nabla}_e \psi_{m'l'}(r) dv \quad (3.2-136)$$

and the subscript e has been used to denote the polarization direction. If now, we agree to normalize the radial factor of $\psi_{m'l}(\vec{r})$ according to Eq. (3.2-119) and consider light of a particular polarization only, the formula for the photoelectric cross section becomes

$$\sigma_{m'l-m'l'} = \frac{2\pi V}{\hbar c} |H'_{m'l, m'l'}|^2 \quad (3.2-137)$$

Inserting Eq. (3.2-135) into Eq. (3.2-137) yields the result

$$\sigma_{m'l-m'l'} = \frac{2\pi e^2 \hbar^2}{m^2 c v} |D_{m'l, m'l'}^{(e)}|^2 \quad (3.2-138)$$

for a transition between particular angular momentum sublevels m, l and m', l' . Eq. (3.2-138) is the result given by Bethe and Salpeter (1957) in their Eq. 69.2.

3.2.3 Reduction of the angular dependence of many-electron matrix elements to analytic formulas*

Before we can apply the preceding formulas to real physical problems in general, we must account, in some approximate fashion, for the possession of more than one electron per atom. In so doing, we must indicate how to average and sum degenerate many-electron transition probabilities over the appropriate initial and final states. For angular momentum eigenstates, this sum and average is dependent on the angular quantum numbers which uniquely specify the angular wave functions that appear in the matrix element. For practical problems it is usually necessary to approximate "true" atomic wave functions by separable product wave functions wherein the coordinates of a given electron appear in only one factor of the product. We will follow this procedure, and, in addition, will neglect configuration interaction. For a discussion of this topic, the reader may consult Hartree (1957), pp. 17 and 159.

Our formulas, therefore, are applicable to Hartree-Fock wave functions, for example, or hydrogenic product wave functions, but are not appropriate for nonseparable wave functions such as the Hylleraas variational functions often used for helium. In the separable approximation to bound-state wave functions, the angular dependence reduces to known spherical harmonics so that all the angular integrations involved in the matrix elements with which we are concerned can be performed (Gaunt, 1928). This is by no means a trivial task, especially for equivalent electrons, so we will not go through all the details. Rather, we confine ourselves to indicating the procedures and giving some results. By the method of Racah algebra (Racah, 1942, 1943, 1949) developed in the early 1940's some time after the initial development period of quantum mechanics, and by subsequent developments thereof (e.g., Kelly, 1959; Rohrlich, 1959), these angular integrations can be reduced to analytic

* The author is indebted to Dr. P. S. Kelly for assistance in the writing of this section.

formulas involving functions of the angular momentum quantum numbers. The earlier methods of Condon and Shortly (1935) can also be used for this purpose, but are more tedious.

We begin this procedure with the total cross section for absorption as given by Eq. (3.3-76) which we can now write formally as

$$\sigma(\omega) = \frac{4\pi^2 e^2 \omega}{3hc} \frac{b(\omega)}{g_i} \sum_{\alpha} \sum_{\beta} |\vec{r}_{\alpha\beta}| \quad (3.2-139)$$

to indicate the required summation over final states and average over initial states.

The number of degenerate initial states, or the statistical weight, of the initial level or term is designated g_i and is equal to $2J + 1$ for an atomic level or $(2L + 1)(2S + 1)$ for a term (see below). Referring to Eq. (3.2-139), it is convenient to define and consider the quantity

$$S_{ij} = \sum_{\alpha(i)} \sum_{\beta(j)} |\vec{r}_{\alpha\beta}|^2 \quad (3.2-140)$$

as this quantity is symmetric in the initial and final states and more or less independent of the remaining factors in the formula for the cross section σ . We follow the usual notation and employ capital letters J , L , and S for the total angular momentum, total orbital angular momentum, and total spin quantum numbers, respectively. For the total magnetic quantum numbers, or z -components of J , L , and S , we employ M_J , M_L , and M_S ,

respectively. The corresponding lower case letters are employed for the individual electron quantum numbers. (For the details of spectroscopic notation the reader is referred to Allen, 1963, Chapt. 4.) The basic degeneracy of an atomic state when there are no external fields present (as in the cases we are considering) is the degeneracy of the $2J + 1$ sublevels, or states, pertaining to the possible values of M_J . We will limit ourselves to LS coupling (Condon and Shortley, 1935) which is usually sufficient for light atoms.

With these limitations in mind, the angular integrations and sums indicated in Eq.(3.2-139) can be carried out. This analysis has been performed explicitly by Rohrlich (1959) for all cases of astrophysical interest. These cases fall into four categories

$$\begin{array}{ll}
 \text{(a)} & \ell^n \cdot \ell' \rightarrow \ell^n \cdot \ell'' \\
 \text{(b)} & \ell^n \rightarrow \ell^{n-1} \ell' \qquad \qquad \qquad (3.2-141) \\
 \text{(c)} & \ell^n \cdot \rightarrow \ell^{n-1} (\ell')^2 \\
 \text{(d)} & \ell^n \ell' \cdot \ell'' \rightarrow \ell^n (\ell')^2
 \end{array}$$

where n , or the numerical superscript, indicates the number of electrons having the ℓ -value to which the superscript is attached. The first two categories normally dominate problems of practical interest involving large numbers of transitions. As examples of these four categories of interest as applied to heated-air problems, we cite the configurational transitions:

$$(a) \quad (1s)^2 (2s)^2 2p \rightarrow (1s)^2 (2s)^2 3s \quad (\text{NIII, OIV})$$

$$l = 0, l' = 1, l'' = 0, n = 2$$

$$(b) \quad (1s)^2 (2s)^2 (2p)^4 \rightarrow (1s)^2 (2s)^2 (2p)^3 3d \quad (\text{OI})$$

$$l = 1, l' = 2, n = 4$$

$$(c) \quad (1s)^2 (2s)^2 (2p)^3 \rightarrow (1s)^2 2s (2p)^4 \quad (\text{OII, NI})$$

$$l = 1, l' = 0, n = 4$$

$$(d) \quad (1s)^2 (2s) (2p) \rightarrow (1s)^2 (2p)^2 \quad (\text{OV, NIV})$$

$$l = 0, l' = 1, l'' = 0, n = 2$$

It is important to note that in case (a) there is a well-defined core $(1s^2 2s^2)$ to which the outer electron (2p or 3s) couples. Thus, the coupling of the core electrons to each other must be specified in addition to the final total coupling of the outer electron to this core. In the other cases, various paren. couplings occur so that one has, effectively, an outer electron coupling to a linear combination of cores. Let us take the specific example under case (a)

$$(1s)^2 (2s)^2 {}^1S 2p {}^2P \rightarrow (1s)^2 (2s)^2 {}^1S 3s {}^2S$$

In each term the core state is a 1S and the outer (2p, 3s) electron couples to this to yield a ${}^2P, {}^2S$ term respectively. As another example, in case (b), the wave function of the $(2p)^4$ combination can be expanded in a fractional parentage coefficient expansion (Racah, 1943) as* (for the

* The p^4 fractional parentage coefficients can be derived from Eqs. 19 and 65 of Racah (1943), using the p^3 fractional parentage coefficients given in Table I of that paper.

specific case of the $1s^2 2s^2 2p^4 3P$ ground term of OI):

$$1s^2 2s^2 2p^4 3P = 1s^2 2s^2 2p^3 \left\{ -\sqrt{\frac{1}{3}} 4S + \sqrt{\frac{5}{12}} 2D - \sqrt{\frac{1}{4}} 2P \right\} p^3 P \quad (3.2-142)$$

We will use the subscript p as in L_p^i to denote that the quantum number to which it is appended belongs to a parent configuration (a core is also a parent--with a fractional parentage coefficient of unity--so the same designation will be used for this case). For the formal definition of the fractional parentage coefficients, see Eq. (3.2-144).

After summation over all magnetic quantum numbers (viz., all strictly degenerate sublevels) the line strength S_{ij} can be written as (Rohrlich, 1959; Bates and Damgaard, 1949):

$$S_{ij} = S(L_i, L_j) S(M_i, M_j) \sigma_{ij}^2 \quad (3.2-143)$$

where L_i symbolizes the triplet of quantum numbers $S^{(i)} L^{(i)} J^{(i)}$ belonging to state i , and L_j the set belonging to state j . M_i and M_j designate for the states i and j the set of all pertinent quantum numbers except J , e.g., for case (a),

$$M_i = \left\{ n, l, l', S_p L_p, L^{(i)}, S^{(i)} \right\}$$

$$M_j = \left\{ n, l, l'', S_p L_p, L^{(j)}, S^{(j)} \right\}$$

where we have taken the left hand side of Eq. (3.2-141) as the "i" state and the right hand side as the "j" state. The remaining factor, σ_{ij}^2 , is defined by

$$\sigma_{ij}^2 = \frac{1}{4\ell^2 - 1} \left[\int_0^\infty R_i(r) R_j(r) r^3 dr \right]^2 \quad (3.2-144)$$

where $R_i(r)$ and $R_j(r)$ are the radial wave functions for the two states i and j , normalized so that

$$\int_0^\infty R^2(r) r^2 dr = 1 \quad (3.2-145)$$

and $\ell >$ is the greater of the two orbital angular momentum values which the "jumping", or "active", electron has in states i and j .

Eq. (3.2-143) shows that the line strength splits into two factors, one of which depends on the line quantum numbers (and not on the parent) and the other depends only on the multiplet to which the line belongs. The definition of $S(\mathcal{L}_i, \mathcal{L}_j)$ is constructed so that if one sums it over all the lines of a multiplet, the result is unity:

$$\sum_{i,j} S(\mathcal{L}_i, \mathcal{L}_j) = 1 \quad (3.2-146)$$

Thus $S(\mathcal{L}_1, \mathcal{L}_j)$ is called the relative line strength. The strength of a multiplet then is given by

$$\sum_{\substack{\text{all lines of} \\ \text{for a given multiplet}}} s_{ij} = \left[\sum_{ij} S(\mathcal{L}_1, \mathcal{L}_j) \right] S(m_1, m_j) \sigma_{ij}^2 \quad (3.2-147)$$

$$= S(m_1, m_j) \sigma_{ij}^2$$

The sum indicated in Eq. (3.2-147) can only be performed if σ_{ij}^2 is the same for all lines in a multiplet. This implies that the radial wave functions are the same for all states in a term. While, of course, this is not strictly true, it is a satisfactory practical approximation for the circumstances with which we are concerned.

$S(m_1, m_j)$ is called the relative multiplet strength. Rohrlich (1959) gives the value of $S(\mathcal{L}_1, \mathcal{L}_j)$ as

$$S(\mathcal{L}_1, \mathcal{L}_j) = (2J^{(i)}+1) (2J^{(j)}+1) W^2(L^{(i)} J^{(i)} L^{(j)} J^{(j)}; S1)/(2S+1) \quad (3.2-148)$$

where $W(abcd;ef)$ is the Racah coefficient (Racah II, 1942, Eq'n 36, also Simon, Vader Sluis, and Biedenharn, 1954, tables. See also the discussion following Eq. (3.2-171).

We have set $S^{(i)} = S^{(j)} = S$ since here we are interested only in transitions which obey the selection rule for ordinary electric dipole radiation that the spin does not change.

Condon and Shortley give the line strengths S_{ij} in terms of a factor $f(SL^{(i)}J^{(i)}, SL^{(j)}J^{(j)})$ such that

$$S_{ij} = f(SL^{(i)}J^{(i)}, SL^{(j)}J^{(j)}) |\gamma^{(i)}L^{(i)}; P; \gamma^{(j)}L^{(j)}|^2 \quad (3.2-149)$$

where the reduced matrix element $|\gamma^{(i)}L^{(i)}; P; \gamma^{(j)}L^{(j)}|$ does not depend on the line quantum number J . This equation factorizes the line strengths into line and multiplet factors as does Eq. (3.2-143), but f is not normalized to unity over all lines. Since Condon and Shortley give the values of the sum of the strengths over all lines, we can easily relate f to our $\mathcal{S}(L_1, L_2)$. The sums needed are

$$\begin{aligned} L \rightarrow L+1 \sum_{J^{(i)}, J^{(j)}} S_{ij} &= (2S+1)L_{>} (4L_{>}^2 - 1) |\gamma^{(i)}L^{(i)}; P; \gamma^{(j)}L^{(j)}L+1|^2 \\ L \rightarrow L &= (2S+1)(2L+1)L(L+1) |\gamma^{(i)}L^{(i)}; P; \gamma^{(j)}L^{(j)}L|^2 \\ L \rightarrow L-1 &= (2S+1)L_{>} (4L_{>}^2 - 1) |\gamma^{(i)}L^{(i)}; P; \gamma^{(j)}L^{(j)}L-1|^2 \end{aligned} \quad (3.2-150)$$

where the symbol $L_{>}$ has been used for the greater of $L^{(i)}$ and $L^{(j)}$.

* γ represents the remaining quantum numbers, of the complete set of commuting observables, which do not need to be considered explicitly, but which exist in principle. As an example, the energy E could belong to the set γ .

Thus we see that

$$S(\mathcal{L}_1, \mathcal{L}_j) = \frac{f(S, L^{(i)}, J^{(i)}; S, L^{(j)}, J^{(j)})}{(2S+1) L_j (4L_j^2 - 1)} \quad L \sim L \pm 1$$

(3.2-151)

$$= \frac{f(S, L^{(i)}, J^{(i)}; S, L^{(j)}, J^{(j)})}{(2S+1) L(L+1) (2L+1)} \quad L \sim L$$

The relative multiplet strengths at this point would be given by Eq. (3.2-150) in terms of the reduced matrix elements $\langle \gamma^{(i)}, L^{(i)}; P: \gamma^{(j)}, L^{(j)} \rangle$. However, the multiplet strengths can be reduced further and cast into a simpler form and we shall do this below. We note here that by comparing Eqs. (3.2-151), (3.2-148) an explicit expression for $f(SL^{(i)}, J^{(i)}; SL^{(j)}, J^{(j)})$ can be obtained for the case $L \sim L \pm 1$:

$$f(SL^{(i)}, J^{(i)}; SL^{(j)}, J^{(j)}) = L_j (4L_j^2 - 1) (2J^{(i)} + 1) (2J^{(j)} + 1) \times W^2(L^{(i)}, J^{(i)}, L^{(j)}, J^{(j)}; S1)$$

(3.2-152)

* An explicit expression for the reduced matrix elements

$|\langle \gamma^{(i)}, L^{(i)}; P: \gamma^{(j)}, L^{(j)} \rangle|^2$ can be obtained from the preceding formulas.

We have not done this herein as we wish to avoid explicit use of this quantity. We use $S(m_i, m_j)$ and σ_{ij}^2 instead, and have only related Condon and Shortley's f to $S(\mathcal{L}_1, \mathcal{L}_j)$ so that the reader who wishes to can use their tables of the f -factors (Table 19, p. 241, Condon and Shortley, 1935).

where again $L_{>}$ is the greater of $L^{(i)}$ and $L^{(j)}$. We shall not concern ourselves with applying Eqs. (3.2-148) (3.2-152) to spectrum lines since it has so far proved impractical to incorporate the details of actual individual lines into a total absorption coefficient calculation. We will assume in this chapter that all the atomic states belonging to a term are degenerate and deal with entire multiplets (or in some circumstances even broader groups of lines) instead of the individual lines themselves. However, the foregoing formulas for the relative line strengths are still of interest because they are closely related to the formulas for the relative multiplet strengths. In fact in some cases the formulas are the same and one needs only to interchange the set of quantum numbers to obtain a multiplet strength from a line strength, as will be seen below.

Returning now to case (a) (Eq. 3.2-148), the formula for $S(m_i, m_j)$ is

$$\begin{aligned}
 S(m_i, m_j) &= S(\ell^n \ell' S_p L_p SL^{(i)}, \ell^n \ell'' S_p L_p SL^{(j)}) \\
 &= (2S+1) (2L^{(i)}+1) (2L^{(j)}+1) \ell_{>} (4\ell_{>}^2 - 1) \\
 &\quad \times W^2(\ell' L^{(i)} \ell'' L^{(j)}; L_p 1)
 \end{aligned}
 \tag{3.2-153}$$

where $\ell_{>}$ is the greater of ℓ' and ℓ'' . If we compare this equation to Eq. (3.2-148), we see that the correspondence $S - L_p$, $L^{(i)} - \ell'$, $J^{(i)} - L^{(i)}$, $L^{(j)} - \ell''$, $J^{(j)} - L^{(j)}$ between the line quantum numbers

(given to the left of the arrows) and the multiplet quantum numbers (given to the right of the arrows) carries the formula for $S(\mathcal{L}_i, \mathcal{L}_j)$ into the formula for $S(m_i, m_j)$ except for factors which are constant within a transition array. These latter factors (t', t'' , and S) do not affect the relative multiplet strengths within a transition array so that the relative multiplet strengths can be obtained from the relative line strengths by the above correspondence. In terms of the Condon and Shortley f-factors, Eq. (3.2-153) becomes

$$S(m_i, m_j) = (2S+1) f(L_p t' L^{(i)}; L_p t'' L^{(j)}) \quad (3.2-154)$$

The reason that the f-function of Condon and Shortley yields both $S(\mathcal{L}_i, \mathcal{L}_j)$ and the case (a) $S(m_i, m_j)$ values is that in both cases one seeks to reduce the matrix element of an operator that depends on only one of two coupled angular momenta. In determining $S(\mathcal{L}_i, \mathcal{L}_j)$ one has S and $L^{(i)}$ coupled to $J^{(i)}$ (as well as S and $L^{(j)}$ coupled to $J^{(j)}$) with the matrix element of the dipole interaction operator being independent of spin coordinates. Thus, the matrix element is reducible to a function of $L^{(i)}$ and $L^{(j)}$ alone. In the case of $S(m_i, m_j)$, L_p and t' are coupled to $L^{(i)}$ (and L_p and t'' are coupled to $L^{(j)}$). The matrix element in this case can be reduced to a function of t' and t'' alone since only this element is non-vanishing. The situation is covered by Eq. 44 given by Racah (1942b). Upon inserting the appropriate quantum numbers LSJ or $L_p t' L$, and summing over magnetic quantum numbers,

it is possible to form two functions which in combination yield the product $S(L_1, L_j) S(m_1, m_j) \sigma_{ij}^2$ for case (a). The functions are

$$|\langle J^{(i)} | P_1 | J^{(j)} \rangle|^2 = (2J^{(i)}+1) (2J^{(j)}+1) W^2(L^{(i)} J^{(i)} L^{(j)} J^{(j)}; S1) \\ \times |\langle L^{(i)} || P_1 || L^{(j)} \rangle|^2$$

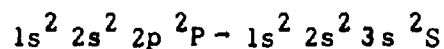
and

$$|\langle L^{(i)} || P_1 || L^{(j)} \rangle|^2 = (2L^{(i)}+1) (2L^{(j)}+1) W^2(L^{(i)} L^{(i)} L^{(j)} L^{(j)}; L_p 1) \\ \times (4L^{(j)}+1) \times \sigma_{ij}^2$$

Going back to Eq. (3.2-139) now, bearing in mind Eqs. (3.2-143) , (3.2-144) , and (3.2-147) , we obtain for the cross section for absorption

$$\sigma(\omega) = \frac{4\pi^2 e^2 \omega}{3\hbar c} \frac{b(\omega)}{g_1} S(m_1, m_j) \sigma_{ij}^2 \quad (3.2-155)$$

Many values of the relative multiplet strengths $S(m_1, m_j)$ are tabulated in Allen's (1963) book, in addition to the Condon and Shortley tabulation of f-factors from which the $S(m_1, m_j)$ can be obtained through Eq. (3.2-154). In order to better illustrate the use of the relative multiplet factors, let us consider some examples in detail. Our original example for case (a) was the non-equivalent electron transition



for NIII, say. Eq. (3.2-153) yields

$$S(m_1, m_2) = 2 \cdot 3 \cdot 1 \cdot 1(1) (3) W^2 (1100;01) = 6$$

since Biedenharn (1954) gives the value $1/3$ for the square of the Racah coefficient. This value agrees with that listed by Allen (1963) on p. 62 in the upper left hand corner of the page.

The arguments of the W coefficients can be permuted in a variety of ways without changing their values (Edmonds, 1957, p. 94).

For example,

$$W (\ell' L^{(i)} \ell'' L^{(j)}; L_p 1) = W (\ell' \ell'' L^{(i)} L^{(j)}; 1 L_p) \quad (3.2-156)$$

The order of the arguments on the right hand side of Eq. (3.2-156) is that which is employed by Burgess and Seaton (1960) and for convenience in comparing our analysis with their paper we shall employ it in the sequel. For electric-dipole transitions, in which $L^{(j)} = L^{(i)} \pm 0, 1$, the Racah coefficient reduces to a simple analytic form (see e.g., Condon and Shortley, p. 238, for the analytic form of the f -functions). In Table 3-1 we give the formulas for $S(m_1, m_2)$ for case (a) based on this analytic form. It is worthy of note that the $\ell - \ell + 1$ and $\ell - \ell - 1$ cases are not independent, but are derivable, one from the other, by an interchange of arguments based on the invariance

$$W^2 (\ell' \ell'' L^{(i)} L^{(j)}; L_p) = W^2 (\ell'' \ell' L^{(j)} L^{(i)}; 1 L_p) \quad (3.2-157)$$

Table 3-1

$$S(m_i, m_j) = (2S+1) (2L^{(i)}+1) (2L^{(j)}+1) t_{>} (4t_{>}^2 - 1) W^2 (t' t'' L^{(i)} L^{(j)}; 1L_p)$$

$$= (2S+1) f(L_p t' L^{(i)}; L_p t'' L^{(j)})$$

(A) $t - t - 1$

$$S(m_i, m_j)$$

$L - L + 1$	$\frac{(2S+1) (L_p + L - t + 1) (L_p - L + t) (L_p + L - t + 2) (L_p - L + t - 1)}{4(L + 1)}$
$L - L$	$\frac{(2S+1) (2L+1) (-L_p + L + t) (L_p + L - t + 1) (L_p + L + t + 1) (L_p - L + t)}{4L(L + 1)}$
$L - L - 1$	$\frac{(2S+1) (L - L_p + t - 1) (L - L_p + t) (L + L_p + t + 1) (L + L_p + t)}{4L}$

(B) $t - t + 1$

$$S(m_i, m_j)$$

$L + 1 - L$	$\frac{(2S+1) (L_p + L - t) (L_p - L + t + 1) (L_p + L - t + 1) (L_p - L + t)}{4(L + 1)}$
$L - L$	$\frac{(2S+1) (2L+1) (-L_p + L + t + 1) (L_p + L - t) (L_p + L + t + 2)}{(L_p - L + t + 1) / 4L(L + 1)}$
$L - 1 - L$	$\frac{(2S+1) (L - L_p + t) (L - L_p + t + 1) (L + L_p + t + 2) (L + L_p + t + 1)}{4L}$

Table 3-1 Relative Multiplet Strengths $S(m_i, m_j)$ for non-equivalent electrons.

The formulas of Table 3-1 may be summed over $L^{(i)}$ to obtain the total strength of the lines of the array which originate in the term $\gamma_p L_p S_p n^t SL^{(i)}$. The result is (Condon and Shortley, 1935, p. 248):

$$t \rightarrow t - 1 \quad (3.2-158a)$$

$$\sum_{L^{(i)}} S(m_i, m_j) = (2S+1) (2L^{(i)}+1) t(2t-1)$$

$$t \rightarrow t + 1 \quad (3.2-158b)$$

$$\sum_{L^{(i)}} S(m_i, m_j) = (2S+1) (2L^{(i)}+1) (t+1) (2t+3)$$

To return now to our examples.

First let us compute the line strength factor $f(SLJ, SL'J')$ for

$$SLJ = 323$$

$$S'L'J' = 323$$

The formula, from Condon and Shortley (1935, Eq. 2⁹2b), is

$$f = (2J+1) \frac{J(J+1) - S(S+1) + L(L+1)}{4J(J+1)} \quad (3.2-159)$$

Inserting the above values into the formula, one obtains $f = \frac{21}{4}$. This is the correct absolute value.

To find Condon and Shortley's tabular entry in table 1⁹ this value must be normalized so that the maximum f value is 100. That is

$$f_{\text{Tab}} = \frac{21}{4} \times a \quad (3.2-160)$$

where a is determined by

$$af_{\text{max}} = 100 \quad (3.2-161)$$

Now, according to Table 1⁹, f_{max} occurs for the $S = 3, L = 2$ to $S = 3, L = 2$ transition for $J = 5, J' = 5$, viz., the 325 to 325 transition. We use Eq. (3.2-159) again and obtain $f_{\text{max}} = \frac{11 \times 24}{5}$. Again, this is the correct absolute value. We determine a from Eqs. (3.2-160) and (3.2-161):

$$a = \frac{100}{f_{\text{max}}} = \frac{500}{11 \times 24}$$

Inserting this value in Eq. (3.2-160) we obtain

$$f_{\text{Tab}} = 9.94$$

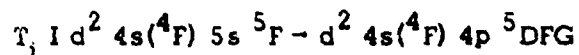
The tabular entry is 9.9. As noted on page 240 of Condon and Shortley, the entries have been sharply rounded off. The line strength $S(\mathcal{L}_i, \mathcal{L}_j)$ is given by Eq. (3.2-151) in terms of f and from this relation we obtain

$$S(\mathcal{L}_i, \mathcal{L}_j) = \frac{f}{(2S+1) L(L+1) (2L+1)} = \frac{\frac{21}{4}}{7 \cdot 2 \cdot 3 \cdot 5} = \frac{1}{40}$$

This agrees with the result obtained from Eq. (3.2-148):

$$S(\mathcal{L}_i, \mathcal{L}_j) = \frac{7 \cdot 7}{7} W^2(2323;31) = 7 \cdot \frac{1}{5 \cdot 7 \cdot 8} = \frac{1}{40} .$$

Next, let us consider a multiplet. We take the example quoted by Condon and Shortley, p. 245:



for which:

$$\begin{array}{ll} L_p = 3 & S = 2 \\ t' = 0 & t'' = 1 \\ L^{(i)} = 3 & L^{(j)} = 2, 3, 4 \end{array}$$

Relative values of $S(m_i, m_j)$ can again be obtained from Table 1⁹ of Condon and Shortley by the correspondence $SLJ \rightarrow L_p t' L^{(i)}$, and $SL'J' \rightarrow L_p t'' L^{(j)}$ which carries the line-strength $f(SLJ; SL'J')$ into the

multiplet strength $f(L_p \uparrow L^{(1)}; L_p \uparrow L^{(0)})$. Thus, the effective $SLJ - SL'J'$ values are 303 - 312;3;4. The 3 entries for $L^{(0)}$ (or J') = 2,3,4 are listed in the box above the "spin = 3" diagonal which appears as:

	2	3	4
0	55.6	77.8	100

In their example on p. 245, Condon and Shortley quote these numbers as the ratios 50:70:90, which can be obtained from the tabular entries by multiplying the latter by 0.90. The values of this configuration are not listed as such by Allen (1963), but do appear under the transition $sd^3 - pd^3$. This is so because the only parent quantum number that appears in Eq. (3.2-153) is L_p , and therefore, in this transition all 4F and 6F parent states are equivalent for calculating $\mathcal{S}(M)$. To obtain absolute values one may use Eqs. (3.2-153) or Table 3-1. From Table 3-1, for $l \rightarrow l+1$ we find

a) $L+1 \rightarrow L$ (F \rightarrow D, $L=2$, $l=0$)

$$\mathcal{S}(m_i, m_j) = 5 \frac{(3+2-0)(3-2+1)(3+2-0+1)(3-2+0)}{4(3)}$$

$$= 25$$

b) $L \rightarrow L$ (F \rightarrow F, $L=3$, $l=0$)

$$\mathcal{S}(m_i, m_j) = 5 \frac{(7)(-3+3+0+1)(3+3-0)(3+3+1+2)(3-3+0+1)}{4 \cdot 3 \cdot 4}$$

$$= 35$$

c) $L - 1 - L$ ($P = G, L = 4, t = 0$)

$$S(m_1, m_j) = 5 \frac{(4-3+0)(4-3+0+1)(4+3+0+2)(4+3+0+1)}{16}$$

$$= 45$$

These display the ratio 50:70:90 quoted by Condon and Shortley.

In the case of hydrogen, our formula (Eq. 3.2-155) must, of course, reduce back to the same result as is obtainable by elementary means. To see that this occurs, we note that

$$L_p = 0$$

$$L^{(i)} = t'$$

$$L^{(j)} = t''$$

where, by Eq. (3.2-153) we obtain

$$S(m_1, m_j) = (2S+1)(2t'+1)(2t''+1)t' > (4t' > ^2 - 1)$$

$$\times W^2(t' t'' t' t''; 10) \quad (3.2-162)$$

From the formula for W for this special case, given by Edmonds* (1957), we have

$$W^2(t' t'' t' t''; 10) = \left[(2t'+1)(2t''+1) \right]^{-1} \quad (3.2-163)$$

* p. 98, Eq. 6.3.2.

Using this result and Eq. (3.2-162) in Eq. (3.2-155) we obtain for the hydrogen cross section:

$$\sigma(\omega) = \frac{4\pi^2 e^2 \omega}{3hc} b(\omega) \frac{l_{>}(4l_{>}^2 - 1)}{2l_{>}^2 + 1} \sigma_{l', l''}^2 \quad (3.2-164)$$

We have used the correspondence $L^{(i)} = l'$, which implies that $g_l = (2S+1)(2l'+1)$. If we insert the explicit form of $\sigma_{l', l''}^2$ given in Eq. (3.2-144) this becomes

$$\sigma(\omega) = \frac{4\pi^2 e^2 \omega}{3hc} b(\omega) \frac{l_{>}}{2l_{>}^2 + 1} \left[\int_0^\infty R_{n'l'}(r) R_{n'l''}(r) r^3 dr \right]^2 \quad (3.2-165)$$

An average f-number is often defined by (Bethe and Salpeter, 1957, Eq. 61.2; cf our Eq. (3.3-86))

$$\begin{aligned} \bar{f}_{n'l', n'l''} &= \frac{l_{>}}{3(2l_{>}^2 + 1)} w_{n'l', n'l''} \left[\int_0^\infty R_{n'l'}(r) R_{n'l''}(r) r^3 dr \right]^2 \left(\frac{2m}{h} \right) \\ &= \frac{l_{>}}{3(2l_{>}^2 + 1)} \left(\frac{w_{n'l', n'l''}}{\text{Ryd}} \right) \left[\int_0^\infty R_{n'l'}(r) R_{n'l''}(r) r^3 dr \right]^2 / a_0^2 \end{aligned} \quad (3.2-166)$$

(where $\text{Ryd} = e^2/2 a_0$ is the Rydberg energy unit).

In terms of this average f-number, our cross section as given by Eq. (3.2-165) can be written

$$\sigma(\omega) = \frac{2\pi^2 e^2}{mc} \bar{f}_{n'l', n'l''} b(\omega)$$

in agreement with Eq. (3.3-87) (the averaging does not alter the constants in the formula).

Coefficients of fractional parentage

Rohrlich's case (a), which we have been discussing so far, does not materially involve equivalent electrons. (The core may, of course, involve them, but case (a) assumes that the core electron quantum numbers remain unchanged.) To proceed to the remaining cases which do involve equivalent electrons, we must define the coefficients of fractional parentage, or fpc, previously alluded to. These arise in the problem of factoring a one-electron wave function out of an antisymmetrized product wave function in such a way that the overall wave function remains antisymmetric. They can be defined by the equation

$$\psi(l^n SL) = \sum_{S_p L_p} F(l^n SL, S_p L_p) \psi\left(\left[l^{n-1} S_p L_p\right] l SL\right) \quad (3.2-167)$$

where $\psi\left(\left[l^{n-1} S_p L_p\right] l SL\right)$ denotes the wave function for a state in which $n-1$ electrons couple together into a parent term $S_p L_p$, and the remaining electron couples to this parent to yield the overall coupling SL . The Racah notation for the fpc which we have denoted by $F(l^n SL, S_p L_p)$ in Eq. (3.2-167) is

$$F(l^n SL, S_p L_p) = \left(l^n SL \left\{ l^{n-1} (S_p L_p) l SL \right\}\right) \quad (3.2-168)$$

Eq. (3.2-167) may be lengthened to include explicitly the angular momentum coupling of the substates distinguished by different magnetic quantum numbers. The more explicit statement is:

$$\psi(t^n S L M_S M_L) = \sum_{S_p L_p} F(t^n S L, S_p L_p) \sum_{M(L_p), m(t)} \sum_{M(S_p), m(s)} C(L_p t L; M(L_p), m(t), M(L)) \cdot C(S_p \frac{1}{2} S; M(S_p), m(s), M(S)) \psi(t^{n-1} S_p L_p M(S_p) M(L_p)) \psi(t m(t) m(s)) \quad (3.2-169)$$

The coefficients $C(j_1, j_2, j_3; m_1, m_2, m_3)$ are Clebsch-Gordan coefficients used earlier (cf. Eq. 3.2-23). They are defined (Condon and Shortley, 1935, Ch. 3) to give the correct fraction of each substate when coupling two angular momenta (j_1 and j_2) to get a third (j_3). They are also known as Wigner, or vector-coupling coefficients, and are referred to by Condon and Shortley as transformation amplitudes for vector addition. They are closely related to the 3-j symbols (Edmonds, 1957, p. 16).

Magnetic quantum numbers are not usually included explicitly in matrix element formulas because the results do not depend on them unless the operator whose matrix element is under consideration is itself not symmetric with respect to the magnetic angle θ . This occurs, for example, in the case of an atom perturbed by an external magnetic field. In the absence of such asymmetric perturbations, the factors of the wave functions which depend on m and θ integrate to one or zero, leaving only sums of

products of Clebsch-Gordan coefficients, which also reduce to unity because of the sum rule (Rose, 1957, Eq. 3.7):

$$\sum_{m_1, m_2} C(j_1, j_2, j_3, m_1, m_2, m_3) C(j_1, j_2, j_3', m_1, m_2, m_3') = \delta_{j_3, j_3'} \delta_{m_3, m_3'}$$

With the foregoing definition of the fpc, the line strength for Rohrlich's case (b) $(t^n - t^{n-1} t')$ may be written as

$$S(m_i, m_j) = S(t^n SL^{(i)}; t^{n-1} S_p L_p t' SL^{(j)}) = nF^2 (t^n SL^{(i)}, S_p L_p) \cdot S(t^{n-1} t S_p L_p SL^{(i)}, t^{n-1} t' S_p L_p SL^{(j)}) \quad (3.2-170)$$

To obtain a formula for case (c), $t^n t' - t^{n-1} (t')^2$, we must expand both t^n and $(t')^2$ with fpc in order to isolate the active electron. However, the fpc for $(t')^2$ are all zero or one, since there is only one possible parent state. In addition, we must recouple the expanded function $t^{n-1} t t'$ in the order $t^{n-1} t' t$ to cause the active electron (viz., the electron for which $t = t'$) to be the last to be coupled on in both states. This is accomplished by the use of the Racah (1943) equation (6), which in our case has the form

$$\begin{aligned} \psi(t^{n-1} S_p L_p, t S' L', t' SL) &= \sum_{S'' L''} U\left(\frac{1}{2} S_p, S_2^1; S' S''\right) U(t L_p t' t'; L' L'') \\ &\times \psi(t^{n-1} S_p L_p, t' S'' L'', t' SL) \times (\text{phase factor}) \end{aligned} \quad (3.2-171)$$

In this formula, the coefficients U are a particular form of the Racah coefficients defined by a sum of products of four Clebsch-Gordan coefficients. Their virtue is to again relieve us of any need to consider Clebsch-Gordan coefficients explicitly.

Tables of the Racah coefficients W and the closely related 6-j coefficients are now generally available (see Biedenharn, 1954; Howell, 1959; Rotenberg, 1959). The relationship of the 3 symbols to each other is given by (see Edmonds, 1957, Ch. 6):

$$\begin{aligned} U(abcd;ef) &= \sqrt{2e+1} \sqrt{2f+1} W(abcd;ef) \\ &= \sqrt{2e+1} \sqrt{2f+1} \begin{Bmatrix} a & b & e \\ d & c & f \end{Bmatrix} (-1)^{a+b+c+d} \end{aligned} \quad (3.2-172a)$$

and their relationship to the Clebsch-Gordan coefficients is given by

$$\begin{aligned} U(abcd;ef) &= \sum_{m_a m_b m_d m_e m_f} C(edc; m_e m_d m_c) C(abe; m_a m_b m_e) C(bdf; m_b m_d m_f) \\ &\quad \times C(afc; m_a m_f m_c) \end{aligned} \quad (3.2-172b)$$

Using Eq.(3.2-171) and the expansion (3.2-167), we can now write the angular factor for Röhrllich's case (c) as

$$\begin{aligned} \mathcal{S}(n_i, m_j) &= \sum_{S''L''} U^2\left(\frac{1}{2} S_p, S''; S''\right) \cdot U^2(\ell L_p L^{(i)}; L'L'') \cdot 2n \cdot F^2(\ell^n S'L', S_p L_p) \\ &\quad \cdot \mathcal{S}(\ell^{n-1} \ell' \ell S''L''SL^{(i)}, \ell^{n-1} \ell' \ell' S''L''SL^{(i)}) . \end{aligned} \quad (3.2-173)$$

We note that S_p, L_p, S', L', S and L all have fixed values determined by the chosen initial and final states, while $S''L''$ takes on all the permitted values for the configuration $l^{n-1} S_p L_p, l' S'' L''$.

To illustrate the use of Eq. (3.2-173), consider our example of case (c):

$$1s^2 2s 2p^4 ({}^4P) - 1s^2 2s^2 2p^3 ({}^4S)$$

The fact that this is really $l^{n-l} l'^{2l-n-1}$ can introduce no more than a phase change into the wave function and, therefore, has no effect upon

$$S(n_1, m_1)$$

We find

$$\begin{aligned} L_p &= 0 & S_p &= 3/2 \\ L' &= 1 & S' &= 1 & S'' &= 2 \text{ or } 1 \\ L^{(i)} &= 1 & & & L'' &= 0 \\ L^{(j)} &= 0 & S &= 3/2 \\ l &= 1 & l' &= 0 & n &= 4 \\ F^2(p^4 3P, 4S) &= \frac{1}{3} & & & & \text{(Rohrlich Table I)} \end{aligned}$$

From the tables:

$$\begin{aligned} U^2 \left(\frac{1}{2} \frac{3}{2} \frac{3}{2} \frac{1}{2} ; 1S'' \right) &= \frac{1}{16} & \text{if } S'' &= 1 \\ &= \frac{15}{16} & \text{if } S'' &= 2, \end{aligned}$$

$$\text{and } U^2(10L1; 10) = 1.$$

Consequently,

$$\begin{aligned}
 \mathcal{S}(m_1, m_j) &= \frac{1}{16} \cdot 2 \cdot 4 \cdot \frac{1}{3} (p^3_{sp} {}^3S {}^4P, p^3_{ss} {}^3S {}^4S) \\
 &+ \frac{15}{16} \cdot 2 \cdot 4 \cdot \frac{1}{3} (p^3_{sp} {}^5S {}^4P, p^3_{ss} {}^5S {}^4S) \\
 &= \frac{1}{6} \cdot 9 + \frac{5}{2} \cdot 15 = 39 .
 \end{aligned}$$

where the values of \mathcal{S} for the non-equivalent electron transitions are obtained from Eq. (3.2-153) as before.

Turning to case (d) , $l^{n_l} l'' - l^{n_l} l'^2$ may be computed without use of f.p.c. since it is not necessary to alter any shell having more than two equivalent electrons. The non-equivalent electron formulas of case (a) may be employed as before, after $l^{n_l} l'^2$ has been recoupled to $(l^{n_l} l') l'$. This is accomplished by using the Racah (1943), Eq. 6, in the form

$$\psi(l^{n_l} S_l L_l, l'^2 S' L', SL^{(j)}) = \sum_{S'' L''} U\left(\frac{1}{2} \frac{1}{2} S S_l; S' S''\right) U(l' l' L^{(j)} L_l; L' L'') \quad (3.2-174)$$

$$\cdot \psi(l^{n_l} S_l L_l, l' S'' L'', l', SL^{(j)}) \cdot (\text{phase factor})$$

Non-zero matrix elements can occur only if S'' and L'' have values equal to those specified for $l^{n_l} l'$ in the state $l^{n_l} S_l L_l, l' S_p L_p, l'' S L$. Therefore, we keep only that term in our expansion for which $S'' = S_p$ and $L'' = L_p$.

Then we have

$$\begin{aligned}
 \mathcal{S}(m_1, m_2) &= U^2 \left(\frac{1}{2} \frac{1}{2} \text{SS}_L; \text{S}'\text{S}'_P \right) U^2 (l' l' L^{(i)} L_L; l' l' L_P) \\
 &\cdot 2 \mathcal{S}(l^n l' l' S_P L_P SL^{(i)}, l^n l' l' S_P L_P SL^{(j)})
 \end{aligned}
 \tag{3.2-175}$$

We illustrate the use of Eq. (3.2-175) with the case (d) example, $1s^2 2s 2p^3 P - 1s^2 2p^2 3P$. Since $1s^2$ is a closed shell the U coefficients are both equal to one. On this account the transition might also be seen as a simple example of case (b), with f.p.c. equal to one.

Using Eq. (3.2-153) in (3.2-175), we find

$$\begin{aligned}
 \mathcal{S}(m_1, m_2) &= 1 \cdot 1 \cdot 2 \mathcal{S}(1s^2 2p 2s 2p^3 P, 1s^2 2p 2p^2 P^3 P) \\
 &= 2 \cdot 3 \cdot 3 \cdot 3 \cdot 1 \cdot 3 \cdot W^2(1101; 11) = 18, \\
 &\text{since } W^2 = 1/9.
 \end{aligned}$$

This result agrees with Allen's tables.

A more complex example will pair the ground state of titanium, which we write (ignoring the closed inner shells) as $3d^2 4s^2 ({}^3F)$, with the excited state $3d^2 ({}^3F) 4s 4p ({}^3G)$. This excited state is actually degenerate, consisting of the two states $3d^2 ({}^3F) 4s ({}^4F) 4p ({}^3G)$ and $3d^2 ({}^3F) 4s ({}^2F) 4p ({}^3G)$. We shall compute the transitions to these two states separately.

The Racah coefficients are

$$U^2\left(\frac{1}{2} \frac{1}{2} 1 1; 0 \frac{3}{2}\right) = 2/3 \quad \text{for the first transition,}$$

$$U^2\left(\frac{1}{2} \frac{1}{2} 1 1; 0 \frac{1}{2}\right) = 1/3 \quad \text{for the second,}$$

and $U^2(0033;03) = 1$ for both.

Again using Eq. (3.2-153) and (3.2-175) we find

$$\begin{aligned} S(m_i, m_j) &= 2/3 \cdot 1 \cdot 2 \cdot 3 \cdot 7 \cdot 9 \cdot 1 \cdot 3 \cdot W^2(0 3 1 4; 3 1) \\ &= 36 \quad \text{since } W^2 = 1/21 . \end{aligned}$$

$S(m_i, m_j)$ for the second transition differs only in the Racah coefficient, since S_p does not appear explicitly in Eq. (3.2-153). Therefore, its value is 18. The sum of these numbers, $36 + 18 = 54$, is the result given by Allen* who lumps degeneracies of this type.

Shore and Menzel (1965) have followed the Racah algebra approach to transition-probability calculations in their compilation of extensive tables of line-strength factors. Their tables cover a large number of the possible transitions involving s, p, and d shells of electrons. Their line strength factor differs from that of Röhrlisch only by the factor $2S + 1$. All values of J have been covered for which $L < 8$ and $S < 4$. The corresponding multiplet strength factors are presented as a table of formulas

for transitions among large classes of open-shell configurations. These multiplet factors are functions of three quantities which are also tabulated. These three quantities are (1) multiplet factors for transitions involving non-equivalent electrons only (corresponding to our Eq. (3.2-153) and Table 3-1, but omitting the factors $(2S + 1) t_{>} (4l_{>}^2 - 1)$ found in Eq. (3.2-153); (2) fractional parentage coefficients -- a complete tabulation for the p- and d- shells, including phases, (3) recoupling coefficients required when the order of angular momentum coupling of a state must be changed before (1) can be applied. The multiplet factor table does not cover such cases as pp' , dd' , (two open p or d shells), $d^n p^n$ (except for $p^n d$ and $d^n p$), and $f^n (n > 1)$.

An excellent compendium of classic papers on angular momentum coupling is now available, including work of Wigner, Pauli, Racah, and many later contributions (Biedenharn and Van Dam, 1965).

Angular factors for photoelectric matrix elements

The algebra involved in the angular-factor reductions in the case of photoelectric absorption is reviewed in the paper by Burgess and Seaton (1960).

3.2.4 Free-free Radiative Transitions*

Although a free electron cannot absorb a photon and simultaneously conserve both energy and momentum, a nearby third particle may accept the necessary recoil momentum and thereby permit the photon absorption. Such a process is called free-free absorption and is generally the dominant radiation absorption effect for photons of energy less than the important photoionization thresholds.

For densities that are not too high, one can associate the photon-absorbing electron with a particular momentum-absorbing ion or atom (hereafter called the ion), and the free-free absorption process may be treated as a radiative absorption transition between two continuum electron states of the ion. Corrections due to momentum absorption by pairs of ions may become important at very high ion densities, and Debye shielding effects and photon absorption by electron pairs may become important at high electron densities. Such effects are ignored here; only the Debye shielding effect will be mentioned in subsection (vi) below.

(i) The Fundamental Cross Section

Both the initial and final states of the absorbing electron are in the continuum spectrum of the ion, so the choice of wave function normalization must be consistent with the "density of states" factor in the Fermi "Golden Rule" (Eq. 3.2-1). This is most evident by writing the basic expression for the transition probability as

$$dw_{\alpha\beta} = \frac{2\pi}{\hbar} \left| \langle \beta | H' | \alpha \rangle \right|^2 \delta(E_i - E_f) \left[\frac{d^3k}{(2\pi)^3} n_{\omega} \right] d\alpha d\beta \quad (3.2-176)$$

* Written by R.R. Johnston

giving the number of transitions per second from an ionic state $|\alpha\rangle$ in $d\alpha$ to a state $|\beta\rangle$ in $d\beta$ due to the interaction H' . Here E_i and E_f are the total energy of the system in the initial and final states, respectively, and the integration over the energy-conserving delta-function has not yet been carried out. The photon "density of states" $\frac{d^3\kappa}{(2\pi)^3} n_\omega$ is consistent with the photon amplitude normalization implicit in H' presented previously (Eq. 3.2-6),

$$H' = -\frac{e}{m} \left(\frac{2\pi\hbar}{\omega} n_\omega \right)^{1/2} \bar{\mathbf{p}} \cdot \hat{\mathbf{e}}_\omega e^{-i\vec{\kappa} \cdot \vec{r}} \quad (3.2-177)$$

and corresponds to an initial state of n_ω photons in a volume $(2\pi)^3$ with polarization $\hat{\mathbf{e}}_\omega$ and wave number $\vec{\kappa}$ in $d^3\kappa$. That is, the incident photon flux is

$$\dot{\Phi} = \left[n_\omega \frac{d^3\kappa}{(2\pi)^3} \right] c \quad (\text{cm}^{-2} \text{sec}^{-1}) \quad (3.2-178)$$

(The electron momentum operator $\bar{\mathbf{p}}$ here and in the following is to be understood as the sum $\sum_{j=1}^J \bar{\mathbf{p}}_j$ over the J electrons of the system.) The state $|\alpha\rangle$ is normalized on the " α -scale" ,

$$\langle \alpha | \alpha' \rangle = \int \langle \alpha | \vec{r} \rangle d^3\vec{r} \langle \vec{r} | \alpha' \rangle = \delta(\alpha - \alpha') \quad (3.2-179)$$

corresponding to one state per interval $d\alpha$, as is evident from the closure relation:

$$\sum_{\alpha} |\alpha\rangle \langle \alpha| = 1 \longrightarrow \int \langle \vec{r} | \alpha \rangle d\alpha \langle \alpha | \vec{r}' \rangle = \delta(\vec{r} - \vec{r}') \quad (3.2-180)$$

Clearly the dimensions of $(\vec{r}|\alpha\rangle)^2 d\alpha$ are $(\text{length})^{-3}$ and the matrix element of any operator O between such states has the dimensions of O . Thus, one may symbolically indicate that $(|\alpha\rangle)^2 d\alpha$ is dimensionless.

Dividing the transition probability (3.2-176) by the incident flux (3.2-178) and using (3.2-177) one obtains - in the usual electric dipole approximation - the result

$$d\tau_{\alpha\beta} = \frac{4\pi^2 e^2}{m^2 \omega c} |\langle \beta | \vec{p} \cdot \hat{\epsilon}_\omega | \alpha \rangle|^2 \delta(E_f - E_i) d\alpha d\beta \quad (\text{cm}^2). \quad (3.2-181)$$

This is the cross section per incident photon with energy in $d(\hbar\omega)$ at $\hbar\omega$ for a transition from a state $|\alpha\rangle$ in $d\alpha$ to state $|\beta\rangle$ in $d\beta$, and the indicated dimensions follow from the discussion above.

Forms of the matrix elements equivalent to (3.2-181) for exact wave functions are easily obtained from commutation relations with the results (see Eq. 3.2-10 and Bethe and Salpeter (1957) § 59 (β))

$$\langle \beta | \vec{p} \cdot \hat{\epsilon} | \alpha \rangle = im\omega_{\alpha\beta} \langle \beta | \vec{r} \cdot \hat{\epsilon} | \alpha \rangle \quad (3.2-182a)$$

$$= \frac{i}{\omega_{\alpha\beta}} \langle \beta | \hat{\epsilon} \cdot \vec{\nabla} V | \alpha \rangle = i \frac{Ze^2}{\omega_{\alpha\beta}} \langle \beta | \frac{\hat{\epsilon} \cdot \vec{r}}{r^3} | \alpha \rangle \quad (3.2-182b)$$

The last of these is the so-called Coulomb "dipole acceleration" form most frequently used in free-free calculations. Here $\hbar\omega_{\alpha\beta} = E_\beta - E_\alpha$ and Z is the nuclear charge. For approximate wave functions the validity of these alternative forms should be considered from the standpoint of the underlying commutation relations. Thus, the "dipole acceleration" form

is obtained from matrix elements of

$$[\vec{p}, H] = \vec{p}H - H\vec{p} = \frac{\hbar}{i} \vec{\nabla} V, \quad (3.2-183)$$

in terms of the exact Hamiltonian H , written $H = \sum (\vec{p}^2/2m) + V$. For exact states $|\alpha\rangle$ and $|\beta\rangle$, V is the sum of the Coulomb interactions and Eq. (3.2-182b) follows. For states $|\alpha\rangle$ and $|\beta\rangle$ which are two eigenstates of some approximate Hamiltonian, use of the associated approximate energies and the form Eq. (3.2-183) with the approximate potential V provides an alternate form of the dipole-acceleration matrix element which may be useful (DeVore, 1965). Finally, if the states $|\alpha\rangle$ and $|\beta\rangle$ are eigenstates of different approximate Hamiltonians, even the validity of Eq. (3.2-183) must be reconsidered.

Averaging over the polarization directions of the incident photon as before (Eq. 3.2-14)

$$\overline{|\langle \beta | \vec{p} \cdot \hat{e} | \alpha \rangle|^2} = 1/3 \sum_{\mu} |\langle \beta | p_{\mu} | \alpha \rangle|^2 = 1/3 |\langle \beta | \vec{p} | \alpha \rangle|^2 \quad (3.2-184)$$

the cross section (3.2-181) may be written

$$d\sigma_{\alpha\beta} = \frac{4\pi^2 e^2}{3m^2 \omega c} |\langle \beta | \vec{p} | \alpha \rangle|^2 \delta(E_i - E_f) d\alpha d\beta \quad (3.2-185)$$

To proceed further, the states $|\alpha\rangle$ and $|\beta\rangle$ and their normalization should be prescribed in greater detail -- most simply in terms of their asymptotic forms. Neglecting for the present effects due to electron exchange, the initial state $|\alpha\rangle$ asymptotically describes an ion in some state i - with wave function, say, $\phi_i(\mathbf{R})$ and energy

W_1 - and a free electron in a state described by the wave function $\chi_{\vec{k}_1}^{(+)}(\vec{r})$ with energy $\epsilon_1 = \hbar^2 k_1^2 / 2m$. That is,

$$\langle \vec{r}, \underline{\alpha} | \alpha \rangle \xrightarrow{|\vec{r}| \rightarrow \infty} \varphi_1(\underline{\alpha}) \chi_{\vec{k}_1}^{(+)}(\vec{r}), \quad (3.2-186)$$

and $E_1 = W_1 + \epsilon_1 + \hbar \omega$.

If one assumes the long-range Coulomb potential to be shielded at large distances, the state $\chi_{\vec{k}_1}^{(+)}(\vec{r})$ asymptotically represents an incident plane wave and outgoing scattered waves -

$$\chi_{\vec{k}_1}^{(+)}(\vec{r}) \xrightarrow{|\vec{r}| \rightarrow \infty} A \left[e^{i\vec{k}_1 \cdot \vec{r}} + f^{(+)}(\epsilon_1, \hat{k}_1 \cdot \hat{r}) e^{ik_1 r / r} \right]. \quad (3.2-187)$$

Here $f^{(+)}(\epsilon_1, \hat{k}_1 \cdot \hat{r})$ is the usual elastic scattering amplitude at energy ϵ_1 in terms of directions measured from that of the incident beam. Normalizing on the \vec{k} -scale determines $A = (2\pi)^{-3/2}$ and $d\alpha = d^3 k_1$, as may be seen from the closure relation,

$$\int \langle \vec{r}' | \underline{\alpha} \rangle d\alpha \langle \alpha | \vec{r} \rangle \xrightarrow{|\vec{r}| \rightarrow \infty} \int \frac{e^{i\vec{k} \cdot \vec{r}'}}{(2\pi)^{3/2}} d^3 k \frac{e^{-i\vec{k} \cdot \vec{r}}}{(2\pi)^{3/2}} = \delta(\vec{r} - \vec{r}').$$

The final state $|\beta\rangle$ similarly represents asymptotically the ion state i and a free electron in a final plane wave state with ingoing spherical waves,

$$\chi_{\vec{k}_f}^{(-)}(\vec{r}) \xrightarrow{|\vec{r}| \rightarrow \infty} (2\pi)^{-3/2} \left[e^{i\vec{k}_f \cdot \vec{r}} + f^{(-)}(\epsilon_f, \hat{k}_f \cdot \hat{r}) e^{-ik_f r / r} \right], \quad (3.2-188)$$

where again the normalization is on the \vec{k} -scale and $d\beta = d^3k_f$. The states $\chi_{\vec{k}}^{(\dagger)}$ are simply related to $\chi_{\vec{k}}^{(\ddagger)}$ in terms of the Wigner time-reversal operation (Goldberger and Watson, 1964, p. 170),

$$\chi_{\vec{k}}^{(\dagger)} = T_0 \chi_{-\vec{k}}^{(\ddagger)} \quad (3.2-189)$$

where T_0 is simply the operator of complex conjugation with neglect of spin. Thus, we have

$$f^{(\dagger)}(\epsilon, \hat{k} \cdot \hat{r}) = \left[f^{(\ddagger)}(\epsilon, -\hat{k} \cdot \hat{r}) \right]^*$$

Finally, $E_f = W_i + \epsilon_f$, and

$$\langle \vec{r}, \underline{R} | \beta \rangle \xrightarrow{|\vec{r}| \rightarrow \infty} \phi_i(\underline{R}) \chi_{\vec{k}_f}^{(\dagger)}(\vec{r}) \quad (3.2-190)$$

With this choice of continuum states, the basic cross section (3.2-185) becomes, after summing over the final electron states,

$$d\sigma_{\alpha\beta} = \frac{4\pi^2 e^2 k_f}{3m \hbar^2 \omega c} \left\{ \int d\Omega_f |\langle \beta | \vec{p} | \alpha \rangle|^2 \right\} d^3k_i \quad (\text{cm}^2) \quad (3.2-191)$$

where we have used $d^3k_f = \left(\frac{mk_f}{\hbar^2}\right) d\epsilon_f d\Omega_f$, and k_f is to be determined from energy conservation, $k_f^2 = k_i^2 + \left(\frac{2m}{\hbar}\right) \hbar\omega$.

The physically significant quantity is the radiation absorption coefficient $\tau(\omega)$, which is the probability per unit length that a photon of angular frequency ω will be absorbed in the medium (see Eq. 3.2-54).

For bound-bound and bound-free processes the radiation-absorbing electron is uniquely associated with a momentum-absorbing ion, so it is convenient to write

$$\tau(\omega) = N_v \sigma(\omega) \quad (\text{cm}^{-1})$$

where N_v is the ion number density, and the cross section $\sigma(\omega)$ has the dimensions $(\text{length})^2 = \text{area}$. For free-free transitions, however, the electrons are no longer uniquely associated with any particular ion, so the electron density is in general independent of the ion density unless thermodynamic equilibrium prevails. Thus, it is convenient to take the free-free absorption coefficient $\tau^{\text{FF}}(\omega)$ proportional to both the electron and the ion densities,

$$\tau^{\text{FF}}(\omega) = N_v N_e \sigma^{\text{FF}}(\omega) \quad , \quad (3.2-192)$$

and the coefficient of proportionality, $\sigma^{\text{FF}}(\omega)$, is frequently called the "free-free cross section" -- although it has dimensions $(\text{length})^5$.

The quantity $d\sigma_{\alpha\beta}$ of Eq. (3.2-191) is the cross section per ion for absorption of a photon of angular frequency ω by a free electron of density $(2\pi)^{-3}$ per unit volume with wave number \vec{k}_1 in d^3k_1 , as is evident from the chosen asymptotic forms (Eqs. 3.2-187 and 3.2-188). Then, if $F_e(\vec{k}) d^3k$ is the fractional number of electrons per unit volume with \vec{k} in d^3k -- normalized to unity -- one obtains

$$\tau^{\text{FF}}(\omega) = N_v N_e \int F_e(\vec{k}_1) \left[(2\pi)^3 d\sigma_{\alpha\beta} \right] \quad .$$

Writing the free-free cross section as

$$\sigma^{\text{FF}}(\omega) = \int F_e(\bar{k}_1) \sigma^{\text{FF}}(\bar{k}_1, \omega) d^3k_1, \quad (3.2-193)$$

one evidently obtains from Eq. (3.2-191)

$$\sigma^{\text{FF}}(\bar{k}_1, \omega) = \frac{(2\pi)^5 e^2 k_f}{3m\hbar^2 \omega c} \int d\Omega_f |\langle \beta | \vec{p} | \alpha \rangle|^2 \quad (\text{cm}^5) \quad (3.2-194)$$

(ii) The one-electron approximation and radial decomposition of the matrix elements

In most applications a one-electron approximation is assumed, according to which the photon-absorbing electron is assumed to move in a static potential $V(\vec{r})$ determined by the average charge distribution of the ion and possibly including some semi-empirical corrections for the effects of ion polarizability and electron exchange (Kivel, 1966; Allen, Kivel, Taylor, and Textoris, 1966; DeVore, 1964). As mentioned above, the choice of asymptotic forms (3.2-186) and (3.2-190) precludes a correct treatment of electron exchange. Accordingly, in this section and in most of the following, electron exchange will be ignored -- except as approximately included in the potential $V(\vec{r})$ -- and will be discussed only at the conclusion of the next section.

Thus, in the one-electron approximation one assumes equalities, for all \vec{r} , in Eqs. (3.2-186) and (3.2-190), with the states $\chi_{\vec{k}}^{(\pm)}(\vec{r})$ taken to be continuum solutions of the single-particle Schrödinger equation

$$\left[-\frac{\hbar^2}{2m} \nabla^2 + V(\vec{r}) \right] \chi_{\vec{k}}^{(\pm)}(\vec{r}) = \left(\frac{\hbar^2 k^2}{2m} \right) \chi_{\vec{k}}^{(\pm)}(\vec{r}) ,$$

satisfying the boundary conditions (3.2-187), (3.2-188). In this approximation the necessary matrix elements become one-electron quantities and are most frequently expressed in the dipole-length or dipole-acceleration forms Eqs. (3.2-182a) and (3.2-182b)

$$\begin{aligned} \langle \beta | \vec{p} | \alpha \rangle &= im\omega \int d^3r \left[\chi_{\vec{k}_f}^{(\pm)}(\vec{r}) \right]^* \vec{r} \chi_{\vec{k}_i}^{(\pm)}(\vec{r}) \\ &= \frac{i}{\omega} \int d^3r \left[\chi_{\vec{k}_f}^{(\pm)}(\vec{r}) \right]^* (\vec{\nabla} V) \chi_{\vec{k}_i}^{(\pm)}(\vec{r}) . \end{aligned} \quad (3.2-195)$$

If the effective single-particle potential is taken to be spherically symmetric a significant simplification results from an angular momentum decomposition of the one-electron states. Let

$$\chi_{\vec{k}_i}^{(\pm)}(\vec{r}) = \sum_{\ell=0}^{\infty} R_{\ell}^{(\pm)}(k_i, r) \sum_m Y_{\ell m}^*(\hat{k}_i) Y_{\ell m}(\hat{r}) , \quad (3.2-196)$$

where the normalized spherical harmonics $Y_{\ell m}$ are from Edmonds (1957). Similarly decomposing the asymptotic form (Eq. 3.2-187) with $A = (2\pi)^{-3/2}$, gives

$$\chi_{\vec{k}_i}^{(\pm)}(\vec{r}) \xrightarrow{r \rightarrow \infty} \sum_{\ell=0}^{\infty} \left[\sqrt{\frac{2}{\pi}} i^{\ell} e^{i\delta_{\ell}} \frac{\sin(k_i r - \ell\pi/2 + \delta_{\ell})}{k_i r} \right] \sum_m Y_{\ell m}^*(\hat{k}_i) Y_{\ell m}(\hat{r}) ,$$

where the scattering amplitude $f^{(\pm)}(\epsilon_i, \hat{k}_i, \hat{r})$ has been expressed in terms of the elastic scattering phase shifts $\delta_{\ell}(\epsilon_i)$ in the usual way

$$f^{(+)}(\epsilon, \hat{k} \cdot \hat{r}) = \frac{4\pi}{k} \sum_{\ell m} e^{i\delta_{\ell}} \sin \delta_{\ell} Y_{\ell m}^*(\hat{k}) Y_{\ell m}(\hat{r}) \quad (3.2-197)$$

Therefore, writing

$$R_{\ell}^{(+)}(k, r) = e^{i\delta_{\ell}} \frac{w_{\ell}(k, r)}{kr} \quad (3.2-198)$$

the function $w_{\ell}(k, r)$ is the solution of

$$\frac{d^2}{dr^2} w_{\ell}(k, r) - \left[\frac{\ell(\ell+1)}{r^2} + \frac{2m}{\hbar^2} V(r) - k^2 \right] w_{\ell}(k, r) = 0 \quad (3.2-199)$$

satisfying the boundary conditions

$$w_{\ell}(k, 0) = 0 \quad (3.2-200)$$

$$w_{\ell}(k, r) \xrightarrow{r \rightarrow \infty} \sqrt{\frac{2}{\pi}} \sin(kr - \ell\pi/2 + \delta_{\ell})$$

and normalized according to

$$\int_0^{\infty} w_{\ell}(k, r) w_{\ell}(k', r) dr = \delta(k - k') \quad (3.2-201)$$

The final state wave function may be similarly expressed

$$\chi_{k_f}^{(+)}(\vec{r}) = \sum_{\ell=0}^{\infty} R_{\ell}^{(+)}(k_f, r) \sum_m Y_{\ell m}^*(\hat{k}_f) Y_{\ell m}(\hat{r}) \quad (3.2-202)$$

Using Eqs. (3.2-189), (3.2-196), (3.2-198) and (3.2-202) one easily finds

$$R_{\ell}^{(+)} = (-1)^{\ell} T_0 R_{\ell}^{(+)} = i e^{-i\delta_{\ell}(\epsilon)} \frac{w_{\ell}(k, r)}{kr} = e^{-2i\delta_{\ell}(\epsilon)} R_{\ell}^{(+)} \quad (3.2-203)$$

The one-electron matrix elements (3.2-195) then become

$$\begin{aligned} |\langle \beta | \vec{p} | \alpha \rangle|^2 &= (4\pi)^{-2} \sum_{\ell_i \ell_i' \ell_f \ell_f'} M_{\ell_f \ell_i} M_{\ell_f \ell_i'}^* (2\ell_i+1)(2\ell_i'+1)(2\ell_f+1)(2\ell_f'+1) \times \\ &\times \begin{pmatrix} \ell_i & \ell_f & 1 \\ 0 & 0 & 0 \end{pmatrix} \begin{pmatrix} \ell_i' & \ell_f' & 1 \\ 0 & 0 & 0 \end{pmatrix} \sum_{\ell} (-1)^{\ell+1} \begin{pmatrix} \ell_i & \ell_i' & \ell \\ 0 & 0 & 0 \end{pmatrix} \begin{pmatrix} \ell_f & \ell_f' & \ell \\ 0 & 0 & 0 \end{pmatrix} \times \\ &\times \begin{pmatrix} \ell_i & \ell_i' & \ell \\ \ell_f & \ell_f' & \ell \end{pmatrix} (2\ell+1) P_{\ell}(\hat{k}_f \cdot \hat{k}_i) \end{aligned} \quad (3.2-204)$$

in terms of the radial integrals

$$M_{\ell_f \ell_i} = im\omega \int_0^{\infty} r^2 dr \left[R_{\ell_f}^{(+)}(k_f, r) \right]^* r R_{\ell_i}^{(+)}(k_i, r) \quad (3.2-205a)$$

$$= \frac{i}{\omega} \int_0^{\infty} r^2 dr \left[R_{\ell_f}^{(+)}(k_f, r) \right]^* \frac{\partial V}{\partial r} R_{\ell_i}^{(+)}(k_i, r) \quad (3.2-205b)$$

and the Wigner 3-j and 6-j symbols (Edmonds, 1957). In obtaining this result the following vector coupling relations are used -- (equation numbers refer to Edmonds, 1957):

$$4.6.3) \int d^2\Omega Y_{\ell_1 m_1} Y_{1 \mu} Y_{\ell_2 m_2} = \left[\frac{3}{4\pi} (2\ell_1+1)(2\ell_2+1) \right]^{1/2} \begin{pmatrix} \ell_1 & \ell_2 & 1 \\ 0 & 0 & 0 \end{pmatrix} \begin{pmatrix} \ell_1 & \ell_2 & 1 \\ m_1 & m_2 & \mu \end{pmatrix}$$

$$4.6.5) \quad Y_{lm}(\hat{k}) Y_{l'm'}(\hat{k}) = \sum_{LM} \left[\frac{(2l+1)(2l'+1)(2L+1)}{4\pi} \right]^{1/2} \begin{pmatrix} l & l' & L \\ 0 & 0 & 0 \end{pmatrix} \begin{pmatrix} l & l' & L \\ m & m' & M \end{pmatrix} Y_{LM}^*(\hat{k})$$

and

$$6.2.8) \quad \sum_{\mu_1 \mu_2 \mu_3} (-1)^{l_1+l_2+l_3+\mu_1+\mu_2+\mu_3} \begin{pmatrix} j_1 & l_2 & l_3 \\ m_1 & \mu_2 & -\mu_3 \end{pmatrix} \begin{pmatrix} l_1 & j_2 & l_3 \\ -\mu_1 & m_2 & \mu_3 \end{pmatrix} \begin{pmatrix} l_1 & l_2 & j_3 \\ \mu_1 & -\mu_2 & m_3 \end{pmatrix} =$$

$$= \begin{pmatrix} j_1 & j_2 & j_3 \\ m_1 & m_2 & m_3 \end{pmatrix} \begin{Bmatrix} j_1 & j_2 & j_3 \\ l_1 & l_2 & l_3 \end{Bmatrix}$$

Integrating over the direction of the outgoing electron and averaging over the direction of the incident electron the free-free cross section (3.2-194) finally becomes

$$\sigma^{FF}(\vec{k}_1, \omega) = \frac{8\pi^4}{3} \left(\frac{e^2}{\hbar c} \right) \frac{k_f}{m\hbar\omega} \sum_{l_i=0}^{\infty} (l_i+1) \left\{ |M_{l_i+1, l_i}|^2 + |M_{l_i, l_i+1}|^2 \right\} \quad (3.2-206)$$

in terms of the radial integrals (3.2-205a), (3.2-205b).

(iii) Relation to Elastic Scattering

For low-energy photons the free-free absorption cross section may be approximately expressed in terms of elastic scattering amplitudes -- a relation discussed by Hundley (1962) and Low (1958) and utilized by many authors (for example, Ohmura and Ohmura (1960), Firsov and Chibisov (1961), and Ashkin (1966)).

The relation may be most easily derived in the one-electron approximation with neglect of exchange, although the result is of more general

validity (John, 1966). In this approximation the basic matrix element (Eq. 3.2-195) may be written

$$\langle \beta | \bar{p} | \alpha \rangle = \left(\chi_{k_f}^{(\beta)} | \bar{p} | \chi_{k_i}^{(\alpha)} \right)$$

where $\chi_{\mathbf{k}}^{(\beta)}$ satisfies a one-electron Schrödinger equation with Hamiltonian $H = H_0 + V$, which may be written in the Lippmann-Schwinger form (Goldberger and Watson, 1964, section 5.3)

$$\chi_{\mathbf{k}}^{(\beta)} = \varphi_{\mathbf{k}} + \frac{1}{\epsilon_{\mathbf{k}} + i\eta - H_0} V \chi_{\mathbf{k}}^{(\beta)}$$

$\varphi_{\mathbf{k}}$ is a plane-wave eigenstate of H_0 with energy $\epsilon_{\mathbf{k}}$. Then, using (3.2-183),

$$\begin{aligned} \langle \beta | \bar{p} | \alpha \rangle &= \frac{1}{\epsilon_f - \epsilon_i} \left(\chi_{k_f}^{(\beta)} | (H\bar{p} - \bar{p}H) | \chi_{k_i}^{(\alpha)} \right) \\ &= \frac{1}{\hbar\omega} \left\{ \left(\chi_{k_f}^{(\beta)} | V\bar{p} | \varphi_{k_i} + \frac{1}{\epsilon_{k_i} + i\eta - H_0} V \chi_{k_i}^{(\alpha)} \right) - \right. \\ &\quad \left. - \left(\varphi_{k_f} + \frac{1}{\epsilon_{k_f} - i\eta - H_0} V \chi_{k_f}^{(\beta)} | \bar{p}V | \chi_{k_i}^{(\alpha)} \right) \right\} \end{aligned}$$

The $\varphi_{\mathbf{k}}$ are momentum eigenstates, so we have

$$\begin{aligned} \langle \beta | \bar{p} | \alpha \rangle &= \frac{1}{\hbar\omega} \left\{ \hbar\mathbf{k}_i \left(\chi_{k_f}^{(\beta)} | V | \varphi_{k_i} \right) - \hbar\mathbf{k}_f \left(\varphi_{k_f} | V | \chi_{k_i}^{(\alpha)} \right) + \right. \\ &\quad \left. + \left(\chi_{k_f}^{(\beta)} | V\bar{p} \left(\frac{1}{\epsilon_i + i\eta - H_0} - \frac{1}{\epsilon_f + i\eta - H_0} \right) V | \chi_{k_i}^{(\alpha)} \right) \right\} \quad (3.2-207) \end{aligned}$$

The scattering amplitudes for elastic electron scattering may be written (op. cit., section 6.2)

$$\begin{aligned}
 f(\epsilon, \hat{k}_i, \hat{k}_f) &= - (2\pi)^2 \frac{m}{\hbar^2} \left(\varphi_{\vec{k}_f} |V| \chi_{\vec{k}_i}^{(+)} \right) \\
 &= - (2\pi)^2 \frac{m}{\hbar^2} \left(\chi_{\vec{k}_f}^{(+)} |V| \varphi_{\vec{k}_i} \right)
 \end{aligned}$$

when $\epsilon_f = \epsilon_i$. Thus, in the limit $\omega \rightarrow 0$, Eq. (3.2-207) may be written

$$\langle \beta | \vec{p} | \alpha \rangle \xrightarrow{\omega \rightarrow 0} \frac{\vec{k}_i - \vec{k}_f}{\omega} \left[\frac{-\hbar^2}{(2\pi)^2 m} f(\epsilon_i, \hat{k}_i, \hat{k}_f) \right] \quad (3.2-208)$$

Expanding the energy-dependent quantities in Eq. (3.2-207) about the mean energy $\bar{\epsilon} = 1/2 (\epsilon_i + \epsilon_f)$, Low (1958, eq. 1.7 N.R.) has shown

$$\langle \beta | \vec{p} | \alpha \rangle = \frac{-\hbar^2}{(2\pi)^2 m} \left\{ \frac{(\vec{k}_i - \vec{k}_f)}{\omega} f(\bar{\epsilon}, \hat{k}_i, \hat{k}_f) - \left(\frac{\vec{k}_i + \vec{k}_f}{2} \right) \frac{\partial f(\bar{\epsilon}, \hat{k}_i, \hat{k}_f)}{\partial \bar{\epsilon}} + O\left(\frac{\hbar\omega}{\bar{\epsilon}}\right) \right\} \quad (3.2-209)$$

Because the cross-term in the square of this matrix element contains the factor $(k_f^2 - k_i^2) \propto \omega$, retention of the first term alone should lead only to relative errors of order $(\hbar\omega/\bar{\epsilon})^2$ in the cross section, aside from possible elastic scattering resonances near energy $\bar{\epsilon}$.

Thus, an approximation to the free-free absorption coefficient useful at low photon energies is given by

$$\sigma^{FF}(k_1, \omega) = \frac{8\pi}{3} \frac{e^2 k_f \bar{\epsilon}}{m^2 c \omega^3} Q_d(\bar{\epsilon}) + O\left(\frac{\hbar \omega}{\bar{\epsilon}}\right)^2$$

(3.2-210)

$$\approx \frac{8\pi}{3} \alpha a_0^3 \left\{ \frac{k_f \bar{\epsilon}}{E_L} \right\}_{a.u.} Q_d(\bar{\epsilon}) \text{ (cm}^5\text{)}$$

In terms of the momentum transfer cross section -- in cm^2 -- which is defined as

$$Q_d(\bar{\epsilon}) = \int d\Omega_f (1 - \cos \theta) |f(\bar{\epsilon}, \cos \theta)|^2 \text{ (cm}^2\text{)} .$$

The bracketed quantity in Eq. (3.2-210) is in atomic units (a.u.), E_L being the photon energy, α the fine-structure constant, and a_0 the Bohr radius. Expressing the scattering amplitude in terms of phase shifts, Eq. (3.2-197), one immediately obtains

$$\begin{aligned} Q_d(\bar{\epsilon}) &= \frac{2\pi a_0^2}{\bar{\epsilon} \text{ a.u.}} \sum_{l=0} \left\{ (2l+1) \sin^2 \delta_{l-2} - 2(l+1) \sin \delta_l \sin \delta_{l+1} \cos(\delta_l - \delta_{l+1}) \right\} \\ &= \frac{2\pi a_0^2}{\bar{\epsilon} \text{ a.u.}} \sum_{l=0} (l+1) \sin^2 \left[\delta_l(\bar{\epsilon}) - \delta_{l+1}(\bar{\epsilon}) \right] \end{aligned}$$

and

$$\sigma^{FF}(k_1, \omega) \approx \frac{16\pi^2}{3} \alpha a_0^5 \left\{ \frac{k_f}{E_L} \right\}_{a.u.} \sum_{l=0} (l+1) \sin^2 \left[\delta_l(\bar{\epsilon}) - \delta_{l+1}(\bar{\epsilon}) \right]$$

(3.2-211)

As is evident from consideration of the asymptotic forms Eq. (3.2-187) and (3.2-188), the zero-frequency relation may be directly derived therefrom and concurs with the familiar arguments that small momentum transfers preferentially sample large radii. Forms equivalent to Eq. (3.2-211) have been so obtained by several authors and differ only in the electron energy at which the phase shifts δ_l are evaluated. Consideration of the validity criteria, Eq. (3.2-209), will resolve such ambiguity in favor of $\bar{\epsilon}$, to order $(\hbar\omega/\bar{\epsilon})^2$ with neglect of resonances, and is substantiated by direct comparison of Eq. (3.2-211) with numerical results by Ashkin (1966).

Modifications to Eq. (3.2-211) due to effects of electron exchange have recently been studied by John (1966), for the particular case of free-free absorption on the neutral hydrogen atom. The cross section is obtained from consideration of the asymptotic forms alone -- with due regard for exchange -- for low photon energies and for electron energies below the first excitation threshold. The result is the same as Eq. (3.2-210), with $Q_d(\bar{\epsilon})$ modified to

$$Q_d(\bar{\epsilon}) = \frac{2\pi a_0^2}{\bar{\epsilon}_{a.u.}} \sum_s \sum_l \omega_s(l+1) \sin^2 \left[\delta_l(\bar{\epsilon}, s) - \delta_{l+1}(\bar{\epsilon}, s) \right] \quad (3.2-212)$$

in terms of a spin statistical factor

$$\omega_s = \frac{(2s+1)}{\sum_s (2s+1)}$$

where s is the total spin of the system. The phase shifts $\delta_l(\bar{\epsilon}, s)$ are those obtained from a correct treatment of electron exchange -- the resultant

symmetry-dependence is manifested in their dependence on s .
As discussed by John, for photon energies such that Eq. (3.2-212) is no longer valid, an adequate treatment of exchange effects requires a detailed many-electron calculation -- such as the close-coupling computations of, for example, Burke (1962).

(iv) Free-free Absorption in the Coulomb Field of Ions:
Hydrogenic Transitions.

The long-range of the Coulomb potential guarantees that for reasonable positive ion densities, free-free transitions in the Coulomb field will dominate the low-frequency radiation absorption mechanisms. Most effects peculiar to such Coulomb transitions are present in the simplest case of free-free absorption in the field of hydrogen nuclei, and accordingly have been most extensively studied. A summary of the hydrogenic results is included in the first subsection below, followed by some non-hydrogenic studies in subsection (v). Finally, modifications due to Debye shielding are considered in subsection (vi).

The hydrogenic free-free absorption.

Radiative transitions in the field of a point charge Ze are called hydrogenic transitions. For such transitions the relevant wave functions and matrix elements may be directly obtained to any desired degree of accuracy and so have been extensively studied -- both as a precise test of physical theory and as an initial approximation to transitions in the field of ions other than hydrogen.

An extensive treatment of continuum Coulomb wave functions and transitions as well as useful approximations thereto are provided by the review article of Alder, et al (1956). Specific application to free-free

absorption and detailed numerical results are presented by Karzas and Latter (1961) and Grant (1958). Only results relevant to the foregoing general theory will be presented here; for details, the above references should be consulted.

As is well-known (Schiff, 1955), the long range of the Coulomb potential modifies the asymptotic forms Eqs. (3.2-187) and (3.2-188), so these become:

$$\chi_{\frac{+}{k}}^{(+)}(\vec{r}) \xrightarrow{|\vec{r}| \rightarrow \infty} (2\pi)^{-3/2} \left\{ e^{i[\vec{k} \cdot \vec{r} + \eta \ln(kr - \vec{k} \cdot \vec{r})]} + f_C^{(+)}(\hat{k}, \hat{r}) \frac{1}{r} \exp\left[\pm i(kr - \eta \ln 2kr)\right] \right\}.$$

$f_C^{(\pm)}(\hat{k}, \hat{r})$ is the Coulomb scattering amplitude (op. cit., eq. 20.10), and the dimensionless parameter η essentially characterizes the interaction of the electron with the field:

$$\eta = -\frac{Ze^2}{\hbar v} = -\frac{Z}{ka_0} = -Z\alpha \left(\frac{c}{v}\right). \quad (3.2-213)$$

Here v and k are the electron velocity and wave number, respectively, a_0 the Bohr radius, and α the fine structure constant. Classical theory applies for $|\eta| \gg 1$ or $(v/c) \ll Z/137$. Further, for $|\eta| \ll 1$ the Coulomb field produces only a small perturbation and Born approximation should be valid. The critical value $|\eta| = 1$ corresponds to an electron kinetic energy Z^2 Rydbergs = $13.6 Z^2$ eV.

For a pure Coulomb field the one electron states are well known. The complete wave functions of Eq. (3.2-194) with the prescribed normalization and asymptotic form are (Alder, et al., eq. II-B40, 41)

$$\langle \vec{r} | \alpha \rangle = (2\pi)^{-3/2} e^{-\eta_i \pi / 2} \Gamma(1+i\eta_i) e^{i\vec{k}_i \cdot \vec{r}} {}_1F_1 \left[-i\eta_i; 1; i(k_i r - \vec{k}_i \cdot \vec{r}) \right]$$

(3.2-214)

$$\langle \vec{r} | \beta \rangle = (2\pi)^{-3/2} e^{-\eta_f \pi / 2} \Gamma(1-i\eta_f) e^{i\vec{k}_f \cdot \vec{r}} {}_1F_1 \left[i\eta_f; 1; -i(k_f r + \vec{k}_f \cdot \vec{r}) \right]$$

in terms of the confluent hypergeometric function. The basic matrix elements are given by

$$|\langle \beta | \vec{p} | \alpha \rangle|^2 = \frac{9Z^2 e^4}{2(2\pi)^5 \omega^2 k_i k_f} \frac{df(\eta_i, \eta_f)}{d\eta_f}$$

in terms of the dimensionless function (Alder, et al., eq. II-E.62, 1956)

$$\frac{df(\eta_i, \eta_f)}{d\eta_f} = \frac{32\pi^3 \eta_i \eta_f}{9\xi^2} \frac{e^{2\pi\eta_i}}{\left(e^{2\pi\eta_i - 1} \right) \left(e^{2\pi\eta_f - 1} \right)} \frac{d}{dx} \left\{ -x \frac{d}{dx} \left| F(-i\eta_i; -i\eta_f; 1; x) \right| \right\}$$

$$x = -\frac{4\eta_i \eta_f}{\xi^2} \sin^2 \theta / 2, \quad \xi = \eta_f - \eta_i$$

Substituting these equations into Eq. (3.2-194) the free-free cross section is obtained

$$\sigma^{FF}(k_i, \omega) = \frac{3}{2} \alpha \frac{Z^2 e^4}{m^2 \omega^3 k_i} f(\eta_i, \eta_f) \text{ (cm}^5\text{)} \quad (3.2-215)$$

A classical calculation of the radiation absorbed by an electron being scattered in a Coulomb field was first carried out by Kramers (1923) - see, for example, Landau and Lifshitz (1962) - with the resulting so-called Kramers cross section given by

$$\sigma_K^{FF}(k_i, \omega) = \frac{16\pi^3}{3\sqrt{3}} \alpha \frac{Z^2 e^4}{m\hbar\omega^3 k_i} \quad (3.2-216)$$

The quantum-theory calculation was studied very early by Gaunt (1930), and it has since been customary to write the result (Eq. 3.2-215) in terms of the Kramers cross section,

$$\sigma^{FF}(k_i, \omega) = g_{FF}(k_i, k_f) \sigma_K^{FF}(k_i, \omega), \quad (3.2-217)$$

defining the so-called "Gaunt factor",

$$g_{FF}(k_i, k_f) = \frac{9\sqrt{3}}{32\pi^3} f(\eta_i, \eta_f) \quad (3.2-218)$$

$$= \frac{1}{3} e^{2\pi\eta_f} (e^{2\pi\eta_i} - 1)^{-1} (e^{2\pi\eta_f} - 1)^{-1} x_0 \frac{d}{dx_0} \left| F(-\eta_i, -\eta_f; 1; x_0) \right|$$

where

$$x_0 = -4\eta_i \eta_f / \pi^2$$

This result was first obtained by Sommerfeld (1951) and numerical values have been extensively tabulated (Karzas and Latter, 1961; Grant, 1958). Some forms of Eq. (3.2-216) useful in applications are

$$\sigma_K^{FF}(k_1, 0) = \frac{16\pi^3}{3^3} \alpha Z^2 \left(E_L^3 k_1 \right)_{a.u.}^{-1} a_0^5 \text{ (cm}^5\text{)}$$

(3.2-219)

$$= \frac{4}{3^3} \alpha^3 \lambda^3 \left(\frac{v_1}{c} \right) \left(\frac{Z^2 \text{ Ryd}}{\epsilon_1} \right) a_0^2 \text{ (cm}^5\text{)}$$

in terms of the fine structure constant α , the Bohr radius a_0 , the photon energy E_L (a.u.), and wave length λ (cm).

A spherical harmonic decomposition of the Coulomb states (Eq. 3.2-214) may be similarly performed (Alder, et al., 1956, II B.3). The radial functions $w_\ell(k, r)$ are given in terms of the regular Coulomb functions $F_\ell(k r)$

$$w_\ell(k, r) = \sqrt{\frac{2}{\pi}} F_\ell(k r) \quad (3.2-220)$$

and the phase shifts $\delta_\ell(\epsilon)$ become the Coulomb phase shifts $\sigma_\ell(\eta) = \arg \Gamma(\ell + 1 + i\eta)$. Evaluation of the radial matrix elements (Eq. 3.2-205) is discussed in detail by Alder, et al. (1956), and Biedenharn (1956) has shown the equivalence of the resulting equation (Eq. 3.2-206) with Eq. (3.2-215). As discussed by Alder, et al. (1956, pg. 452) the main contribution to the ℓ -sum in Eq. (3.2-206) is from values $\ell \sim \eta_1$, although the convergence is slow - particularly for low photon energies. It is of interest to study the dependence of this dominant ℓ ($=\ell_D$) on the photon energy $\hbar\omega$. The semi-classical, most-probable electron deflection angles are tabulated by Alder, et al. (1956) in their table II.7 in terms of $\xi = (\eta_f - \eta_i)$. Interpreting the deflection angles in terms of angular momenta, the rough correspondence shown in Table 3-2 is obtained.

Table 3-2

ξ^2	$t_D/\eta \sim$
0.1	12.
0.2	5.7
0.4	3.2
0.6	2.5
0.8	1.8
1.0	1.5

Approximating $t_D/\eta \sim 1/\xi$, one obtains

$$t_D \sim (\epsilon_i/h\nu).$$

A similar result is obtained from the expansions of Burgess (1958).

The complexity of the expression (Eq. 3.2-218) for the Gaunt factor has stimulated considerable effort to obtain approximations which are reliable in the various domains of interest. A critical summary of the approximations is provided by Grant (1958).

From an asymptotic evaluation of the hypergeometric function in Eq. (3.2-218), Menzel and Pekeris (1935) have obtained an approximation suitable for $\epsilon_i \ll 1$ and $\epsilon_i \ll \epsilon_f$,

$$g_{FF}^{MP}(k_i, k_f) \sim 1 + \frac{0.1728(1 + \epsilon_i/\epsilon_f)}{(1 - \epsilon_i/\epsilon_f)^{2/3}} \left(\frac{\text{Ryd}}{\epsilon_f}\right)^{1/3} - \frac{0.0496 \left(1 - \frac{484}{15} \frac{\epsilon_i}{\epsilon_f} + \frac{\epsilon_i^2}{\epsilon_f^2}\right) \left(\frac{\text{Ryd}}{\epsilon_f}\right)^{2/3}}{(1 - \epsilon_i/\epsilon_f)^{4/3}} + \dots$$

(3.2-221)

A similar technique was employed by Burgess (1958) for asymptotic approximations to the Coulomb radial matrix elements (Eq. 3.2-205) valid for $\epsilon_i \gg 1$, $\epsilon_f \ll \epsilon_f$ and $\epsilon \ll \eta_i$.

As discussed at the beginning of this section, the Born approximation is expected to be valid if $|\eta| \gg 1$, or if the photon energy is small:

$$g_{FF}^B(k_i, k_f) = \frac{\sqrt{3}}{\pi} \ln \left(\frac{k_i + k_f}{k_f - k_i} \right). \quad (3.2-222)$$

This displays the usual logarithmic divergence at small photon energies due to the infinite range of the pure Coulomb field. In practice, shielding effects of other electrons effectively limit the range of the field and so remove this divergence - as discussed in subsection (vi) below. Partial allowance for the long-range Coulomb distortions of the Born approximation plane waves by Elwert (1939) lead to a simple modification of Eq. (3.2-222),

$$g_{FF}^{BE}(k_i, k_f) = \left(\frac{e^{-2\pi\eta_i - 1}}{e^{-2\pi\eta_f - 1}} \right) \left(\frac{k_i}{k_f} \right) g_{FF}^B(k_i, k_f) \quad (3.2-223)$$

of considerably wider applicability.

In the limit $|\eta| \gg 1$ the "semi-classical" or WKB approximation is expected to be valid. Using WKB wave functions the free-free matrix elements may be evaluated (Alder, et al., 1956), with the resulting Gaunt factor

$$g_{FF}^C(k_i, k_f) = \frac{\sqrt{3}}{2\pi} e^{+\pi\eta} \left\{ x \frac{d}{dx} \left[K_{1/2} |x| \right]^2 \right\}_{x = |\xi|} \quad (3.2-224)$$

in terms of the modified Bessel function $K_{1/2} |x|$.

A useful approximation to g_{FF}^C for $|\xi| > 1$ is

$$g_{FF}^C(k_i, k_f) \sim 1 + 0.21775|\xi|^{-2/3} - 0.01312|\xi|^{-4/3}, \quad (3.2-224a)$$

a result which more closely approximates Eq. (3.2-218) than does the Menzel-Pekeris expansion (Eq. 3.2-221) - see Grant (1958, eq. 14). From this, the Kramers result is seen to be valid in the limit $\xi \gg 1$.

Grant has compared the above approximation with detailed numerical evaluation of Eq. (3.2-218). Better than one per-cent accuracy is obtained by the various approximations in the following domains of validity:

$(k_f/k_i) = 1.0 - 1.025,$	$ \eta_f \geq 30.0$: semi-classical (3.2-224)
$= 1.025 - 1.30,$	$ \eta_f \leq 0.1$: Born-Elwert (3.2-223)
	$ \eta_f \geq 5.0$: semi-classical (3.2-224)
$= 1.30,$	$ \eta_f \leq 0.1$: Born-Elwert (3.2-223)
	$ \eta_f \geq 2.5$: semi-classical (3.2-224)

From the tables of Alder, et al. (1956), the semi-classical Gaunt factor agrees with the quantum mechanical to within three percent for all $\eta_i \geq 1.0$ and $\xi \geq 0.1$.

In most applications the electron distribution function $F_e(\bar{k}_i)$ of Eq. (3.2-193) is Maxwellian. With Eq. (3.2-219) the Coulomb free-free absorption coefficient $\kappa_{FF}(\omega)$ may be written in terms of the Maxwell-average Gaunt factor $\langle g_{FF}(\omega) \rangle$,

$$\kappa_{FF}(\omega) = N_v N_e \frac{4\alpha^4 Z^2}{3^2 3\pi} \lambda^3 \left(\frac{Ryd}{kT} \right)^{1/2} a_0^2 \langle g_{FF}(\omega) \rangle \quad (\text{cm}^{-1}) \quad (3.2-225)$$

Values of $\langle g_{FF}(\omega) \rangle$ are contained in Karzas and Latter (1961).

(v) Free-free absorption on non-hydrogenic ions

A satisfactory treatment of free-free absorption in the fields of ions other than hydrogen would require extensive numerical treatments of, for example, Hartree-Fock ionic states perturbed by continuum electron states which are obtained from, say, close-coupling calculations. As yet, such detailed treatments are not available.

Fortunately, however, for low-energy photons the long range Coulomb field of charge Z_1 dominates the momentum-absorbing interaction and the non-Coulomb portions of the ionic field result in only small modifications of the hydrogen-results of the preceding section. On the other hand, high energy photons tend to sample the shorter range non-Coulomb field and so require the more detailed calculations.

From the discussion of Table 3-2, above, the angular momenta dominating the Coulomb absorption cross section (Eq. 3.2-206) are in the neighborhood of $l_D \sim (e_1/h\nu)$. Further, one expects departures from the pure Coulomb field to be limited to some range R , and so to contribute to the sum (Eq. 3.2-206) only through terms $l \sim L = k_1 R = (R/a_0)(e_1/\text{Ryd})^{1/2}$. Thus one expects substantial departure from the Coulomb results only when the dominant terms themselves become modified; that is, when $L \sim l_D$ or $h\nu \sim \frac{a_0}{R} e_1$.

In a one-electron spherically symmetric approximation, the states in a pure Coulomb field are given by Eq. (3.2-220)

$$w_l^C(k, r) = \sqrt{2/\pi} F_2(kr) \xrightarrow{r \rightarrow \infty} \sqrt{\frac{2}{\pi}} \sin(kr - l\pi/2 - \eta \ln 2kr + \sigma_l) ,$$

where σ_ℓ is the Coulomb phase shift given by

$$\sigma_\ell(\eta) = \text{Arg } \Gamma(\ell + 1 + i\eta) .$$

As described by Schiff (1955, § .20) the short-range departure from the pure Coulomb field results in an additional phase shift δ_ℓ for $r > R$, according to

$$w_\ell(k, r) = \sqrt{\frac{2}{\pi}} e^{i\delta_\ell} \left[F_\ell(kr) \cos \delta_\ell + G_\ell(kr) \sin \delta_\ell \right], \quad (r \geq R) \quad (3.2-226)$$

$$\xrightarrow{r \rightarrow \infty} \sqrt{\frac{2}{\pi}} e^{i\delta_\ell} \sin \left(kr - \frac{\ell\pi}{2} - \eta \ln 2kr + \sigma_\ell + \delta_\ell \right)$$

where one expects $\delta_\ell(k) \neq 0$ only for $\ell \lesssim kR$. The function $G_\ell(kr)$ in Eq. (3.2-226) is the solution of the Coulomb equation which is irregular at the origin and asymptotically approaches $\cos(kr - \ell\pi/2 - \eta \ln 2kr + \sigma_\ell)$.

The slow convergence of the ℓ -sum in Eq. (3.2-206) is best treated by explicitly separating the terms $\ell \leq L$ for which $\delta_\ell \neq 0$ and summing the remaining series in terms of the Coulomb result (Eq. 3.2-217) for charge Z_I :

$$\psi_{FF}(k_i, \omega) = g_{FF}(k_i, k_f) \psi_K^{FF}(k_i, \omega) + \quad (3.2-227)$$

$$\frac{8-4}{3} \alpha \frac{k_f}{m\omega} \sum_{\ell_i=0}^L (\ell_i+1) \left\{ \left| M_{\ell_i+1, \ell_i} \right|^2 + \left| M_{\ell_i, \ell_i+1} \right|^2 - \left| M_{\ell_i+1, \ell_i}^C \right|^2 - \left| M_{\ell_i, \ell_i+1}^C \right|^2 \right\}$$

The M_{l_f, l_i}^C are from Eq. (3.2-205) in terms of the actual solutions (Eq. 3.2-226), and the M_{l_f, l_i}^C are the Coulomb radial matrix elements which may be expressed in terms of hypergeometric functions (Alder et al., 1956; Gordon, 1929) and have been approximated by Burgess (1958).

DeVore (1964) has recently carried out a one-electron approximate calculation for the nitrogen ion N^+ . The potential $V(r)$ of Eq. (3.2-199) was taken to be the unperturbed static Hartree-Fock potential of the ion, and effects of exchange and polarization were neglected. Comparison of the resulting numerical solutions of Eq. (3.2-199) with the asymptotic form (Eq. 3.2-226) for large r determined the phase shifts δ_l . For electron energies $\epsilon \leq 0.36$ Ryd, the s- and p-wave phase shifts were large, and the d-phase shifts were less than two percent of the s- values. Higher angular momenta were ignored, and the free-free absorption cross section was obtained from Eq. (3.2-227) with $L = 2$ and photon energies $h\nu \leq 0.01$ Ryd. Comparison with hydrogen ion results indicates only small differences for $h\nu \leq 0.01$ - despite the large s- and p-wave phase shifts. This result substantiates the general discussion at the beginning of this section.

The predominance of the asymptotic domain in the absorption of low-energy photons led Peach (1965) to evaluate the radial matrix elements (Eq. 3.2-205) in terms of the asymptotic wave functions (Eq. 3.2-226) alone, modified at small radii to ensure convergence of integrals over the irregular solution. This approach corresponds to the familiar Coulomb approximation

of Bates and Damgaard (1949) and Burgess and Seaton (1960) . The Coulomb integrals are evaluated numerically and the results tabulated in convenient form. In terms of the Kramers' cross section (Eq. 3.2-219) - with $Z = Z_1$ - Peach's results may be expressed as a "Gaunt factor" defined by

$$\frac{\pi}{\sqrt{3}} g_{FF}^P = \frac{1}{4} \sum_{l_i, l_f} l_{>} G^2(\epsilon_i, l_i, \epsilon_f, l_f) \cos^2 \left[\delta_{l_f}(\epsilon_f) - \delta_{l_i}(\epsilon_i) + \pi \chi(\epsilon_i, l_i, \epsilon_f, l_f) \right] \quad (3.2-228)$$

Here $l_f = l_i \pm 1$ only and $l_{>}$ is the greater of (l_i, l_f) . The functions G and χ are tabulated for l_i, l_f equal (0-3) and a range of values of ϵ_i and $\hbar\omega$. For low-energy electrons the phase shifts may be obtained from the quantum defect method (Burgess and Seaton, 1960) .

A similar result follows from Eq. (3.2-211) and the corresponding Gaunt factor may be written

$$\frac{\pi}{\sqrt{3}} g_{FF}^{EL} = \frac{1}{n_i n_f} \sum_{l=0} (l+1) \sin^2 \left[\delta_l + \sigma_l - \delta_{l+1} - \sigma_{l+1} \right] \quad (3.2-229)$$

and $\sigma_{l+1} = \sigma_l + \tan^{-1} \left(\frac{n}{2l+1} \right)$. In the limit of zero photon energy (Peach, 1965, eq. 32) and vanishing phase shifts δ , (Eq. 3.2-228-229) reduce to the same expression.

In view of the slow rate of convergence of the l -sum for Coulomb interactions it appears most convenient to follow Eq. (3.2-227) and sum explicitly only over those l -values for which δ_l is non-vanishing. Then, for example, Eq. (3.2-229) becomes (in terms of the hydrogen Gaunt factor $g_{FF}^H(Z_1)$ with charge Z_1)

$$g_{FF}^{\text{Ion}} = g_{FF}^H(Z_1) + \frac{\sqrt{3}}{\pi\eta_i\eta_f} \sum_{l=0}^L (l+1) \left[\sin^2(\delta_{l+\sigma_l} - \delta_{l+1} - \sigma_{l+1}) - \frac{\eta^2}{\eta^2 + (l+1)^2} \right] \quad (3.2-230)$$

This form appears to be the most useful approximation to the (anticipated) small modification of the Coulomb Gaunt factor due to the non-Coulomb short range ionic field. Inclusion of electron exchange effects follows the treatment of John (Eq. 3.2-212 and 1964, 1966).

(vi) Effects of Debye shielding

As discussed in connection with Eq. (3.2-222) the logarithmic divergence of the Coulomb Gaunt factor for small photon energies is a manifestation of the assumed infinite range of the potential. A small- ω expansion of the exact result (Eq. 3.2-218) - using Eq. II E-66b of Alder, et al. (1956) leads directly to Eq. (3.2-222), as does the elastic scattering approximation (Eq. 3.2-210) with the known Coulomb scattering amplitude. This last formulation displays most clearly the origin of the divergence in the small angle scattering - and hence large impact parameters.

As is well known the assumption of a pure Coulomb potential is valid only near the ion; the interaction is screened at large radii by other electrons. For moderate densities and high temperatures an exponentially-screened Debye potential is a useful approximation to the actual potential responsible for the free-free absorption. That is,

$$V(r) = -\frac{Ze^2}{r} e^{-\alpha r}, \quad (3.2-231)$$

where

$$\alpha^2 = \frac{4\pi e^2}{kT} \sum_i n_i Z_i (Z_i + 1) \quad (3.2-232)$$

for a gas at an electron temperature T_e with n_i ions per cm^3 of type i and charge Z_i .

As the Born approximation correctly exhibits the low photon energy divergence a Born calculation of the scattering amplitude for potential $V(r)$ of Eq. (3.2-231) in the low photon energy approximation (Eq. 3.2-210) may be expected to demonstrate the effects of shielding on the low frequency Gaunt factor. The result of such a calculation is that the Coulomb Born Gaunt factor (Eq. 3.2-222) is replaced by

$$g_{FF}^{BD}(k_i, k_f) = \frac{\sqrt{3}}{2} \left(\frac{1}{2} \right) \left\{ \ln \frac{(k_f + k_i)^2 + \alpha^2}{(k_f - k_i)^2 + \alpha^2} + \frac{\alpha^2}{(k_i + k_f)^2 + \alpha^2} + \frac{\alpha^2}{(k_i - k_f)^2 + \alpha^2} \right\} \quad (3.2-233)$$

a result not diverging at $\omega \rightarrow 0$.

A WKB-approximation of more general validity - for small α and not too small ω or too large ϵ_1 - has been obtained by Green (1958),

$$g_{FF}^G(k_1, \omega) = \left[1 - 2\mu^2 \left(\frac{\text{Ryd}}{\hbar\omega} \right) \right] g_{FF}(k_1', \omega) + O(\mu^3), \quad (3.2-234)$$

in terms of the Coulomb Gaunt factor $g_{FF}(k_1', \omega)$ at the same frequency ω but lower energy $\epsilon_1' = k_1'^2 \text{Ryd} = \epsilon_1 - 2\mu Z^2 \text{Ryd}$. The dimensionless parameter μ is related to the screening constant α through

$$\mu = \frac{\alpha a_0}{Z}$$

The Maxwellian velocity average of (Eq. 3.2-234) has been compared with detailed machine calculations and has proved useful over an extensive temperature-density range. To first order in μ , one may use (see Eq. 3.2-226)

$$\langle g_{FF}^{\text{shielded}}(\omega) \rangle \approx \langle g_{FF}(\omega) \rangle - \left[\langle g_{FF}(\omega) \rangle - g(k_1=0, \omega) \right] \left(2\mu Z^2 \frac{\text{Ryd}}{kT} \right) \quad (3.2-235)$$

As the expression (Eq. 3.2-235) is only accurate to first order in μ it is most useful in determining when screening effects may safely be neglected. Numerical evaluation of the velocity averages of Eq. (3.2-234) should be suitable for most cases of interest.

(vii) Free-free absorption on neutral atoms

The short range of the electron-atom interaction relative to the Coulomb force results in much smaller free-free radiation absorption cross sections on atoms than on ions - typically smaller by several orders of magnitude (DeVore, 1965).

A convenient though rough measure of the relative importance of atoms in free-free absorption is provided by the work of Firsov and Chibisov (1961). Assuming s-wave interactions only, for electron energies less than a few eV, the momentum transfer cross section was approximated by the zero-energy elastic scattering cross section $\sigma_{el}^{e1}(0)$ in Eq. (3.2-210). The Maxwellian velocity-average may then be performed and the result compared with the Kramers cross section. When the relative numbers of ions and atoms is estimated by the Saha equation, the condition that the atomic and ionic frequency-integrated free-free absorption be equal yields the result

$$N_{atom} \sigma_{el}^2 = 2.2 \times 10^{26} \theta^{-5/2} e^{-\epsilon_1/\theta} \quad (3.2-236)$$

Here θ is the temperature and ϵ_1 the ionization potential of the atom in eV, σ_{el} is the zero-energy elastic scattering cross section in 10^{-16} cm^2 , and N_{atom} is the atom density (cm^{-3}). For a given temperature, ionization energy, and cross section (Eq. 3.2-236) then provides a critical density above which atomic free-free absorption is expected to dominate and below which ionic absorption should dominate. In obtaining Eq. (3.2-236), use was made of the fact that the absorption per atom is much less than the absorption per ion, so equal absorption contributions necessarily implies $N_{atom} \sim N$, the total particle density (atoms and ions).

Few detailed studies of the free-free absorption on neutral atoms have as yet been carried out. A general treatment is of equivalent complexity to the case of non-hydrogenic ions - discussed at the beginning of subsection (v) above - so the resort to extensive approximation is necessary.

Due both to its relative simplicity and to its particular relevance in astrophysical applications, the free-free absorption on neutral hydrogen has been most extensively studied. Early work by Wheeler and Wildt (1942) employed the acceleration radial matrix element (Eq. 3.2-205b) in the cross section (Eq. 3.2-206), using Born approximation wave functions and the unperturbed Hartree potential of the hydrogen atom - without polarization or exchange.

Chandrasekhar and Breen (1946) employed similar approximations - differing principally in the replacement of the Born approximation s-wave by a numerical solution in the assumed potential. The result is a much larger cross section, approaching an order of magnitude greater than the result of Wheeler and Wildt at $\lambda \sim 2\mu$ and $T = 6300^\circ\text{K}$.

Most recent studies have employed the phase shift approximation. As emphasized by Ohmura (1964) this formulation has the particular virtue that variationally determined phase shifts are generally more accurate than variational wave functions. Ohmura and Ohmura (1960, 1961) included s-wave phase shifts only, with allowance for polarization and exchange according to Eq. (3.2-212), and found the results of Chandrasekhar and Breen (1946) to be reduced by 40-60 per cent as a result.

Finally, a very detailed treatment of the phase-shift approximation was carried out by John (1964, 1966). Numerical solutions in the static Hartree potential of the atom were obtained - with inclusion of exchange - for angular momentum states $l = 0, 1, 2$ and electron energies less than one Rydberg. It was found that

inclusion of the effects of exchange increased the importance of the higher phase shifts ($l \geq 1$), and the results obtained were 30-40 percent less than those of Chandrasekhar and Breen (1946). Detailed comparison of the results obtained by use of the numerical wave functions in Eq. (3.2-206) with the phase shift approximation (Eq. 3.2-211) for the initial and final electron energies independently ranging from 0.01 to 0.1 Ryd indicate at worst 3 percent difference in p-waves and 12 percent in the s-waves. As the photon energy in the worst case is $h\nu = 99 \epsilon_1$, the agreement is remarkable in view of Eq. (3.2-209).

A variational method for direct determination of the hydrogen free-free matrix element itself has recently been proposed by Khare and Rudge (1965) which is somewhat reminiscent of the Schwinger variational procedures of scattering theory. Employing simple trial wave functions, the authors were able to obtain results substantially in agreement with the numerical results of John.

For atoms other than hydrogen relatively few results are available. DeVore (1964, 1965) has studied the free-free absorption by neutral nitrogen, assuming an unperturbed Hartree-Fock potential and an effective polarization potential

$$v_p(r) = \frac{-\alpha}{(r^2 + r_p^2)^2}$$

for two values of α and r_p . Numerical solutions to Eq. (3.2-199) were obtained for $l = 0, 1, 2$, and the cross section was evaluated from Eq. (3.2-206).

An approach essentially equivalent to that of DeVore has been pursued by Kivel et al. at AVCO (1966) for both atomic oxygen and nitrogen. A semi-empirical exchange potential akin to the Slater exchange approximation was included and various constants in the potentials were normalized to agree with results of electron-scattering calculations. The gross features of the resulting cross sections are in reasonable agreement with the phase shift approximation Eq. (3.2-211). In a recent report Kivel (1966) has further explored the dependence of the approximate exchange interaction on the configuration of the free electron plus atom through a study of the corresponding Hartree-Fock equations. To obtain results consistent with the experimental work of Taylor (1963), Kivel finds it necessary to evaluate separately the free-free cross sections for each of the participating atomic configurations.

A comparison of similarly obtained cross sections for argon with various phase shift approximations has recently been published by Ashkin (1966). The various approximations differ in their choice of energy-centering of the phase shifts in Eq. (3.2-211). The photon energy illustrated is $\hbar\omega \sim 1.8$ eV and the range of initial electron energies ϵ_1 is .01 to 1.0 Ryd. For $\epsilon_1 \geq 0.05$ Ryd ($\hbar\omega/\epsilon_1 \leq 2.7$) the use of the average energy $\bar{\epsilon}$ of Eq. (3.2-210) leads to essential agreement with the numerical results. For energies $.03$ Ryd $< \epsilon_1 < .05$ Ryd Ashkin finds that a formula due to Holstein (1965) gives results in best agreement with the numerical results.

Holstein retains the difference $(\vec{k}_1 - \vec{k}_2)^2$ in Eq. (3.2-208) explicitly and evaluates the scattering amplitude $f(\epsilon, \cos\theta)$ only at the mean energy $\bar{\epsilon}$. Clearly,

for $\hbar\omega/\epsilon_1 \ll 1$, all these results are equivalent to Eq. (3.2-210).

The RAND report of Hundley (1962) introduces the use of effective-range expansions for the evaluation of the low-energy phase shifts of Eq. (3.2-211). Peach (1965) suggested estimating ion phase shifts by the "quantum defect" method, which has been demonstrated by Moiseiwitsch (1963) to correspond to an effective-range expansion.

Dalgarno and Lane (1966) have employed the effective-range expansion of O'Malley, et al. (1961) which is more correctly applicable to atoms. The authors obtain useful velocity-averaged absorption coefficients in terms of a few atomic parameters and some conveniently tabulated numerical functions. The approximations employed assume low temperatures - as atomic absorption may be expected to be dominated by ion absorption at high temperatures - and retain only the s-wave phase shift in Eq. (3.2-211). As shown by O'Malley, et al. (1961) the zero-order elastic scattering cross section is expected to have a low-energy dependence of the form

$$q_0(\cdot) = \frac{4\pi}{k^2} \sin^2 \delta_0(k)$$

$$= 4\pi (D_1 + D_2 \epsilon^{1/2} + D_3 \epsilon \ln \epsilon + D_4 \epsilon + D_5 \epsilon^{3/2} + \dots) a_0^2 \quad (3.2-237)$$

where D_1, D_2 , and D_3 may be written in terms of the scattering length $A a_0$ and the atomic polarizability αa_0^3 according to

$$D_1 = A^2, \quad D_2 = \frac{2\pi}{3} \alpha A, \quad D_3 = \frac{8}{3} \alpha^2 A.$$

If one approximates the momentum-transfer cross section of Eq. (3.2-210) by the elastic scattering cross section $q_0(c)$, the explicit energy dependence of Eq. (3.2-237) allows direct evaluation of the Maxwell-averaged absorption coefficient, which is expressed in terms of the D_i 's and certain tabulated functions of temperature alone. For most applications of astrophysical interest the approach of Dalgarno and Lane appears eminently suited, particularly in view of the large numbers of atomic species and states commonly present in the gas.

3.3 Line broadening*

Reference has been made a number of times in Chapter 2 and in sections 3.1 and 3.2 of this chapter to the finite width of spectral lines and to their frequency-dependent profiles $b(\nu)$ which have to be taken quantitatively into account in opacity calculations on hot gases. The study of line shapes and line broadening influences is an active and difficult research field of long standing (see for example the reviews of Baranger (1962), Griem (1964) and Alier (1963)). It is thus not the purpose of this section to make a detailed review of the field, but rather to record established results of line broadening studies which are of direct application to the study of hot-gas opacities.

It is well known that the experimentally recorded profiles of spectrum lines in emission or absorption depend upon three classes of influences: a) instrumental effects, b) intrinsic properties of emitting or absorbing particles and, c) environmental effects. In the theoretical discussion of opacities it is often assumed that purely instrumental effects have already been allowed for. Intrinsic properties of the emitting or absorbing atom or molecule give rise to its 'natural' width which is usually so small compared to other effects that it can be neglected. Two classes of environmental effect are however important and often occur together. The first of these depends upon the random motion of the absorbing or emitting particle, the component of which motion in the line of sight gives rise to a Doppler broadening of the line. The second of these results from the influences of collisions of neighboring particles on the emitter or absorber and is thus called collision broadening. Both effects are strongly temperature dependent. All of these contributors to line shapes are briefly discussed below.

* Written by R. W. Nicholls

a) Instrumental Profile. Geometrical optics determines the gross size of the slit image on the detector. The slit width is always reduced as far as possible so that most of the instrumental broadening arises from diffraction effects. The finite size of the spectrograph implies that a finite and truncated wave front reaches the detector from the slit. A diffraction image of the slit of finite angular width is thus formed. In what follows it will be assumed that this is either negligible relative to other causes, or can be allowed for.

b) Natural Profile. The Lorentz profile of Eqs. (3.1-4a, b, c) is retained in the quantum formulation

$$\alpha_{\nu} = \frac{e^2 f}{mc} \frac{\frac{\Gamma}{4\pi}}{(\nu - \nu_0)^2 + \left(\frac{\Gamma}{4\pi}\right)^2} \quad (3.3-1)$$

where $\Gamma = \Gamma_U + \Gamma_L$ = sum of widths of U and L levels according to the uncertainty principle. If L is the ground state, $\Gamma_L \sim 0$ and $\Gamma_U = \frac{1}{t}$ where t is the lifetime of the upper state.

The central maximum is very narrow ($w = \frac{\Gamma}{2\pi}$) (often negligible compared to other broadening influences) and the wings can be fairly extensive. The algebraic form of the natural profile (Eq. (3.3-1)) is retained with appropriate redefinition of parameters in the quantitative description of the collisionally broadened line profile (see Eq. (3.3-3)).

c) Thermal Profile. The random motion in line of sight of the absorbing (or emitting) atoms implies a thermal of Doppler profile of the form

$$I_{\nu} = I_0 \exp \left(-\beta c^2 \frac{(\nu - \nu_0)^2}{\nu_0^2} \right) \quad (3.3-2)$$

where $\beta = \frac{u}{2kT}$, and u = molecular weight and T = temperature.

d) Collision Broadening. Collision broadening is a result of motion of neighbors and of environment. A complete theoretical discussion of the complicated matter of collision broadening is outside the scope of this review (see Griem, 1964). Line broadening by collision results from collisions with

Atoms of same kind - (Self Broadening, or "Holtsmark" Broadening)

Atoms of a different kind - (Lorentz broadening)

Ions
Electrons } - (Stark Broadening)

Two types of theories, collisional and statistical, have been developed to explain the effects. In the former, the truncation of wave trains by collisions is examined by classical or quantum methods, often for uncharged perturbers. In the latter, the influence of the average electric field strength of neighboring charge carriers is taken into account statistically and the Stark Effect invoked (Aller, 1963; Griem, 1964; Baranger, 1962).

The practical result of collision broadening is to produce a line with a profile similar in form to Eq. (3.3-1) but with width parameters Γ_{natural} and $\Gamma_{\text{collision}}$. Thus

$$a_{\nu} = \frac{\frac{\pi e^2 f}{m c} \left(\frac{\Gamma_n + \Gamma_c}{4\pi} \right)}{(\nu - \nu_0)^2 + \left(\frac{\Gamma_n + \Gamma_c}{4\pi} \right)^2} \quad (3.3-3)$$

Nearly always the influence of Γ_c is much greater than Γ_n and gives rise to lines with very wide wings.

e) Effects of Fields. If the gas has external magnetic and electric fields applied through it in addition to the microfields of collisions, Stark and Zeeman broadening have to be considered.

In most typical situations of interest to this review more than one broadening influence is present. For example, natural and thermal broadening often occur in low pressure laboratory sources. Thermal and collision broadening (illustrated in Fig. 3-4) often dominate the scene at higher pressures. If $f_1(\nu)$ and $f_2(\nu)$ are the frequency profiles of the two independent effects, the combination of two effects is represented by the convolution or 'folding' integral

$$F(\nu) = \int_{-\infty}^{\infty} f_1(\nu - \nu') f_2(\nu') d\nu' \quad (3.3-4)$$

A number of analytical and numerical methods have been developed to treat specific cases of this integral. For example the combined application of

natural and thermal broadening was treated by Voigt (see Mitchell and Zemansky, 1934) and the volume absorption coefficient is

$$k_v = k_0 \frac{a}{\pi} \int_{-\infty}^{\infty} \frac{\exp(-y^2) dy}{a^2 + (x-y)^2} \quad (3.3-5)$$

where

$$x = \frac{2(\nu - \nu_0) \sqrt{\ln 2}}{W_D} \quad (3.3-6a)$$

$$y = \frac{2 \sqrt{\ln 2} \Gamma}{W_D} \quad (3.3-6b)$$

$$a = \frac{W_n}{W_D} \sqrt{\ln 2} \quad (3.3-6c)$$

W_n = natural or Lorentz width at 1/2 intensity
 $= \Gamma / 2\pi$

W_D = Doppler or thermal width at 1/2 intensity = $\frac{2\nu_0}{c} \sqrt{\frac{2kT \ln 2}{\mu}}$ (3.3-6d)

Tables of these so-called Voigt Profiles are available for parametric interpolation (Van der Hulst and Resnick, 1947; Hummer, 1965). Because collision broadening can often be expressed in terms of a Lorentzian profile (see Eq. (3.3-3)), collision and thermal broadening can also be treated in this way. Hansen, (1964) has recently treated the problem of combined Stark (ionic) and Doppler broadening by analytic approximation.

The thermally and collision-broadened line often has a central core which is dominated by thermal effects and wings which are dominated by collision effects. In this case the natural line profile exerts a negligible effect.

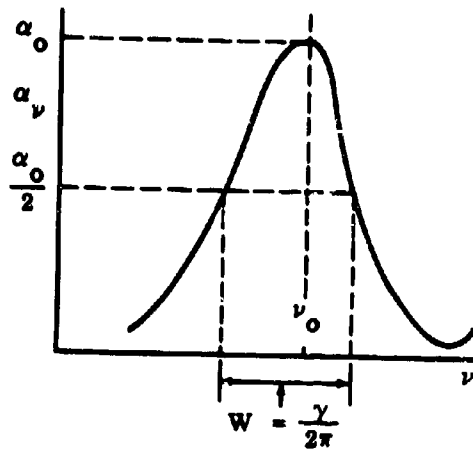


FIG. 3.1 LORENTZ PROFILE

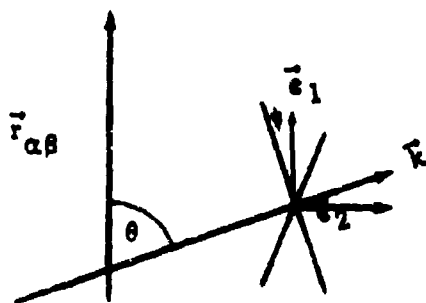


FIG. 3-2 DIRECTIONAL RELATIONSHIPS BETWEEN THE DIPOLE MATRIX ELEMENT VECTOR $\vec{r}_{\alpha\beta}$, THE PROPAGATION VECTOR \vec{k} , AND THE UNIT POLARIZATION VECTORS $\vec{\epsilon}_1$ and $\vec{\epsilon}_2$.

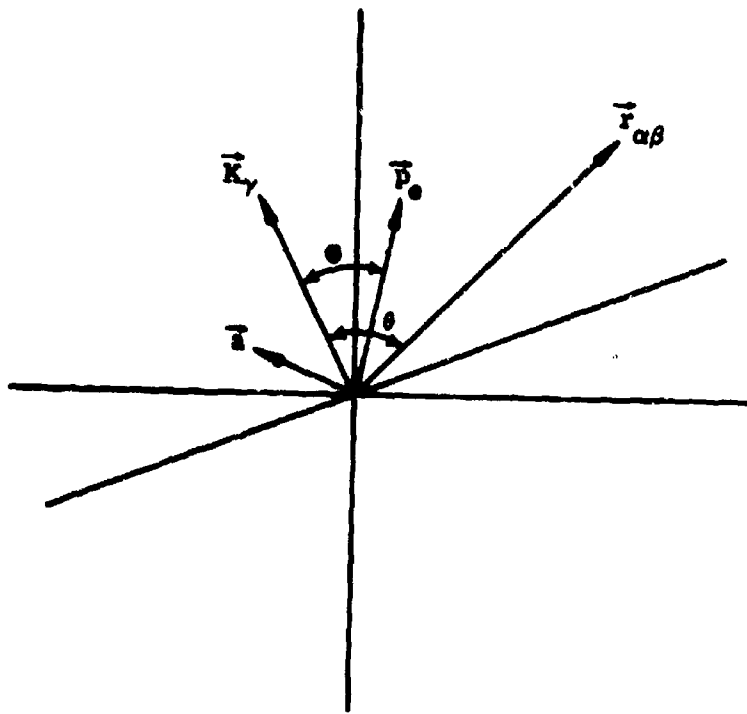


FIG. 3-3 DIAGRAM INDICATING THE VECTORS INVOLVED
IN THE PHOTOELECTRIC OR RECOMBINATION
PROCESS, AND THE ANGLES BETWEEN THEM.



FIG. 3-4 REPRESENTATIVE LINE
PROFILE SHOWING
THERMAL CENTER AND
COLLISION WINGS

Chapter 4. THEORY OF MOLECULAR ABSORPTION

It was pointed out in Section 3.2 that the quantity which determines the probability of a U-L electric dipole transition for an atomic system is the transition strength matrix element $S_{UL} = \left| e\vec{r}_{\alpha\beta} \right|^2$ (see Eqs. (3.2-14) and (3.2-20)). In this chapter we shall adopt the notation

$$S_{UL} = \left| R_e \right|^2 = \left| \int \psi_U^* \underline{M} \psi_L d\tau \right|^2 \quad (4.1-1)$$

where $R_e \left(= e\vec{r}_{\alpha\beta} \right)$ is the transition moment, ψ_U and ψ_L are the complete wave functions of the upper and lower states, \underline{M} is the electric dipole moment and $d\tau$ is the element of configuration space. Similar matrix elements to S_{UL} control higher and other pole transitions (Allen, 1963). Transition probability parameters such as absorption coefficients, oscillator strengths, Einstein A and B coefficients, are, apart from constants, the product of S_{UL} with appropriate powers of frequency (see Eqs. (4.1-17), (4.1-18), (4.1-19)).

In this chapter we discuss the form that S_{UL} takes for molecular transitions. We also review the molecular transition probability parameters which are determined by S_{UL} . For the purposes of this chapter the absorption coefficient is the most important of these, and we review calculations which have been made during the past few years on the molecular contributions to the absorption coefficient of heated air in Chapter 7.

4.1 The Born-Oppenheimer approximation and its consequences

The internal degrees of freedom of the molecule influence the transition strength matrix element of a molecular spectral feature. Consider the $U, v', J', \Lambda', M' \rightarrow L, v'', J'', \Lambda'', M''$ transition. U and L are the upper and lower electronic states, or components of multiplets. For the other quantum numbers, primes refer to the upper levels and double primes refer to the lower levels. v is the vibrational quantum number, J is the total or rotational quantum number, Λ is the quantum number of the component of the electronic angular momentum along the internuclear axis, and M , the magnetic quantum number (which should not be confused with \underline{M} the electric dipole moment) refers to the component of J in the direction

of an externally applied magnetic field. It takes $2J + 1$ values.

Born and Oppenheimer (1927) proposed a molecular model in which it was assumed that the electronic state of the molecule was negligibly affected by the nuclear vibration and rotation. This assumption allows the complete molecular wave function to be written in Eq. (4.1-2) as the product of factors which take account of the electronic, the vibrational and the rotational motion independently. A discussion of vibration-rotation interaction effects is postponed until Section 4.3. The total energy of the molecule is written in Eq. (4.1-3) as the sum of the three components E_{elect} , E_{vib} and E_{rot} .

$$\Psi_{e,v,J,\Lambda,M} = \psi_e(\underline{r}_e, r) \frac{\psi_v(r)}{r} \psi_{J\Lambda M}(\theta, \chi, \varphi) \quad (4.1-2)$$

$$E = E_{\text{elect}} + E_{\text{vib}} + E_{\text{rot}} \quad (4.1-3)$$

$\Psi_{e,v,J,\Lambda,M}$ is the complete molecular wavefunction of the electronic state e , vibrational level v , with J , Λ , and M defined as above.

$\psi_e(\underline{r}_e, r)$ is the electronic wavefunction written in subsequent equations as ψ_u or ψ_l for upper or lower states respectively. The \underline{r}_e represent electron coordinates relative to the internuclear axis, r is the internuclear separation, $\psi_v(r)$ is the vibrational wavefunction of the one dimensional oscillator in the v 'th level appropriate to a particular molecular potential (centrifugal effects have been neglected). $\psi_{J\Lambda M}(\theta, \chi, \varphi)$ is the wavefunction of the symmetric top rotator. θ, χ, φ are the Euler angles of the molecular coordinate system relative to the fixed one.

The dipole moment \underline{M} can be resolved into contributions \underline{M}_e arising from the molecular electrons and \underline{M}_n arising from the nuclei.

$$\underline{M} = \underline{M}_e + \underline{M}_n \quad (4.1-4)$$

where
$$\underline{M}_e = -\sum_s e \underline{r}'_s = \left\{ -\sum_s e \underline{r}_s \right\} \cdot \underline{D}(\theta, \chi, \varphi) \quad (4.1-5)$$

\underline{r}'_s is the position vector of the s 'th electron relative to external axes and \underline{r}_s is the position vector of the s 'th electron relative to the figure axis of the molecule. $\underline{D}(\theta, \chi, \varphi)$ is the dyadic appropriate to the transformation of axes. Its elements are the direction cosines of the angles between the coordinate systems. The element $d\tau$ may be written

$$d\tau = d\tau_e dv = d\tau_e r^2 \sin \theta d\theta d\varphi d\chi \quad (4.1-6)$$

where dv is the volume element for the vibrator and rotator and $d\tau_e$ is the element for electrons.

From Eqs. (4.1-1), (4.1-2), (4.1-4), (4.1-6) R_0 may now be written

$$\begin{aligned} R_{Lv}^{Uv'J'\Lambda'M'} &= \int \psi_u^* \psi_{\underline{y}'} \psi_{J'\Lambda'M'} (\underline{M}_e + \underline{M}_n) \psi_L \psi_{\underline{y}''} \psi_{J''\Lambda''M''} d\tau_e dv \\ &= \int \psi_u^* \psi_{\underline{y}'} \psi_{J'\Lambda'M'} (\underline{M}_e) \psi_L \psi_{\underline{y}''} \psi_{J''\Lambda''M''} d\tau_e dv \\ &\quad + \int \psi_u^* \psi_L d\tau_e \int \psi_{\underline{y}'} \psi_{J'\Lambda'M'} \underline{M}_n \psi_{\underline{y}''} \psi_{J''\Lambda''M''} dv \end{aligned}$$

for a molecular line. Orthogonality between ψ_U and ψ_L reduce the second integral on the right hand side to zero.

Using Eqs. (4.1-5) and (4.1-6) the first member may be rewritten as

$$\left| R_{L'V''J''\Lambda''M''}^{U'V'J'\Lambda'M'} \right| = \int \psi_{V'} \left(\int_U \psi_{L'}^* \Sigma \mathbf{L}_z \psi_V d\tau \right) \psi_{V''} d\tau \int \psi_{J'\Lambda'M'} |D(\theta, \chi, \varphi)| \psi_{J''\Lambda''M''} d\Omega$$

where $d\Omega = \sin \theta d\theta d\phi$ (4.1-7)

The first integral on the right hand side of Eq. (4.1-7) when summed, if necessary, over degenerate electronic states and squared is called the band strength $S_{L'V''}^{U'V'}$. The second integral determines the selection rules. It has been studied for various types of molecular transitions by Dennison (1926), Kronig and Rabi (1927), Rademacher and Reichs (1926, 1927), Schadee (1964) and others. When summed over the degenerate quantum numbers M' and M'' and squared it is the Hönl-London (1925), or line intensity, factor $S_{J''\Lambda''}^{J'\Lambda'}$.

After squaring and summing over degeneracies Eq. (4.1-7) thus becomes

$$S_{L'V''J''\Lambda''}^{U'V'J'\Lambda'} = |R|^2 = S_{L'V''}^{U'V'} \cdot S_{J''\Lambda''}^{J'\Lambda'} \quad (4.1-8)$$

$S_{L'V''J''\Lambda''}^{U'V'J'\Lambda'}$ is the strength matrix of the individual molecular band line. $S_{L'V''}^{U'V'}$ is the band strength defined in Eq. (4.1-9) and is a very important quantity (see the discussion of Section 4.4). It can be factored into two terms controlled respectively by electronic and vibrational aspects of the motion of the molecule. $S_{J''\Lambda''}^{J'\Lambda'}$ is the Hönl-London factor (see Section 4.2 for a more complete discussion) or line intensity factor. It is often a quotient of

simple polynomial functions of J and Λ and is well known for all branches of most allowed molecular transitions.

The band strength $S_{Lv''}^{Uv'}$ is an average, with respect to the vibrational wave functions,*

$$S_{Lv''}^{Uv'} = \left| \int \psi_{v'} R_e(r) \psi_{v''} dr \right|^2 \quad (4.1-9)$$

of the electronic transition moment $R_e(r)$ defined in Eq. (4.1-10).

$$R_e(r) = \int \psi_u^* M_e \psi_L^* d\tau_e = \int \psi_u^* |-\sum e_L r_s| \psi_L d\tau_e \quad (4.1-10)$$

The electronic transition moment is thus an average with respect to electronic wave functions of the electric dipole moment.

* Footnote:

In the case of infrared vibration-rotation transitions where $\psi_U = \psi_L$, Eq. (4.1-9) becomes

$$S_{Lv''}^{Uv'} = \left| \int \psi_{v'} M \psi_{v''} dr \right|^2 \quad (4.1-9a)$$

See discussion in Section 4.4.

If $R_e(r)$ is independent of r , Eq. (4.1-9) becomes

$$S_{Lv'}^{Uv'} = R_e^2 \left| \int \psi_{v'} \psi_{v''} dr \right|^2 = R_e^2 q_{v'v''} \quad (4.1-11)$$

On the other hand, as is much more realistic, if $R_e(r)$ varies with r in a polynomial fashion

$$R_e(r) = \sum_n a_n r^n,$$

it is possible (Fraser, 1954) to use the r -centroid $\bar{r}_{v'v''}$, where

$$\bar{r}_{v'v''} = \frac{\int \psi_{v'} r \psi_{v''} dr}{\int \psi_{v'} \psi_{v''} dr}; \quad (4.1-12a)$$

$$(\bar{r}_{v'v''})^n = \frac{\int \psi_{v'} r^n \psi_{v''} dr}{\int \psi_{v'} \psi_{v''} dr} \quad (4.1-12b)$$

to write Eq. (4.1-9) as

$$\begin{aligned} S_{Lv'}^{Uv'} &= \left| \int \psi_{v'} \sum_n a_n r^n \psi_{v''} dr \right|^2 = \left| \sum_n a_n \int \psi_{v'} \psi_{v''} r^n dr \right|^2 \\ &= \left| \sum_n a_n \bar{r}_{v'v''}^n \right|^2 \left| \int \psi_{v'} \psi_{v''} dr \right|^2 = R_e^2 (\bar{r}_{v'v''})^n q_{v'v''} \end{aligned} \quad (4.1-13)$$

The vibrational overlap integral square $q_{v'v''}$ in Eq. (4.1-11) and Eq. (4.1-13) is called the Franck-Condon factor

$$q_{v'v''} = \left| \int \psi_{v'} \psi_{v''} dr \right|^2 \quad (4.1-14)$$

It is responsible for the operation of the Franck-Condon Principle in the determination of relative band intensities. The r -centroid is a characteristic internuclear separation associated with the band. Franck-Condon factors and r -centroids are discussed more fully in Section 4.3.

Finally, using Eqs. (4.1-8) and (4.1-13) the total line strength is written in Eq. (4.1-15) as the product of the square of the electronic transition moment, the Franck-Condon factor, and the Hönl-London factor.

$$S_{L\nu''J''\Lambda''}^{U\nu'J'\Lambda'} = R_e^2 (F_{\nu'\nu''}) \cdot q_{\nu'\nu''} \cdot S_{J''\Lambda''}^{J'\Lambda'} \quad (4.1-15)$$

The sum rules for the Hönl-London factors and Franck-Condon factors are

$$\sum_{J'} S_{J''\Lambda''}^{J'\Lambda'} = 2J'' + 1, \quad \sum_{J''} S_{J''\Lambda''}^{J'\Lambda'} = 2J' + 1 \quad (4.1-16a)$$

$$\sum_{\nu''} q_{\nu'\nu''} = 1 = \sum_{\nu'} q_{\nu'\nu''} \quad (4.1-16b)$$

A useful interpretation of Eq. (4.1-15) is that $R_e^2(r)$ controls the magnitude of the transition strength for the whole band system, $q_{\nu'\nu''}$ determines its distribution from band to band in the system and $S_{J''\Lambda''}^{J'\Lambda'}$ influences the distribution from line to line in a band. This is an approximate point of view because both $R_e(F_{\nu'\nu''})$ and $q_{\nu'\nu''}$ influence the distribution of transition strength from band to band. However, $q_{\nu'\nu''}$ can vary by many orders of magnitude from band to band in a system and $R_e(F_{\nu'\nu''})$ varies

relatively slowly across a system. Nicholls and Stewart (1962) and Tatum (1967) have discussed these topics more fully.

Any application of Eq. (4.1-15) to the study of molecular intensities requires a good knowledge of $R_e(r)$, $q_{v'v''}$, and $S_{J''\Lambda''}^{J'\Lambda'}$ for all of the contributing transitions. These factors are thus discussed in some detail in following sections.

A number of molecular transition probability parameters may now be defined in terms of $S_{Lv''J''\Lambda''}^{Uv'J'\Lambda'}$. It is well known (Allen, 1963) that the general expressions for oscillator strength f , and the Einstein A and B coefficients are: (see also Eqs. (3.2-14), (3.2-20), (3.2-21) and (3.2-62)

$$|gf| = |g_U f_{UL}| = |g_L f_{LU}| = \frac{8\pi^2 \nu_{UL} S_{UL}}{3 h e^2} \quad (4.1-17)$$

$$g_U A_{UL} = \frac{64\pi^4 \nu_{UL}^3 S_{UL}}{3 h c^3} \quad (4.1-18)$$

$$|g_U B_{UL}| = |g_L B_{LU}| = \frac{8\pi^2 S_{UL}}{3 h^2} \quad (4.1-19)$$

where g is the statistical weight. In the case of a molecular line we make the following substitutions:

$$g_U = d_U(2J' + 1); \quad g_L = d_L(2J'' + 1)$$

$$S_{UL} = R_e^2(\bar{r}_{v'v''}) q_{v'v''} S_{J''\Lambda''}^{J'\Lambda'}$$

d_U and d_L are the degeneracies of the electronic states U and L and are $(2S + 1)$ for Σ states ($\Lambda = 0$) and $2(2S + 1)$ for other electronic states (Davidson, 1962). The spectroscopic notation is standard (Herzberg, 1950).

Eqs. (4.1-17), (4.1-18), and (4.1-19) are thus rewritten as follows for a molecular line:

$$d_U(2J' + 1) f_{L\nu''J''}^{U\nu'J'} \downarrow = d_L(2J'' + 1) f_{L\nu''J''}^{U\nu'J'} \uparrow = \frac{8\pi^2 m}{3 h e^2} \nu_{L\nu''J''}^{U\nu'J'} R_e^2(F_{\nu'\nu''}) q_{\nu'\nu''} S_{J''\Lambda''}^{J'\Lambda'} \quad (4.1-20)$$

$$d_U(2J' + 1) A_{L\nu''J''}^{U\nu'J'} = \frac{64\pi^4}{3 h c^3} (\nu_{L\nu''J''}^{U\nu'J'})^3 R_e^2(F_{\nu'\nu''}) q_{\nu'\nu''} S_{J''\Lambda''}^{J'\Lambda'} \quad (4.1-21)$$

$$d_U(2J' + 1) B_{L\nu''J''}^{U\nu'J'} \downarrow = d_L(2J'' + 1) B_{L\nu''J''}^{U\nu'J'} \uparrow = \frac{8\pi^2}{3 h^2} R_e^2(F_{\nu'\nu''}) q_{\nu'\nu''} S_{J''\Lambda''}^{J'\Lambda'} \quad (4.1-22)$$

The arrows indicate whether a transition is upward ($L \rightarrow U$) or downward ($U \rightarrow L$).

For the purposes of this discussion perhaps the most important transition probability parameter is the absorption coefficient. As pointed out in Chapter 2 the three most commonly defined absorption coefficients, when integrated over a spectral feature are:

$$\text{Atomic (or molecular)} \quad \int \alpha_\nu d\nu = \frac{\pi e^2}{m c} f_{LU} \quad (\text{cm}^2/\text{atom}) \quad (4.1-23)$$

$$\text{Volume} \quad \int u_\nu d\nu = \frac{\pi e^2}{m c} N_L f_{LU} \quad (\text{cm}^{-1}) \quad (4.1-24)$$

$$\text{Mass} \quad \int \kappa_\nu d\nu = \frac{\pi e^2}{m c \rho} N_L f_{LU} \quad (\text{cm}^2/\text{gm}) \quad (4.1-25)$$

α_ν is the optical cross section and u_ν is the reciprocal of the photon mean free path. Eq. (4.1-24) is rewritten in Eq. (4.1-26) for a molecular line

$$\int u_\nu d\nu = \frac{8\pi^3}{3hc} \frac{N_{L\nu''J''}}{d_L(2J''+1)} \nu_{L\nu''J''}^{U\nu''J''} R_e^2(\bar{r}_{\nu''\nu''}) q_{\nu''\nu''} S_{J''\Lambda''}^{J'\Lambda'} \quad (4.1-26)$$

This equation may be modified, as in Eq. (4.1-27), to take account of the line shape $b(\nu)$ where

$$\int b(\nu) d\nu = 1 .$$

$$\text{Thus } u_\nu d\nu = \frac{8\pi^3}{3hc} \frac{N_{L\nu''J''}}{d_L(2J''+1)} \nu_{L\nu''J''}^{U\nu''J''} R_e^2(\bar{r}_{\nu''\nu''}) q_{\nu''\nu''} S_{J''\Lambda''}^{J'\Lambda'} b(\nu) d\nu . \quad (4.1-27)$$

As was pointed out in Section 3.3, various instrumental, thermal, and environmental influences control $b(\nu)$ *. It is very difficult to propose a completely satisfactory theoretical form for it which will satisfy all circumstances. A Voigt (see Van der Hulst and Reesnick, 1947; Hummer, 1965) profile is often used to take account of the combined effects of thermal and collision broadening. The last influence produces a line shape similar in general form though much broader than the Lorentz shape produced by natural broadening. One procedure which is often used is to use a Lorentz profile (Eq. (4.1-28)) in which the half width at half height σ is a variable parameter which can be modified as circumstances warrant.

$$F(\nu) = \frac{1}{\pi} \frac{\sigma}{\sigma^2 + (\nu - \nu_{L\nu''J''}^{U\nu''J''})^2} \quad (4.1-28)$$

*Footnote:

An often unconsidered source of apparent broadening is unresolved or only partly resolved rotation structure as in the case of components of Λ -doubling (Herzberg, 1950).

Eqs. (4.1-26) and (4.1-27) and equations derived from them have been the bases of a number of the calculations of the molecular contributions to absorption coefficients of hot air. These calculations are reviewed in Chapter 7.

A formal summation over all the lines of a band is possible in each of Eqs. (4.1-20) - (4.1-26) to produce similar equations which apply to the whole $v'v''$ band. In the summations, an approximation of the form

$$\sum v^n R_e^2 q S = \bar{v}^n R_e^2 q \sum S = \bar{v}^n R_e^2 q (2J+1) \quad (4.1-29)$$

is involved where n is 0, 1, or 3. It is assumed in such an approximation that a characteristic frequency \bar{v} can be assigned to a whole band. This is a fair approximation for a band whose rotational structure is not too greatly developed and which does not extend over too great a frequency range. Care must be taken not to force such approximations on cases where they do not reasonably apply.

The following equations for integrated bands result

$$d_U f_{Lv''}^{Uv'} \downarrow = d_L f_{Lv''}^{Uv'} \uparrow = \frac{8\pi^2 m}{3 h e^2} v_{v'v''} R_e^2(\bar{v}_{v'v''}) q_{v'v''} \quad (4.1-30)$$

$$d_U A_{Lv''}^{Uv'} = \frac{64\pi^4}{3 h c^3} v_{v'v''}^3 R_e^2(\bar{v}_{v'v''}) q_{v'v''} \quad (4.1-31)$$

$$d_U B_{Lv''}^{Uv'} \downarrow = d_L B_{Lv''}^{Uv'} \uparrow = \frac{8\pi^2}{3 h^2} R_e^2(\bar{v}_{v'v''}) q_{v'v''} \quad (4.1-32)$$

$$\int_{\text{Band}} d_U v = \frac{8\pi^3}{3 h c} \frac{N_{Lv''}}{d_L} v_{v'v''} R_e^2(\bar{v}_{v'v''}) q_{v'v''} \quad (4.1-33)$$

It is often convenient to rewrite Eq. (4.1-33) so as to take account of the contributions of bands (or parts of bands) which fall within the frequency increment $\Delta\nu$. Thus

$$\bar{\mu}_\nu = \frac{1}{\Delta\nu} \sum_{\text{Bands}} \int_{\text{Bands}} k_\nu d\nu \quad (4.1-34)$$

Eqs. (4.1-30) - (4.1-33) have been used to interpret band intensity measurements in absorption or emission in terms of transition probability parameters. Eq. (4.1-34) has been used in preliminary "broad band" estimates of opacities of hot gases.

In some experiments vibrational lifetimes $\tau_{\nu'}$ have been measured. They are related to Einstein A coefficients by

$$\tau_{\nu'} = \frac{1}{\sum_{\nu''} A_{\nu'\nu''}} \quad (4.1-35)$$

A formal summation procedure, similar in principle to that of Eq. (4.1-29), has been used to define the oscillator strength f_{LU} of the whole band systems. Summation is over all ν' which combine with a given ν'' .

$$d_L f_{LU} = d_L \sum_{\nu'} f_{\nu''\nu'} = \frac{8\pi^2 m}{3 h e^2} \sum_{\nu'} \nu_{\nu'\nu''} R_e^2(f_{\nu'\nu''}) q_{\nu'\nu''} \quad (4.1-36)$$

If an effective $\bar{\nu}$ for the system can be defined, and if $R_e(r)$ is a constant, Eq. (4.1-36) can be rewritten, (using Eq. (4.1-16b)

$$d_L f_{LU} = \frac{8\pi^2 m}{3 h e^2} \bar{\nu} \bar{R}_e^2 \sum_{v'} q_{v'v''} = \frac{8\pi^2 m}{3 h e^2} \bar{R}_e^2 \bar{\nu} \quad (4.1-37)$$

Dividing Eq. (4.1-37) by Eq. (4.1-30)

$$f_{LU} = \frac{f_{v''v'} \bar{\nu}}{q_{v'v''} \nu_{v'v''}} \quad (4.1-38)$$

Eq. (4.1-38) should be used with extreme care, if at all, in view of the somewhat gross assumptions involved in the definition of $\bar{\nu}$ and \bar{R}_e .

It is clear from the discussion of Eqs. (4.1-20)-(4.1-22), (4.1-26), (4.1-27), (4.1-30)-(4.1-34), (4.1-38), that a good knowledge of $\nu, R_e(r), q_{v'v''}, S_{J''\Lambda''}^{J'\Lambda'}$ and N_L is necessary before they can be used in theoretical studies of opacities. The factors which control N_L are discussed in Volume 1 by Gilmore and in Chapter 7 of this volume. Although it might appear that ν is always known in principle, from spectroscopic research this is not always the case, particularly when one is dealing with $\nu_{LV''J''}^{UV'J'}$ in very hot gases where high values of J' will be excited. Unambiguous band analyses have been carried out for a relatively small number of bands of each system and those analyses which have been carried out usually involve only those J -values excited in common laboratory sources running at temperatures under 1000°K . Extrapolation of the low temperature analyses to high degrees of rotational development using the usual equations (Herzberg, 1950) for $\nu_{LV''J''}^{UV'J'}$ can be a somewhat naive procedure for no account is taken of possible perturbations at high J numbers. The same argument holds to a lesser extent for extrapolation of vibrational analyses.

A review is now made in subsequent sections of Hönl-London factors, Franck-Condon factors, r -centroids, electronic transition moments and band strengths, their properties and methods by which they may be obtained.

4.2 The Hönl-London Factors $S_{J''\Lambda''}^{J'\Lambda'}$

The line strengths for a symmetric top model of a diatomic molecule were first studied with the old quantum theory by Hönl and London (1925). They were re-investigated by Dennison (1926), Rademacher and Reiche (1927), Kronig and Rabi (1927), Hill and Van Vleck (1928), Budo (1937), and Earls (1935), using quantum mechanics, for branches of bands of allowed transitions and for most common coupling cases. Herzberg (1950), Johnson (1949), Jevons (1932), Mulliken (1931), and others list tables of the Hönl-London factors for these cases. Schlapp (1932), Kovacs (1960) and others have studied the factors for forbidden transitions. Schadee (1964) and Tatum (1967) have compiled tables for important transitions. The sum rules for Hönl-London factors were given in Eq. (4.1-16a). As a simple example, the Hönl-London expressions for allowed singlet, $\Delta\Lambda = 0$ transitions are given for the P, Q and R branches by the following equations

$$S_J^R = \frac{(J'' + 1 + \Lambda'')(J'' + 1 + \Lambda'')}{J'' + 1} = \frac{(J' + \Lambda')(J' - \Lambda')}{J'}$$

$$S_J^Q = \frac{(2J'' + 1)\Lambda''^2}{J''(J'' + 1)} = \frac{(2J' + 1)\Lambda'^2}{J'(J' + 1)}$$

$$S_J^P = \frac{(J'' + \Lambda'')(J'' - \Lambda'')}{J''} = \frac{(J' + 1 + \Lambda')(J' + 1 - \Lambda')}{J' + 1}$$

As the selection rule $\Delta J = 0, \pm 1$ determines the P, Q or R branch concerned, it is only necessary to specify the branch and the J-value in the superscripts and subscripts to the factors. For branches of bands of higher multiplicity the K value has to be specified (Johnson, 1949). The intensity profile in a branch is determined from line to line by $S_J \exp(-E_J/kT)$ for thermally maintained populations. In $J = J'$ for emission and $J = J''$ for absorption the early literature S_J was written as i_J and called the intensity factor.

4.3 Franck-Condon Factors and r-Centroids, Vibrational Wavefunctions and Molecular Potentials

A strict vibrational selection rule ($\Delta v = \pm 1$) applies to infrared vibration-rotation transitions and which involve a single parabolic (Simple Harmonic Oscillator) potential. In this case, the potential (electronic state) is common to the upper and the lower vibrational levels. The vibrational wave functions of Eq. (4.1-9a) are Hermite functions and are mutually orthogonal. M is assumed to be linear in r . Under these circumstances (see Herzberg, 1950, p. 80) $S_{Lv}^{Uv'}$ vanishes unless the above selection rule applies. Realistic potentials are somewhat anharmonic and thus some weak infrared vibration-rotation bands are observed for transitions which break the selection rule. Infrared vibration-rotation transitions are only observed in heteronuclear molecules. Homonuclear molecules, because of their symmetry, have no permanent dipole moment and are thus infrared inactive.

The Franck-Condon principle takes the place of a strict selection rule for vibrational transitions between different electronic states by specifying their relative probabilities. In the qualitative discussion of the photodissociation of diatomic molecules, Franck (1925) pointed out that a spontaneous electronic transition affects neither the instantaneous position nor momentum of the nuclei. Thus the most preferred molecular transitions are "vertical" ones in which r does not change on the energy-internuclear separation diagrams. Further the molecule is, on a time average basis, most

likely to be found near the turning points (r_{\min} or r_{\max}) of its oscillation, and thus those $v'-v''$ transitions are most likely to occur where one of the turning points of the upper level v' is nearly equal to one of the turning points of the lower level v'' .

Condon (1926) placed this suggestion on a quantitative basis and showed (Condon, 1928) that it was the square of the overlap integral of vibrational wave functions (or Franck-Condon factor as it was called by Bates, 1952) which was a measure of the relative probability of the $v'-v''$ transition. This is consistent with Franck's suggestion, as the vibrational wave functions have large antinodes in the region of r_{\min} and r_{\max} . When the overlap between these regions of the two wave-functions is large, the Franck-Condon factor will be large. Thus 'vertical' transitions at the turning points of molecular oscillations will be most probable.

Other transitions are not forbidden. Their relative strength will be determined by the amount of non-cancelled overlap between their wave functions. Condon (1947) has given a very good review of the circumstances leading to the development of the principle.

It is thus the purpose of this section to review our knowledge of Franck-Condon factor $q_{v',v''}$ arrays and related quantities for important electronic band systems of diatomic molecules.

$$q_{v',v''} = \left| \int \psi_{v'} \psi_{v''} dr \right|^2 \quad (4.3-1)$$

Considerable effort has been expended, particularly over the past two decades, to provide tables of Franck-Condon factors for important band systems. Spindler (1965) lists some of the more recent calculations.

The first requirement for calculation of q-arrays is a knowledge of the vibrational wave functions appropriate to the molecule in the upper and lower states of the transitions. Once these are known, a number of derived quantities of the wavefunctions including q-values can be calculated. The wave functions are solutions of the one-dimensional Schroedinger Eq. (4.3-2) for the linear single particle oscillator of reduced mass $\mu = M_1 M_2 / (M_1 + M_2)$ moving under the action of the 'rotationless' molecular potential $U(r)$. (We discuss the effect of vibration-rotation interaction later.)

$$\frac{d^2 \psi_v}{dr^2} + \frac{8\pi^2 \mu}{h^2} [E_v - U(r)] \psi_v = 0 \quad (4.3-2)$$

The specification of a realistic molecular potential provides the first problem. No completely realistic non-numerical analytic potential is available. All analytic potentials are empirical, and plausible representations of what has been thought to be a reasonable approximation to molecular behavior. The parabolic or simple harmonic potential was the first to be used. Eq. (4.3-2) has closed solutions (Hermite functions) for such potentials. The model is only realistic at very low values of vibrational quantum number. Manneback (1951), Condon (1928) and others have produced limited arrays of 'harmonic oscillator' q-values for a number of transitions. Aitken (1951) produced a large number of arrays of them for many band systems on the Harvard Mark I Computer. An attempt was made by Gaydon and Pearse (1939) to overcome some of the lack of realism of the parabolic potential by linearly distorting its wave functions to fit an equivalent Morse potential. Although the resulting functions are non-orthogonal, they were used with some success by a number of workers. Pillow (1949),

Nicholls (1950), and others extended and applied the method to many transitions (see list of references given by Nicholls and Stewart (1962)).

The Morse (1929) potential, Eq. (4.3-3) has had the greatest popularity in molecular spectroscopy for many years, because, among other properties, it does predict the correct vibrational energy level array E_v for many cases. Although it is an empirical suggestion, it does have some physical plausibility in the adequate representation of the mechanical anharmonicity of many molecular states. There are nevertheless relatively severe theoretical objections to it (e.g., it often predicts the incorrect dissociation energy $D_e = \omega_e^2/4\omega_e x_e$, $U(0)$ is non-infinite, etc.)

$$U(r) = D_e \left[1 - \exp - \beta (r - r_e) \right]^2 ; \beta = 2 \left(\frac{2\pi^2 c}{h} \mu \omega_e x_e \right)^{1/2} \quad (4.3-3)$$

The vibrational wave functions for the Morse potential are also known in closed form and have been the basis of a number of calculations of Franck-Condon factors. Some of these calculations were performed on desk calculators (Jarman and Nicholls, 1954) when it was not common to have access to digital computers. A number of approximate methods for evaluation of 'Morse' Franck-Condon factors were thus developed (Fraser and Jarman, 1953; Jarman and Fraser, 1953; Fraser, 1954; Wu, 1952). Franck-Condon factor arrays were computed for a large number of astrophysically and aeronomically important arrays by these methods (Jarman, Fraser and Nicholls, 1953, 1955; Fraser, Jarman and Nicholls, 1954; Nicholls, Fraser and Jarman, 1959; Nicholls, Fraser, Jarman and McEachran, 1960). Access to computers allowed the direct

computation of Morse Franck-Condon Factor Arrays (using a program which first computed the wave functions (Nicholls, 1961)). Over 85 Franck-Condon factor arrays have been computed to high quantum numbers by this method, some of which have been published (Nicholls, 1960; 1961; 1962 a,b,c,d; 1963a; 1964a,b; 1965 a,b,c,d; Ory, 1964a,b; Halman and Laulicht, 1965). Not only have radiative transitions been studied but also excitation and ionization transitions whose cross sections are to some extent controlled by the Franck-Condon factor (Craggs and Massey, 1959) have also been studied in a number of important cases (Nicholls, 1961; 1962a; 1965e; Wacks and Krauss, 1961; Wacks, 1964).

One major limitation of 'Morse' Franck-Condon factor arrays is the inability of the Morse potential to represent with realism the behavior of all molecules. Rydberg (1931, 1933), Klein (1932), Dunham (1932) developed methods of constructing molecular potentials numerically from location of the classical turning points of the oscillator at each value. Rees (1946) placed this method on a sound analytic basis. The starting point for such calculations was measured molecular constants, particularly the B_v values derived from band analysis. Jarman (1959, 1960), Vanderslice, Mason, Maisch and Lippincott (1959, 1960) and Hurley (1962) have demonstrated the equivalence of Rydberg and Klein's WKB method (which would be expected to hold at high v values) and Dunham's representation of the potential at low v values. The basis of the method has been reviewed by Gaydon (1953), Gilmore (1965), and Spindler (1965), Jarman (1959, 1960), Vanderslice and co-workers (see Steele, Lippincott and Vanderslice, 1962 and references therein) and others have computed realistic Rydberg-Klein-Dunham-Rees potentials for many molecular electronic states. Gilmore (1965) has made a recent definitive and exhaustive

study of the potential energy curves by this method for all the known states of N_2 , O_2 , NO and their ions.

The end results of such work is a list of r_{\min} and r_{\max} for each vibrational level for which measured values of G_v and B_v (Herzberg, 1950) were used. A rectification of such a list into $U(r)$ at equally spaced intervals of r is necessary and has been performed in different ways by different workers.

Computer-oriented methods have been developed by Jarman (1961, 1963a,b), Cooley (1961a,b), and Cashion (1963) for the numerical solution of equation (40) appropriate to a numerical potential produced in the manner described above. These methods depend on the analysis of Numerov (1933). The resulting wave functions have then been used to compute Franck-Condon factors by straightforward numerical integration of their products. Jarman (1963b) has discussed criteria which wavefunctions arising from these methods must satisfy. A number of other workers (Zare, Larson, and Berg, 1965; Spindler, 1965) have used Cooley's program to obtain wavefunctions for the computation of Franck-Condon factor arrays for a number of important band systems.

A comparison between arrays of Franck-Condon factors computed from realistic molecular potentials and from Morse potentials indicates that in general there is good agreement between the two arrays at low quantum numbers and less good agreement at high quantum numbers although in some cases the agreement at high quantum numbers is much better than might have been a priori expected. If there is a very great divergence between the potentials then there will be a divergence between the arrays.

All of the above discussion of Franck-Condon factors relates to a rotationless model of the molecular vibrator (in the $J=0$ state). It is tacitly assumed that the coupling between vibration and rotation is small and that the centrifugal energy $\frac{\hbar^2}{8\pi^2 I} \frac{1}{2} (J(J+1) - \Lambda^2)$ of molecular rotation which should really be added to $U(r)$ in equation (40) has a negligible effect on the molecular potential. This assumption is not always valid, particularly for light, rapidly rotating molecules such as hydrides, and in principle the Eq. (4.3-2) of which ψ_v is the solution should have the centrifugal energy term added to $U(r)$. Pekeris (1934) solved Eq. (4.3-2) for a Morse potential to which the rotational energy barrier has been added. Herman and Rubin (1955) and Herman, Rothery, and Rubin (1958) have examined vibration rotation interaction, using Morse-Pekeris wave functions, for vibration-rotation spectra. Fraser (1958) examined the effect of vibration-rotation interaction using the analytic approximation with perturbation correction (Fraser, 1954b). Learner (1961) made a similar study of hydrides (particularly OH) and computed overlap integrals by numerical integration of Morse-Pekeris wave functions, James (1960, 1961) made a similar study using harmonic and anharmonic oscillators and perturbation methods. Haycock (1963) extended Fraser's work with particular emphasis on hydrides. The result of these studies would seem to indicate that vibration-rotation effects are important in the case of light molecules, particularly hydrides. For heavier molecules the effect appears to be small, but more work is needed before this conclusion can be considered to be firmly established. Nearly all of the work that has so far been done has been for molecular transitions where the effect is expected to be large.

It is very likely to be a small effect for the transition considered to be important on hot air.

So far we have limited the discussion of Franck-Condon factors to transitions between discrete vibrational levels, for which the sum rule (Eq. (4.1-16b)) holds. There is an important class of molecular transitions which however, involve unbound continuum states in one of the levels. For example, the dissociation continuum of the O_2 Schumann-Runge of the O_2 Herzberg I systems, involve transitions between the $v'' = 0$ level of the $X^3\Sigma_g^-$ ground state and levels above the dissociation limit of the $B^3\Sigma_u^-$ and the $A^3\Sigma_u^+$ states respectively in cold O_2 . For hot O_2 other values of v'' are incorporated. The wave function $\psi_{cont}(r, \nu)$ of the unbound state is a function of energy as well as internuclear separation and cannot be normalized in the same way as bound state wave functions. Normalization is carried out with respect to energy and involves the asymptotic amplitude (see for example Jarman and Nicholls, 1964). A Franck-Condon density $q_{v'', cont}(\nu)$ is defined in Eq. (4.3-4)

$$q_{v'', cont}(\nu) = \left| \int \psi_{v''}(r) \psi_{cont}(r, \nu) dr \right|^2 \quad (4.3-4)$$

and the Franck-Condon factor for the whole continuum is

$$q_{v'', cont} = \int q_{v'', cont}(\nu) d\nu \quad (4.3-5)$$

Under these circumstances the sum rule (Eq. (4.1-16b)) is replaced by

$$\sum_{v'} q_{v'v''} + \int q_{v''\text{cont}}(v) dv = 1 \quad (4.3-6)$$

The element of the volume absorption coefficient in the continuum is

$$d\mu_v = \mu_v dv = \frac{\pi e^2}{mc} \frac{N_{Lv''}}{dL} \frac{df}{dv} dv = \frac{\pi e^2}{mc} N_{Lv''} R_{\bullet}^2(r) dq_{\text{cont}} \quad (4.3-7)$$

Jarman and Nicholls (1964, 1966) have recently computed Franck-Condon densities for the Schumann-Runge Continuum from $v'' = 0$, using wave functions derived from realistic potentials and also for the Herzberg I Continuum from $v'' = 0, 1, 2$. The densities were compared with measured absorption coefficients, and using Eq. (4.3-7) $R_{\bullet}(r)$ was determined.

An earlier approach to this sort of problem derives from the suggestion of Winans and Stueckelberg (1928), that from a Franck-Condon point of view it will be the terminal antinode of the continuous wavefunction which plays an important part in the overlap integral. They thus suggested that in the absence of firm knowledge of the form of the continuum wavefunction it should be replaced by a δ function at one classical turning point (r_1') of the oscillator. The Franck-Condon density is then $|\psi_{v''}(r_1')|^2$. This ingenious idea was tested by Coolidge, James and Present (1936) in an H_2 transition using a Dunham potential and a differential analyzer to obtain realistic wave functions. They obtained good agreement between the two results. However a similar test carried out by Jarman and Nicholls (1964) for the O_2 Schumann-Runge transition led to no agreement between the two methods. Ditchburn and Young (1962) used the δ function method for comparison with experimental measurements on the O_2 Herzberg I continuum.

A large enough number of Franck-Condon Factor arrays have now been calculated under similar circumstances that the systematics of these arrays can be studied. Two related aspects of these systematics have been investigated: The Geometry of the Condon Loci, The Geometry of the Franck-Condon Factor Surface.

It was a very early observation in molecular spectroscopy that the most commonly observed bands of a system lie in well defined regions of the v', v'' plane on and around an open limbed, quasi-parabolic curve which is roughly symmetric about $v' = v''$ and whose vertex is in the region of $(0,0)$. Condon (1926) in a semiclassical discussion was able to show that for a simple harmonic oscillator potential the strong bands would indeed lie on a parabolic locus in the $v'v''$ plane. The parabolae have thus been called 'Condon Parabolae'. For band systems where Δr_e is very small, the parabola collapses into a diagonal line. As Δr_e increases the parabola widens, its vertex moves away from $(0,0)$ and subsidiary "parabolae" nested within the primary outer parabola develop. Detailed examination of these loci of the stronger bands show that they are not parabolic but lie on open curves which remind one of parabolae. They are by no means all symmetric about $v' = v''$. They are in fact the projection on the $v'-v''$ plane of the three dimensional surface of $q_{v',v''}$ vs v' and v'' .

The definition of $q_{v',v''}$ (Eq.(4.3-1) makes it natural to see whether the shape of the Condon loci can be predicted by requiring agreement in r between one antinode of one wave function and one of the other. The primary locus runs through those v' and v'' values for which there is overlap between one terminal antinode of one wave function with one terminal antinode of the other (Nicholls, 1962e). The subsidiary loci run through

those v' and v'' for which there is overlap between a terminal antinode of one wavefunction and a subsidiary antinode of the other (Nicholls, 1963b; Murty and Nicholls, 1966). This analysis has been very fully investigated by Murty (1964) who has shown that each locus has six possible segments of which three usually occur.

The systematic variation in shape of the Condon loci with Δr_e is a reflection of a similar behavior of the $q_{v',v''}$ surfaces. It has been described elsewhere (Nicholls, 1964d) how with increase in Δr_e the surfaces change from a diagonal ridge to a series of nested horseshoe-shaped ridges whose apex moves steadily away from (0,0). It has been possible to represent this behavior by a series of plots (one for each v', v'') of $\log q_{v',v''}$ vs. $\log \theta' \Delta r_e$. θ' is the harmonic mean of the θ 's in the exponents of the two Morse potentials (Eq. (4.3-3)) and $\theta' \Delta r_e$ is thus a transition parameter characteristic of the whole system (Nicholls, 1964c, 1965f). The curves have a systematic undulatory shape as would be expected, and can be used for the rough interpolation of Franck-Condon factors.

The r-centroid approximation defined in Eq. (4.1-12a,b) is another important derived quantity of vibrational wave-functions used in the interpretation of intensities of molecular spectra. Fraser (1954) has shown that as a result of the compact nature of the wavefunction product $\psi_{v'} \psi_{v''}$ (see Eq. (4.3-8a)) that Eq. (4.1-12b) is a good approximation for band systems for which $\mu_A \omega_e \sim 10^4$ (μ_A in amu and ω_e in cm^{-1}), $0.01A < \Delta r_e < 0.25A$ and for which v' and v'' do not greatly exceed 10.

This approximate property allows one to resolve the integral of the product of $\psi_{v'}$, $\psi_{v''}$ and a polynomial function of r into the product of the vibrational overlap integral and the polynomial taken at an argument $\bar{r}_{v',v''}$ (see Eq. (4.1-13)).

The r -centroid is a characteristic r -value associated with the $v'-v''$ transition and recent work has shown that it may be identified with the 'Franck-Condon principle' value of r for the $v'-v''$ transition in question as is demonstrated below. Eqs. (4.1-12a, b) imply that

$$\delta(r - \bar{r}_{v',v''}) = \frac{\psi_{v'} \psi_{v''}}{\int \psi_{v'} \psi_{v''} dr} \quad (4.3-8a)$$

and thus that under Fraser's conditions the wavefunction product should have approximately comparable properties to a δ -function at the r -centroid. A recent study using tabulated Morse wavefunctions for a number of systems (Nicholls, 1966) has confirmed this view for many bands on the primary Condon Locus.

The r -centroid also satisfies the relationship (Nicholls and Jarman, 1956)

$$U'(\bar{r}_{v',v''}) - U''(\bar{r}_{v',v''}) = E_{v'} - E_{v''} \quad (4.3-8b)$$

which has been the basis for many calculations of r -centroid arrays and also for a theoretical demonstration that the r -centroid is the Franck-Condon principle value of r (Nicholls, 1966).

Arrays of r-centroids have been computed for many band systems by a number of methods, some of which are based on Eq. (4.3-8b) and some of which involve direct calculation of the integral quotient of Eq. (4.1-12). The properties, methods of calculation and arrays of r-centroids have been fully discussed in a number of papers (Nicholls and Jarman, 1955, 1956, 1959; Nicholls, Parkinson, Robinson, and Jarman, 1956; Nicholls and Stewart, 1962; Nicholls, 1965g, 1966). The r-centroids are related to the r_e 's and the turning values $r_{1,2}'$ and $r_{1,2}''$ of the oscillators in the v' and v'' levels (Nicholls and Jarman, 1959). It is also possible to relate r-centroids and Franck-Condon factors to the expectation value $\bar{r}_{v'}$ or $\bar{r}_{v''}$ of r in the level v' or v'' through the equation

$$\bar{r}_{v' \text{ or } v''} = \sum_{v'' \text{ or } v'} \bar{r}_{v'v''} q_{v'v''} \quad (4.3-9)$$

(Nicholls and Jarman, 1955). That is the expectation $\left(= \int \psi_{v' \text{ or } v''}^2 r dr \right)$ value is a weighted average of r-centroids and Franck-Condon factors for all transitions out of the level concerned.

One of the most useful properties for applications of the r-centroid is its monotonic dependence on wavelength $\lambda_{v'v''}$ or frequency $\nu_{v'v''}$ for the bands of a system.

When $r_e' > r_e''$, $\bar{r}_{v'v''}$ increases monotonically with $\lambda_{v'v''}$. When $r_e' < r_e''$, $\bar{r}_{v'v''}$ decreases monotonically with $\lambda_{v'v''}$. This behavior, and the two possible types of $\bar{r}_{v'v''}$ surfaces (the three-dimensional representation of $\bar{r}_{v'v''}$ as a function of v' and v'')

which it implies, is directly related to the two types of $\lambda_{v',v''}$ surface. In both, $\lambda_{v',c}$ is less than $\lambda_{0,v''}$. When $r'_e > r''_e$, $\lambda_{vv} > \lambda_{00}$ and conversely. The monotonic relationship allows simple interpolation of uncalculated $\bar{f}_{v',v''}$ values and also allows $\lambda_{v',v''}$ or $\nu_{v',v''}$ to be used as independent variables in place of $\bar{f}_{v',v''}$ in some applications in the rescaling of measured intensities to provide a table of band strengths (see section 4.4).

After a number of $\bar{f}_{v',v''}$ arrays had been calculated it was observed that $\bar{f}_{v'+1, v''+1} - \bar{f}_{v',v''}$ was approximately constant for each of the $v'-v''$ sequences. The constant was different for each sequence. The theoretical justification for this was provided and it gave a simple means of making up an $\bar{f}_{v',v''}$ -array once the leading entries $\bar{f}_{v',0}$ $\bar{f}_{0,v''}$ for the sequences and the constant differences were known. The constant differences imply that the $\bar{f}_{v',v''}$ -surface is approximately plane.

4.4 The electronic transition moment and band strengths

The electronic transition moment $R_e(r)$ is the final of the three factors which control a line strength. It is formally defined in Eq. (4.1-19) and because of our poor detailed knowledge of molecular electronic wave functions, we are forced to study it experimentally. The electronic transition moment enters into a discussion of molecular transition probabilities from a number of standpoints. It is of course interesting in its own right as a knowledge of its magnitude and variation with r for a large number of different systems gives greater understanding of problems

of molecular structure. It has been pointed out a number of times in the preceding discussion that from a transition probability point of view it is the band strengths $S_{\nu_1\nu_2}$ or the product $R_e^2(\bar{r}_{\nu_1\nu_2}) q_{\nu_1\nu_2}$ which is a more important quantity than either of its factors. In the applications discussed below we shall thus look on $R_e(r)$, $q_{\nu_1\nu_2}$ and $\bar{r}_{\nu_1\nu_2}$ as means to the end of determination of reliable and smoothed band strengths.

$R_e(r)$ has been studied experimentally in three main ways:

- a) From intensities of emission spectra
- b) From intensities of absorption spectra
- c) From measurement of lifetimes of states.

The consequences of these will be discussed briefly in turn. Discussion of examples of these which have applications to thermal radiation from air is deferred to Chapter 7.

The emission intensity $I_{\nu_1\nu_2}$ of a molecular band is given by (Nicholls and Stewart, 1962)

$$I_{\nu_1\nu_2} = K N_{\nu_1} \nu_{\nu_1\nu_2}^4 R_e^2(\bar{r}_{\nu_1\nu_2}) q_{\nu_1\nu_2} = K N_{\nu_1} \nu_{\nu_1\nu_2}^4 S_{\nu_1\nu_2} \quad (4.4-1)$$

K is a constant which allows for units and geometry. In emission, geometrical considerations make absolute measurements very difficult to make, and thus this equation has been used in many relative measurements of band intensities. There are a number of other practical difficulties associated with overlap in structure between adjacent bands which can add significantly to possible errors in measured $I_{\nu_1\nu_2}$. These will not be discussed in detail here.

One obvious application of Eq. (4.4-1) is to measure $I_{\nu_1\nu_2}$ band

by band by photographic or photoelectric means and to interpret relative $S_{v'v''}$ band by band from

$$S_{v'v''} = I_{v'v''} / KN_{v'} v'^4 v'' \quad (4.4-2)$$

That approach requires either a knowledge of $N_{v'}$ (e.g., from demonstrated thermal excitation of spectra in a furnace or shock-tube) or the determination of relative $S_{v'v''}$ along progressions of bands for which $N_{v'} = \text{const.}$ The method has been applied to furnace-excited C_2 spectra for example, by King (1948), Phillips (1954, 1957) and Hagan (1962), and others. The method, while straightforward in application has the disadvantage that the relative error varies from band to band. Strong bands have profiles of large area and are, in general more accurately measured than weak bands.

An alternative application of Eq. (4.4-1) (Fraser, 1954a) is to plot $(I_{v'v''} / q_{v'v''} v'^4 v'')^{1/2}$ vs $\bar{r}_{v'v''}$ for progressions of bands in which v' is common in each. This plot is equivalent to $N_{v'}^{1/2} R_e(r)$ vs. r . It has been applied to many band systems (see Nicholls and Stewart, 1962; Nicholls, 1954). The result is a set of segments (one for each $v' = \text{const}$ progression of bands) which delineate the relative variation of $R_e(r)$ with r . The segments are displaced in ordinate from each other by an amount controlled by $N_{v'}^{1/2}$. Rescaling procedures allow all of the segments to be placed on the same ordinate scale and provide a knowledge of $N_{v'}$. All the measured intensities have then played a role in the delineation of $R_e(r)$, and a smooth empirical curve can be fitted by least squares methods to the final set of points.

If the aim of such work is to study $R_{\theta}(r)$ per se, then the procedure outlined above can be used with the reservation that $\bar{r}_{\nu',\nu''}$ is an approximately defined quantity. If the aim is however, to provide a set of smoothed $S_{\nu',\nu''}$ ($=R_{\theta}^2/q$) values from the smoothed $R_{\theta}(r)$ curve and the Franck-Condon factors, the discussion of the preceding section on r-controids indicates that $(I/q\nu^4)^{1/2}$ could equally well have been plotted against ν or λ in progressions because of the monotonic relationship between $\bar{r}_{\nu',\nu''}$ and wavelength or frequency. Further, provided that no large extrapolation is made outside the range of $\bar{r}_{\nu',\nu''}$ (or λ or ν) for the system this procedure will also allow estimates to be made of relative band strengths for bands not measured, providing that a consistent estimate of $q_{\nu',\nu''}$ and $\bar{r}_{\nu',\nu''}$, λ or ν is available for each of them so that the correct ordinate of the $R_{\theta}(r)$ plot can be read off.

It should also be pointed out in this connection that while different forms of $R_{\theta}(r)$ will obviously result from the use of each $q_{\nu',\nu''}$ (and $\bar{r}_{\nu',\nu''}$) arrays calculated on the basis of a different model of $U(r)$, that the compensation achieved between division by $q_{\nu',\nu''}$ in the determination of $R_{\theta}(r)$, and multiplication by $q_{\nu',\nu''}$ in the determination of $S_{\nu',\nu''}$ will make the eventual smoothed $S_{\nu',\nu''}$ arrays less sensitive to the model of potential used that has often been thought.

The relative $S_{\nu',\nu''}$ arrays (often expressed on a scale where $S_{0,0}$ is 100) can be, and have been in some cases, placed on an absolute scale by comparison with absolute absorption coefficients for a few bands or by use of lifetime measurements (see for example, Nicholls, 1964d). One advantage of emission measurements, in spite of their relative nature, is that, in general more bands of a system are excited in emission than are observed in cold absorption (see however the remarks below).

If the aim of the work is the provision of data on $R_e(r)$, the realism of model of potential used to compute $q_{v',v''}$ arrays is of great importance as is the adequacy of the r-centroid approximation for the band system under consideration. There has been relatively little discussion of any possible systematic difference in behavior of $R_e(r)$ with r from band system to band system. Bates (1949) proposed that the dependence upon r would be most strong for perpendicular ($\Delta\lambda = \pm 1$) transitions than for parallel ($\Delta\lambda = 0$) transitions. The change of the electronic structure is more severe in the former than the latter. In one survey which was made of the meagre experimental data (Nicholls, 1962a), support was found for Bates' proposal.

The band absorption coefficient (Eq. (4.1-33)) has been used by a number of authors in recent years to provide information on band oscillator strengths, and in some cases on the behavior of $R_e(r)$ with r from a plot of $(\mu_v(\text{band})/v_{v',v''} q_{v',v''})^{1/2}$ vs $\bar{r}_{v',v''}$. See for example Bathke (1959a,b), Marr (1964a,b), Treanor and Wurster (1960). One advantage of absorption work is that absolute absorption coefficients can be measured directly in most cases (when N_L is known). While much absorption work has been done on the $v''=0$ progression in cold gas samples, the technically more difficult time resolved shock-tube spectroscopy of hot gases is being increasingly used. Band oscillator strengths are a commonly measured parameter in such work and more bands per system are in principle accessible than when using cold gas samples.

Eq. (4.1-35) has been used during the past decade to interpret lifetimes $\tau_{v'}$ of vibrational levels in terms of $R_e(r)$. The lifetime is the reciprocal of the sum of Einstein A-coefficients of all (v',v'') transitions which combine with v' . Consequently care has to be exercised when interpreting lifetime measurements that the sum is realistic, that no competing processes to

radiation depopulate the level, nor that it is being populated by unsuspected cascade transitions.

Three techniques have been developed for the measurement of molecular lifetimes.

a) The delayed coincidence method (Heron, McWhirter & Rhoderick, 1954, 1956; Brannen, Hunt, Adlington and Nicholls, 1955; Bennett & Dalby, 1959, 1960a,b; Dalby, 1964; Schwenker, 1965).

b) The decay of discharge method (Jeunhomme, 1965; Wentinck, 1964)

c) The phase shift method (Demtröder, 1962; Brewer et al., 1962; Lawrence, 1965; Hesser and Dressler, 1965).

In the delayed coincidence technique the spectrum feature is repetitively excited by a chopped electron beam and detected through a monochromator with a photomultiplier. Electrical delays are inserted in the detector circuit and the lifetime is inferred from the slope of a semilogarithmic plot of coincidence (with respect to the exciting pulse) counting rate vs. delay time. This is a modification of a commonly used method in nuclear physics. Provided cascading and other secondary effects do not occur it is a very accurate method and has been exploited to the full by Bennett and co-workers. The results are usually extrapolated to zero pressure to avoid the influence of secondary processes, and a dependence of $\tau_{v'}$ upon v' is often found which is not surprising.

In the decay of radiation from a discharge the decay of the radiation of a spectral feature from a pulsed discharge is studied. Care must be taken in interpretation of the results that a single atomic process (radiation) is

being observed and not the cumulative effect of a number of overlapping processes in the discharge. The method is in principle quite simple.

In the phase shift method the spectral feature of interest is excited by a sinusoidally modulated electron beam of controllable frequency. The lifetime can be inferred from either a measurement of amplitude or phase (relative to the electron beam) of the output signal. The phase measurements are used in practical application. This method is being used with great success on molecules of astrophysical interest at Princeton observatory.

In the interpretation of all of these methods, some prior knowledge of the number of bands making a significant contribution to the sum over v'' of the $A_{v',v''}$ has to be known, before $\tau_{v'}$ can be interpreted in terms of $R_e^2(F_{v',v''})$. In simple cases (e.g., (0,0) bands of systems where no other contributors to the $v' = 0$ progression) make a contribution,

$$\tau_{v'} = \frac{1}{A_{0,0}} \quad (4.4-3)$$

from which $R_e(F)_{v',v''}$ can be immediately inferred. In cases where there is more than one contributor the "branching ratios" have to be estimated, often approximately by use of the Franck-Condon factor ratios.

Lifetime measurements have been used in a number of cases to place relative band strengths on an absolute basis (Nicholls, 1964c).

PART B

SPECTRAL AND MEAN ABSORPTION COEFFICIENTS OF HEATED AIR

**Chapter 5. HISTORICAL REVIEW:
RESEARCH ON HOT GAS ABSORPTION COEFFICIENTS SINCE 1900**

In Part A of this volume an account was given of the theoretical bases both in radiative transfer theory and also in quantum mechanics, on which calculations of spectral and mean absorption coefficients of heated air can be made. In Part B, which follows, a detailed description was given of actual calculations which have been made particularly during the past two decades of these absorption coefficients. Typical illustrative results of such calculations are also presented as part of a larger more comprehensive compilation which forms another volume of this series.

Before making the detailed description of actual calculations it will be valuable for orientation purposes briefly to review in this chapter the development of theoretical research on absorption coefficients of hot gases made during this century. Much of this work has had a strong astrophysical motivation.

The importance of radiation absorption coefficients of heated gases in the detailed quantitative description of stellar atmospheres was increasingly realized during the decade 1915-1926. During this period it became clear that the purely convective models of stellar atmospheres were not adequate to account for the observed facts, and that in some way the radiation flux must be included in any realistic account of stellar structure. Schwarzschild (1906) had in fact already begun to lay the foundation of radiative stellar models. Between 1915 and 1926 Eddington (1926) made a systematic application of radiative transfer theory to stellar atmospheres, and with E. A. Milne (1924)

was primarily responsible for establishing the direct physical significance of radiative stellar models. The work of this period, including the early calculations of absorption coefficients, is described in Eddington's classic book (1926) which stands as a monument to and closes the initial period of development of radiative stellar models. The historical significance of Eddington's book is heightened by its position relative to the formulation of quantum mechanics. It appeared just at the onset of the major period of development of the subject and before the results of this development were available. Also, it appeared just after Kramer's (1923) remarkable derivation of semiclassical absorption coefficients, and Rosseland's (1924) discovery of the correct mean absorption coefficient to use for stellar interiors. These two developments enabled Eddington and Milne* to provide a solid physical basis for the radiative aspects of stellar structure.

The next period of development involved the application of quantum mechanics to the study of absorption coefficients. Among the principal papers in which complete quantum mechanical discussion of continuous radiative processes were made are those of Oppenheimer (1928, 1929), Gaunt (1930), and Stobbe (1930). The classic paper of Born and Oppenheimer (1927) is of fundamental importance in the discussion of molecular contributions.

Following the formal quantal descriptions of elementary processes which contribute to the spectral absorption coefficients, Strömberg (1932, 1933) carried out the first systematic and detailed calculations of the mean absorption coefficient $1/\bar{u}_R$ defined by Rosseland as the most appropriate

254

* It is interesting to note that Milne independently obtained the same results as Kramers (1923) for the semiclassical photoelectric cross section. His paper (Milne, 1924) appeared in the same journal, the Philosophical Magazine, just two months after Kramers'. Because of Kramers' prior publication, the semiclassical cross sections are ordinarily attributed to him, and Milne's paper is now remembered primarily for the connection between the photoelectric and recombination cross sections first given in it.

for discussion of radiative transfer in stellar interiors:

$$\Lambda_R = \frac{1}{\bar{\mu}_R} = \frac{\int \frac{1}{\mu'(v)} \frac{dB(v)}{dT} dv}{\int \frac{dBv}{dT} dv} \quad (5-1)$$

(The quantity $\bar{\kappa}_R = \bar{\mu}_R/\rho$ is often used, and is called the "Rosseland Mean Opacity", see section 2.5)

The next important development was the paper of Menzel and Pekeris (1935) which provided a very extensive analysis of hydrogenic matrix element formulae with tables of numerical values to correct the Kramers' semiclassical approximation. In addition, they discussed, analyzed, and made improvements to previous approximate formulae for the spectral and mean absorption coefficients. Papers by Marshak and Bethe (1950), and Morse (1960) for the first time considered interparticle interactions in the calculation of occupation numbers for study of opacity and thermodynamic properties of gases at high temperatures and densities. These authors adopted the suggestion of Slater and Krutter (1935) to apply the Fermi-Thomas method to the calculation of occupation numbers and/or other thermodynamic properties under conditions of temperature and pressure of astrophysical interest. This was the origin of the use of the ion-sphere model in opacity calculations. Its original use, by Wigner, Seitz, Slater, and others, was in the theory of metals. But, as pointed out by Slater and Krutter (1935), it is also advantageous for thermodynamic calculations under conditions of high temperature and pressure. It permits more detailed consideration to be made of interparticle interactions than the previous "excluded volume" type corrections* which are more or less

* Discussions of studies of truncation with early cutoffs and corrections for the partition function may be found in Fowler (1936). See also Fermi (1924), and Urey (1924).

intuitive in nature. The Thomas-Fermi calculations of Slater and Krutter (1935), using the ion-sphere model, provided the necessary ground work for the Marshak-Bethe (1960), and Morse (1940) calculations. This original ion-sphere theory was more or less intuitively based, without any statistical justification. H. Mayer (1947) was the first to work out a detailed statistical mechanics foundation for this theory.

With the development of nuclear weapons during the second World War, it was recognized that conditions in and around the fireball of a nuclear explosion would be similar to those in a star. Thus, in order to predict these conditions, it was necessary to consider the opacity both of the materials used in the construction of a nuclear weapon, and of the air surrounding such a weapon, after heating caused by the nuclear explosion has taken place. The first calculations of the opacity of air were therefore carried out* under the Manhattan project by Hirschfelder and Magee (1945). Later, a much more extensive general development of opacity calculation theory was provided by Mayer (1947), although he did not carry out any explicit calculations for air in that (1947) report. The Hirschfelder-Magee calculations covered a very extensive temperature-density range, but with a limited number of contributing components. This work was later extended to include a few more components and to include a consideration of Planck mean absorption coefficients as well as Rosseland means (Hirschfelder and Magee, 1958/1947). Their calculations were based on Morse's method with some simplifications (i.e., neglect of excited states and pressure ionization).

* The associated equation-of-state calculations were carried out by Fuchs, Peierls, Christy, and others. See LA 296 or LA 2000.

As stated above, Mayer (1947) gave the first statistical discussion, based on the canonical ensemble, of the ion-sphere theory for obtaining occupation numbers. He also included explicit consideration of free-bound electron-electron interactions in his treatment, thus giving more accurate and detailed formulae for the occupation number calculations than had previously been available. In addition, he considered the effects of line transitions on the opacity for the first time.

Because of the complexity of this problem, previous investigators had limited themselves to the so-called "continuous" opacity, that is, absorption due to the photoelectric and free-free processes, and scattering. At the suggestion of E. Teller, Mayer performed the first realistic estimates of the line effect, both by means of a statistical theory which he developed (see also Goody, 1952, who developed it independently) and by direct calculation (Kivel and Mayer, 1965/1954). Specific lines or groups of idealized lines had been used for some time in low-temperature radiation transport studies (Elsasser, 1938) but these were traditionally confined to relatively narrow frequency regions in contrast to the extremely broad regions involved in a high-temperature opacity calculation.

Further history of opacity calculations carried out under the Manhattan project and afterwards has been reviewed by H. Mayer (1964). It is not our purpose here to provide a definitive historical survey, and thus we limit the discussion to the most significant developments in absorption coefficient and opacity calculations, specifically those that are most concerned with air, per se. After 1945, opacity calculations were continued under

government sponsorship at the Argonne National Laboratory (Moszkowski and Meyerott, 1957; Keller and Meyerott, 1952a, 1952b; Brachman and Meyerott, 1953; Keller and Meyerott, 1955), and at Rand Corp. (Gilmore and Latter, 1955; Meyerott, 1955), as well as at Los Alamos (Cox, 1964; Kivel and Mayer, 1965/1954).

Astrophysical studies of many aspects of opacities and absorption coefficients did not stop during the war nor later, of course. At about the time of Morse's work, Wildt (1939) suggested that bound-free absorption by H^- was a significant factor in determining radiative energy flow in the outer layers of the sun. This proved to be a particularly fruitful suggestion, and precipitated an outburst of calculations of wave functions and absorption coefficients of H^- (Chandrasekhar, 1945a, b). We will not attempt to trace the purely astrophysical work beyond this point. An extensive discussion and evaluation of this work has been given by Cox (1965).

At the time of Wildt's suggestion, rough calculations of the H^- photodetachment cross section already existed (Jen, 1933; Massey and Smith, 1936) whereby he was able to assess the importance of the absorption due to this process. Also at this time, Massey, Bates, and colleagues had already started detailed calculations of a number of photoelectric cross sections of upper-atmospheric and astrophysical interest. For example, Bates, Buckingham, Massey and Unwin (1939) calculated the photoelectric cross section for the ground state of oxygen using the self-consistent-field method.* Following this calculation, Bates went on to obtain similar cross sections for the neighboring elements boron, carbon, nitrogen, flourine, and neon. These

* So did Yamanouchi and Kotani, Proc. Phys. Math. Soc., Japan 22, 60 (1940).

calculations were interrupted by World War II, and resumed shortly thereafter. In 1946 Bates published a very substantial review paper on the characteristics of radiative cross sections for a wide variety of elements, listing the calculations which had been made to that date. This paper also reviews the basic quantal formulas, including for the first time, explicit values of some of the angular factors in the matrix elements. Concomitant with this review paper, Bates (1946b) gave approximate formulae for the photoelectric cross sections of light atoms and ions, using Slater screening-constant wave functions. This work included results for N^+ and O^+ .

Later, Bates and Seaton (1949) published still more accurate calculations on oxygen, nitrogen and carbon; detailed calculations of this type have of course, continued and multiplied (further references will be found in Section 8.1). Most significant to the present study is the work of Burgess and Seaton (1960). By generalizing the Coulomb Approximation of Bates and Damgaard (1949) these authors obtained a very general and widely-applicable method of obtaining photoionization cross sections. Results for excited states can be obtained just as well as for (in fact better than) ground states. The accuracy and relative simplicity of this method lends itself well to large-scale calculations of the type required for gases at high temperatures. The methods of Burgess and Seaton were first applied to a calculation of the continuous absorption coefficients of heated nitrogen and oxygen (10,500 - 13,000°K) by Peach (1962). The results were in reasonable (although not precise) agreement with experiment. A generalization of this so-called "quantum-defect" method to free-free transitions has been reported

(Norman, 1963) but so far no applications of it have appeared in the American literature. A more careful and elaborate generalization of this method to free-free transitions has appeared quite recently (Peach, 1965) in which the author promises to apply the results to opacity calculations in a subsequent paper.

Returning now to more recent work on air opacity calculations per se, an approximate method for detailed inclusion of contributing lines in air (or air constituent) opacity calculations appears to have been first attempted by Moszkowski and Meyerott (1951) and by Kivel and Mayer (1965/1954). Until about the mid-fifties, and except for the work of Hirschfelder and Magee (1945, 1958/1947), the emphasis in opacity research was on atomic opacities at high-temperature or high density conditions, or both. Starting in the mid-fifties, additional calculations were begun which provide information in the lower-temperature regions which are of particular application to re-entry problems and to the outer layers of fireballs, and where molecules exist or predominate (Meyerott, 1955; Kivel and Bailey, 1957; Kivel, Mayer and Bethe, 1957).

At this time, the U.S. Air Force, through the Rand Corp., the Air Force Special Weapons Center, the Air Force Cambridge Research Center, and other sub-agencies, began to sponsor extensive new opacity-calculation projects, a number of which were carried out at industrial laboratories such as Aeronutronic Systems, Inc., Newport Beach, Calif., AVCO Corp., Everett, Mass., General Atomic, La Jolla, Calif., and Lockheed Missiles and Space Co., Palo Alto, Calif. The discussion in subsequent chapters will remain principally

within the context of these investigations, many of which are described only in unpublished contract reports and have not appeared in the journal literature. The new round of atomic air opacity calculations began with the work of Gilmore and Latter (1955). In 1957, Plass, Mayer, Wright, Rosengren, Schlesinger, Sashkin, and Browne produced an extensive report which contained an elaborate analysis of Mayer's earlier (1947) ionic method of calculation with additional formal theory supplementing the earlier report. It also included an analysis of a hydrodynamic opacity model due to Wheeler and Fireman. Following this, Armstrong, Holland, and Meyerott (1958) reported on an extensive hydrogenic calculation for air in the temperature region (2-20 eV) where atomic bound states predominate. This calculation was based on Mayer's ionic method, but with additional improvements such as inclusion of configuration splitting and large numbers of excited states, including some multiply-excited states. Shortly after this, Bernstein and Dyson (1959) completed a similar calculation with a cruder hydrogenic model but which covers the impressive array of elements from hydrogen to fluorine.

Following the lead of Bernstein and Dyson, Stewart and Pyatt (1961) performed the first large-scale atomic opacity calculation including lines (in the hydrogenic approximation), and also covering a wide variety of elements. At the same time, Armstrong, Buttrey, Sartori, Siegert, and Weisner (1961) performed a much more limited calculation of the Planck mean absorption coefficient of N, O, and air, but which employed for the first time, relatively accurate non-hydrogenic line f-numbers (this calculation was

subsequently refined by Armstrong and Aroeste, 1964). The computer code developed by Stewart and Pyatt in their calculation was later used for an explicit calculation for air (Freeman, 1963) of absorption coefficients, opacities, and some thermodynamic data. The temperature range of the original calculation was extended so that the air results cover temperatures from 1.5 eV to 2,250 eV. A combination of these two approaches (viz., that of Armstrong, et al., and of Stewart and Pyatt) led subsequently to a large-scale calculation for air, similar to that of Stewart and Pyatt, but using non-hydrogenic matrix elements (cf. Peach, 1962) for both lines and photoelectric continuum by Armstrong, Johnston, and Kelly (1965).

Concomitant with the rise in interest in atomic opacity calculations, there was also a rise in interest in the low-temperature, molecular calculations for air. Following the work of Meyerott (1956), and of Kivel and Bailey (1957), there appeared reports on work by Meyerott, Sokoloff, and Nicholls (1960), of Breene (1958), of Breene and Nardone (1962), of Churchill, Hagstrom, and Landshoff (1963), of Churchill, Armstrong and Mueller (1965), and of Ashley (1964) on molecular contributions to opacity of air in the 2000^o-20,000^o range.

In 1963, an "Opacity" conference was organized by the Air Force Weapons Laboratory and Los Alamos Scientific Laboratory, and held at Kirtland Air Force Base, New Mexico. The proceedings were published in toto in the Journal of Quantitative Spectroscopy and Radiative Transfer (JQSRT), Vol. 4, Sept./Oct., 1964. This conference, and a succeeding one held in 1964 (whose proceedings were similarly published in JQSRT,

Vol. 5, Jan./Feb., 1965) proved to be of considerable catalytic significance to the field. A number of older, important calculations and considerable information, previously unavailable in the open literature were thereby brought into the public domain. These conferences also provided the stimulus for a number of authors to publish calculations which would otherwise have remained in unpublished reports. The conference proceedings constitute an excellent source of reference information and general orientation to the state of research in the field. In addition to the detailed calculations of absorption coefficients, cross sections, and opacities, a few review papers and books, most of them relatively recent, have appeared which deal with the subject and we conclude this chapter with brief reference to them.

Review Papers - The first significant review paper on absorption coefficients, and dealing with photoelectric absorption, is probably that of Bates (1946). This paper reviews detailed atomic structure calculations of absorption from the ground states of atoms and ions of laboratory and astrophysical interest. Thus, while this paper is important for general theory and orientation, the results discussed and presented are not sufficiently extensive to be of much value for large-scale air calculations. A later review by Weissler (1956) is in a similar vein, but is more extensive, and covers experimental studies of photoelectric-effect phenomena as well as theoretical investigations. The paper of Burgess and Seaton (1960) applies quantum-defect methods to large scale photoelectric calculations for the first time and also includes a valuable review of many previous calculations. It also provides a very general

and practical method for computing approximate photoionization cross sections. In 1961, Armstrong, Sokoloff, Nicholls, Holland, and Meyerott published a review paper covering the molecular and atomic absorption-coefficient calculations that had been carried out up to that time at the Lockheed Research Laboratories in Palo Alto, Calif. The review article by Cox (1965), should be consulted for discussion of specifically astrophysical calculations. The review article by Ditchburn and Öpik (1962) provides an excellent bibliography on photoionization processes.

Books - The book "Quantitative Spectroscopy and Radiative Transfer" (Penner, 1959) treats absorption coefficients and opacities of molecular origin. Its primary orientation, however, is towards combustion and lower-temperature applications. The review article by Baranger (Spectral Line Broadening in Plasmas, 1962) provides an elegant and comprehensive account of modern line-broadening theory which is essential for any realistic treatment of atomic lines in high-temperature radiative problems. A particularly germane book is "Plasma Spectroscopy" by Griem (1964). It reviews many of the topics which we discuss below. Since Griem was active in the development of modern line-broadening theory, his book is especially valuable as an additional reference on this subject. In addition, he gives extensive tables of relevant atomic structure data, and discusses line and continuous emission, ionization and excitation equilibria, and radiation transfer in extended laboratory sources. It also contains a thorough discussion of experimental techniques and measurements. Hydrogenic emission and absorption coefficients, and ionization equilibrium are discussed extensively in "Astrophysics",

Vol. I, 2nd Edn., (Aller, 1963), who also gives an excellent discussion of approximate solutions to the transfer equation. He touches only lightly, however, on the Rosseland mean opacity. The recent book "Atomic Theory of Gas Dynamics" of Bond, Watson, and Welch (1965) contains an extensive chapter on opacities including (in the open literature for the first time) some of the theory and formalism developed by Mayer (1947). This excellent book also contains an extensive background and discussion of the atomic and molecular processes of interest in gases at high temperatures.

Russian Work - Before concluding this brief survey, mention should be made of Russian work in opacity calculations. We have not surveyed this literature in detail; entry to it can be gained through the work of Raizer (1960), and through the quantum-defect, Coulomb approximation calculations of Biberman, Norman, et al. (Biberman and Norman, 1960; Biberman, Norman and Ul'ianov, 1961, 1962; Biberman, Vorob'ev and Norman, 1963; Biberman and Norman, 1963; Norman, 1963; and Vorobyov and Norman, 1964). Another useful reference is the work of Levinson and Nikitin (1965).

Experimental Work - There is also, of course, some experimental work in this field. The amount is meager, however, compared to the extensive theoretical studies that have been carried out, as the experiments are generally very hard to perform and on this account are often imprecise. For this aspect of the subject, reference should be made to Keck et al. (1959), Boldt (1959), to the book by Griem (1964), and to the Opacity Conference issues of JQSRT (Vol. 4, 1964; Vol. 5, 1965).

Statistical Models - As mentioned earlier, statistical models of absorption both for lines and for photoelectric edges have been proposed and worked out. Since our emphasis has been on numerical computations of detailed spectral features, we will not review the statistical work here, but rather refer the interested reader to the sources Mayer, (1947), Goody, (1964), Stewart and Pyatt (1961), and to the brief discussion of Bond et al. (1965).

We will now proceed to discuss the general features of spectral and mean absorption coefficients in Chapter 6. The development of the low-temperature molecular absorption-coefficient calculations will be considered in some detail in Chapter 7, and the recent large-scale high temperature atomic calculations will be reviewed in Chapter 8.

Chapter 6. GENERAL FEATURES OF AIR ABSORPTION COEFFICIENTS

6.1 Spectral absorption coefficients

The aspect of absorption of radiation in a gas considered in this book is that which involves elementary interactions between the radiation photons and the individual particles of which the gas is composed. This is the dominant type of absorption process unless the gas is relatively dense and highly ionized, in which case absorption may occur by excitation of collective modes involving the combined simultaneous action of many particles. In this book it is assumed that collective effects* play no significant role or are out of the frequency range of interest. Thus only the elementary interactions involving individual gas particles need be considered. (On this point see Kahn, 1959; Salpeter, 1960)

Let the number density of particles of type s in the state J be denoted by N_{sJ} , and let the cross-section for absorption of a photon of frequency ν by a particle of type s in a transition which carries the particle from the state J to the state J' be denoted by $\sigma_{sJJ'}(\nu)$. Then the absorption coefficient μ_ν in cm^{-1} is given by

$$\mu_\nu = \sum_{s, J, J'} N_{sJ} \sigma_{sJJ'}(\nu) \quad (6.1-1)$$

(see Eq. (2.1-6c) in which α is replaced by σ .)

* We refer here to collective effects among the atoms, ions, or molecules. The electrons of a single atom or molecule are susceptible to a collective description and such models are mentioned briefly in sec. 8.1.

where the sum is extended over all particle species s and their initial and final states J and J' . The density of particles of type s in quantum state J may be written

$$N_{sJ} = N P_{sJ} \quad (6.1-2)$$

where N is the density of particles of all types, P_{sJ} is the probability that a particle chosen at random is of type s and is in the state J .

It is clear from Eqs. (6.1-1) and (6.1-2) that calculation of the absorption coefficient falls naturally into two distinct parts. The first is the calculation of the probabilities or "occupation numbers" P_{sJ} , which is a problem in statistical mechanics and has little to do with the radiation field, and the second is the calculation of the cross-sections σ , which is a problem in the quantum theory of radiation and to a first approximation can be undertaken without reference to the various particle densities. The problems encountered in performing these calculations vary markedly with temperature and density. For this reason it is convenient to discuss the problem with respect to several distinct temperature-density regions characterized by qualitative differences in the effects which are dominant in determining μ_ν (Armstrong, Sokoloff, Nicholls, Holland, and Meyerott, 1961).

Cold air consists almost exclusively of N_2 and O_2 ; hence, at sufficiently low temperatures, only the cross-sections for these two molecules need be considered. As the temperature is raised, N_2 and O_2 interact to form the various oxides of nitrogen. For example, at normal

density, and temperature kT in the range 0.4 to 1.0 eV, NO is formed and plays a significant role in determining the absorption coefficient. In addition to the formation of new molecular species, dissociation and ionization of the molecules also occur. Thus, at around $kT = 0.6$ eV, important contributions are made by N_2^+ and O^- . At temperatures of about 1 eV, dissociation is practically complete, and as the temperature is further increased the main contribution comes from atoms, ions, and free electrons. The problem of obtaining cross-sections for molecular species is much more difficult than the corresponding atomic problem; hence, the point at which the molecular particle density becomes so low that molecules may be neglected in the absorption coefficient calculation constitutes a natural and useful point of division of the problem.

A similar division occurs in the statistical mechanical calculations of occupation numbers. In some temperature-density regions, the interactions among particles may be neglected without introducing serious errors into the calculation of occupation numbers for the various species. At sufficiently high densities, however, the effects of interparticle interactions must be included, with a consequent increase in the difficulty of performing the calculations.

As a rather arbitrary demarcation between the regions where molecular effects may be neglected and where they make a significant contribution, let us choose a molecular contribution to the absorption coefficient which is generally less than about 1 percent of the atomic contribution over the optical frequencies. From the results of Churchill,

Armstrong and Mueller (1965) the temperature-density points corresponding to this demarcation may be found.

The curve labeled M in Fig. 6-1 is the locus of these points, and divides the temperature-density plane into two regions labeled atomic and molecular. The curve labeled I in Fig. 6-1 divides the plane into two regions according to whether the interactions among particles may or may not be neglected. Again an arbitrary criterion has been selected for determining the curve, namely, that the Coulomb interaction energy between ions be 1/50 of their thermal kinetic energy, i.e.,

$$\frac{Z^2 e^2}{r} = \frac{1}{50} \left(\frac{3}{2} kT \right) \quad (6.1-3)$$

where r , the average distance between ions, is obtained from the density.

The curve shown is obtained in Fig. 6-1 from Eq. (6.1-3) after some smoothing.

Further subdivisions over the parameter ranges may also be made. In Fig. 6-2 (from Armstrong, Sokoloff, Nicholls, and Meyerott, 1961) the temperature ranges over which the various processes make significant contributions are indicated, without reference to the density dependence of the effects.

It has been traditional in opacity work to divide the absorption coefficient into two parts. The so-called continuum part is composed of those contributions that are relatively smooth functions of frequency, and the line contribution is the absorption due to discrete (or "bound-bound") atomic and molecular transitions. The continuum contribution involves photoelectric and photodissociation (bound-free) absorption, inverse bremsstrahlung (free-free)

absorption and scattering. Simple, but not very accurate formulas for these contributions for many-electron atoms can be obtained on the basis of hydrogenic models and much work along these lines has been done. In atomic opacity calculations the line contribution has until recently simply been neglected because of its complexity. On the other hand, it is the principal consideration in molecular absorption. In Part B, we will proceed from low to high temperature absorption coefficients. Thus molecular absorption is reviewed in Chapter 7 and atomic absorption is reviewed in Chapter 8.

6.2 Mean absorption coefficients

The Planck and Rosseland mean absorption coefficients defined in Chapter 2 can be written as *

$$\bar{\mu}_P = \frac{15}{\pi^4} \int_0^{\infty} u^3 e^{-u} \mu(u, T) du \quad (6.2-1)$$

and

$$(\bar{\mu}_R)^{-1} = \frac{15}{4\pi^4} \int_0^{\infty} \frac{u^4 e^{-2u}}{\mu(u, T) (e^u - 1)^3} du \quad (6.2-2)$$

respectively, where $u = hv/kT$. These formulae can be obtained from Eqs. (2.4-15) and (2.5-6) of Chapter 2 by use of the expression for the integral of the Planck function

$$B = \int_0^{\infty} B(\nu) d\nu = \frac{2\pi^4 k^4 T^4}{15 c^2 h^3} \quad (6.2-3)$$

and by interchanging the order of differentiation and integration in the integral

$$\int_0^{\infty} \frac{dB_\nu}{dT} d\nu \quad (6.2-4)$$

* We write $\mu(\nu) = \mu(u, T)$ to avoid the suggestion that $\mu(\nu)$ depends only on u .

to write

$$\int_0^{\infty} \frac{dN}{dT} dv = \frac{d}{dT} B = \frac{8\pi^4 k^4 T^3}{15c^2 h^3} \quad (6.2-5)$$

In Eqs. (6.2-1) and (6.2-2), the factor $1-e^{-u}$ that differentiates between μ and μ' has been absorbed into the weighting functions.

It is useful (and traditional) to call the factors multiplying $\mu(v)$ in Eqs. (6.2-1) and (6.2-2) weighting functions; $W_P(u)$ and $W_R(u)$. Eqs. (6.2-1) and (6.2-2) can thus be written

$$\mu_P = \int_0^{\infty} W_P(u) \mu(u, T) du \quad (6.2-6)$$

$$(\bar{u}_R)^{-1} = \Lambda_R = \int_0^{\infty} \frac{W_R(u)}{\mu(u, T)} du \quad (6.2-7)$$

Graphs of the weighting functions

$$W_P(u) = \frac{15}{\pi^4} u^3 e^{-u} \quad (6.2-8a)$$

and

$$W_R(u) = \frac{15}{4\pi^4} \frac{u^4 e^{-2u}}{(e^u - 1)^3} \quad (6.2-8b)$$

are shown in Fig. 6-3. By inspection or differentiation it can be easily verified that $W_P(u)$ has its maximum at $u = 3$. We can similarly show that $W_R(u)$ has a maximum where

$$u_M = 4 \left(\frac{e^{u_M} - 1}{e^{u_M} + 2} \right) \quad (6.2-9)$$

μ_M is thus just a little less than 4 (since $(e^u - 1)/(e^u + 2) < 1$) . In fact Eq. (6.2-9) can be solved graphically to obtain $\mu_M \approx 3.74$.

The weighting function curves shown in Fig. 6-3 clearly show the frequency regions, at a given temperature, that dominate the calculation of each mean. Since $\bar{\mu}_p$ is a direct mean and the contributions to it are additive, further comment is unnecessary. The Rosseland mean coefficient $(\bar{\mu}_R)^{-1}$, is however, a harmonic mean, or, physically, a mean free path rather than strictly a mean absorption coefficient, and as such merits further discussion.

Following Mayer (1947) we divide the absorption coefficient into two parts

$$\mu = \mu_c + \mu_l \quad (6.2-10)$$

where μ_c is the continuous, or slowly varying part and μ_l is the rapidly varying line contribution. If we further introduce the notation

$$r(u) = \mu_l / \mu_c \quad (6.2-11)$$

such that $\mu = \mu_c(1 + r)$, Eq. (6.2-7) for Λ_R can now be rewritten as

$$\Lambda_R = \int_0^{\infty} \frac{W_R(u) du}{\mu_c(1+r)} \quad (6.2-12)$$

thus

$$\Lambda_R = \int_0^{\infty} \frac{W_R(u)}{\mu_C} du - \int_0^{\infty} \left(\frac{r(u)}{1+r(u)} \right) \frac{W_R(u)}{\mu_C} du \quad (6.2-13a)$$

$$\Lambda_R = \Lambda_C - \Lambda_L \quad (6.2-13b)$$

where Eq. (6.2-13b) defines a notation for the continuous and line contributions to the Rosseland mean free path respectively, in terms of the two integrals in Eq. (6.2-13a). This expression shows explicitly how the lines reduce the mean free path from the value Λ_C that it would have in the presence of continuous processes alone.

The effect of a strong line can be shown in the following way. We write $r(u)/(1+r(u))$ as $\frac{1}{1+1/r(u)}$ and note that a strong line implies

$$\frac{1}{r(u_0)} \ll 1 \quad (6.2-14)$$

where u_0 is the position of the line.

Then

$$\frac{r(u_0)}{1+r(u_0)} = 1 - \frac{1}{r(u_0)} + \left(\frac{1}{r(u_0)} \right)^2 + \dots \quad (6.2-15)$$

The line contribution to Λ_R from the small frequency region Δu_0 about u_0 where u is large is

$$\Delta \Lambda_L = \frac{W_R(u_0)}{u(u_0)T} \Delta u_0 \left[1 - \frac{1}{r(u_0)} \right] \quad (6.2-16)$$

to first order in $\frac{1}{r(u_0)}$. The zero order term precisely cancels the contribution of Λ_C , leaving only a first order contribution to Λ_R from this interval. Thus to lowest order the line eliminates the entire transmission over the interval. Its zero-order effect on Λ_R depends only on the width of the spectral region which it blacks out, and is independent of the strength of the line. The first order correction term is

$$\Delta \Lambda_R = \frac{W_R(u_0)}{r(u_0)\mu_C} \Delta u_0 = \frac{W_R(u_0)}{\mu_L} \Delta u_0 \quad (6.2-17)$$

which, as one would expect, does not depend upon u_C , since $\mu_L \gg \mu_C$ in this region. For a simple model of rectangular, non-overlapping lines of widths Δu_1

$$\begin{aligned} \mu_L(u_1, T) &= \mu_1, \frac{-\Delta u_1}{2} \leq u \leq \frac{+\Delta u_1}{2} \\ &= 0, u \text{ otherwise} \end{aligned} \quad (6.2-18)$$

these results imply that to first order in $[r(u_0)]^{-1}$

$$\Lambda_R = \int_0^\infty \frac{W_R(u) du}{u_c} - \sum_i \frac{W_R(u_i)}{u_c} \Delta u_i \quad (6.2-19)$$

$$+ \sum \frac{W_R(u_i)}{u_i} \Delta u_i$$

This equation follows from Eq. (6.2-13) if the first two terms of Eq. (6.2-15) are used for $r(u)/[1+r(u)]$. The last term of Eq. (6.2-19) is negligible if the lines are sufficiently strong.

For Lorentz and Doppler line shapes, the integrations over the line profiles can still be performed (Mayer, 1947) leading to an approximate result with the same form as Eq. (6.2-19) but with $\frac{\Delta u_0}{2}$ being replaced by $\pi/2$ or 1.0 times a quantity w , called the wingspread of the line*. For the Lorentz dispersion shape

$$b(\nu) = \frac{w/\pi}{(\nu-\nu_0)^2 + w^2} \quad (6.2-20a)$$

$$\int b(\nu) d\nu = 1 \quad (6.2-20b)$$

with conventional half-width w , the wingspread is given approximately by

$$w = \frac{hw}{kT} \left(\frac{u_0}{\pi w u_c} \right)^{1/2} \quad (6.2-21a)$$

* 276
Mayer defines the wingspread of a line as the distance between the line position $u_0 = h\nu_0/kT$ and the frequency $u = h\nu/kT$ at which $r = 1$, i.e., where the line absorption coefficient is equal to the continuum absorption coefficient.

where

$$\mu_0 = \int \mu_\ell(\nu) d\nu = \frac{\pi e^2 N_{\nu} f}{mc} \quad (6.2-21b)$$

is the absorption coefficient integrated over the line or, loosely speaking, the integrated line strength. Thus, for the Lorentz shape, the first approximation to Λ_ℓ for a single line is

$$\Lambda_\ell = \frac{\pi}{2} \times 2\omega \times \frac{W_R(u_C)}{u_C} \quad (6.2-22)$$

so that a line of this type approximately blacks out a frequency interval $\Delta\nu = \pi\omega kT/h$, or

$$\Delta\nu \text{ (blacked out)} = w \left(\frac{\pi \mu_0}{w \mu_C} \right)^{1/2} = \left(\frac{\pi w \mu_0}{\mu_C} \right)^{1/2} \quad (6.2-23)$$

(For further discussion, including the problem of overlapping strong lines, and the formulas for the Doppler-broadened case, see Mayer, 1947.)

We will conclude this section with a brief discussion of the weak line case. From Eq. (6.2-13), we define a weak line by

$$r(u) \ll 1 \quad (6.2-24)$$

In this approximation, we can expand $r/(1+r)$ as

$$\frac{r(u)}{1+r(u)} = r(u) [1 - r(u) + \dots] \quad (6.2-25)$$

Thus, to the same order of approximation that strong lines black out a frequency interval completely (neglect of $\frac{1}{r(u_0)}$), weak lines may be neglected completely. The first-order contribution of a weak line follows from Eq. (6.2-25) and Eqs. (6.2-13a,b)

$$\Lambda_L \approx \int_0^\infty R(u_0) \frac{W_R(u)}{\mu_c} du = \int_0^\infty \frac{\mu_L(u_0)}{\mu_c^2} W_R(u) du \quad (6.2-26)$$

If, as is usually the case, the variation of the line profile is quite rapid compared to variations in $W_R(u)$ and μ_c , the integration in Eq. (6.2-26) can be immediately performed. The result is

$$\Lambda_L = \frac{\mu_0}{\mu_c^2} W_R(u) \Big|_{u=u_0} \quad (6.2-27)$$

where again μ_0 is the integrated line absorption coefficient. From this result it is evident that the contributions of weak lines to Λ_R are additive and independent of the line width. The contribution of a given line depends only on its strength*, in distinction to the strong-line case where just the opposite situation prevails. We can now state a consistent first-order approximate formula for Λ_R in the presence of weak $\left(\frac{\mu_L}{\mu_c} \ll 1\right)$ and of strong, $\left(\frac{\mu_L}{\mu_c} \gg 1\right)$ non-overlapping rectangular lines. The

* as defined in Eq. (6.2-21b).

formula is

$$\Lambda_R \approx \int_0^{\infty} \frac{W_R(u) du}{\mu_C(u, T)} - \sum_{i(s)} \frac{W_R(u_i)}{\mu_C(u_i, T)} \Delta u_i$$

(6.2-28)

$$+ \sum_{i(s)} \frac{W_R(u_i) \Delta u_i}{\mu_{sl}(u_i, T)} - \sum_{j(w)} \frac{\mu_O^{wl}(j)}{\mu_C^2(u_j, T)} W_R(u_j)$$

In this formula, the Δu_i are the (reduced) widths of the strong lines and the $\mu_O^{wl}(j) = \frac{\pi e^2}{mc} N_V f_j$ are the integrated weak-line absorption coefficients. The letters wl and sl have been used in appropriate places in the formula to distinguish weak lines and strong lines, respectively.

Although these formulas and their equivalents for more realistic line profiles are descriptive and qualitatively very useful in providing physical intuition, it has been found both practical and convenient in the most recent calculations of mean absorption coefficients (Stewart and Pyatt, 1961; Freeman, 1963; Armstrong, Johnston, and Kelly, 1965) to perform analytic or detailed numerical integrations over the line profiles with the aid of high-speed digital computers. If this is done, lines of intermediate strength can be accurately accounted for, together with overlapping lines.

Huebner (1964) has presented a valuable review of the subdivisions of the temperature, density, and atomic number domain with brief comments on the principal contributors to the opacity within these various regimes. We present below a slightly condensed version of Huebner's summary. The reader should note that this summary covers a considerably wider domain of temperature, density and atomic number than we undertake to cover in Part B.

MAJOR CONTRIBUTIONS TO THE ROSSELAND MEAN OPACITY IN VARIOUS T , η , Z REGIONS

(after Huebner, 1964)

To acquire an orientation for the relevance of the theories, methods, and approximations which are applicable to the calculation of the Rosseland mean opacity and to emphasize the importance and the difficulty of obtaining good estimates of the line absorption contribution to this opacity one may consider a three-dimensional space with temperature, compression, and atomic number as the three coordinate axes. Dividing each of the three axes in their positive directions into three regions, which for simplicity shall be labeled as low, medium, and high, one obtains 27 major categories for opacity calculations. No sharp dividing lines can be established since the regions must overlap to some extent. Nevertheless, this division creates a useful concept, especially if one deals with mixtures of elements which is predominantly the case.

The low and medium ranges of temperature are divided approximately at the temperature above which molecular effects are unimportant, i.e., $kT_{l,m} \approx 2$ eV. In the medium temperature range atomic line transitions predominate. The high temperature range is defined to have as its lower limit a temperature above which atoms are essentially stripped of all electrons, therefore reducing bound-bound (line) transitions and incidentally also bound-free absorption edges (photo effect) to a small number which, with increasing temperature, rapidly approaches zero. Heavy atoms can be considered stripped at about 10 keV, light elements at a few eV; this corresponds to $kT_{m,h} \approx 2Z^2$ eV.

At the very lowest compressions (large expansions) of matter in the gaseous state interaction between free electrons and ions, atoms, and molecules is small, collision broadening is negligible and, unless there is a very large number of lines, as may be the case with molecular bands or heavy elements, line absorption may be neglected. Taking into account the heavy element effect on the number of lines, the division between low and medium compression* regions is approximately $\eta_{l,m} \approx 10^{-3} Z^{-4}$. The division between the medium and high compression ranges may be taken at a compression above which pressure ionization is so large that only 1s electrons are bound (and perhaps electrons in the $n-2$ shell in the case of heavy elements). This compression is at $\eta_{m,h} \approx 10^2$ except for heavy elements at low temperature $\eta_{m,h} \approx 10^3$.

The low range of the atomic number coordinate shall cover the light elements for which atomic line absorption can be calculated for each line individually. This task becomes cumbersome at $Z_{l,m} \approx 20$. For medium Z elements it is usually possible to group some lines and approximate their collective effect and treat the remaining lines individually. The

* Compression is defined as $\eta = \rho/\rho_0$, where ρ_0 is the density at standard conditions.

division between medium and high Z elements may be taken at $Z \approx 50$. For heavy elements most of the lines can be grouped and the effect of these groups may then be approximated. It is usually not necessary to consider individual lines in this range.

Not all of the 27 possible regions delineated above are of interest to present day science and technology. A brief discussion of relevant methods for calculating opacities in the various regions and an outline of some of the phases which require improvements follows.

1. Low temperature, low compression, low atomic number. Opacity in this region is of interest in upper atmosphere physics and also in theories for the formation of proto-stars. Molecular bands due to vibrational and rotational spectra are frequently the least accurate quantities entering in the calculations. Although the line widths of the transitions are small, the number of transitions in a band is large and the collective effect is significant. Quantities such as dissociation constants, f -numbers, and band structures are best taken from the tables and graphs compiled predominantly from experimental data (Herzberg, 1950). Great efforts have been under way for some time now to fill one of the largest gaps, that of the f -numbers, by experimental methods notably shock tube techniques, pressurized cells, and lifetime measurements. More reliable calculations are also made of the Franck-Condon factors.

Another important contribution to opacity at low temperatures are the absorption and scattering by agglomeration of particles (grains) such as droplets or dust. Vapor pressure, droplet size, latent heats, etc. are determined by thermodynamic considerations. The grain size in relation to the wavelength of the radiation and the complex index of refraction which depends on the chemical composition of the grains must be known before the absorption coefficient can be calculated (Van De Hulst, 1957). For small grains the difference between gas temperature and internal temperature of the grains can be neglected except at the very lowest densities where the number of inelastic collisions with gas molecules is too low to establish equilibrium.

Continuous processes such as molecular dissociation, atomic bound-free transitions, Thomson scattering, etc. are of some importance.

2. Low temperature, low compression, medium atomic number. In high altitude atmospheric phenomena concerned with ablation from re-entry bodies, meteorites, or with debris from nuclear explosions, contributions to the opacity come mainly from grains, molecular effects, and continuous atomic transitions. Opacities of medium Z elements of interest in the formation of proto-stars are mostly due to grains and probably to a lesser extent due to other molecular effects.

Contributions from grains and molecules are similar to the ones discussed in region 1.

The atomic continuous processes can be calculated from the knowledge of atomic energy levels and occupation numbers. Most energy levels are tabulated (Moore, 1949, 1952, 1958) and the occupation numbers can be obtained from the Boltzmann and Saha equations.

3. Low temperature, low compression, high atomic number. Except for possibly studies on debris from nuclear explosions, no applications are known. Continuous atomic transitions, molecular, and grain effects are probably the most important contributions to the opacity in this region. Very little work has been done in this region.

4. Low temperature, medium compression, low atomic number. This is a region of interest in astrophysics, and in technical fields; for example, in rocket design. Excepting the upper range of compressions in this region, pressure broadening makes molecular band absorption the dominant effect (see Section 4.3). Grain absorption and scattering can be important.

A new effect, that of the negative ion, notably the negative hydrogen ion, enters opacity calculations. The binding energy of the extra electron in hydrogen is about 0.75 eV. The bound-free and free-free processes (Bremsstrahlung) of these negative ions can dominate the absorption coefficient.

Line effects due to atomic bound-bound transitions become also important. Stark broadening of lines must be considered for the lightest elements in addition to collision broadening.

For light elements the number of lines is too small to apply statistical averaging and therefore they should be treated individually; however, techniques such as application of the Elsasser model to sum over an entire series appear to give reasonably good results (Stewart and Pyatt, 1961). Line strengths and atomic energy levels are tabulated. Rayleigh scattering and resonance scattering by bound electrons can be significant. Occupation numbers can be obtained from the Boltzmann and Saha equations.

5. Low temperature, medium compression, medium atomic number. Interest in this region is mostly in the fields of technology. Processes contributing to the opacity and methods of calculation are similar to the ones in region 4. Resonance and Rayleigh scattering are less important, since the number of lines is large. Many lines can be grouped and their average effect estimated. Methods of calculating line absorption as discussed by Goody (1964) may be applicable in this region, and also at higher temperatures.

6. Low temperature, medium compression, high atomic number. Gaseous reactors can be cited as an example of application of opacities in this region. Very little is known about molecular bands for heavy elements. Since the number of lines and the line density are very large, it seems that one can neglect the effect of molecular bands. It is entirely impractical to treat lines individually. Various approximate methods may be used to estimate line absorption. One can sample individual lines in some small frequency ranges, calculate the line absorption in these ranges and then interpolate to get the total line absorption. Another approximation is to space lines evenly throughout the entire frequency range (Sziklas, 1961).

Energy level and line strength data are very sparse for heavy elements, and the Slater approximation to the Hartree-Fock self-consistent field calculation is tedious and time consuming. Thomas-Fermi-Dirac calculations give probably the next best estimate to energy level data (for references, see Section 4.4.1).

7. Low temperature, high compression, low atomic number. This region is almost exclusively of interest in astrophysical problems. Besides the usual grain effects and absorption due to the negative hydrogen ion, conductive opacity (a measure of resistance to energy transport by electron conduction) shows its effect by lowering the total opacity below that of the radiative opacity. Energy transport by electron conduction competes with or, borrowing terminology from the field of electrical networks, is in shunt with energy transport by radiation. Nearly complete pressure ionization precludes existence of molecules and of most lines. Free-free transitions and Compton scattering are important.

Energy levels and occupation number calculations become problematic when the compression is so high that the Coulomb interaction energy for free electrons is greater than the thermal energy.

8. Low temperature, high compression, medium atomic number. Astrophysical problems have some limited interest in opacities of this region. Processes contributing to opacity and their calculations are similar to those of region 7. Energy levels can be calculated from the Thomas-Fermi-Dirac potentials.

9. Low temperature, high compression, high atomic number. No specific applications or calculations of opacity are known to the author. Continuous radiative absorption and electron conduction will dominate, but some lines in the lower compression range of the region may be important.

10. Medium temperature, low compression, low atomic number. The opacity in this region is almost entirely due to continuous atomic transitions. There is some resonance and Rayleigh scattering but bound-free absorption is dominant. The Kramers' formula for bound-free transitions and hydrogenic Gaunt factors are commonly used. This method becomes unreliable, particularly

for the less ionized atoms in the range $10 \leq Z \leq Z_{1,m} \approx 20$. (Bethe and Salpeter, 1957.)

For the low ionization stages energy levels are available in tables and for highly ionized atoms building the ions up, using screening constants, gives satisfactory results. Occupation numbers may be obtained from the Saha equation.

11. Medium temperature, low compression, medium atomic number. Bound-free absorption and scattering by free electrons dominate the opacity. Many energy levels for low ionization stages are available in tables and may be corrected for other relevant ionization stages with the use of screening constants. Unavailable levels can be readily calculated using the Thomas-Fermi potential or the Slater approximation to the Hartree-Fock method. Occupation numbers are obtained from the Saha equation.

For highly ionized atoms (usually for temperatures above 100 eV) energy levels are calculated from occupation numbers and screening constants and occupation numbers are calculated from energy levels with the aid of Fermi-Dirac statistics. Iterations are carried out until the degeneracy parameter has converged under the condition that the total number of electrons (bound and free) is conserved (Mayer, 1947).

Cross sections for the bound-free transitions from all but the lowest lying levels are difficult to obtain with accuracy. The opacity has its strongest dependence on these transitions when the calculations are most difficult. The large number of electron configurations will "split" the bound-free absorption edges and distribute them around the position of the edge for the average configuration.

12. Medium temperature, low compression, high atomic number. To the author's knowledge there is no interest in opacities in this region at this time. Continuous effects should dominate.

13. Medium temperature, medium compression, low atomic number. This is another region of great interest in astrophysics. Although the number of lines is small, they are pressure broadened and their absorption is best taken into account on an individual basis. Hydrogenic oscillator strengths and Gaunt factors are tabulated (Kargas and Latter, 1961) and are usually used.

Energy levels and occupation numbers may be obtained by the method outlined for region 11. However, since for the position of the lines the difference between energy levels is important and not their absolute value, all levels should be obtained by one and the same method. Shifting of lines with respect to one another or with respect to their series limits (photo electric edges) can change the opacity significantly through the creation or closing of "windows" in the frequency spectrum.

Bound-free transitions are important and conductive opacity can be significant in the low temperature-high compression range of this region.

14. Medium temperature, medium compression, medium atomic number. Opacities in this region are of interest in astrophysical problems and also in the design and effects studies of nuclear weapons.

Line effects are very important. There are many lines and they are collision broadened; therefore, they may be grouped and their collective effect estimated (Mayer, 1947). Absorption of many lines may still have to be calculated on an individual basis. Statistical procedures may be applied to decide which of these lines can be grouped (Moszkowski, 1960, 1962).

In the low temperature range of this region energy levels are tabulated or may be calculated by the Hartree-Fock-Slater method, and occupation numbers can be obtained by means of the Saha equation. For higher temperatures energy levels are most conveniently obtained from Thomas-Fermi potentials, and the occupation numbers by Fermi-Dirac statistics.

Bound-free absorption can be important but is difficult to calculate and is therefore usually not very accurate. Compton scattering is strong in the upper temperature range of this region. Conductive opacity reduces the radiative effects on the total opacity in the corner of this region where temperature is low and compression is high.

15. Medium temperature, medium compression, high atomic number. This region of opacity calculations is of interest in nuclear weapons work. Calculations are similar to those in region 14, except here almost all lines can be grouped and their collective effect estimated. The Hartree-Fock-Slater method for calculating energy levels is too tedious to be useful. Continuous opacity is again important at the upper temperature range of this region while conductive opacity is significant in the low temperature-high compression range.

16. Medium temperature, high compression, low atomic number. Opacities are of astrophysical interest. Pressure ionization reduces lines to a very small number or makes line transitions completely impossible. If lines are present they must be treated individually; their effect can be quite important due to the large pressure broadening. At the lower temperature range of this region conductive opacity is also important. Energy levels are obtained most conveniently from screening constants.

17. Medium temperature, high compression, medium atomic number. Opacities are calculated very similarly to those in region 16. Lines are a little more likely to occur. Energy levels and occupation numbers are calculated by methods similar to the ones discussed in region 11.

18. Medium temperature, high compression, high atomic number. This region has no application to the author's knowledge. Line opacity and conductive opacity can be expected to make contributions but the two effects tend to cancel. Bound-free absorption and scattering predominate.

19. High temperature, low compression, low atomic number. Opacity is entirely due to continuous processes, mainly free-free absorption and Compton scattering. As the temperature approaches $2mc^2$ electron-positron pair production begins to dominate the absorption processes, but even only at a small fraction of this temperature the high energy tail of the photon distribution creates enough electron pairs which have a long lifetime at low compressions to increase Compton scattering by several powers of ten (Sampson, 1959).

20. High temperature, low compression, medium atomic number. Opacity calculations are essentially the same as in region 19; however, in the low temperature range of this region bound-free absorption can be of greater importance.

21. High temperature, low compression, high atomic number. There are no applications of opacities in this region known to the author. Calculations would presumably be similar to those of regions 19 and 20 with increased absorption due to bound-free transitions.

22. High temperature, medium compression, low atomic number. Opacities in this region are of interest in the calculations of stellar models. Contributions to the opacity are similar to those of region 19, but the increase in Compton scattering due to electron pair creation does not occur until somewhat higher temperatures - several tens of keV - are reached (Sampson, 1959). The increased density shortens the lifetime of electron pairs and, therefore, a higher production rate is required to get the same effect as the Compton scattering.

A few lines are possible near the low temperature limit of this range. Bound-free absorption is important. Energy levels and occupation numbers may be calculated as described for region 11.

23. High temperature, medium compression, medium atomic number. Opacities are again of interest to theories about stellar interiors. Similar to region 22 bound-free absorption and Compton scattering are important. The number of lines is somewhat larger and many of them can be grouped to estimate their absorption. Energy levels are most conveniently obtained from Thomas-Fermi potentials, and the occupation numbers by Fermi-Dirac statistics.

24. High temperature, medium compression, high atomic number. This region is of interest in nuclear weapons work. Calculation of opacities is similar to those of region 23. Lines can be grouped and their absorption estimated.

25. High temperature, high compression, low atomic number. Opacity is predominantly continuous due to bound-free and free-free absorption and Compton scattering. Energy levels can be obtained from screening constants. Electron-positron pair production begins to dominate absorption processes as the temperature approaches $2mc^2$. However, below this threshold energy Compton scattering does not increase as significantly as it did for similar temperatures at low and medium compressions (Sampson, 1959).

26. High temperature, high compression, medium atomic number. Opacity calculations are similar to those of region 25. Energy levels may be obtained from the Thomas-Fermi potential; occupation numbers from Fermi-Dirac statistics. A few lines may exist and pressure broadening will make them important.

27. High temperature, high compression, high atomic number. The opacity may be calculated similar to that of region 26. Some groups of lines may be important.

6.3 Inequalities and bounds on mean absorption coefficients

In calculations of the Rosseland and Planck mean absorption coefficients, it is advantageous to have limits for the values to be expected for these quantities. This is particularly true when one includes considerations of the line contribution, since it has such a wildly fluctuating, complicated frequency dependence. Bernstein and Dyson (1959) have presented a theorem which places an upper limit on the Rosseland mean opacity. This theorem is based on the Schwartz inequality

$$\left[\int f g dx \right]^2 \leq \int f^2 dx \int g^2 dx \quad (6.3-1)$$

If f^2 is chosen to be the Rosseland mean integrand, and g^2 is chosen proportional to the absorption coefficient $\mu(\nu)$, then $\int f g dx$ is a definite integral independent of $\mu(\nu)$, and the integral $\int \mu(\nu) d\nu$ can be evaluated by means of the Thomas-Reiche-Kuhn f-number sum rule. Their result may be given as (cf. also Bond, Watson, and Welch, 1965)

$$\bar{\mu}_R/\rho = \kappa_R \leq \bar{\mu}_O/\rho = \kappa_O \quad (6.3-2)$$

where

$$\kappa_O = \frac{Z}{A} \left(\frac{Ryd}{kT} \right) 4.43 \times 10^5 \text{ cm}^2/\text{gm} \quad (6.3-3)$$

In this relation Z is the atomic number, A is the atomic weight, and Ryd is 13.6 eV when kT is also expressed in eV.

Unfortunately, at low density the upper limit of Eq. (6.3-2) is many orders of magnitude higher than the continuous opacity, which should be the dominant contribution (at sufficiently low density). Hence it would be convenient if an upper limit could be obtained closer to the true value even if, perhaps, more effort might be needed in its calculation. An advance in this direction was made by Armstrong (1962) by applying the Schwartz inequality in a different manner, as follows.

Recalling the definition of the Planck mean absorption coefficient

$$\bar{\mu}_p = \frac{15}{\pi^4} \int_0^{\infty} e^{-u} u^3 \mu(u) du \quad (6.3-4)$$

with

$$u = hv/kT, \quad (6.3-5)$$

we can apply Schwartz's inequality with

$$f^2 = \frac{15}{4\pi^4} \frac{u^4 e^{2u}}{u(u) (e^u - 1)^3} \quad (6.3-6)$$

and

$$g^2 = \frac{15}{\pi^4} u^3 e^{-u} u(u) \quad (6.3-7)$$

to derive

$$\frac{\bar{\mu}_P}{\bar{\mu}_R} \approx I^2 \quad (6.3-8)$$

where

$$I = \frac{15}{2\pi^4} \int_0^\infty \frac{\mu^{7/2} e^{\mu/2} d\mu}{(e^\mu - 1)^{3/2}} \quad (6.3-9)$$

The value 0.9743 for I was obtained by numerical integration, and inserting this result into Eq. (6.3-8) yields

$$\bar{\mu}_R \approx 1.053 \bar{\mu}_P \quad (6.3-10)$$

The Planck mean μ_P is much more tedious to compute than the Bernstein-Dyson $\bar{\mu}_0$, but it generally gives a lower value and is a quantity of some interest in its own right. It does not depend on the detailed shape of the lines, in distinction to the Rosseland mean, so it is still much easier to compute than the Rosseland mean. The values of these two means for the continuum absorption coefficient of air data given by Armstrong (1959) were compared and the ratio $\bar{\mu}_P/\bar{\mu}_R$ was found to range from a minimum of 1.1 at the low-density, high-temperature end of the parameter range, to a maximum of 7 or 8 at the high-density, low-temperature end. On the other hand, for air we can take the Bernstein-Dyson bound κ_0 as $1.5 \times 10^6 \text{ cm}^2/\text{gm}$ ($Z/A = \frac{1}{2}$) at $kT = 2\text{eV}$, which is the low-temperature end of the parameter range referred to above, and $\kappa_0 = 1.5 \times 10^5 \text{ cm}^2/\text{gm}$ at 20 eV, the high-temperature

and. Using the extreme κ_C values given by Armstrong (1959), namely,

$$\kappa_C \approx 3.2 \times 10^3 \text{ cm}^2/\text{gm} \quad \begin{array}{l} kT = 2 \text{ eV} \\ \rho \sim 5.4 \times 10^{-3} \text{ gm/cm}^3 \end{array} \quad (6.3-11)$$

$$\kappa_C \approx 0.25 \text{ cm}^2/\text{gm} \quad \begin{array}{l} kT = 20 \text{ eV} \\ \rho \sim 10^{-7} \text{ gm/cm}^3 \end{array} \quad (6.3-12)$$

we obtain for the ratio κ_O/κ_R , in the case of the Dyson bound,

$$\frac{\kappa_O}{\kappa_K} = \frac{1.5 \times 10^6}{3.2 \times 10^3} = 4.7 \times 10^2 \quad (6.3-13)$$

$$\frac{\kappa_O}{\kappa_K} = \frac{1.5 \times 10^5}{0.25} = 6.0 \times 10^5 \quad (6.3-14)$$

From this empirical "check", the inequality (Eq. (6.3-10)) would appear to be much nearer an equality than the inequality (Eq. (6.3-2)). Physically, it is easy to see why the relationship between $\bar{\mu}_P$ and $\bar{\mu}_R$ might hold. Fig. 6-4 shows the general case of a line superimposed on the continuum. The Planck mean obtains its dominant contributions when μ_ν is large as at A.

On the other hand $\bar{\mu}_R$ obtains its dominant contributions from regions of small values of μ_ν as at B and C. We can realistically make the contribution of this line to $\bar{\mu}_R$ as small as we please by passing to physical conditions such that the line becomes progressively more narrow and peaked (low density, low temperature). The Planck mean is invariant to this distortion, depending only on the area under the curve -- which is preserved under all but the most severe physical conditions*. At the opposite, but physically unrealistic, extreme, we could distort the line shape to be flat (i.e., constant in frequency) over a width w much greater than the span of the two weighting functions but still such that $\mu w = \text{constant}$. Then the weighting integrals could be performed, giving unity in both cases and the two means would be equal. Perhaps a clearer explanation, however, resides in the fact that a harmonic mean of any function, say

$$\bar{\mu}_H = \frac{1}{\frac{1}{\Delta x} \int_{\Delta x} \frac{dx}{\mu(x)}} \quad (6.3-15)$$

is always less than the corresponding direct mean

$$\bar{\mu}_D = \frac{1}{\Delta x} \int_{\Delta x} \mu(x) dx \quad (6.3-16)$$

* As long as the line width is small compared to kT , which is usually the case.

This is easily seen by setting

$$f = \frac{1}{\sqrt{u(x)}} \quad (6.3-17a)$$

and

$$g = \sqrt{u(x)} \quad (6.3-17b)$$

in the Schwartz inequality. Eq. (6.3-1) , and integrating over the range Δx .

This immediately yields

$$\bar{u}_H \leq \bar{u}_D \quad (6.3-18)$$

Except for the factor 1.053 this is the same as Eq. (6.3-10). Hence, it appears that the weighting functions are somewhat superfluous. The equality occurs when both functions are constant over Δx .

Another approach to the problem of bounds has been taken by Liberman (1962) who wrote a general factorization formula

$$\int_0^{\infty} \frac{W'(u) du}{\mu'(u)} \int_0^{\infty} \mu^t \mu'(u) du \geq \left\{ \int_0^{\infty} [W(u) \mu^t]^{1/2} du \right\}^2 \quad (6.3-19)$$

where

$$\mu'(u) = \mu(u) (1 - e^{-u}) \quad (6.3-20)$$

and

$$W'(u) = \frac{15}{4\pi^4} \frac{\mu^4 e^u}{(1 - e^{-u})^2} \quad (6.3-21)$$

On the left hand side of Eq. (6.3-19), the first integral is the reciprocal of μ_R , and the second integral may be evaluated by means of f-number sum rules for $l = 2, 1, 0, -1, -2$. (The Bernstein-Dyson theorem corresponds to $l = 0$.) Apparently, the bound for $l = 2$, i.e., $\bar{\mu}_2$, is also considerably superior to $\bar{\mu}_0$ as was shown by computation for hydrogen compared with the Bernstein-Dyson continuum opacity values. Liberman's result for $l = 2$ may be written as

$$\bar{\mu}_R \leq \bar{\mu}_2 = \frac{1}{(19.112)^2} \int_0^{\infty} u^2 \mu'(u) du \quad (6.3-22)$$

Armstrong (1965) has recently noted that since $e^{-u} (1+u) \leq 1$, one can write

$$\int u^2 (1+u) e^{-u} \mu(u) du \leq \int u^2 \mu(u) du \quad (6.3-23)$$

from which it easily follows that

$$\int u^3 e^{-u} \mu(u) du \leq \int u^2 (1 - e^{-u}) \mu(u) du \quad (6.3-24)$$

Eqs. (6.3-4), (6.3-20), and (6.3-22) may then be combined to give

$$\bar{\mu}_P \leq 56.3 \bar{\mu}_2, \quad (6.3-25)$$

which offers an opportunity to examine the relative utility of $\bar{\mu}_P$ and $\bar{\mu}_2$ as upper bounds for $\bar{\mu}_R$.

Let us consider the two idealized model absorption coefficients shown in Fig. 6-5 . For the first model portrayed in Fig. 6-5 we understand that $\mu = 0$ unless $u \ll 1$. In this case we note that

$$u^2 (1 - e^{-u}) \approx u^3 \approx u^3 e^{-u} \quad , \quad (6.3-26)$$

and therefore, calling this first model $\mu^{(1)}(u)$, we can write

$$\int u^3 e^{-u} \mu^{(1)}(u) du \approx \int u^2 \mu'(u) du \quad , \quad (6.3-27)$$

with the result that

$$\bar{\mu}_p^{(1)} \approx 56.3 \bar{\mu}_2 \quad . \quad (6.3-28)$$

For the second model, we understand that the absorption coefficient peaks at a value of $u^{(2)} \gg 1$. (In Fig. 6-5 this value is arbitrarily represented as $u^{(2)} = 7$) . We can now write that

$$\int u^3 e^{-u} \mu^{(2)} du \approx C \int u^2 \mu' du \quad , \quad (6.3-29)$$

with

$$C \approx e^{-u^{(2)}} [1 + u^{(2)}] \ll 1 \quad , \quad (6.3-30)$$

and therefore

$$\bar{\mu}_p^{(2)} \approx 56.3 C \bar{\mu}_2 \quad (6.3-31)$$

For $u^{(2)} \sim 6$, 56.3 C is equal to unity, and for $u^{(2)} \gg 6$, $56.3 \text{ C} \ll 1$.

Since $u = hv/kT$, these models are idealized representations of high temperature [$u^{(1)}$] and low temperature [$u^{(2)}$] absorption, with "high" and "low" defined by the relative size of kT and the range of typical ionization edges and absorption frequencies taken for hv . We can thus conclude qualitatively that for temperatures of the order of typical atomic ionization potentials and larger, $\bar{\mu}_2 < \bar{\mu}_p$ and constitutes a better bound for $\bar{\mu}_R$. On the other hand for temperatures below these ionization potentials, the inequality in Eq. (6.3-10) is expected to be more useful.

These conclusions are also indicated from the behavior of the functions that weight $\mu(\nu)$ in the defining integrals for $\bar{\mu}_p$ and $\bar{\mu}_2$. The function $u^3 e^{-u}$ cuts off the high-frequency absorption (compared with kT), whereas $u^2(1-e^{-u})$ does not, but rather, increases monotonically. Thus, at low temperatures where most of the absorption potential lies far ahead of kT in the form of lines and edges, $\bar{\mu}_p < \bar{\mu}_2$. However, at high temperatures kT has already passed most of the absorption potential (which lies toward $u = 0$ in the free-free continuum), and $\mu(\nu)$ is decreasing monotonically, with the result that $\bar{\mu}_2 < \bar{\mu}_p$.

Some confirmation of these predictions can be obtained by a comparison of results. Liberman has computed $\bar{\kappa}_2 = \bar{\mu}_2/\rho$ for hydrogen for a range of densities at $kT = 5, 10$ and 20 eV . Figs. 6-6 (5 and 10 eV) and 6-7 (20 eV) show his results in comparison with the Stewart-Pyatt (1961) results for $\bar{\kappa}_p$ and $\bar{\kappa}_R$, which include line contributions. For $kT = 5 \text{ eV}$,

$\bar{\kappa}_p$ is about 1.5 times $\bar{\kappa}_2$ for the densities shown, and this ratio clearly increases with kT , while a rough calculation indicates that $\bar{\kappa}_p$ becomes approximately equal $\bar{\kappa}_2$ at about 3-4 eV, and then presumably $\bar{\kappa}_p < \bar{\kappa}_2$ when $kT \gtrsim 3$ eV. Also, as kT increases, $\bar{\kappa}_R$ approaches $\bar{\kappa}_2$. The suspicious behavior of $\bar{\kappa}_R$ vs. $\bar{\kappa}_2$ at the low-density end of the 20 eV curve (where $\bar{\kappa}_R$ appears to be on the verge of crossing $\bar{\kappa}_2$) is probably due to the Compton scattering contribution included in the Stewart-Pyatt results, but omitted in the sum rule.

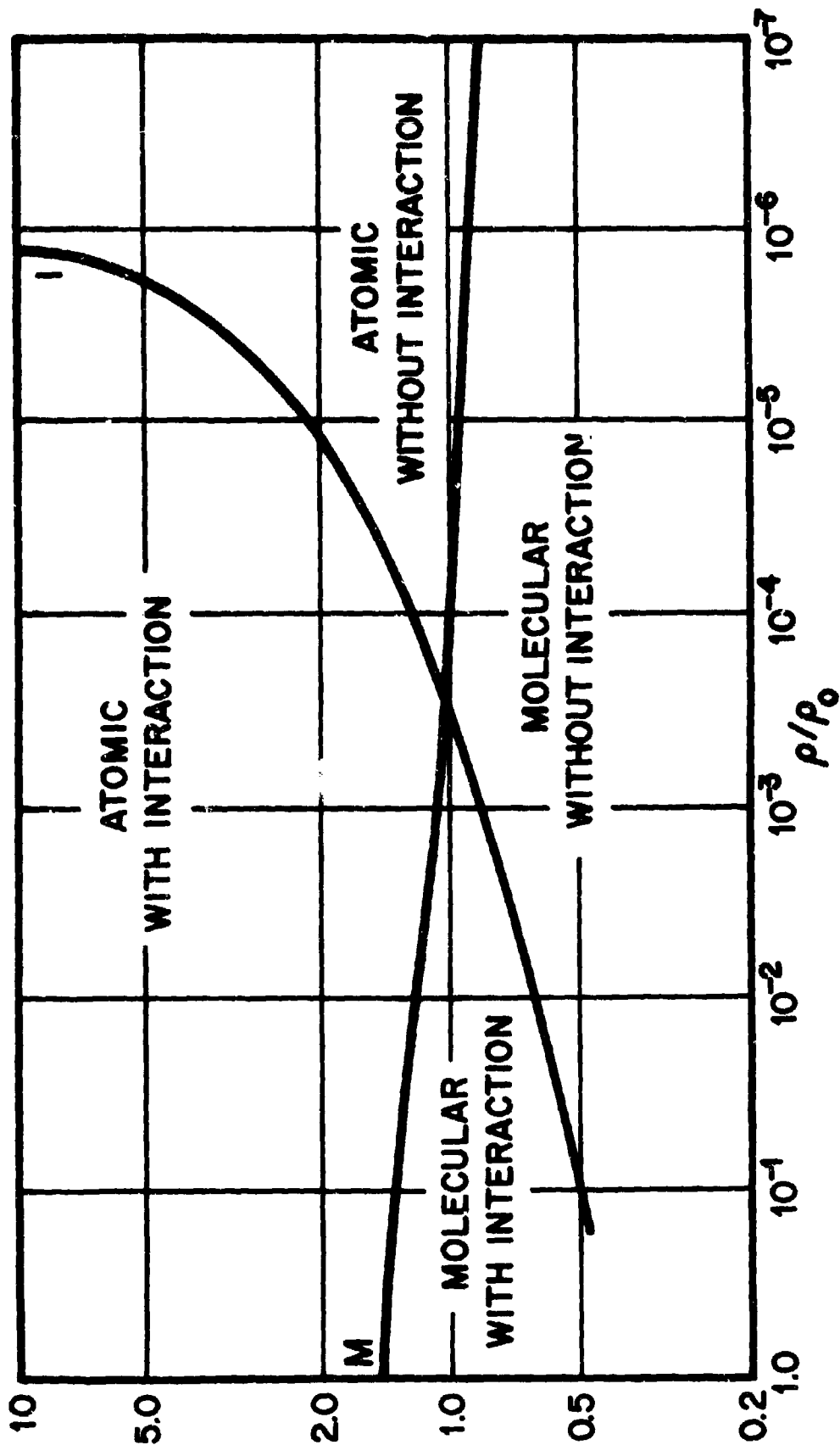


FIG. 6-1 SUBDIVISION OF TEMPERATURE-DENSITY PLANE INTO MOLECULAR AND ATOMIC REGIONS AND INTO REGIONS WHERE INTERACTION CAN AND CANNOT BE NEGLECTED FOR AIR.

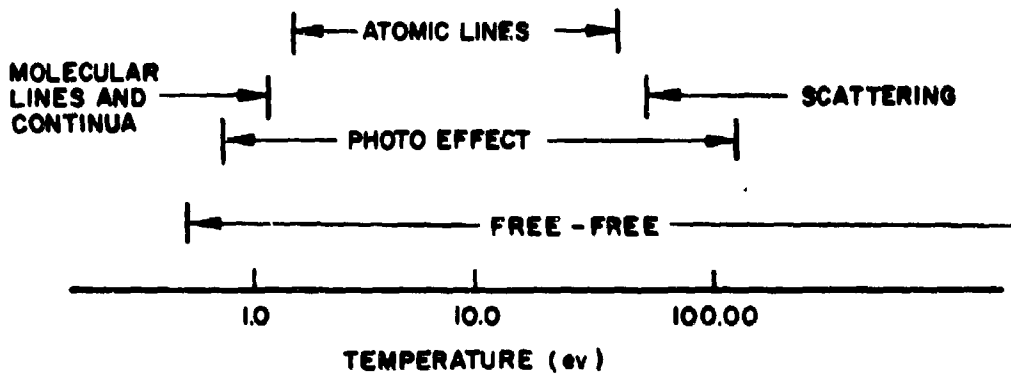


FIG. 6-2 EFFECTS WHICH CONTRIBUTE TO THE ABSORPTION COEFFICIENT OF AIR AS A FUNCTION OF TEMPERATURE

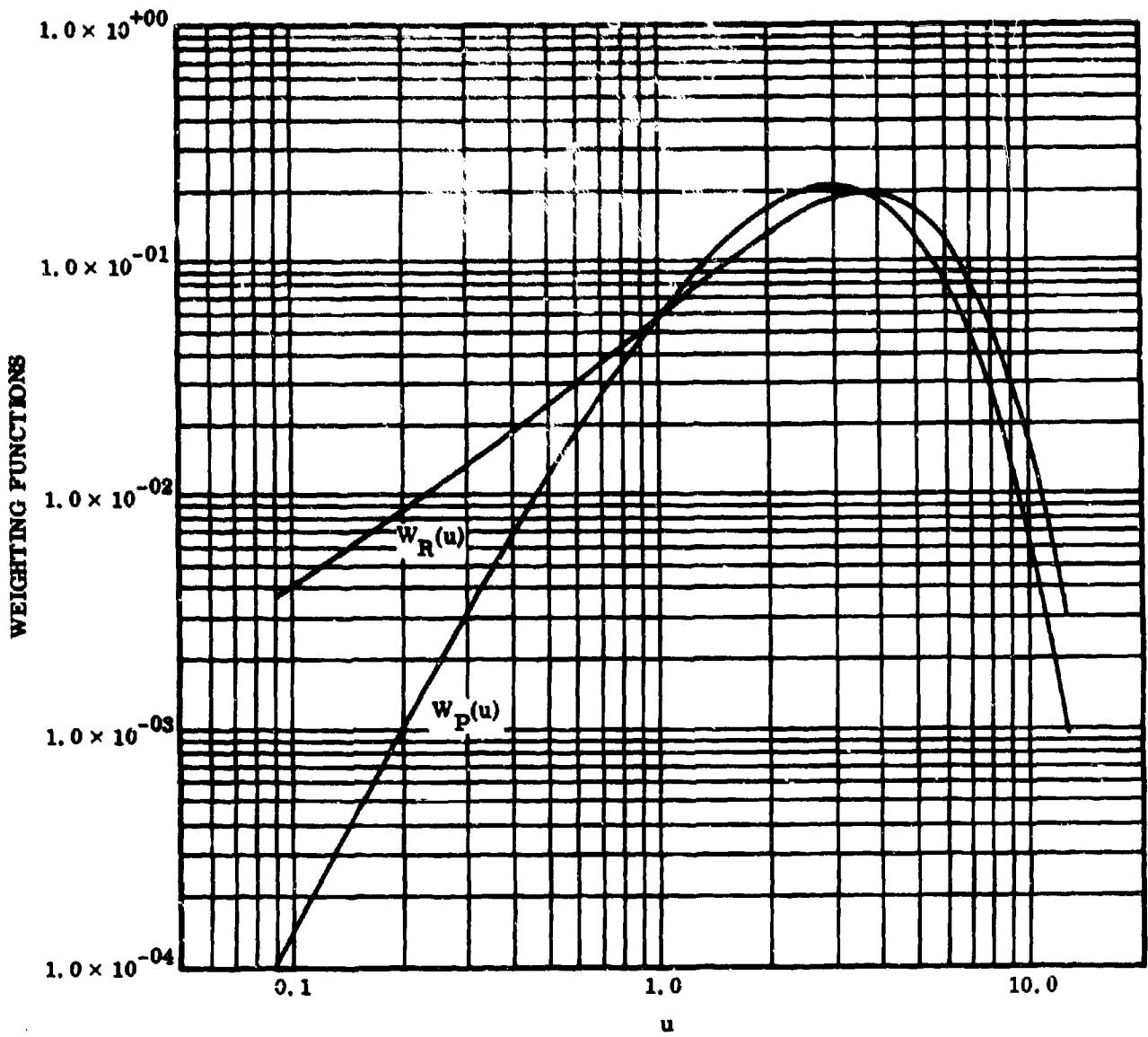


FIG. 6-3 PLANCK AND ROSSELAND WEIGHTING
FUNCTIONS AS GIVEN BY EQS. (6.2-8)

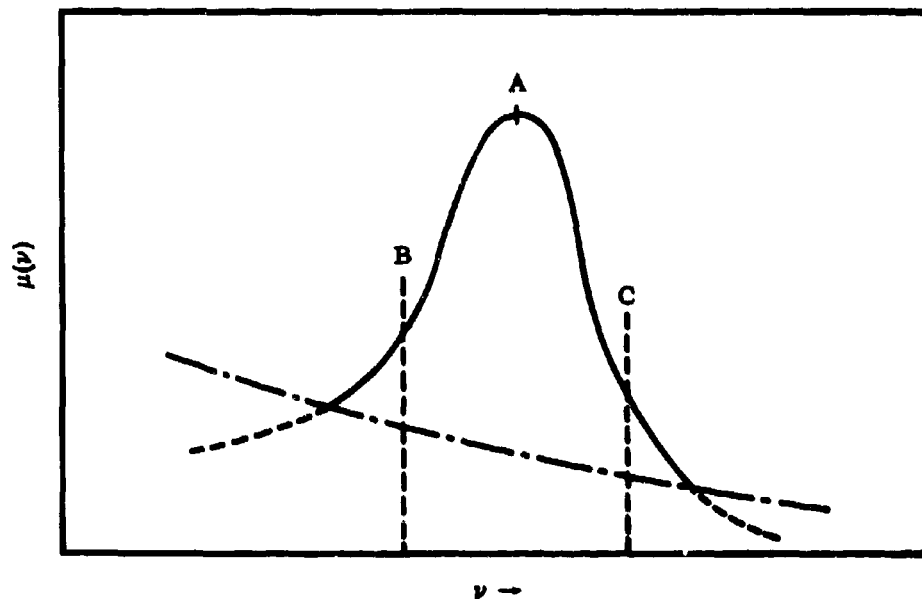


FIG. 6-4 SCHEMATIC ILLUSTRATION OF SPECTRUM LINE SUPERIMPOSED ON CONTINUUM BACKGROUND. THE REGION BETWEEN B AND C IS THE LINE CORE, AND THE REGIONS TO THE LEFT AND RIGHT OF B AND C, RESPECTIVELY, ARE THE LINE WINGS.

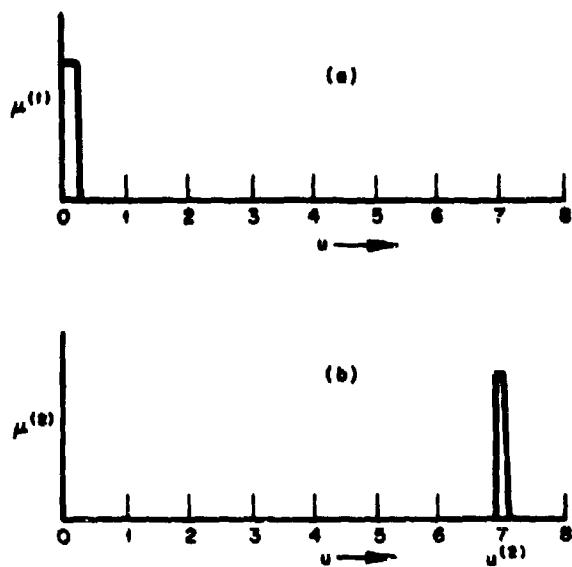


FIG. 6-5 SIMPLIFIED MODEL ABSORPTION COEFFICIENTS WHICH ILLUSTRATE THE DOMINANT TREND IN (a) HIGH-TEMPERATURE ABSORPTION AND (b) LOW-TEMPERATURE ABSORPTION

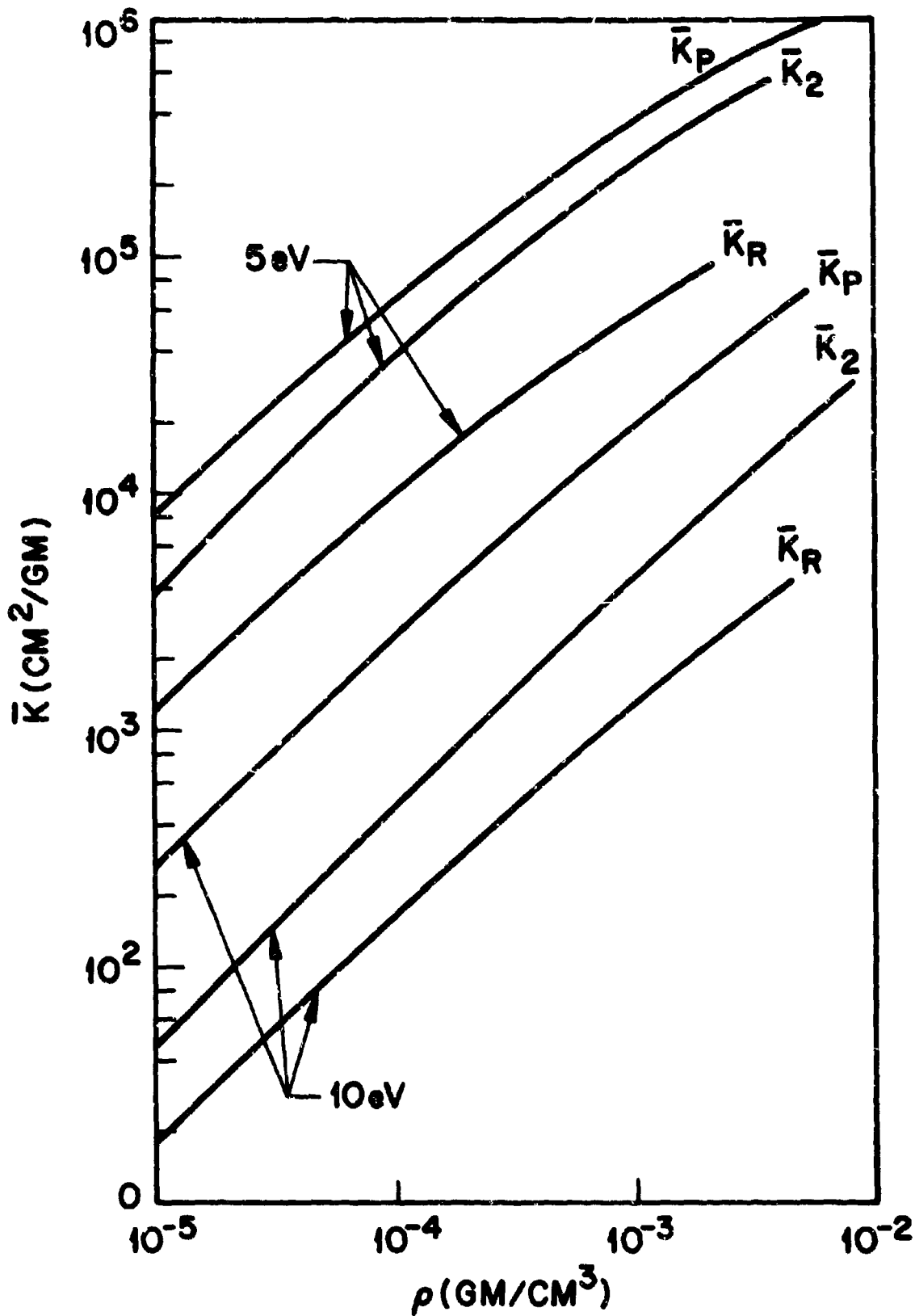


FIG. 6 - 6 UPPER BOUNDS ON THE PLANCK (\bar{K}_P) AND ROSSELAND (\bar{K}_R) MEAN ABSORPTION COEFFICIENTS: A COMPARISON OF THE MAGNITUDES OF \bar{K}_P AND \bar{K}_R AS A FUNCTION OF DENSITY WITH LIBERMAN'S \bar{K}_2 FOR HYDROGEN AT TEMPERATURES OF 5 AND 10 eV.

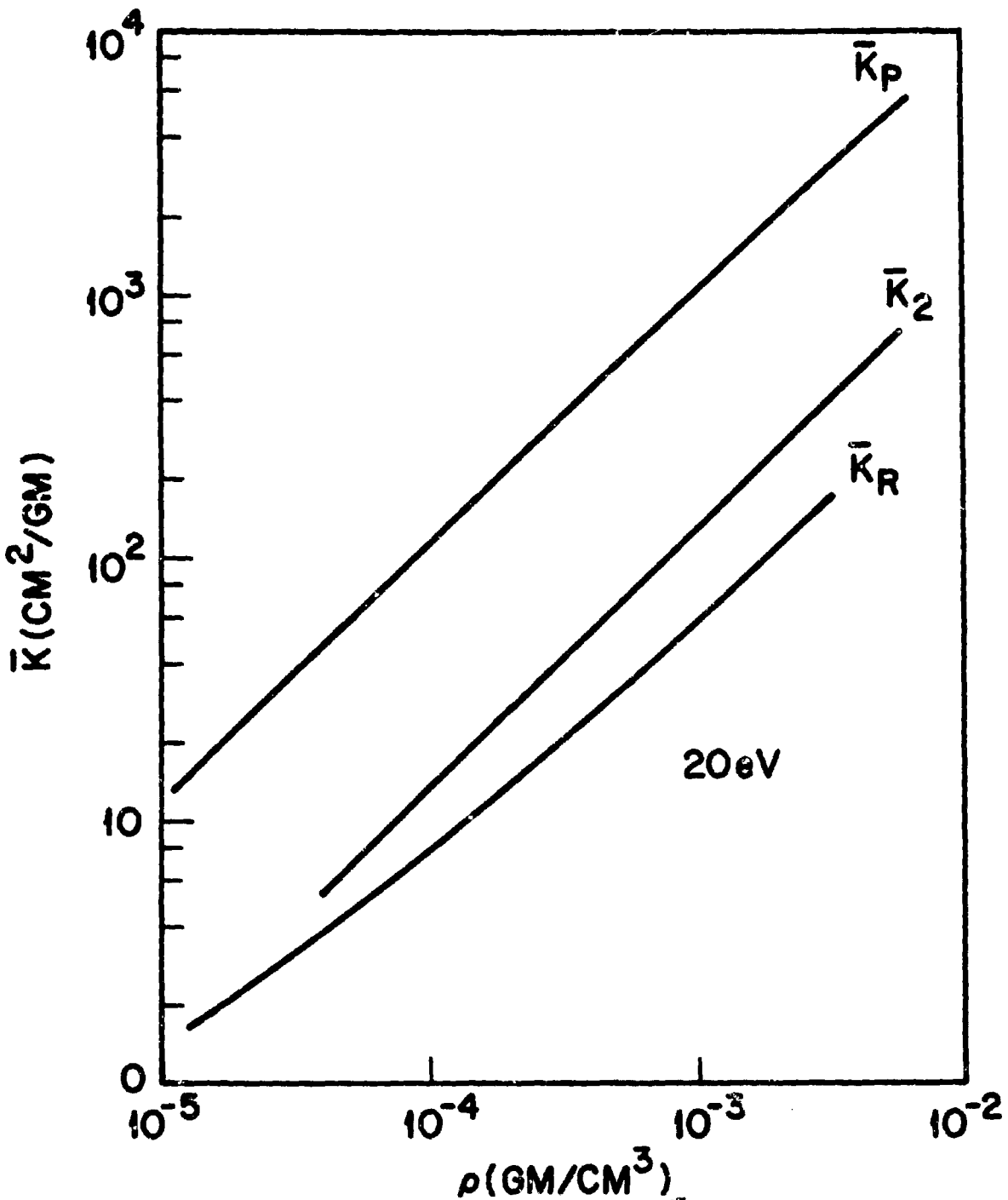


FIG. 6-7 UPPER BOUNDS ON THE PLANCK (\bar{K}_P) AND ROSSELAND (\bar{K}_R) MEAN ABSORPTION COEFFICIENTS: A COMPARISON OF THE MAGNITUDES OF \bar{K}_P AND \bar{K}_R AS A FUNCTION OF DENSITY WITH LIBERMAN'S \bar{K}_2 FOR HYDROGEN AT A TEMPERATURE OF 20 eV.

Chapter 7. MOLECULAR ABSORPTION COEFFICIENTS

In this chapter we discuss the molecular contributions to the opacity of relatively low temperature ($< 1 \text{ eV}$) air. Molecular species and transitions which make important contributions are reviewed in section 7.1. Less important molecular contributions are discussed in section 7.2. A review is made in section 7.3 of actual calculations of the molecular aspects of air opacities based on the theory of Chapter 4.

One difference between the approach to the (low temperature) molecular calculations of this chapter and the (high temperature) atomic calculations of Chapter 8 should be pointed out. Both require independent study of population and transition probability parameters. They differ however in the way by which contributing spectral features are taken into account. Detailed molecular theory is less comprehensively developed than atomic theory. Thus a priori selection of the probably important contributory molecular spectra of those species which are expected to be present on thermodynamic grounds is made from general knowledge of the spectra of the species. Atomic theory is however, well enough developed that a completely theoretical allowance can be made not only for the structure of atomic species expected to be present but also for all transitions between the predicted energy levels.

7.1 Molecular species and transitions of importance

The major constituents of air are N_2 and O_2 which react chemically when heated to form NO . The heating also causes some ionization. Thus N_2 , O_2 , NO and some or all of their ions might be expected to be major molecular contributors to the absorption coefficient of air at temperatures below say $12,000^\circ K$ (about 1 eV). Above 1 eV, dissociation of diatomic species rapidly becomes complete and major contributions to the absorption coefficient come from atoms, atomic ions and free electrons. At relatively low temperatures, say below a few thousand degrees, contributions from the triatomic species CO_2 , H_2O and NO_2 (formed from chemical reactions) must also be considered.

In this section we review band systems of the above six major diatomic molecular species and indicate which of them are major contributors to the absorption coefficient. In section 7.2 possible minor contributors are discussed, and in section 7.3 a review is made of calculations over the past two decades of the molecular contribution to the absorption coefficient which have taken these transitions into account. The discussion is mainly confined to the conventional optical region of the spectrum: 1000 Å - 10,000 Å which includes the near vacuum ultraviolet and the near infrared with the ultraviolet and visible regions.

There is an incorrect yet widely held point of view that all electronic transitions and band systems of N_2 , O_2 , NO and their ions are well known, completely studied and analyzed, and that all possible molecular

constants have been definitively established and tabulated. Conventional spectroscopic studies have, of course been carried out on these molecules for many years, but new band systems and new bands of old systems continue to be discovered. This is the pattern of contemporary molecular spectroscopy. Relatively few band systems per molecule, relatively few bands per system and relatively few lines per band have been definitively measured and analyzed in the overall study of diatomic species. The relatively recent identification of the $D^3\Delta_u - a^1\Delta_g$ Chamberlain system of O_2 in the airglow spectrum (see Chamberlain 1958, 1961) and the discovery of the $D^2\Pi_u - A^2\Pi_u$ Janin-d'Incan system of N_2^+ (see Janin and d'Incan, 1958; Grandmontagne, d'Incan and Janin, 1959; Tanaka, Namioka and Jursa, 1961) and a number of new systems of NO (Miescher, 1962) are examples of continuing research on molecules, some of whose spectra have been known for many years.

The relatively fragmentary and changing state of our knowledge of the qualitative (wavelength) and quantitative (intensity) aspects of the spectroscopy of N_2 , O_2 , NO and their ions has had an important influence on the progress of theoretical studies on the absorption coefficient of heated air as will become clear in the discussion of following sections. Definitive opacity calculations require a firm knowledge of the positions (wavelengths) of all possible contributing features and of the transition probability parameters of each. Our knowledge of both of these aspects of the spectra of the six important diatomic species has been incomplete because of the motivation of much of conventional molecular spectroscopic research. One major aim of such work is the determination of molecular

constants from which molecular structure may be inferred and discussed. Band systems are excited and measured so that sufficient vibrational and rotational analyses may be made to determine for each electronic state such vibrational constants as $\omega_e, \omega_e x_e, \omega_e y_e$ and such rotational constants as B_e (from which the equilibrium internuclear separation r_e may be determined) α_e etc. Some of these symbols have been discussed in Chapter 4 and are more fully discussed by Herzberg (1950). When sufficient bands have been identified and measured to provide the vibrational constants, and sufficient bands have been rotationally analyzed to provide the rotational constants, the motivation disappears for more extensive measurements and analyses which, except for uncovering perturbations and predissociations, will not provide much more information on molecular structure. Thus perhaps only 20% of the known bands of a system have been rotationally measured and analyzed. Seldom have vibrational levels been followed to the dissociation limit of the electronic state. Few laboratory sources of spectra excite high temperatures such as are discussed in opacity calculations, and thus the positions of rotational lines at very high rotational quantum numbers (say >100) which are excited in high temperature sources have not been measured. The prediction of the position of such lines by extrapolation of the series of expressions determined from analyses of lines of lower quantum numbers has high probability for error. Systematic rotational analyses of high temperature spectra of carbon containing molecules of importance in astronomy is being carried out by Phillips and his colleagues at Berkeley (Phillips, 1963). Some years ago Mesdames Gibson and Buttery at Lockheed made some rotational analyses to high quantum numbers of N_2^+ bands excited

in a shock tube (Gibson, 1962). The determination of molecular potentials by the Klein-Dunham procedure often requires a firmer knowledge of vibrational and rotational constants than has been provided by conventional analyses (see discussion of Gilmore, 1965). A rough average statement might be that of the less than 10 bands systems per diatomic molecule which are known, less than 50 bands per system have been identified and less than 5-10 bands per systems have been subjected to rotational analysis of less than about 50 lines per branch. The 'best' constants for band systems treated in opacity calculations are displayed in Volume 3 of this series and have been supplied after a critical review of the literature by Gilmore.

Pearse and Gaydon (1963), Wallace (1962a, b) have provided most valuable compilations of known molecular spectra which illustrate a number of the above points. Tyte and Nicholls (1964a, b, 1965) and colleagues are producing identification atlases of molecular spectra.

From the above remarks we may conclude that in a practical sense molecular contributions to hot air opacity, and the manner in which they are allowed for, differ from atomic contributions in two ways:

- a) Although there are far fewer band systems per molecule than lines per atom, the closely packed, multi-line structure of the band systems, which becomes more extensive at higher temperatures as the high rotational levels become excited give rise to broader regions of opacity than are contributed by atomic lines at the same temperature.

b) Our detailed theoretical knowledge of molecular spectra and molecular structure is far less comprehensive than the comparable state of development of atomic theory. Thus in theoretical studies of molecular opacity, appeal has to be made to experimental knowledge of molecular spectra to decide which spectral features should be included in the opacity calculations. In atomic calculations the theory is comprehensive enough not to have to make so direct an appeal to experiment.

With the above remarks as background, we now review a partial list of band systems for the important species N_2 , O_2 , NO and their ions. Gilmore (1965b) in a discussion of the known potential energy curves of the electronic states of these molecules has in his Table 1 made a complete list of all known electronic transitions between the states. Some of these transitions are only known by virtue of one or two bands as may be seen by comparing his list with the detailed compilation of Wallace. Accordingly we list here the major band systems of the species in Tables 7-1 - 7-6 which also contain information on wavelength extension of the systems. These tables are illustrated in Figs. 7-1 - 7-6 with simplified energy level arrays on which the electronic states and transitions are indicated.

Table 7-1
MAJOR BAND SYSTEMS OF N₂

<u>Wavelength Range (Å)</u>	<u>Name</u>	<u>Transition</u>
Far Vacuum U.V.	Birge-Hopfield, Worley,	(i, j, p, q, r, s, t, u, v) - X ¹ Σ _g ⁺
920-1644	Birge-Hopfield (a)	b ¹ Π _u - X ¹ Σ _g ⁺
955-1438	Birge-Hopfield (b) - Worley	b' ¹ Σ _u ⁺ - X ¹ Σ _g ⁺
1205-2602	Lyman-Birge-Hopfield	a ¹ Π _g - X ¹ Σ _g ⁺
1333-2004	Wilkinson-Mulliken	a' ¹ Σ _u ⁻ - X ¹ Σ _g ⁺
2019-2232		B ³ Σ _u ⁻ - X ¹ Σ _g ⁺
2034-2761	Fifth Positive	l _g ⁻ - a' ¹ Σ _u ⁻
2138-2733	Herman-Kaplan	E ³ Σ _g ⁺ - A ³ Σ _u ⁺
2224-3661	Gaydon-Herman Singlet Systems	(b, l, p', d, m, o, r', k, d'', g, s', d', h, e) - a ¹ Π _g
2256-2904	Fourth Positive	C ³ Π _u - B ³ Π _g
2263-2855	Kaplan's Second	y ¹ Π _g - w ¹ Δ _u
2333-5060	Vegard-Kaplan	A ³ Σ _u ⁺ - X ¹ Σ _g ⁺
2369-2477	Lofthus	Z ¹ Δ _g - w ¹ Δ _u
2687-5482	Second Positive	C ³ Π _u - B ³ Π _g
4166-5076	Goldstein-Kaplan	C' ³ Π _u - B ³ Π _g
4273-4 _μ	First Positive	B ³ Π _g - X ³ Σ _u ⁺
5047-6336	Gaydon-Green	probably ³ Σ _g ⁻ - ³ Π
6058-8900	Infra-red Afterglow	B' ³ Σ _u ⁻ - B ³ Π _g

Table 7-2
MAJOR BAND SYSTEMS OF O₂

<u>Wavelength Range (Å)</u>	<u>Name</u>	<u>Transition</u>
1958-5720	Schumann-Runge	$B^3\Sigma_u^- - X^3\Sigma_g^-$
2540-6541	Herzberg II	$c^1\Sigma_u^- - X^3\Sigma_g^-$
2562-4881	Herzberg I	$A^3\Sigma_u^+ - X^3\Sigma_g^-$
2570-2630	Herzberg III	$D^3\Delta_u - X^3\Sigma_g^-$
3650-4840	Broida-Gaydon	$A^3\Sigma_u^+ - b^1\Sigma_g^+$
3700-4380	Chamberlain Airglow	$C^3\Delta_u - a^1\Delta_g$
5795-8645	Atmospheric	$b^1\Sigma_g^+ - X^3\Sigma_g^-$
1.27 - 1.58 μ	Infra-red Atmospheric	$a^1\Delta_g - X^3\Sigma_g^-$
1.91 μ	Noxon	$b^1\Sigma_g^+ - a^1\Delta_g$

Table 7-3
MAJOR BAND SYSTEMS OF NO

<u>Wavelength Range (Å)</u>	<u>Name</u>	<u>Transition</u>
1455-1888	B''	$B'' - X^2\Pi$
1461-3459	γ	$A^2\Sigma - X^2\Pi$
1462-2392	ϵ	$D^2\Sigma - X^2\Pi$
1475-1870	γ'	$E^2\Sigma - X^2\Pi$
1504-2060	B'	$B'^2\Delta - X^2\Pi$
1910-2415	δ	$c^2\Pi - X^2\Pi$
2018-6511	θ	$B^2\Pi - X^2\Pi$
5225-8021	Ogawa 1	$B'^2\Delta - B^2\Pi$
6000	Feast 1	$D^2\Sigma - A^2\Sigma$
7725-9733	Ogawa 2	$b^4\Sigma^- - a^4\Pi$
1.1 μ	Feast 2	$E^2\Sigma - A^2\Sigma$
1.36 - 5.33 μ	Vibration-Rotation	$X^2\Pi - X^2\Pi$

Table 7-4
MAJOR BAND SYSTEMS OF N₂⁺

<u>Wavelength Range (Å)</u>	<u>Name</u>	<u>Transition</u>
1377-2060	Second Negative	$C^2\Sigma_u^+ - X^2\Sigma_g^+$
2240-3070	Janin d' Incan	$D^2\Pi_g - A^2\Pi_u$
2913-5865	First Negative	$B^2\Sigma_u^+ - X^2\Sigma_g^+$
5516-17706	Meinel	$A^2\Sigma_u - X^2\Sigma_g^+$

Table 7-5
BAND SYSTEMS OF O₂⁺

<u>Wavelength Range (Å)</u>	<u>Name</u>	<u>Transition</u>
2060-6103	Second Negative	$A^2\Pi_u - X^2\Pi_g$
6992-7891	First Negative	$b^4\Sigma_g^- - a^4\Pi_u$

Table 7-6
BAND SYSTEM OF NO⁺

<u>Wavelength Range (Å)</u>	<u>Name</u>	<u>Transition</u>
1160-1680	Miescher-Baer	$A^1\Pi - X^1\Sigma^+$

Different transitions of course dominate different regions of the spectrum and to various extents. In the calculations which are reviewed in section 7.3 the most common molecular and atomic contributors to the spectral absorption coefficient of heated air are listed in Table 7-7.

These certainly seem to be the major contributors, but the Tables 7-1 - 7-6 and Figs. 7-1 - 7-6 raise the possibility that other transitions (e.g., N_2^+ Meinel, Janin-d'Incan, N_2 Birge-Hopfield, etc.) should eventually be incorporated in the calculations. Many of the transitions listed in Table 7-7 are spectroscopically quite complicated. For example each band of the N_2 First Positive system has 27 branches. Nicholls (1962) has recently discussed many of these systems and what is known of their transition probability in the context of aeronomical (auroral and airglow) luminosities. Spectroscopic data for many of these transitions are listed by Gilmore in Volume 1 of this series.

Table 7-7
MOST COMMONLY TREATED ATOMIC AND MOLECULAR CONTRIBUTORS
TO THE ABSORPTION COEFFICIENT OF HEATED AIR

Atomic Contributors

O^- , O , N : Photoelectric transitions

e : Free-free transitions

Molecular Contributors

N_2

First Positive, Second Positive, Lyman-Birge-Hopfield, Birge-Hopfield

N_2^+

First Negative

O_2

Schumann-Runge

NO

β , γ , Vibration-rotation

NO_2

7.2 Less important molecular species and transitions

Minor contributors to the absorption spectrum of air which have to be considered briefly are: a) contributions from minor constituents of the atmosphere; b) contributions from other band systems of major constituents than those listed in Table 7-7. So far very little quantitative account has been taken of minor contributors in calculations of absorption coefficients.

Gilmore (1965a) has made a recent assessment of the relative importance of minor contributors and has made approximate quantitative estimates of their effects.

The minor atmospheric constituents are CO_2 and H_2O . NO_2 formed from chemical reactions in heated air also has to be considered. As the temperature rises, diatomic dissociation and reaction products of these molecules also have to be considered. Such products as CO , OH , CH , CN , NH are probably present in small amounts and all have band systems which could contribute to the absorption coefficient. Their parent triatomic molecules are in such relatively small concentration that the effect of such diatomics would probably be quite small except in spectral regions where the effect of major contributors is small and the air is effectively transparent.

In the vacuum ultraviolet region of the spectrum Gilmore (1965a) calls attention to the possible importance of the Birge-Hopfield $b^1\Pi_u - X^1\Sigma_g^+$

and $b^1\Sigma_u^+ - X^1\Sigma_g^+$ systems, particularly bands of them which originate in absorption from high vibrational levels (~ 10) of the $X^1\Sigma_g^+$ state. He is able to explain Wray and Teare's (1962) measurements of absorption coefficient of N_2 and 1270 Å as a function of temperature, in terms of contributions from these band systems. There are many other band systems of N_2 in the vacuum ultraviolet which may also make some contributions (see the review of Wilkinson, 1961). Intensity data for all of them is very sparse. The CO Fourth Positive System ($A^1\Pi - X^1\Sigma$) may also make a contribution in the vacuum ultraviolet absorption under conditions of a significant concentration of CO. It makes such a contribution in the solar atmosphere (Goldberg, Parkinson and Reeves, 1965). NO also has many systems (Miescher, 1962) which may contribute. Possible consideration should be given to the Wilkinson-Mulliken $a^1\Sigma_u - X^1\Sigma_g$ systems of N_2 and the Hopfield-Birge systems $B^1\Sigma^+$ and $b^3\Sigma^+ - X^1\Sigma$ of CO.

Gilmore points out that in the visible region of the spectrum the major constituents of air are transparent and in this region some of the minor contributors may have significant effects. Account has been taken of the very complex spectrum of NO_2 (Mueller, 1963) in a number of calculations of absorption coefficient. It is very difficult to deal with this spectrum in such calculations in any more than semi-empirically. It undoubtedly plays a role at low temperatures.

The CN Red ($A^2\Pi-X^2\Sigma$) and Violet ($B^2\Sigma-X^2\Sigma$) systems may make some contribution because the N arises from a major constituent. Their spectroscopy is fairly well known. They lie in the same spectral region as the N_2 First Positive and N_2^+ First Negative Systems, and for this reason discrimination between contributions from CN and the N_2 and N_2^+ may present difficulties. Absolute band strengths are available from some CN Violet (Nicholls, 1964) bands. While intensities for CN Red have been measured (Dixon and Nicholls, 1957) there is not agreement between recent lifetime measurements (Wentinck, Isakson and Morreal, 1964; Jeunehomme, 1965) using the same method. Jeunehomme's measurements appear to be the more reliable.

Although firm spectroscopic knowledge of them is fragmentary, some account may also have to be taken of N_2 and CO systems whose lowest electronic states are in the first two or three excited states of the molecules. N_2 First and Second Positive band systems are strong contributors and in this position. There are other contending N_2 systems in the same position about which much less is known, e.g., Herman-Kaplan ($E^3\Sigma_g^+ - A^3\Sigma_u^+$), Fourth Positive ($D^3\Sigma_u^+ - B^3\Pi_g$), Goldstein-Kaplan ($C^3\Pi_u - B^3\Pi_g$), Fifth Positive ($x^1\Sigma_g^- - a^1\Sigma_u^-$), etc. and a number of others (see Fig. 1) (see Pearse and Gaydon, 1962; Wallace, 1962a; Lofthus, 1960). There are a number of similarly situated systems of CO e.g., Cameron ($a^3\Pi - X^1\Sigma$) Third Positive ($b^3\Sigma - a^3\Pi$) and a number of others. Some of these systems are admittedly weak (i.e., difficult to excite in emission) others are of

moderate strength. Until they have been shown to have negligible transition probabilities they should not necessarily be ruled out as possible contributors to the spectrum of heated air.

The obvious minor contributors to the near infrared spectrum of heated air are NO_2 CN Red, N_2 Infrared Afterglow ($B^3\Sigma_u^- - B^3\Pi_g$), CO Asundi ($a^3\Sigma^+ - a^3\Pi$), N_2^+ Meinel ($A^2\Pi - X^2\Sigma$), NO Ogawa ($b^4\Sigma^- - a^4\Pi$), in addition to the vibration-rotation spectrum of NO, NO_2 , CO, CO_2 , N_2O , CN and NO^+ .

Until we know more of the probable relative populations of the minor species and of the general qualitative and quantitative spectroscopy of the types of band systems cited above, it is profitless to speculate further on their probable contributions.

7.3 Review of calculations of the molecular contribution to the absorption coefficient of heated air

Calculations on the opacities of hot gases have been made for many years in astrophysical situations; such work is the heart of traditional astrophysics (Aller, 1963). It is directed towards an understanding of planetary and stellar envelopes and various models of them. The calculations often involve gross average absorption coefficients of a relatively small number of contributing species. The Planck- and Rosseland Mean absorption coefficients were thus developed in astrophysical discussions of stellar atmospheres, and for the solutions of the appropriate equations of transfer.

During the past two decades as interest in the earth's atmosphere increased, similar, but more detailed calculations of the absorption coefficient

of air have been undertaken. The calculations have been made for a wide range of temperatures and densities, and have taken account of chemistry and of as many spectral features of known atmospheric constituents as possible. Those contributors to the air absorption coefficient which have been thought to be most important were listed in Table 7.7. The motivation of recent quantitative work on absorption coefficients is of specific interest in such artificially induced high temperature aeronomical phenomena as high altitude nuclear explosions (in which radiation is a very important mode of energy transfer), and the entry of high speed bodies (meteors, spacecraft and missiles) into the atmosphere.

While the first calculations were of broad average absorption coefficients, our current knowledge of air constituents, chemistry, and spectroscopy of air constituents, incomplete though it be, has recently led to a number of more detailed calculations of increasing sophistication. It is the purpose of this section to review what studies have been made and to attempt to place them in perspective. Nearly all of them have been made on the assumption of the existence of thermal equilibrium. Non-equilibrium effects undoubtedly occur and are difficult to allow for. A discussion of such phenomena is given in Volume 4.

Many of the calculations of absorption coefficient of heated air are unfortunately only described in reports of contract-supported research, which are not universally available nor completely abstracted. No claim can be made here that all such reports have been reviewed. Some of the work has, of course been published in the open literature, and it is hoped that a representative selection of such papers are discussed below.

The original studies which were necessarily classified at the time were made in connection with nuclear weapons development in the early 1940's at Los Alamos. Some of these reports have now been declassified. Two 'Opacity' conferences co-sponsored by the Los Alamos Laboratory and the Air Force Special Weapons Laboratory were held at Kirtland AFB in the summers of 1963 and 1964 and were particularly useful for a general orientation of the field. Two status reports (Huebener and Stewart 1964, 1965) arising in part from the conferences provide a fairly comprehensive, author-supplied list of workers in the field and studies being made. The second of the conferences was published in toto in The Journal of Quantitative Spectroscopy and Radiative Transfer, Volume 5, No. 1, Jan./Feb. 1965. The papers in that proceedings (some of which are referred to here) provide a good orientation in the current state of the field.

All the molecular calculations were based, in principle, on Eqs. (4.1-27), (4.1-33) and (4.1-34). The earliest calculations involved very broad averages, later calculations, although they also involved averages took account of individual band systems, and later individual bands of the systems. The latest calculations incorporate a study of the absorption coefficient line by line of each band. It is clear from the above equations that in common with atomic contributions all of the calculations involve two stages:

- a) Statistical Thermodynamic considerations to evaluate N_L for each contributing species as a function of overall temperature and density
- b) Spectroscopic considerations for the frequency of the spectral feature and the strength factors $S_{el} = R_e^2(\bar{r}_{v'v''}) q_{v'v''}$ and $S_{J''\Lambda''}^{J'\Lambda'}$

The studies reviewed below include the early pioneer work of the 1940's (section 7.3.1), the approximate, yet more detailed calculations of the 1950's (section 7.3.2), and the recent entirely computer-based work of the 1960's (section 7.3.3) in which a realistic attempt is made to take the effect of all probable absorbers into quantitative account.

7.3.1 Early Work of the 1940's

The earliest discussion of the molecular contribution to the opacity of heated air was by Hirschfelder and Magee (1945) and Magee and Hirschfelder (1947). They made a preliminary quantitative discussion of such phenomena as the luminosity of the shock wave which accompanies a nuclear explosion, and the effect of the opacity of the surrounding heated air in impeding reducing energy loss by radiation. They made estimates of the contribution to the mean absorption coefficients from bound-free photoionization transitions of O^- , N^- , O , N , free-free transitions of electrons in ionic fields and of the molecular species O_2^- and NO_2 . The Rosseland mean was estimated over the temperature range 2000-20,000°K. The emphasis was not at all on the minutiae of spectroscopic detail of the absorption coefficient. In all of this work, which remained classified for about 10 years, and in common with many of the more recent calculations, thermodynamic equilibrium was assumed.

7.3.2 Approximate methods of 1950's

During the 1950's and as a result of renewed interest in nuclear explosions and re-entry phenomena, a series of theoretical studies of heated air absorption coefficients were carried out at Rand, Lockheed, AVCO Los Alamos and other laboratories.

Much of the work was based, insofar as molecular contributions were concerned, on Eq. (7.3-1), written in a number of equivalent forms,

$$\mu_{\nu} \sim \sum N_L R_e^2 (F_{\nu, \nu''}) q_{\nu, \nu''} S_{J, J''} \nu_{J, J''} b(\nu) \quad (7.3-1)$$

where the summation is over the spectral features which fall at ν . Many of the calculations used the tables of Gilmore (1955) for the population factors N_L . The differences between the studies reviewed here is predominantly in the way in which the meagre transition probability data was used and in the averaging techniques were employed. The absorption coefficient has often been calculated, as indicated in Eq. (4.1-33) in a series of increments $\Delta\nu$ using a 'smeared rotational structure' averaging procedure. According to Eq. (4.1-29) the band oscillator strength may be written

$$f_{\nu, \nu''} \sim \nu_{\nu, \nu''} R_e^2 (F_{\nu, \nu''}) q_{\nu, \nu''} \quad (7.3-2)$$

Thus from Eqs. (4.1-33) and (7.3-2) the average absorption coefficient in $\Delta\nu$ is

$$\bar{\mu}_{\nu} = \frac{1}{\Delta\nu} \sum_{\text{Bands}} \sum_{\Delta\nu} N_L f_{\nu, \nu''} \Delta\nu \quad (7.3-3)$$

Lack of information on $R_e(r)$ for a number of band systems at the time of these early calculations forced the use of an "electronic oscillator strength" f_{el} for a whole band system (see Eq. (4.1-36), where

$$f_{el} \sim \bar{\nu} \overline{R_e^2} \quad (7.3-4)$$

$\bar{\nu}$ is a characteristic average frequency for the whole band system, and $\overline{R_e^2}$ is similarly a characteristic average of the transition moment square.

Eq. (7.3-2) may thus be approximately written: (see Eq. (4.1-37))

$$f_{v'v''} = f_{el} q_{v'v''} \quad *$$
(7.3-5)

Finally Eq. (7.3-3) may be approximately written

$$\bar{u}_v^{\Delta v} = \frac{1}{\Delta v} \sum_{\text{Bands}} \sum_{\Delta v} N_L f_{el} q_{v'v''} \Delta v$$
(7.3-6)

This equation has been the basis of a number of calculations discussed below.

Meyerott (1955) briefly reported on, and gave tables of discrete and continuous contributions, total and Planck Mean Absorption Coefficients of heated air at the temperatures 6000°, 8000°, 12,000°, 18,000°K, for the density ratios 10, 1, 10⁻³, 10⁻⁶, in 0.25 eV increments of the spectrum from 1 eV to 12 eV. No detailed band structure was assigned and a smoothed

* Footnote

Very approximate equations such as Eq. (7.3-5) have led to the use in some of the literature on absorption coefficients of such erroneous equations as

$$f_{\text{spectral feature}} = f_{el} f_{\text{vib}} f_{\text{rot}} \quad (7.3-5a)$$

which, since oscillator strength is (frequency x transition strength) apart from a constant, is a meaningless statement. It is the transition strength which is separable (under well defined circumstances) into factors for vibration rotation and electronic motion. Recall

$$S_{L'v''J''\Lambda''}^{Uv'J'\Lambda'} = R_e^2 (f_{v'v''}) q_{v'v''} S_{J''\Lambda''}^{J'\Lambda'} \quad (4.1-14)$$

absorption coefficient was computed. Lack of information on band strengths or even electronic oscillator strengths of systems forced him to use an estimated $f_e = 0.2$ for all contributing band systems. The data were presented so that contributions from different band systems could easily be rescaled when f_e values became available.

Meyerott (1956) published the bases of the 1955 calculations and presented extended tables of data. He used Eq. (7.3-6) and a 'smeared' rotational structure assumption. Gilmore's (1955) tables were used for N_L , and the following contributors (Table 7.8) were included:

Table 7.8

-
- 1) N_2 : First Positive, Second Positive and
Lyman-Birge Hopfield Systems
 - 2) N_2^+ : First Negative
 - 3) NO : β and γ systems
 - 4) NO_2 :
 - 5) O^- , O, N, N_2 Photoelectric (bound-free)
transitions
 - 6) e : Free-Free
-

This list is very similar to Table 7.7. Where firm data specific to a contributor was not known, an appropriate approximation had to be used.

f_e was set equal to 0.2 for all diatomic band systems. Tables of approximate Franck-Condon factors were available from the work of Fraser, Jarman and Nicholls (see references in section 4.3). Measured room temperature absorption coefficients of NO_2 were used. Insofar as the contributions from atomic species, these are discussed more fully in section 7.4. Branscomb and Smith's (1955) experimental and Bates and Massey's (1943) theoretical photo-dissociation cross sections for O^- were used. A hydrogenic model was used for the bound-free photoelectric cross-sections of O, N, N_2 (see p. 180 of Aller, 1962) and for the free-free contribution.

Tables were given of μ_ν for each contributor and in total at frequency interval equivalent to $\Delta(kT) = 0.5$ for 3000° , 6000° , 8000° and $18,000^\circ$, density ratios of 1 and 10^{-3} over the wavelength range of 1700\AA -5 microns.

Although admittedly approximate in many details this was the first set of absorption coefficient calculations in which an attempt was made to take quantitative account of a number of atomic and molecular contributors. It laid the groundwork of more extensive calculations in a number of laboratories.

Meyerott (1958), in a discussion of the radiant heat transfer from the bow shock wave to re-entering hypersonic vehicles presented a further refined version of the previous calculations in which specific values of f_{e1} were assigned to each molecular

transition. The measurements of Marmo (1953) and Weber and Penner (1957) (see Penner, 1959) were used to assign f_{e1} of 0.008 and 0.0025 to the NO β and γ systems respectively. The measurements of Ditchburn and Heddle (1953, 1954) (now thought to be overestimated) were used to assign the value 0.259 to the O₂ Schumann-Runge system (including the photodissociation continuum). Experimental work from the AVCO laboratory (see below) was used to provide provisional f_e values of 0.02, 0.07, and 0.20 for the N₂ First and Second Positive and N₂⁺ First Negative Systems respectively.

An experimental and theoretical program on emission from shock heated air was started in the AVCO laboratories at about the same time. The relation between emission and absorption coefficients has been pointed out earlier.

Keck, Kivel and Bethe (1957) of AVCO discuss in their first paper a simplified theory to take account of NO emissions. They used a distorted SHM method to compute $q_{v,v'}$ -values for the NO β and γ systems. They also state an expression for the average emission from the gas. In a second paper (1959) Keck, Camm, Kivel and Wentinck interpret a mainly experimental study of hot air emission from shock tubes in terms of the underived expression

Eq. (7.3-7) based on a formal smearing of band structure

$$\mu_{\lambda} = \pi r_o [X] f_{el} \varphi \frac{hc}{kT} \exp \left[- \frac{hc}{kT} \left(\frac{1}{\lambda_{oo}} - \frac{1}{\lambda} \right) \right] \quad (7.3-7)$$

It appears that the basis of the averaging procedure has been to assign to each band in the system just a Q-Branch ($\Delta J = 0$) to represent all rotational structure, whether or not a Q-Branch is formally allowed or not. All of the band intensity is then supposed to be vested in the fictitious Q-Branch over the profile of which summations or integrations can be made. In Eq. (7.3-7)

$$r_o = \frac{e^2}{mc^2} \quad = \text{radius of classical electron}$$

$$f_{el} = \frac{8\pi^2 mc}{3h\lambda} |R_e|^2 \quad = \text{electronic f-number of the band system}$$

$$[X] \quad = \text{concentration of absorbing species}$$

φ is a dimensionless quantity resulting from formal integration over the assigned Q-Branch and =

$$\frac{kT}{hc} \frac{1}{Q_V'' Q_R'' (B_e' - B_e'')} \sum_{E_R} q_{V'V''} \exp(-E_{V'} + E_{rot})/kT$$

λ_{00} is the wavelength of the (0,0) band of the system. Q_V'' and Q_R'' are the vibrational and rotational contributions to the partition function of the ground state. The E 's are vibrational and rotational energies of the upper state. On the assumption of thermal equilibrium, Keck et al. state that the emission power over the wavelength band $(\Delta\lambda)$ of the spectral slit is

$$\left(\frac{dI}{dA d\Omega d\lambda} \right) = \pi r_0^2 2hc^2 f_{el} [X] \langle \varphi \rangle \lambda^{-5} \frac{hc}{kT} \exp(-hc/kT\lambda_0) \quad (7.3-8)$$

where $\langle \varphi \rangle = \langle \varphi \rangle_{\Delta\lambda} = \frac{\lambda^6}{\Delta\lambda} \int_{\lambda - \frac{\Delta\lambda}{2}}^{\lambda + \frac{\Delta\lambda}{2}} \lambda^{-6} \varphi d\lambda$

They were thus able by a comparison between the power profiles of measured emission spectra and those predicted from Eq. (7.3-8) to assign those f_{el} values to each of the transitions which make theory and experiment agree. These were in part the f_{el} numbers used by Meyerott (1958). The theoretical method has been used subsequently by a number of workers, for in spite of its approximate averaging procedure, it is well adaptable to computer application. Golden and Miller (1963) used the method to compute

the spectral absorption coefficients of band systems of atmospheric gases and metallic oxides, and to plot (by computer) their results graphically. Temperatures were, characteristically 1000° (1000)6000 $^{\circ}$. The best available input data from the literature were used. Ashley (1964) used the method to study emission from equilibrium air over the wavelength range 3800A-6500A, for temperatures 1000° K(1000)8000, 12,000(6000)24000 $^{\circ}$ K and for density ratios $1(10^{-1})10^{-6}$. He also used selected experimental input data, and replaced f_{el} by $\frac{\nu}{3R_{\infty}} \left| \frac{R_e(\bar{r}_{v'v''})}{e a_0} \right|^2$ where $R_e(\bar{r}_{v'v''})$ were from the compilation of Keck, Allen and Taylor (1964) which is not entirely without objection. Main and Bauer (1965) has used the method to study opacities of carbon-air mixtures from 3000° to $10,000^{\circ}$ and wavelengths from 1400A to 2 microns.

Main and Bauer, Ashley, and Golden and Miller all provide clear discussions of the theoretical basis of Eq. (7.3-7). Patch, Shackelford and Penner (1962) have carried out similar calculations using the same method and have demonstrated, for NO, equivalence between the method of calculation based on Eq. (7.3-7) and that used by Meyerott based on Eq. (7.3-6)

Meyerott, Sokoloff and Nicholls (1960) extended Meyerott's earlier work and employed improved experimental data in calculations based on Eq. (7.3-6). Contributions from N_2 (First Positive, Second Positive), N_2^+ (First Negative), O_2 (Schumann-Runge), NO_2 (β, γ) were calculated in addition to those from O^- , O, N, and e. Gilmore's (1955) tables of N_L were used. Franck-Condon factors were obtained as before from the work of Nicholls and co-workers, f_{el} values from the AVCO laboratory were used for N_2 and N_2^+ systems. Weber and Penner's measured values were again used for NO systems and Ditchburn and Heddle's

measurements were used for O_2 . Calculations were made over the following ranges of parameters

T: 1000(1000), 4000(2000)8000, 12,000^oK

ρ/ρ_0 : $1(10^{-1}) 10^{-6}$

λ : 1.9837 microns to 1167 Å in 0.25 eV intervals.

A typical result of such calculations of absorption coefficient is displayed in Figs. 7-7 and 7-8 for conditions ($T = 6000^{\circ}K$, $\rho/\rho_0 = 1$) which emphasize molecular contributions.

The relative contribution of each band system is indicated as a function of temperature for atmospheric densities in Fig. 7-7.

There are many limitations to the accuracy of this calculation, but the results are probably realistic to an order of magnitude. It could have been improved by using a version of Eq. (7.3-1) but the necessary band strengths were not available at the time. Armstrong, Sokoloff, Nicholls, Holland and Meyerott (1961) reviewed the development of this sort of calculation which, apart from the improvement which could be effected by use of band strength represents almost the ultimate in such 'smeared' or 'smoothed' model calculations.

7.3.3 Calculations with the SACHA Code in 1960's

The next improvement in such calculations takes account of the detailed rotational structure of the contributing molecular absorbing band systems. The amount of labor involved in this is enormous and is only possible by recourse to large scale computing facilities. The only known work of this nature has been done during the past 5 years in the Lockheed Research Laboratories by Churchill, Hagstrom, Landshoff and Mueller. A comprehensive computer code: S(spectral) A(bsorption) C(oefficient) of H(eated) A(ir) has been written which takes account of the detailed structure of the spectrum line by line.

The first calculations of this research program were described in a report by Churchill, Hagstrom and Landshoff (1963). The essentials of this work, with some extensions, were recently published (Churchill and Meyerott, 1965) and the latest results of this program are described by Churchill, Armstrong and Mueller (1965) and typical results from this work are included in the tables in Table 7-12. Churchill, Armstrong and Mueller's report includes a discussion of the contribution from atomic species, as described in detail in section 7.4 below.

The calculations with the SACHA code are based, in principle on Eq. (7.3-1). The absorption coefficient μ_ν at a frequency ν in a rotational line is given by

$$\mu_\nu = N_{Lv''J''} B_{Lv''J''}^{Uv'J'} h\nu_{Lv''J''}^{Uv'J'} b(\nu) \quad (7.3-9)$$

Now, from Eq. (4.1-32)

$$B_{Lv''J''}^{Uv'J'} = \frac{8\pi^3}{3 h^2 c} \left| R_e(\bar{r}_{v'v''}) \right|^2 q_{v'v''} \frac{S_{J''}}{2J''+1} \quad (7.3-10)$$

where $S_{J''}$ is a simplified notation for the Hönl-London factor of the J'' line in a specific branch considered.

Further from statistical mechanical considerations in equilibrium air

$$N_{LV^nJ^n} = \frac{N(2J^n+1) \omega_I \exp(-E_{LV^nJ^n}/kT)}{Q} \quad (7.3-11)$$

N is the particle density of the species in all levels which can in principle be obtained from Gilmore's (1955) tables. ω_I is the nuclear spin statistical weight. Q is the total partition function which has a contribution from each electronic state n . Two values of n are U and L; there are in principle many others, i.e.,

$$Q = \sum_n Q_n \quad (7.3-12)$$

Further Q_n may be factored for each electronic state into contributions from each of the internal degrees of freedom of the molecule. That is,

$$Q_n = Q_{el} \cdot Q_{vib-rot} \cdot Q_{nuclear} \quad (7.3-13)$$

where

$$Q_{el} = \omega_\Lambda (2S+1) \exp(-v_{00}hc/kT) \quad (7.3-14a)$$

$$Q_{vib-rot} = \sum_{v=0} \exp[-G_0(v)hc/kT] \cdot Q_{rot}^v \quad (7.3-14b)$$

$$Q_{rot}^v = \int_0^\infty (2J+1) \exp[-F_v(J)hc/kT] dJ \approx \frac{kT}{hcB_v} \quad (7.3-14c)$$

$$Q_{nuclear} = (2I_a+1)(2I_b+1)/3 \quad (7.3-14d)$$

Nearly all of the spectroscopic symbols are conventional (Herzberg, 1950).

w_Λ is the statistical weight for orbital angular momentum (1 or 2) depending on whether Λ is zero or nonzero. I_a and I_b are the spins of the two nuclei and ρ is a symmetry number which is 2 for homonuclear molecules and 1 for heteronuclear molecules. It should not be confused with the line width. The approximate formula developed by Bethe (1942) and corrected by Brinkley (see Brinkley, Kirkwood and Richardson, 1944) for $Q_{\text{vib-rot}}$ is

$$Q_{\text{vib-rot}} = \frac{1}{1 - \exp(-1.4388 \omega_0/T)} \frac{1}{1.4388 B_0} (1 + \gamma T) \quad (7.3-14e)$$

ω_0 and B_0 are vibrational and rotational constants for the $v=0$ level.

γ is Bethe's correction for anharmonicity and non-rigidity.

$$\gamma = \frac{1}{1.4388 \omega_0} \left[\frac{2\omega_0 x_0}{\omega_0} + \frac{\alpha_0}{B_0} + \frac{8B_0}{\omega_0} \right] \quad (7.3-14f)$$

With these substitutions Eq. (4.3-11) may be rewritten:

$$N_{Lv''J''} = N_{\text{total}} \frac{Q_L}{Q_{\text{total}}} \frac{w_I(2J''+1) \exp \left[-\{G_0(v'') + F_{V''}(J'')\} \frac{hc}{kT} \right]}{(2S+1) w_\Lambda Q_{\text{nuclear}} Q_{\text{vib-rot}}} \quad (7.3-15)$$

where $E_{Lv''J''}$ has been replaced by $hc[v_{00} + G_0(v'') + F_{V''}(J'')]$. v_{00} is in the Boltzmann factor which controls N_{total} , the concentration of the absorbing species.

$$\text{Write } P_{n''} = Q_{n''}/Q_{\text{total}} \quad (n''=L \text{ here}) \quad (7.3-16)$$

which is the fractional population of the n'' 'th electronic state.

This allows the definition of a function H which contains only molecular constants

$$H_{n''v''J''}^{n'v'J'} = \frac{8\pi^2 L_0}{3hc} \frac{\omega_I}{(2S+1) \omega_\lambda Q_{\text{nuclear}}} \nu_{n''v''J''}^{n'v'J'} R_e^2(f_{v'v''}) q_{v'v''} S_{J''\Lambda''}^{J'\Lambda'} \quad (7.3-17)$$

$$\text{Also define } E_{v''J''} = [G_0(v'') + F_{v''}(J'')] hc/k \quad (7.3-18)$$

$L = 2.6875 \times 10^{19}$ particles per cc and is Loschmidt's number.

Eq. (7.3-9) may now be written in compact form using Eqs. (7.3-10), (7.3-15) (7.3-17) and (7.3-18)

$$u_\nu = \left[\frac{N_{\text{total}} P_{n''}}{L_0 Q_{\text{vib-rot}}} \right] H_{n''v''J''}^{n'v'J'} \exp(-E_{v''J''}/T) \pi b(\nu) \quad (7.3-19)$$

This is the equation on which the SACHA code is based. H and E are quantities which are characteristic of the isolated molecule and are thus independent of temperature and density. Temperature and density control the dimensionless bracketed term and the exponent. H has the dimensions of $(\text{length})^{-2}$. The line profile b has the dimensions of $(\text{length})^{+1}$.

The equation is thus dimensionally consistent as u_ν has the dimensions $(\text{length})^{-1}$. While there is provision in the general SACHA code for any line profile function it has been found useful to employ the physically reasonable Lorentz form (see Eq. 7.3-20) which represents pressure broadened lines, and to use the line width parameter σ as a controllable assignable constant which can be varied from calculation to calculation in parameter studies.

$$b(\nu) = \frac{1}{\pi} \frac{\sigma}{\sigma^2 + (\nu - \nu_{n''v''J''}^{n'v'J'})^2} \quad (7.3-20)$$

The six band systems: N_2 First and Second Positive, N_2^+ First Negative, NO β and γ , O_2 Schumann-Runge were incorporated in the first set of calculations (Churchill, Hagstrom and Landshoff, 1963). Such a calculation requires a detailed examination of the spectroscopic structure of each band system and of the branch structure of each band within the system. This procedure is reviewed in Appendix A1 where the necessary spectroscopic properties of the above six band systems are listed and illustrated. The procedure has also been discussed by Churchill and Meyerott (1965). An atlas of all important lines of the six systems is assembled by computer on magnetic tape. The following computed data is stored (for further computations) for each line

$$\nu \text{ (frequency)} \quad \alpha \text{ (identification parameter)} \quad H_\alpha, \quad E_\alpha$$

The identification parameter α is an octal number formed from the upper and lower vibrational and rotational quantum numbers, a branch (of the band) identification number and the band system identification number. The calculation of ν , H and E for each line involves recourse to the spectroscopic structure of the band system and the Eqs. (7.3-21), (7.3-17) and (7.3-18)

$$\nu_{n''v''J''}^{n'v'J'} = \nu_0 + G'_0(v') - G''_0(v'') + F'_{v'}(J') - F''_{v''}(J'') \quad (7.3-21)$$

In the Churchill, Hagstrom and Landshoff (1963) calculations, the following input data was used in the calculation of H . The statistical weight and frequency data were calculated from standard spectroscopic data (Herzberg, 1950). The constant R_0 approximation was adopted and the values of R_0 were taken from the measurements of Treanor and Wuster (1960) (O_2) Bennett and Dalby (1959) (N_2^+) and the recommendations of Meyerott, Sokoloff and

Nicholls (1960) for the other systems. Franck-Condon factors were taken from the calculated values of Nicholls (1960, 1961, 1962). The Hönl-London factors were calculated appropriate to the branch of the band under consideration (see discussion of Section 4.2).

The final atlas tape for these calculations contained data for 151,528 lines are as listed in Table 7.9.

Table 7.9

<u>System Number</u>	<u>Band System</u>	<u>Number of Lines Treated</u>
1	O ₂ Schumann-Runge	13,836
2	N ₂ First Positive	58,476
3	N ₂ Second Positive	16,750
4	N ₂ ⁺ First Negative	21,306
5	NO β	15,760
6	NO γ	25,400
Total:		151,528

The atlas tape was then used in the line by line calculation of μ_{ν} from Eq. (7.3-19). Population factors N_{total} were taken from Gilmore's (1955) tables.

The wealth of data which emerges from such accurate calculations requires that some averaging or merging be done before the data is printed or plotted. Two types of averages have been computed using the SACHA code: a) mean absorption coefficients and transmissions for use in transport calculations; b) incremental absorption coefficients for each contributor summed over small frequency intervals (see Eq. (7.3-3)). The mean absorption coefficients are discussed here as they were the major end result of the calculations of Churchill, Hagstrom, and Landshoff (1963).

It is recalled from the discussion in Chapter 2 on radiation transport that the effective absorption coefficient μ'_ν which incorporates the effect of stimulated emission is given by

$$\mu'_\nu = \mu_\nu (1 - \exp - h\nu/kT) \quad (7.3-22)$$

The obvious average absorption coefficient to consider (see b above) is the incremental coefficient

$$\bar{\mu}'_{\nu, \Delta\nu} = \frac{1}{\Delta\nu} \int_{\nu}^{\nu+\Delta\nu} \mu'_\nu d\nu \quad (7.3-23)$$

$\Delta\nu$ is chosen to be large relative to the width of individual lines yet narrow enough to contain only a few lines. Calculations of this nature were made in later applications of the SACHA code (see on).

It will also be recalled (see Section 6.2) that two mean absorption coefficients can be defined for use in radiative transfer studies.

a) The Planck Mean $\bar{\mu}_P(T)$ is used in optically thin cases

$$\bar{\mu}_P(T) = \frac{\int \mu'_\nu B_\nu d\nu}{\int B_\nu d\nu} \quad (7.3-24)$$

b) The Rosseland Mean $\bar{\mu}_R(T)$ is used in optically thick cases

$$\frac{1}{\bar{\mu}_R} = \frac{\int \frac{1}{\mu'_\nu} \frac{dB_\nu}{dT} d\nu}{\int \frac{dB_\nu}{dT} d\nu} \quad (7.3-25)$$

Both of these can be and have been evaluated using the SACHA code.

$B_\nu(T)$ is the Planck function.

In cases between the optically thin and the optically thick limits it is more useful to define a transmission function $\text{Tr}(\nu)$.

The transmission of an isothermal homogeneous slab of material of thickness x is

$$\text{Tr}(\nu_j) = \exp\left[-\left\{\sum_{\alpha} u'_{\alpha}(\nu_j) + u'_c(\nu_j)\right\} x\right] \quad (7.3-26)$$

where α sums over the lines and c refers to continua. The average transmission at ν is

$$\overline{\text{Tr}}^{\Delta\nu}(\nu) = \frac{1}{\Delta\nu} \int_{\Delta\nu} \text{Tr}(\nu) d\nu \quad (7.3-27)$$

In many practical applications the contribution of the continuum can be neglected. Thus an average absorption coefficient can be defined from Eq. (7.3-27) in Eq. (7.3-28)

$$\bar{\kappa}(\nu) = \frac{-\ln \overline{\text{Tr}}^{\Delta\nu}(\nu)}{x} \quad (7.3-28)$$

This equation has been the basis of a number of calculations using the SACHA code and Eqs. (7.3-26), (7.3-27), (7.3-22) and (7.3-19). Average absorption coefficients $\bar{\kappa}(\nu)$ and average transmissions $\overline{\text{Tr}}(\nu)$ have been computed as a function of temperature, slab thickness, line width (σ) for a number of representative frequencies. Curves are given of these quantities by Churchill,

Hagstrom and Landshoff for the temperature range $1000^{\circ} < T < 12,000^{\circ} \text{K}$, the density range $1 < \rho/\rho_0 < 10^{-4}$ and for optical paths from cm to 10^9 cm. σ was set at 1 cm for this work and $\Delta\nu$ was set at 100 cm^{-1} . Calculations were made at each 2000 cm^{-1} from about $18,000 \text{ cm}^{-1}$ to $50,000 \text{ cm}^{-1}$. Typical results of this work are shown in Fig. 7-9.

The SACHA code was also used by Churchill and Hagstrom (1964) to compute the contribution to the absorption coefficient of air from the NO vibration-rotation spectrum.

It will be recalled from Eq. (4.1-8a) that the transition strength in this case is

$$S_{v'J', v''J''}^{v'J', v''J''} = \left| \int \psi_{v'} \cdot \underline{M} \cdot \psi_{v''} \, dr \right|^2 S_{J', J''} = S_{v', v''} S_{J', J''} \quad (7.3-29)$$

where $\psi_{v'}$ and $\psi_{v''}$ are both vibrational wave functions of the same family and are mutually orthogonal, \underline{M} is the total dipole moment, and $S_{J', J''}$ is the Hönl-London factor. Assuming electrical anharmonicity, the dipole moment is expanded as far as quadratic terms

$$M(\xi) = M\left(\frac{r-r_e}{r_e}\right) = p_0 + p_1 \xi + p_2 \xi^2 \quad (7.3-30)$$

Thus the integrated band absorption coefficient (which is often a measured quantity from which the empirical constants p_0 , p_1 and p_2 may be determined) is

$$\begin{aligned}
 \int_{\text{Band}} \mu_{\nu} dv &= \frac{8\pi^3}{3hc} \nu_{\nu' \nu''} N_{\nu''} \left[\int \psi_{\nu'} \psi_{\nu''} (p_0 + p_1 \xi + p_2 \xi^2) \right]^2 \\
 &= \frac{8\pi^3}{3hc} \nu_{\nu' \nu''} N_{\nu''} \left[p_1 \int \psi_{\nu'} \psi_{\nu''} \xi dr + p_2 \int \psi_{\nu'} \psi_{\nu''} \xi^2 dr \right]^2
 \end{aligned}
 \tag{7.3-31}$$

The term involving p_0 has vanished due to the orthogonality of the ψ 's .

Providing the vibrational wave functions are known, the integrals on the right hand side can in principle be calculated, and thus Eq. (7.3-31) can be used to determine p_1 and p_2 if integrated intensities of two bands have been measured. The fundamental and the first overtone (1-0 and 2-0) bands are usually employed. In this way the vibrational band strength $S_{\nu' \nu''}$ of Eq. (7.3-29) can be determined. Churchill and Hagstrom determined this as follows in a preliminary step of their calculations of the NO vibration-rotation spectrum. Breene and Todd (1958) had made some calculation of the vibrational matrix elements of Eq. (7.3-31) based on wave functions appropriate to Lippincott's (1953, 1955) potential for the ground state of NO. They went through the procedure outlined above, using Fenner and Weber's (1953) integrated intensity measurements on the fundamental and first overtone bands of NO. Schurin and Clough (1963) remeasured the fundamental and obtained a somewhat higher value. Churchill and Hagstrom thus scaled Breene and Todd's values to become consistent with Schurin and Clough's measurements, and used the new arrays of $S_{\nu' \nu''}$ in the H functions of the SACHA code.

An atlas of $\nu, \alpha, H,$ and E values for each of the 25,610 lines was then generated as described above for electronic transitions. Gilmore's (1955) data for N were used and average absorption coefficients and transmissions

were calculated from $1200(200)2000(500)9000 \text{ cm}^{-1}$, for temperatures between 1000° and 5000° at density ratios $1(10^{-1})10^{-4}$ and for optical path lengths between 1 and 10^6 cm. A parameter study was also conducted on the line width parameter σ . Values of 1.0, 0.1 and 0.01 cm^{-1} were used.

Churchill and Meyerott (1965) describe in detail an improvement on the calculations of Churchill, Hagstrom and Landshoff in which contributions from the molecular transitions listed in Table 7.10 were taken into account.

Table 7.10

<u>System Number</u>	<u>Band System</u>	<u>Number of Lines Treated</u>
1	O ₂ Schumann-Runge	4,611
2	N ₂ First Positive	48,785
3	N ₂ Second Positive	20,369
4	N ₂ ⁺ First Negative	3,216
5	NO β	18,518
6	NO γ	31,429
7	NO vibration-rotation	25,610
8	N ₂ Birge-Hopfield (b ¹ Σ_u^+ - X ¹ Σ_g^+)	38,983

The basis of the method was almost the same as described above for the 1963 calculations. Gilmore's (1955) population data were employed and the NO vibration-rotation and N₂ Birge-Hopfield contributions have been added. No f_{e1} (or R_e) was available for the N₂ Birge-Hopfield system

so a provisional value of 0.1 was assigned to f_{el} . The Franck-Condon factors employed were those of Nicholls (1965).

Average transmission and average absorption coefficients were calculated for much the same range of parameters as are presented in Volume 3 of this series.

A model study was conducted on the line-width parameter and values of 1, 0, 0.1 and 0.001 (cm⁻¹) were used.

Finally the most recent application of the SACHA code by Churchill, Armstrong and Mueller (1965, 1966) to the molecular part of the absorption coefficient of air must be described. It is the most extensive study so far made, and takes account of the contributors listed in Table 7.11. The atomic constituents and high temperature results are discussed in Chapter 8.

Table 7.11 Contributors to the Absorption Coefficient of Heated Air

-
- 1: Schumann-Runge bands of O₂
 - 2: N₂: First Positive
 - 3: N₂: Second Positive
 - 4: N₂: Birge-Hopfield (b' ¹Σ_u⁺ - X¹Σ_g⁺)
 - 5: N₂⁺: First Negative
 - 6: NO: β
 - 7: NO: γ
 - 8: NO: vibration-rotation
 - 9: O₂: Schumann-Runge Continuum
 - 10: NO₂
 - 11: O⁻ Photodetachment
 - 12: electrons (free-free in presence of ions)
 - 13: N Photoionization
 - 14: O Photoionization
-

Contributors 1-8 were treated by the SACHA code in the manner discussed below. Contributors 9-12 were continua and were treated in a semi-empirical way. Contributors 13 and 14 were treated by the PIC code and are discussed in Chapter 8.

Insofar as the use of the SACHA code in the treatment of contributors 1-8 is concerned, a number of refinements were used which had not been employed in previous application. Firstly, band strengths $S_{\nu' \nu''}$

$$S_{\nu' \nu''} = R_e^2 (\bar{F}_{\nu' \nu''}) q_{\nu' \nu''} \quad (7.3-32)$$

were employed wherever possible in place of the constant R_e approximation used previously. The band strengths of aeronomically important band systems compiled by Nicholls (1964) were used with some additions to fill in 'windows' in those tables. Also a new EQUILIBRIUM code was written and used to compute the densities of absorbing species. This code takes account of the newest thermodynamic information on 12 molecular species (including molecular ions) 21 atomic species (including single, double and triply ionized atomic ions) and electrons present in heated air. Data from this code was used in place of the classic tables of Gilmore (1955) which have been used in all previous work. A complete description of the EQUILIBRIUM code including a printout and data cards is provided in Appendix B of Churchill, Armstrong and Mueller's report.

Most previous applications of the SACHA code have provided average absorption coefficients or transmissions because of the vast amount of output involved. In contrast the output of this application (appendix 1 of Churchill, Armstrong and Mueller's report) is a 385 page listing of the absorption coefficient of air for each of the contributors listed in Table 7.11, and the total absorption coefficient, over the energy range range 0.60(0.10)10.70 eV over the temperature range 1000(1000)24,000^oK and over the density ratio range $10(10^{-1})10^{-6}$. The results of this study are reproduced in full in Volume 3 of this series and are illustrated here in Fig. 7-10 and Table 7-12. Fig. 7-10 compares the spectral absorption coefficient of 12,000^oK normal density air as a function of photon energy as calculated by Churchill, Armstrong, and Mueller (1965) and by Meyerott, Sokoloff, and Nicholls (1960). Table 7-12 is a reproduction of a typical page of the 385 pages of computer print-out referred to above.

The above discussion is a review of progress in the studies of the past twenty years on the molecular contribution to hot air. Further improvements will probably involve the incorporation into SACHA of contributions for minor constituents when more is known of them, refinement of the experimentally determined input data on line and band strengths, and improvements on the form of $b(\nu)$ which is employed. All of these improvements require much supporting laboratory research. In particular our detailed experimental and theoretical understanding of the phenomena which control molecular line shapes is not very deep.

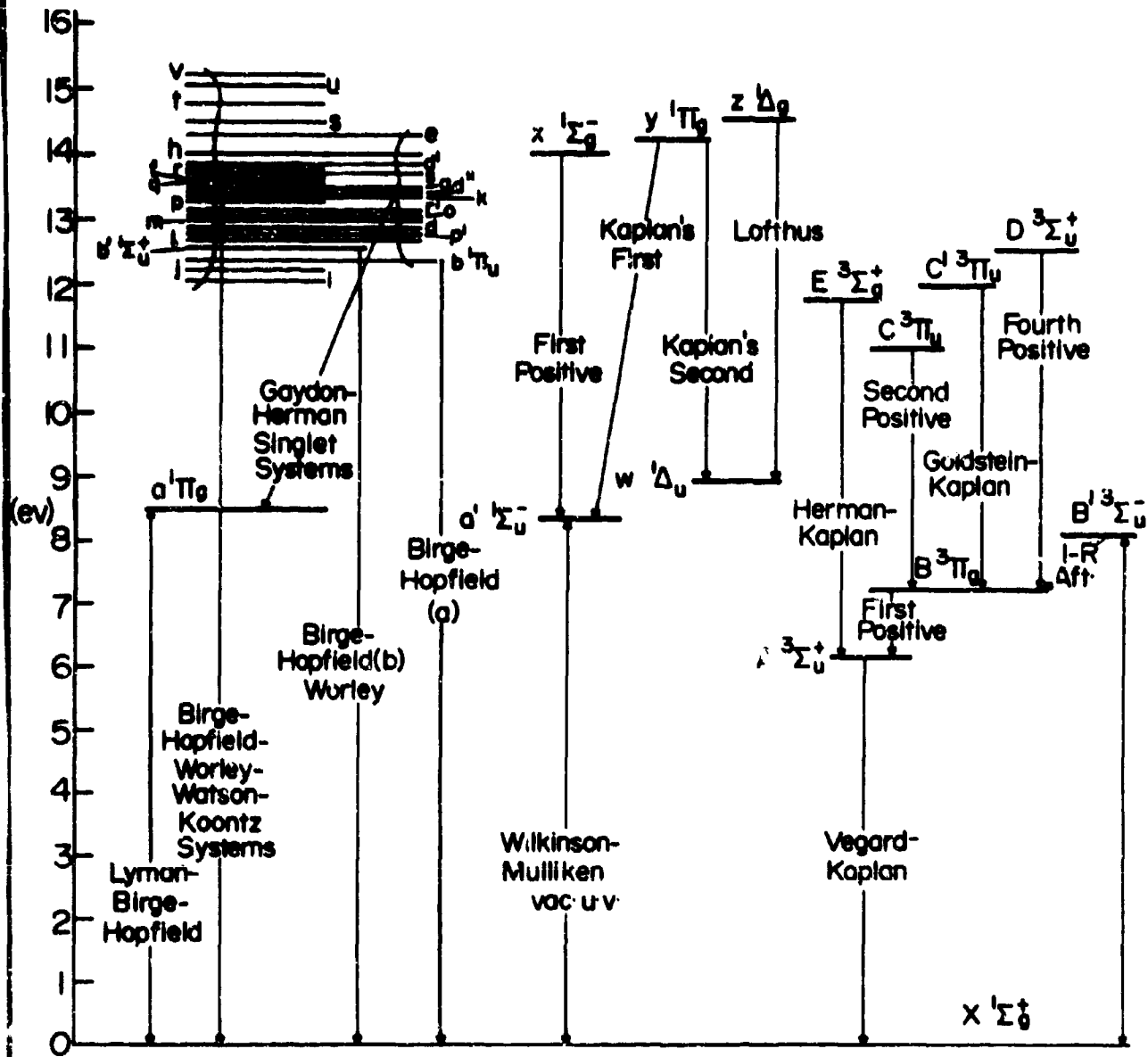


FIG. 7-1 ENERGY LEVEL DIAGRAM FOR N_2

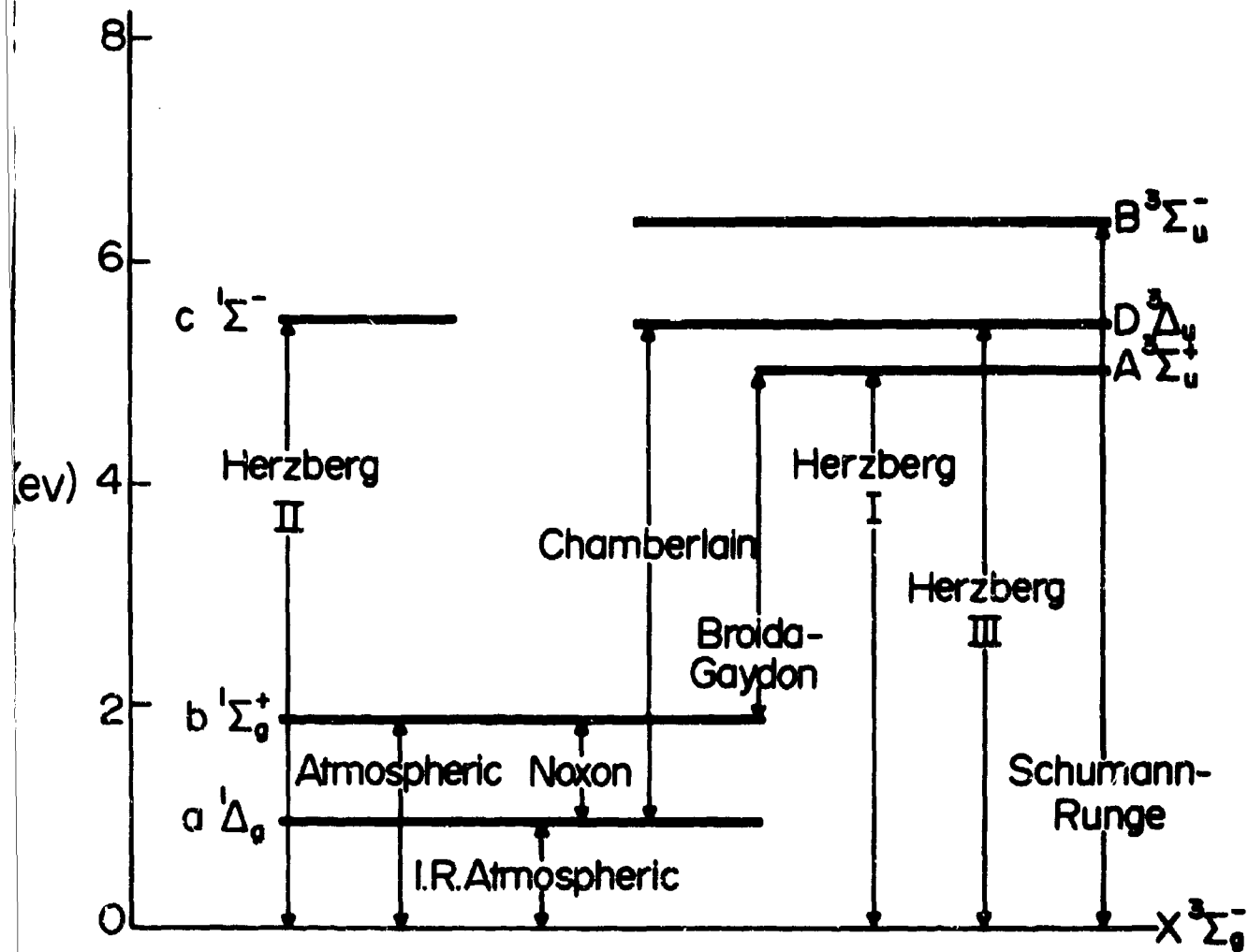


FIG. 7-2 ENERGY LEVEL DIAGRAM FOR O_2

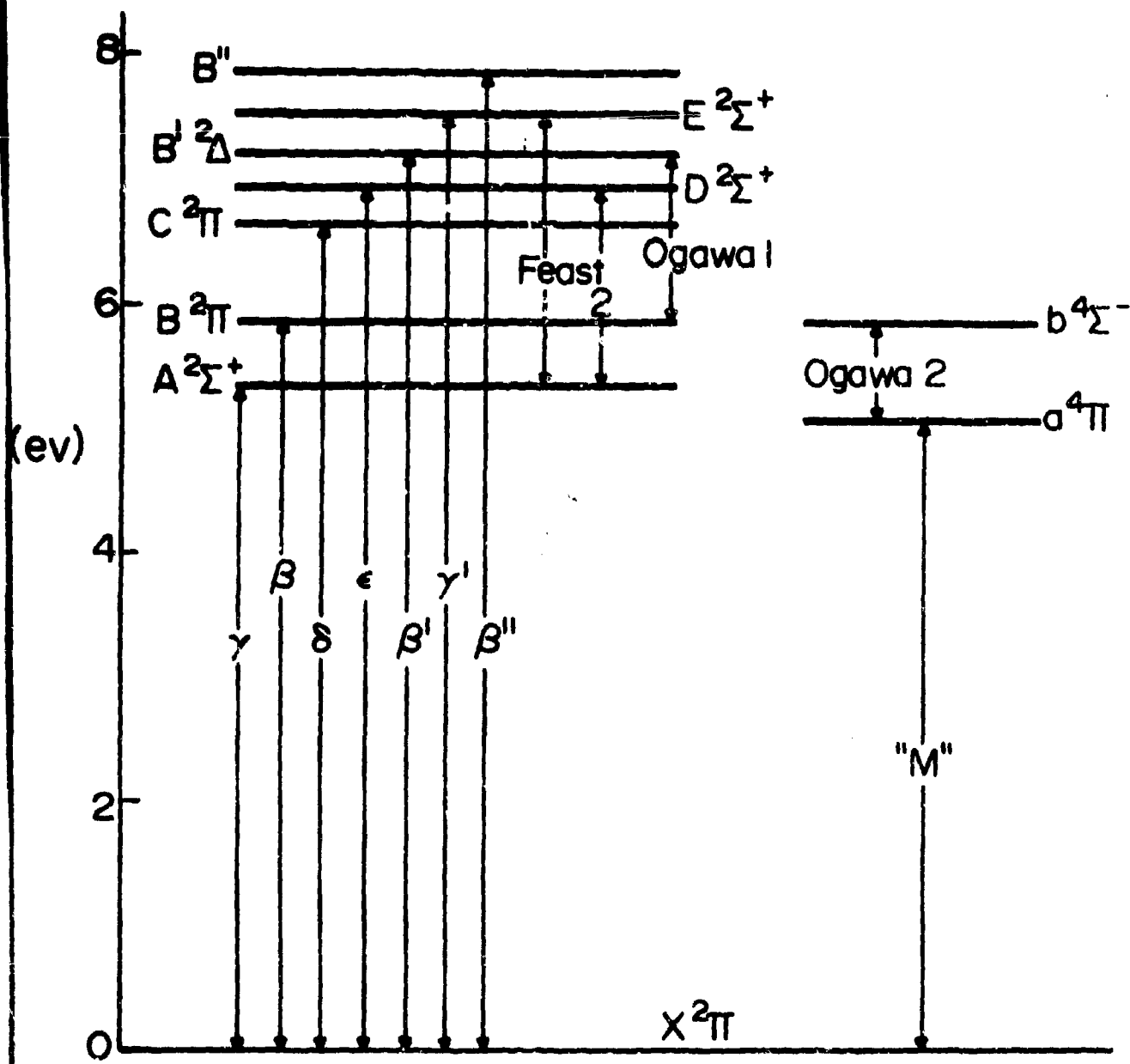


FIG. 7-3 ENERGY LEVEL DIAGRAM FOR NO

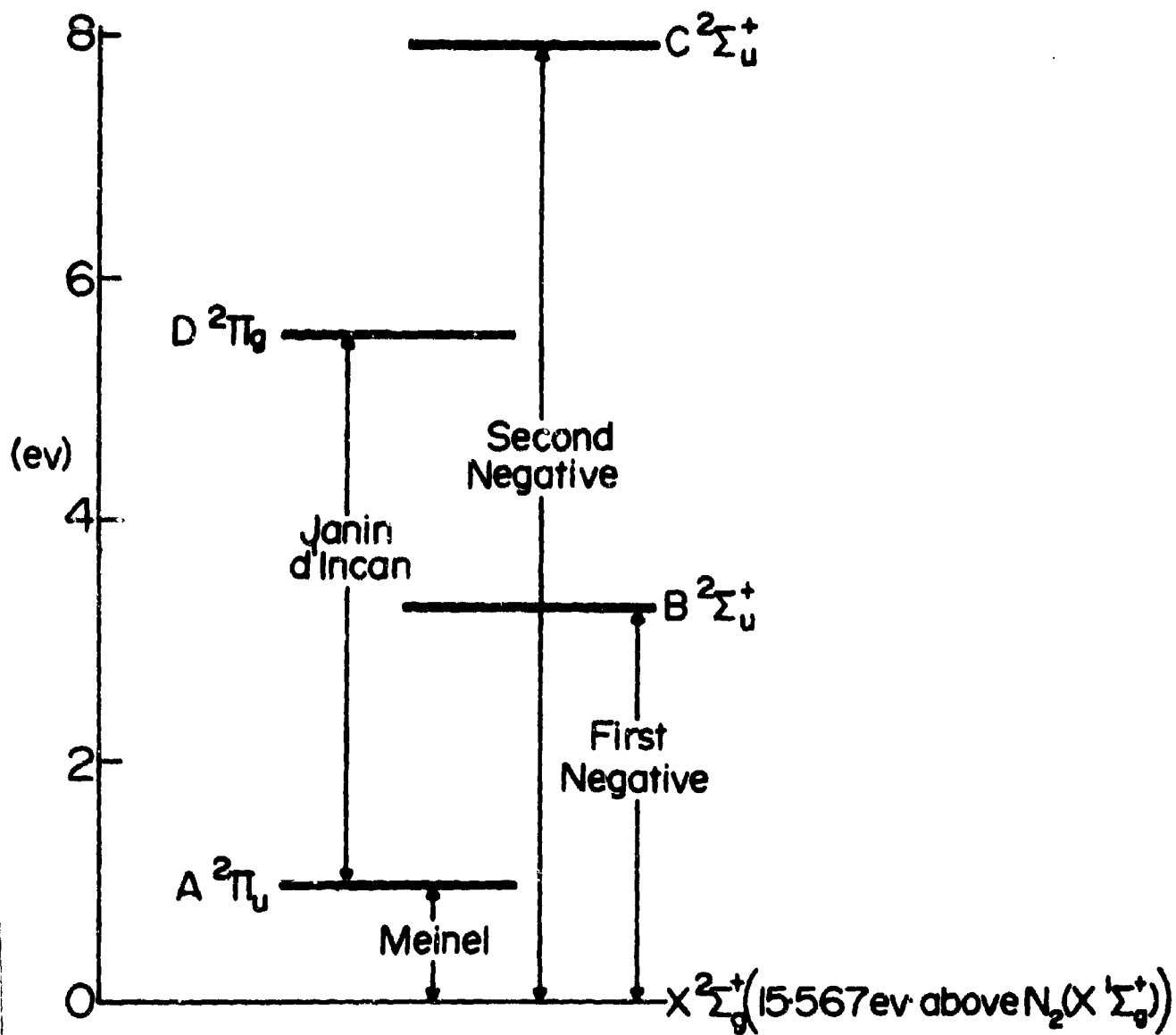


FIG. 7-4 ENERGY LEVEL DIAGRAM FOR N_2^+

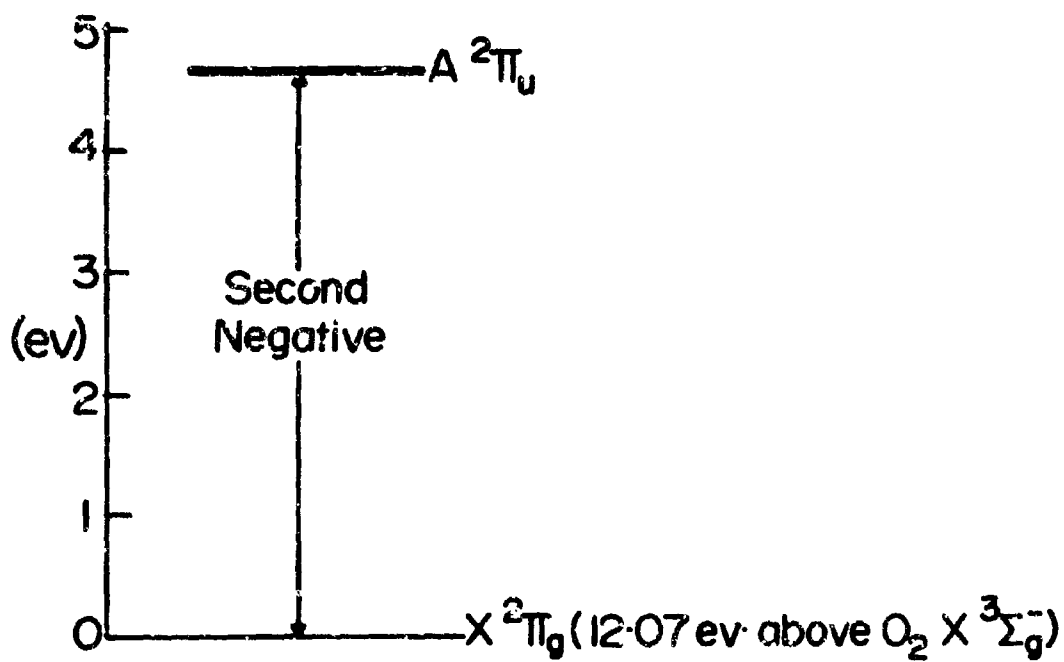
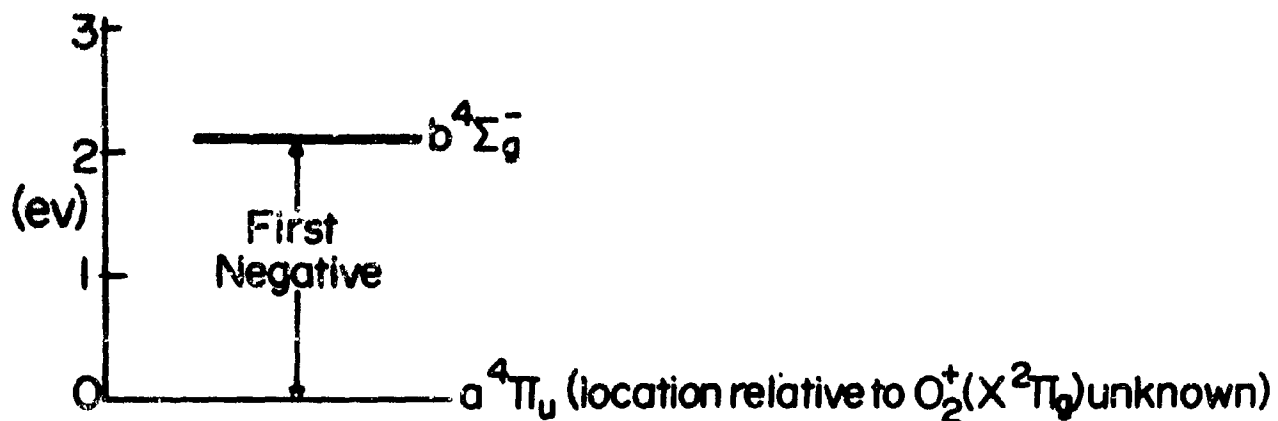


FIG. 7-5 ENERGY LEVEL DIAGRAM FOR O_2^+

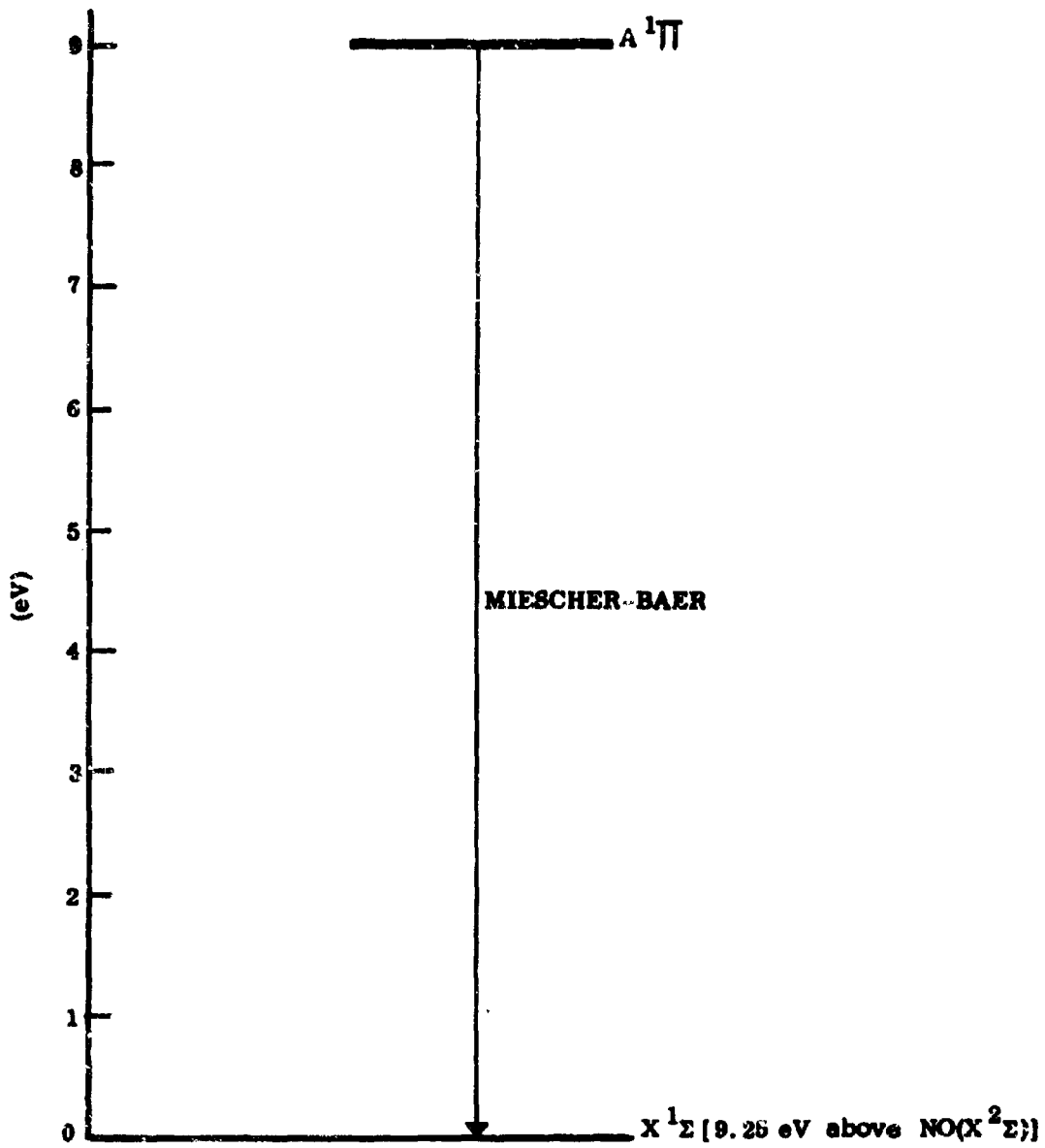


FIG. 7-6 ENERGY LEVEL DIAGRAM FOR NO^+

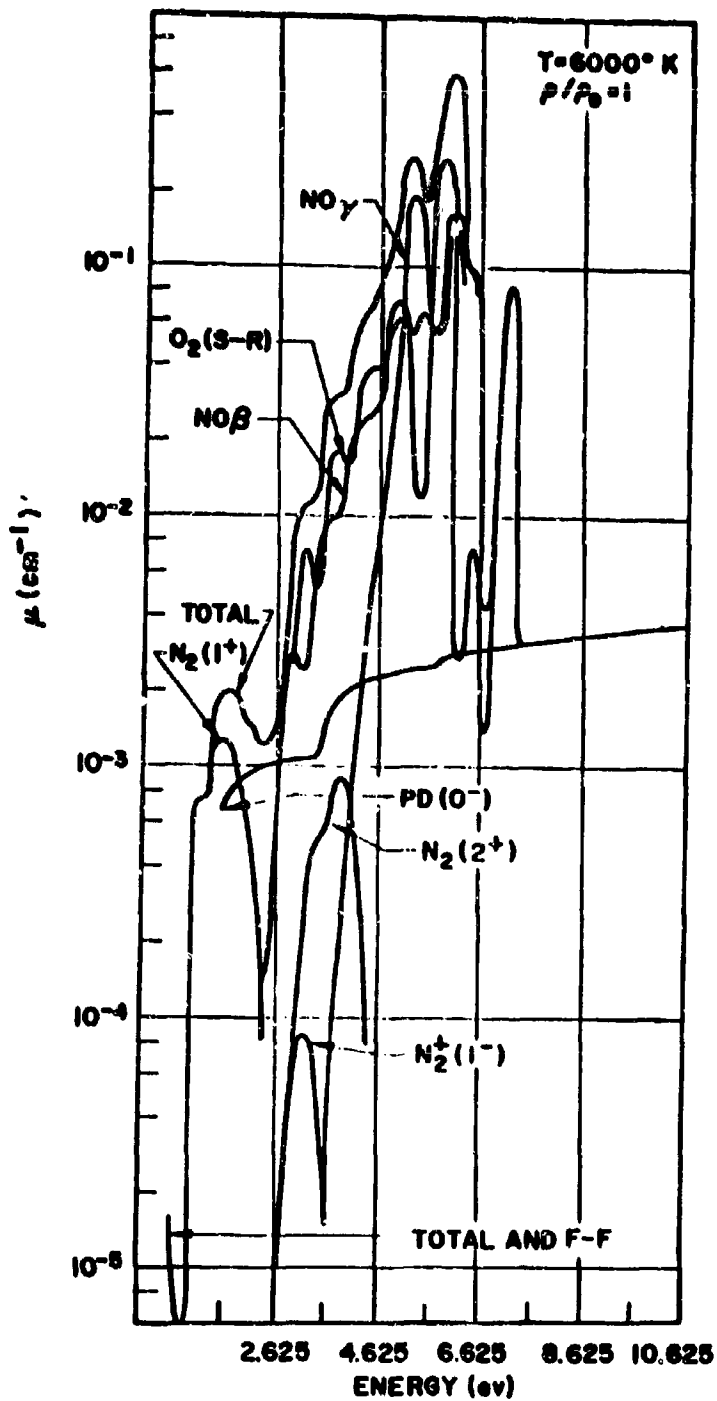


FIG. 7-7 SPECTRAL ABSORPTION COEFFICIENT vs PHOTON ENERGY FOR AIR:
(T = 6000°K, $\rho/\rho_0 = 1$) FROM CALCULATIONS OF MEYEROTT,
SOKOLOFF, AND NICHOLLS (1960)

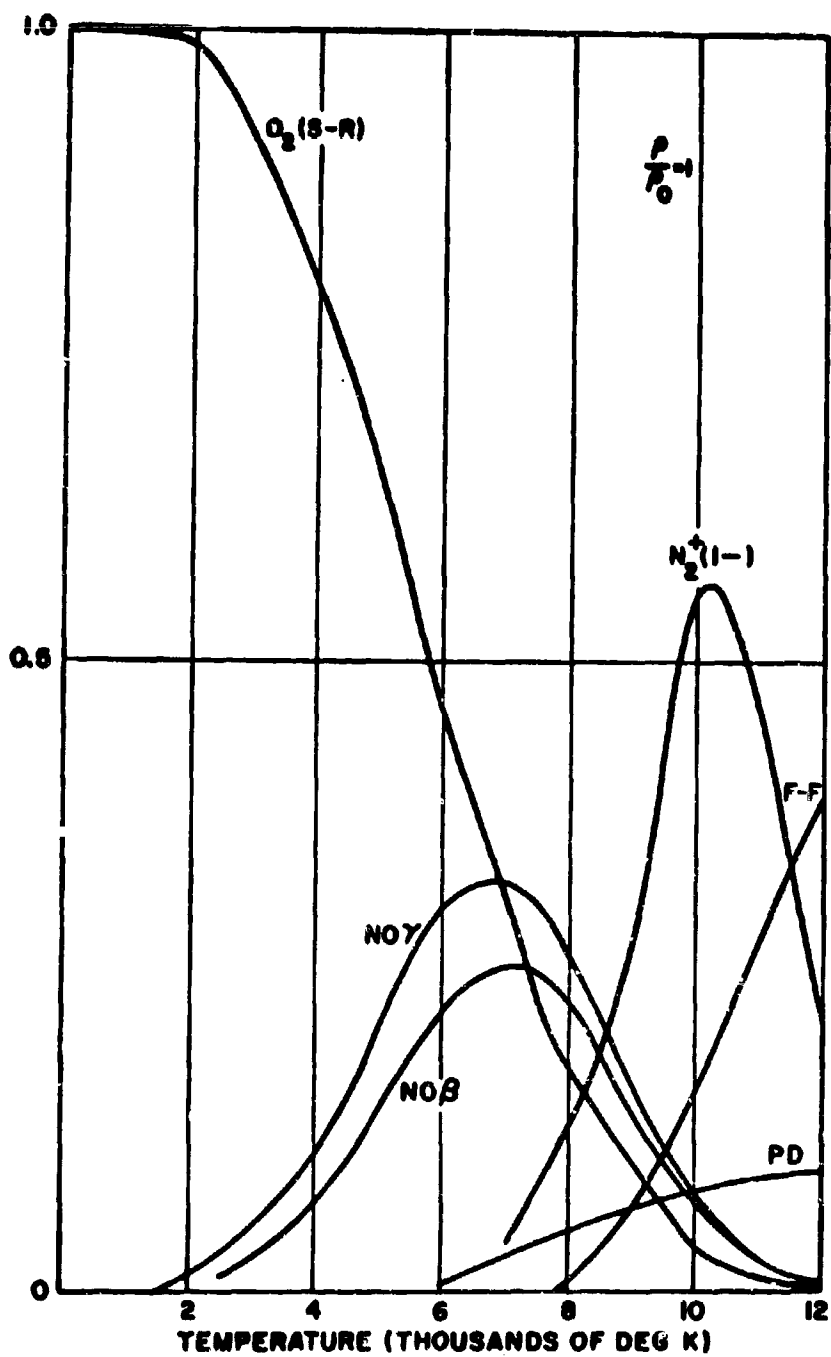


FIG. 7-8 RELATIVE CONTRIBUTION OF MOLECULAR TRANSITIONS: ($\rho/\rho_0 = 1$)
 IN CALCULATIONS OF SPECTRAL ABSORPTION COEFFICIENT OF AIR
 BY MEYEROTT, SOKOLOFF, AND NICHOLLS (1960)

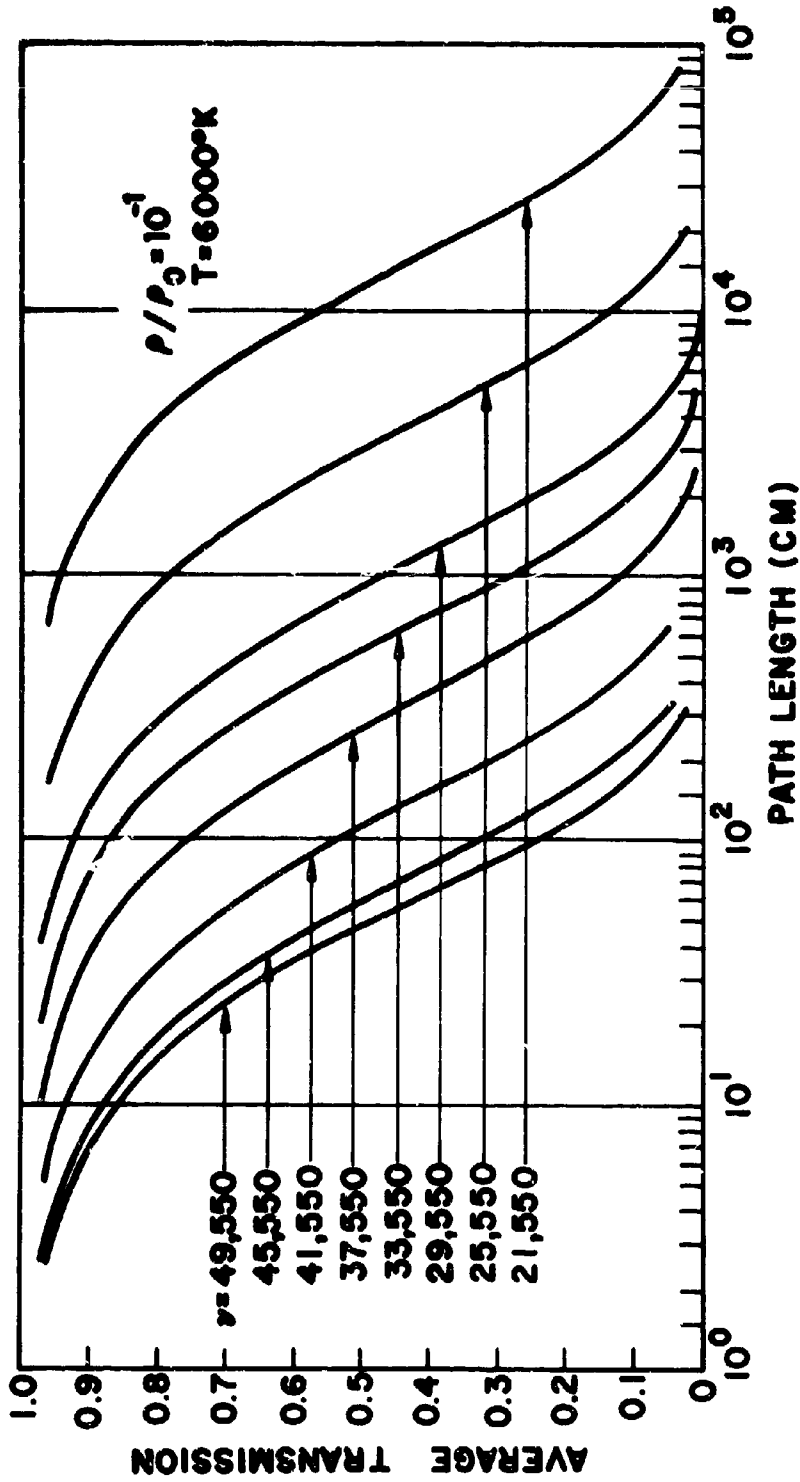


FIG. 7-9 AVERAGE TRANSMISSION OF OPTICAL RADIATION THROUGH A SLAB OF HEATED AIR AS A FUNCTION OF PATH LENGTH FROM THE WORK OF CHURCHILL, HAGSTROM, AND LANDSHOFF (1963)

Chapter 8. ATOMIC ABSORPTION COEFFICIENTS

It has been pointed out in Chapters 6 and 7 that absorption coefficient and opacity calculations have two parts: a) calculation of occupation numbers of absorbing species by statistical mechanics and, b) calculation of absorption cross sections for each of the species involved by quantal methods. The calculation of occupation numbers is treated in some detail in Volume 1 of this series and is also discussed elsewhere in this volume. In this chapter we are mainly concerned with a discussion of quantal methods for the calculation of cross sections of atomic constituents of heated air.

A review was made in Chapter 3 of the basic quantum theory of radiation from which was derived specific formulae for atomic absorption processes. These formulae involve atomic constants, energy and or angular momentum eigenvalues, and integrals over molecular or atomic wavefunctions. The theory is applied with some modifications to molecules in Chapter 4 where it is shown that because some of the basic integrals involving molecular wavefunctions cannot be evaluated, appeal has to be made to experiment. The way in which this works out for molecular contributions to air opacities is described in Chapter 7. However, for atoms, the situation is much more favorable. There is a wide choice of atomic models which provide knowledge of energy levels, wavefunctions and complete radial integrals to varying degrees of accuracy.

8.1 Survey of atomic models

The amount of work involved in formulating an atomic model and solving it for the desired features varies tremendously with the degree of accuracy required, and as in the molecular case, with the amount of empirical information which is available, or which one desires to use.

The choice of an atomic model is somewhat complicated by the fact that no one model will yield all needed information to a consistently high degree of accuracy. For example, the Hartree-Fock method, or model, yields radial wave functions of quite adequate accuracy for most absorption-coefficient calculations, but the energy eigenvalues one obtains thereby are typically in error by about 0.5 eV per electron (the so-called correlation energy) for light atoms. (For references see Table 8-1.) Since we are concerned with spectral absorption coefficients, and with temperatures for which kT may not be much larger than 0.5 eV, this error could be significant, if, for example, these energies were used to determine a line or a photoelectric edge position. Most of the error in such line or edge positions can usually be avoided either by an elaborate choice of screening constants or by use of experimental energy levels (or both, i.e., the screening constants can be evaluated empirically. See Stewart and Pyatt, 1961.).

The simplest model is, of course, the hydrogenic, independent-electron model. This is at one and the same time, the most comprehensive and useful, but least accurate model available. Most of the opacity calculations performed until recently employ either a strict hydrogenic approximation or some rather limited departure from it. At the opposite extreme

Table 6-1
A SURVEY OF ATOMIC MODELS

Model	General	Wave Functions	Atomic Potentials	Radial Integrals	Energy Levels
Hydrogen	Tuller and Salpeter (1957) Sternheimer (1958, 1965) Meyer (1967) Moshinsky and Poshenko (1969) Kleinman and Lohr (1970) Chen, Rank, and Chaudhuri (1987)	See "General"	See "General"	See "General"	
Self-Consistent Field-Quantum Screening Theory	Slater (1969) <i>Methods</i> II-7 Mayer (1967)	Major (1966)		Vanmommery (1968, 1983)	Laporte (1989)
Quasiparticle Approximation Quasiparticle-Quasiparticle Screening	Kelly, Reinhold, and Armstrong (1989)	Slater and Thompson (1974) Slater (1975) Reynolds and Ruckenstein (1980) Gidycz (1984)			
Superconductivity					Slater (1974, 1986, 1988) Lichten and Liebman (1987), Chap. VI Slater (1978), § 20
Wigner	Lichten and Liebman (1987), Chap. VI Slater (1978), § 20	Chap. VI		Lichten and Liebman (1987), Chap. VI	
Formal-Thomas	Quasiparticle (1989) Lichten (1989) Slater (1989) Slater and Reinhold (1989) Tuller and Reynolds (1989) March (1987) Moshinsky and Slater (1969) Feynman, Hellmann, and Taylor (1949) Chen and Ashkin (1987)	Reynolds and Reinhold (1989)			Lichten (1989) Reynolds and Quasiparticle (1989)
Slater, Hartree-Fock (6-7)	Slater (1974) Slater (1989) Pratt (1989)				
Asymptotic/Approximate (6-7)	Reynolds and Major (1989) Slater (1989) Slater et al. <i>Phys. Rev. B</i> (1989) Kelly, Reinhold, and Armstrong (1989)	Reynolds and Kelly (1989) P. S. Kelly (1989)		P. S. Kelly (1989) Reynolds (1989)	Slater and Kelly (1989) P. S. Kelly (1989)
Hartree-Fock-Slater	Slater (1989)	P. S. Kelly (1989) Kelly, Reinhold, and Armstrong (1989)			Reynolds and Hellmann (1989)
Reynolds/7 With Correlation Corrections	Slater and Thompson (1989) Kelly, Reinhold, and Armstrong (1989) P. S. Kelly (1989) Slater et al. <i>Phys. Rev. B</i> (1989)			Alkhalil (1989) Alkhalil and Thompson (1989)	
Collective Models					
All Models: Matrix Elements Angular Integrals for Spin-Orbit Corrections Wave Functions					

would be the Hartree/Hartree-Fock models with corrections for correlation; however, it will probably not be practicable to use such advanced and computationally complicated models in a general opacity calculation for some years to come.

In Table 8-1 we give a list of various atomic models which have been, or can be used to calculate atomic features needed for opacity studies, together with principal references to these models. The list is indicative only, and not rigorous nor exhaustive, but is sufficiently complete that the reader should have little difficulty in extending it. The lack of a reference under a particular atomic feature for a particular model may mean that it is not possible to compute that feature by means of the model, that it has not been done, that it has not come to our attention, or that we consider it unimportant for opacity applications. Non-separable variational methods are not included since they have not been widely nor very successfully applied to the general many-electron problem. For an application of this method to the ground state of oxygen, see Breene (1962).

In addition to the references in the table, mention should be made of the tabulation of atomic (and molecular) f-numbers, relative multiplet strengths, and general atomic structure information by C. W. Allen (1964), and the National Bureau of Standards Bibliography of atomic oscillator strengths (Wiese, Smith and Glennon, 1966). We should also explicitly point out that the extensive calculations of radial dipole integrals in the Hartree-Fock-Slater approximation by Kelly (1964b, 1965) permits practical use to be made of this model in large-scale air opacity calculations (see Armstrong,

Johnston and Kelly, 1965). The most comprehensive tabulation of hydrogenic Gaunt factors for free-free transitions, as well as f-numbers and Gaunt factors for bound-bound and bound-free transitions, is that of Karzas and Latter (1961). The hydrogenic radial dipole integrals tabulated by Green, Rush, and Chandler (1957) can be used to advantage for same-shell transitions (see Section 8.4), and for limited improvements on a strict hydrogenic model.

It is not appropriate in the present context to give a detailed description of each of these models; the details are readily available in the literature cited. We will, however, describe the "hydrogenic model" in the next section because of its basic importance, and then discuss a comparison of some of the most important features of the non-hydrogenic models which have been used in practice. We present a bibliography on photoelectric absorption in Table 8-2 because of the basic importance of this process in atomic absorption of heated air. The bibliography is similar to that of Ditchburn and Öpik (1962), but with a different emphasis and up-dated references. We have attempted to include the most important general references, and as many as possible of the papers dealing with nitrogen and oxygen. Additional references may be found in Ditchburn and Öpik (1962). A similar table has been compiled for free-free processes, and is presented in Table 8-3.

Table 8-2

Important References on Photoelectric Absorption Cross Sections

Kramers (1923)
Milne (1924)
Oppenheimer (1928, 1929)
Gaunt (1930)
Stobbe (1930)
Maue (1932)
Menzel and Pekeris (1935)
Massey and Smith (1936)
Hall (1936)
Sommerfeld (1939)
Bates, Buckingham, Massey and Unwin (1939)
Bates and Massey (1943)
Bates (1946a,b)
Bates and Seaton (1949)
Seaton (1951)
Weissler (1956)
Bethe and Salpeter (1957)
Seaton (1958)
Kelly and Armstrong (1959)
Armstrong and Kelly (1959)
Armstrong (1959, 1964b)
Burgess and Seaton (1960)
Dalgarno and Parkinson (1960)
Karzas and Latter (1961)
Cooper and Martin (1962)
Cooper (1962)
Dalgarno, Henry, and Stewart (1964)
Johnston (1964)
Burgess (1964)

Table 8-3

Important References on Free-Free Absorption Cross Sections

Kramers (1923)

Menzel and Pekeris (1935)

Sommerfeld (1939)

Wooler and Wildt (1942)

Chandrasekhar and Breen (1946)

Mayer (1947)

Berger (1956)

Bethe and Salpeter (1957)

Grant (1958)

Karzas and Latter (1961)

Breene, Jr., and Nardone (1960, 1961, 1963)

Brussaard and Van de Hulst (1962)

Peach (1965)

8.2 Hydrogenic and simple-Coulomb-force models

The hydrogenic model of the atom was quite naturally an archetype for opacity calculations. This model predicts the gross features of the periodic table and many of the qualitative regularities of atomic spectra. In addition, most features of many-electron atoms become hydrogenic or nearly hydrogenic in the limit of large orbital or angular quantum numbers. The reason for this is that the higher the value of the quantum number an electron has, the smaller is the fraction of its time that is spent at small distances. At large distances from the nucleus, the residual ion (or "core") acts as a hydrogenic point charge to the electron.

One aspect of the realism of a hydrogenic model is its prediction, in agreement with experiment, of a Rydberg-Ritz-type formula for atomic term values of the form

$$E_{LS} = - I_{LS} + \frac{Z_e^2 \times \text{Ryd}}{(n - \Delta_{LS})^2}$$

where the atomic term is denoted by L, S for orbital and spin angular momentum respectively, and Ryd is the Rydberg unit (13.605 eV). The hydrogenic shell quantum number is denoted by the integer n . The "quantum defect" Δ_{LS} is a measure (together with the ionization potential I_{LS}) of the departure from strictly hydrogenic behavior. The ionization potential I depends strongly on the angular momentum coupling (L-S value) of the core, or of the residual ion with charge Z_e , Δ depends most strongly on the one-electron orbital angular momentum, l . For s- and

p-levels ($l = 0$ and 1) in N and O, Δ is roughly $1.5 - 1.0$. For d-levels ($l = 2$) it drops sharply to about $.05$ or smaller. When $l > 2$, Δ is always very close to zero.

The L-S terms (E_{LS}) for a given l and n usually cluster about an average value which depends on l . The average is often used to represent the entire group of terms in approximate calculations.

The word Term is applied to the group of levels associated with L and S and which differ only in J , the inner quantum number associated with the vector sum of L and S . The energy differences of these levels differing only in J is due to spin-orbit interaction, and is usually negligible for high-temperature air radiation studies (in view of the overall uncertainties in this type of problem). The center-of-gravity or any other convenient average of the levels of different J is taken to be the term energy.

The words "hydrogenic model" do not imply a unique set of formulas, as a variety of more or less independent corrections can be made on formulas strictly applicable to hydrogen, in order to account for non-hydrogenic features. Even the terminology "hydrogenic f-numbers or matrix elements" is rather loose when used in an opacity context. What is usually implied is a Kramers-Gaunt approximation with the Gaunt factor taken to be independent of frequency or energy. We will not propose a precise definition of the hydrogenic model but will present in this section, formulas and results, obtained from hydrogenic formulas by some correction or other. Perhaps the prototype of this model is the set of formulas presented by Mayer (1947) and improved by Stewart and Pyatt (1961).

8.2.1 Photoelectric Cross Sections

A most useful starting point, because of its simplicity, is the Kramers (1923) semiclassical expression for the photoelectric cross section per electron. Compton (1926) gives the Kramers' formula for the absorption coefficient per electron in the n -th shell as:

$$\sigma = \frac{64\pi^4}{3^3} \frac{Z^4 e^{10} m \lambda^3}{c^4 h^6 a_n n^3} \left(\lambda \leq \frac{I}{hc} \right)$$

$$= 0 \quad \left(\lambda > \frac{I}{hc} \right)$$
(8.2-1)

where λ is the wavelength of the incident radiation (cgs units), m is the electron mass, I the ionization potential, and a_n is the "statistical weight" of an electron in the shell. If we take $a_n = n^2$, this formula can be reduced to

$$\sigma = \frac{2^4 e^2 h}{3^3 mc} \cdot \frac{I_n^2}{n(h\nu)^3} \quad h\nu \geq I_n$$

$$= 0 \quad h\nu < I_n$$
(8.2-2)

* Since Eq. (8.2-1) is a semiclassical expression, spin is neglected and it is not summed over the usual two final spin states of the free electron. Therefore, we should also neglect spin in the sum over initial states.

where $I_n = \frac{Z^2 e^2}{2n^2 a_0}$ is the ionization potential of the n-th shell with $a_0 = \hbar^2 / me^2$ the Bohr radius. Eq. (8.2-2) is also the result obtained from Mayer's (1947) Eq. 2.21 if one divides the latter expression by $2n^2$ to account for the fact that it is for a complete shell of electrons, and has been corrected to account for spin weights (see footnote on preceding page). The expression, Eq. 78.15, given by Bethe and Salpeter (1957),

$$\sigma \text{ (a.u.)} = \frac{Z^4 \alpha}{3\sqrt{3} \pi^2 \nu^3 \text{ a.u.} n^3} \quad (8.2-3)$$

is equivalent to Mayer's expression when converted to cgs units. (In Eq. (8.2-3), a.u. signifies atomic units and $\alpha = e^2 / \hbar c$ is the fine-structure constant.)

Now the difference between Eq. (8.2-3) and the exact expression for hydrogen (Eq. (3.2-99) with hydrogen wave functions inserted for the $R_{nl}(r)$) is usually a factor of order unity (Gaunt, 1930; Menzel and Pekeris, 1935) called the Gaunt factor $g_{bf}^{(n)}(\nu)$. In view of the simplicity of the Kramers expression and the complexity of the exact hydrogen expression, it is convenient to write the exact photoelectric absorption coefficient for hydrogen as

$$\mu_{bf}(\nu) = \sum_n N_v^{(n)} \left(\frac{2^4 e^2 \hbar}{3\sqrt{3} mc} \right) \frac{1}{n} \frac{I_n^2}{(h\nu)^3} g_{bf}^{(n)}(\nu) \quad (8.2-4)$$

where $N_v^{(n)}$ is the number density of absorbing hydrogen atoms in each state n , and $g_{bf}^{(n)}(\nu)$ is the Gaunt factor. It is defined strictly as the ratio of the exact hydrogen expression to the Kramers' expression for the absorption coefficient.

We can make a straightforward approximate generalization to other atoms by replacing the hydrogenic I_n by the ionization potential of the other atom* and inserting as an additional factor in Eq. (8.2-2) the number of electrons in each shell of the non-hydrogenic atom. In contrast to hydrogen, non-hydrogenic atoms are not degenerate in l and we can further break down the summation indicated in Eq. (8.2-2) to specify subshells of given angular momentum l . The result is then

$$\mu_{bf}(\nu) = \sum_{n,l} N_v^{(n,l)} n(n,l) \left(\frac{2^4 \pi^2 h}{3mc} \right) \frac{I_n^2}{n(h\nu)^3} g_{bf}^{n,l}(\nu) \quad (8.2-5)$$

where we have used $n(n,l)$ to indicate the number of electrons in the n,l subshell. This formula, with $g_{bf}^{n,l}(\nu)$ set equal to unity, was used by Stewart and Pyatt (1961) for bound-free absorption studies as follows. They define a Stromgren D-function, $D(u) = u^3 \kappa$, where $u = h\nu/kT$ and $\kappa = \mu/\rho$ with ρ the mass density in gm/cm^3 , and where μ is the linear absorption coefficient in cm^{-1} . Eq. 18 of Stewart and Pyatt (1961) then states

$$D(u) = D_{ff}(u) \frac{\Gamma}{\langle Z^2 \rangle} \left(\frac{kT}{\text{Ryd}} \right) \frac{p_i m_i}{n_j} \frac{(I_j)^2}{(kT)^2} \quad (8.2-6)$$

* These can be obtained from experiment or approximately from screening constants; see references given in Table 8.1.

where m_j is what we have called $n(n, \ell)$ in Eq. (8.2-5), n_j is our n , I_j is our I_n , $\frac{P_1 \rho}{AM_1} = N_V^{(n, \ell)}$, ρ again is the mass density, A the atomic number, M_1 is the atomic mass unit, and $Ryd = e^2/2 a_0 = 13.6 \text{ eV}$. The free-free D-function which they use is given by

$$D_{ff} = \frac{\langle Z^2 \rangle}{A} \left(\frac{Ryd}{kT} \right)^2 \frac{1}{\Gamma} \left[\frac{64\pi\alpha a_0^2}{3/3 M_1} \right] \quad (8.2-7)$$

where $\alpha = e^2/\hbar c$ is the fine structure constant. Substituting Eq. (8.2-7) into Eq. (8.2-6), with use of the definitions of κ and $D(u)$ yields the result

$$\mu = (P_1 \rho) \frac{\Gamma}{\langle Z^2 \rangle} \left(\frac{kT}{Ryd} \right) \frac{m_1}{n_j} \frac{I_1^2}{(kT)^2} \cdot \frac{\langle Z^2 \rangle}{A} \left(\frac{Ryd}{kT} \right)^2 \frac{1}{\Gamma} \left[\frac{64\pi\alpha a_0^2}{3/3 M_1} \right] \quad (8.2-8)$$

In view of the equivalences stated above, and the cancellation of factors (including their mean square ionic charge $\langle Z^2 \rangle$ and their degeneracy parameter Γ which we have not defined) Eq. (8.2-8) is identical with Eq. (8.2-5) if $g_{bf}^{n, \ell}(\nu) = 1$.

A convenient way of writing Eq. (8.2-5) which also accounts for configuration splitting (Armstrong, Holland and Meyerott, 1958) is to consider the total absorption coefficient for a given atomic term, T , specified by n , ℓ , L , and S (L = total angular momentum, S = total spin). We replace $N_V^{(T)}$, the number density of atoms in the state, or term T , by

$$N_V^{(T)} = P_T N_V \quad (8.2-9)$$

where P_T is the fraction in this state ("fractional occupation number") and N_V the total number density. It will now be assumed that the wavefunction is separable and thus that the many-electron wave function consists of a product of one electron wavefunctions. If this assumption is made, a single electron wavefunction can be factored out of the total many-electron function (Eq. (8.2-12)) and employed in a one-electron-transition matrix element (Eq. (8.2-11)). Then a one-electron-transition dipole matrix element which initially has the form,

$$\int \psi^*(\vec{r}_1, \vec{r}_2, \dots, \vec{r}_N) \vec{r}_1 \psi(\vec{r}_1, \vec{r}_2, \dots, \vec{r}_N) d^3\vec{r}_1 d^3\vec{r}_2 \dots d^3\vec{r}_N \quad (8.2-10)$$

in an N-electron atom, simplifies to

$$\int \psi^*(\vec{r}_2, \dots, \vec{r}_N) \psi(\vec{r}_2, \dots, \vec{r}_N) d^3\vec{r}_2 \dots d^3\vec{r}_N \times \int \varphi^*(r) \vec{r} \varphi(r) d^3r \quad , \quad (8.2-11)$$

where we have factored ψ according to

$$\psi(\vec{r}_1, \vec{r}_2, \dots, \vec{r}_N) = \varphi(\vec{r}_1) \psi(\vec{r}_2, \dots, \vec{r}_N) \quad , \quad (8.2-12)$$

and the factor on the left of Eq. (8.2-11) is the overlap of the passive electron wave functions.

Now, strictly speaking, the factorization is not as simply done as Eq. (8.2-12) would indicate. The reason for this is that electrons obey Pauli statistics and the total wave function $\psi(\vec{r}_1, \vec{r}_2, \dots, \vec{r}_N)$ must be antisymmetric in the coordinates of all the electrons. This is usually taken into account by employing wave functions of a determinantal form (Slater, 1960). In order to describe analytically the ejection of a single

electron from a system containing several electrons, we must find the matrix element for a transition involving just the one electron, which will in general be a very complicated integral over the coordinates of that electron. An integration over the coordinates of the remaining, or "passive" electrons will also appear in the matrix element but this will only be of an overlap type. That is to say, there will be no operator in the matrix element connecting the initial and final coordinates of the passive electrons.

We will not here go into this problem in any detail. The effect of the antisymmetry of the electrons is to replace the simple factorization indicated in Eq. (8.2-12) by a linear combination of such factored terms over different parent terms of the residual N-1 electron system (core or ion are words often employed). That is to say, Eq. (8.2-12) should more properly be written

$$\Psi(\vec{r}_1, \vec{r}_2, \dots, \vec{r}_N)_{SL} = \sum_{S_p L_p} F(l^q SL, S_p L_p) \psi(\vec{r}_1, \vec{r}_2, \dots, \vec{r}_N)_{S_p L_p} \quad (8.2-13)$$

where S and L denote the total spin and total angular momentum of the term which is to be the initial state, S_p and L_p denote the values of S and L for the possible parent terms of the N-1 electron core, and the coefficients $F(l^q SL, S_p L_p)$ are called coefficients of fractional parentage. These coefficients, sometimes called OFP or FPC for short, were implicitly introduced by Bacher and Goudsmit (1934), and the algebra governing their behavior was first worked out by Racah (1943). (See also Rose, 1957.) If there are no electrons equivalent to the factored one (i.e., having the same value of n and l) in the parent configuration, then the factorization reduces to the simple expression,

Eq. (8.2-12).^{*} We will assume that the overlap integrals are unity. This is not, of course, strictly true since the other orbitals do change when one electron is ejected, but it is a good approximation under most circumstances (10% or better). We will also use ψ_{pC} which are normalized to the number of equivalent electrons. By this means we can omit the factor $n(n, l)$ which appears in Eq. (8.2-5).

An absorption coefficient according to this hydrogenic approximation can now be written as

$$\mu_{TTp}^{(n,l)}(\nu) = N_V \left(\frac{2^4 h e^2 I_T^2}{3/3 mc n(h\nu)^3} \right) P_T F^2 \left(l^{nSL}, S_p L_p \right) \left(g_{nl}^{e, l+1}(\nu) + g_{nl}^{e, l-1} \right) \quad (8.2-14)$$

where the dipole selection rule $l \rightarrow l \pm 1$ is explicitly acknowledged.

The symbols in Eq. (8.2-14) have the following meanings

I_T = Ionization energy of atomic term T .

N_V = Total number density of gas particles

P_T = Fraction of total number density N_V which are in term T

$$\left(\sum_{\substack{\text{all terms} \\ \text{all species}}} P_T = 1 \right)$$

$g_{nl}^{e, l'}(\nu)$ = Bound free Gaunt factor for initial bound state n, l ,
final free state e (energy of free electron), l' .

* In the foregoing analysis we have, for simplicity, suppressed the spin wave functions and sums, and the sums over magnetic quantum numbers,

$$\sum_m C(l L_p L; m M_p M) \psi_{l, m}(\vec{r}_1) \psi_{L_p M_p}(\vec{r}_2, \dots, \vec{r}_N) , \text{ which}$$

permit the coupling of the core and one-electron angular momenta to the specific total L and S ($C(l L_p L; m M_p M)$ are Clebsch-Gordan coefficients -- see Chapter 3). We have also neglected the effect of radial exchange.

ν = Photon frequency; obeys conservation equation

$$h\nu = \epsilon + I_T$$

T : Symbol for LS coupling term T ; specifies total angular momentum and total spin L and S , respectively. A unique energy E_T or ionization potential I_T can be assigned such a term by using e.g., the center of gravity of the component J- levels:

$$E_T = \frac{\Sigma(2J+1) E_J}{(2L+1)(2S+1)}$$

$F^2(\ell^q SL, s_p L_p)$ = Fractional parentage coefficient, or fraction of term T of the configuration ℓ^q (specified by LS) which arises from the parent term T_p (specified by $L_p S_p$) of the configuration ℓ^{n-1} .

q = Number of electrons of angular momentum ℓ , (which comprise the configuration ℓ^q , which couples to the term SL).

T_p = Symbol for LS coupling term of the parent or core, which remains after one electron has been ejected from the initial system by photoionization.

The squared fractional parentage coefficients of the more important terms needed in air studies are given in Table 8.4 for configurations involving one or two angular momentum subshells. (For more complicated cases involving three or more subshells, see Armstrong and Kelly (1959) or Rohrlich (1959).) The non-trivial results in this table are taken from Menzel and Goldberg (1936). The remainder have been included here for the convenience of the reader who may not be familiar with the methods of computing them.

Table 8.4 Percentages of Terms Arising from Shell of Equivalent Electrons (after Menzel and Goldberg, 1936)

Configuration	Term	Percentage
sp^2	2D	$p^2(^1D)$, $sp(\frac{3}{2}^3P + \frac{1}{2}^1P)$
	4P	$p^2(^3P)$, $sp(2^3P)$
	2P	$p^2(^3P)$, $sp(\frac{1}{2}^3P + \frac{3}{2}^1P)$
	2S	$p^2(^1S)$, $sp(\frac{3}{2}^3P + \frac{1}{2}^1P)$
s^2p	2P	$s^2(^1S)$, $sp(\frac{3}{2}^3P + \frac{1}{2}^1P)$
p^2	3P	$p(2^2P)$
	1D	$p(2^2P)$
	1S	$p(2^2P)$
s^2p^2	3P	$s^2p(2^2P)$, $sp^2(\frac{4}{3}^4P + \frac{2}{3}^2P)$
	1D	$s^2p(2^2P)$, $sp^2(2^2D)$
	1S	$s^2p(2^2P)$, $sp^2(2^2S)$
s^2p^4	3P	$sp^4(\frac{4}{3}^4P + \frac{2}{3}^2P)$
	1D	$sp^4(2^2D)$
	1S	$sp^4(2^2S)$
sp^5	3P	$sp^4(\frac{8}{3}^4P + \frac{1}{3}^2P + \frac{5}{3}^2D + \frac{1}{3}^2S)$
	1P	$sp^4(3^2P + \frac{5}{3}^2D + \frac{1}{3}^2S)$
p^3	4S	$p^2(3^3P)$
	2D	$p^2(\frac{3}{2}^3P + \frac{3}{2}^1D)$
	2P	$p^2(\frac{3}{2}^3P + \frac{5}{6}^1D + \frac{2}{3}^1S)$
p^4	3P	$p^3(\frac{4}{3}^4S + \frac{5}{3}^2D + ^2P)$
	1D	$p^3(3^2D + ^2P)$
	1S	$p^3(4^2P)$

Table 8.4 (cont'd)

Configuration	Term	Parentage
p^5	$2P$	$p^4(3^3P + \frac{5}{3} 1^1D + \frac{1}{3} 1^1S)$
s^2p^3	$4S$	$sp^3(\frac{5}{4} 5^5S + \frac{3}{4} 3^3S)$
	$2D$	$sp^3(\frac{3}{2} 3^3D + \frac{1}{2} 1^1D)$
	$2P$	$sp^3(\frac{3}{2} 3^3P + \frac{1}{2} 1^1P)$
sp^3	$5S$	$sp^2(3^4P)$
	$3S$	$sp^2(\frac{1}{3} 4^4P + \frac{8}{3} 2^2P)$
	$3D$	$sp^2(\frac{4}{3} 4^4P + \frac{3}{2} 2^2D + \frac{1}{6} 2^2P)$
	$1D$	$sp^2(\frac{3}{2} 2^2D + \frac{3}{2} 2^2P)$
	$3P$	$sp^2(\frac{4}{3} 4^4P + \frac{5}{6} 2^2D + \frac{1}{6} 2^2P + \frac{2}{3} 2^2S)$
	$1P$	$sp^2(\frac{5}{6} 2^2D + \frac{3}{2} 2^2P + \frac{2}{3} 2^2S)$
sp^4	$4P$	$sp^3(\frac{5}{4} 5^5S + \frac{5}{3} 3^3D + 3^3P + \frac{1}{12} 1^1S)$
	$2P$	$sp^3(\frac{5}{12} 3^3D + \frac{1}{4} 3^3P + \frac{4}{3} 3^3S + \frac{5}{4} 1^1D + \frac{3}{4} 1^1P)$
	$2D$	$sp^3(\frac{9}{4} 3^3D + \frac{3}{4} 3^3P + \frac{3}{4} 1^1D + \frac{1}{4} 1^1P)$
	$2S$	$sp^3(3^3P + 1^1P)$

In order to use Eq. (8.2-14), we also need the Gaunt factors $g_{nl}^{\epsilon, l \pm 1}$. The most comprehensive tables of these quantities have been given by Karzas and Latter (1961) and earlier partial results were given by Bethe (1933), by Mayer (1947), and by Armstrong and Kelly (1959). These factors have a slowly varying frequency dependence, particularly near threshold where they are most important. This can be seen from Figs. 8-1, 8-2, and 8-3, taken from Karzas and Latter. On this account it often suffices to use the threshold ($\epsilon = 0$) values of the Gaunt factors as a constant approximation over all frequency values. Accordingly, we have included (Table 8.5) a table of threshold values for a large variety of states.

Table 8.5 Asymptotic Bound-Free Gaunt Factors

$$g_{n_1 l} = (g_{n_1 l}^{\infty, l-1} + g_{n_1 l}^{\infty, l+1}).$$

n_1	Angular momentum l							
	s	p	d	f	g	h	i	j
3	1.06160	1.09768	0.76259
4	1.18	1.25	1.13	0.606
5	1.2901	1.3661	1.3526	1.0369	0.44309
6	1.3957	1.4724	1.5109	1.3360	0.87216	0.30932
7	1.4955	1.5724	1.6372	1.5539	1.2183	0.68851	0.20827	...
8	1.5900	1.6643	1.7479	1.7233	1.4908	1.0323	0.51789	0.13638

The values for $n = 3$ are taken from Mayer (1947), the values for $n = 4$ have been computed from the radial integral, $\left(R_{nl}^{n', l'} \right)^2$ values given in Bethe and Salpeter (1957), and the remainder $\left(R_{nl}^{n', l'} \right)$ are from Armstrong and Kelly (1959).

An analytic formula for the threshold Gaunt factor values has been given by Armstrong and Kelly (1959). Their result can be written

$$g_{nl}^{n', l+1} = \lim_{n' \rightarrow \infty} \frac{\sqrt{3\pi}}{2^5} \left\{ \frac{(l+1) + \frac{1}{2}}{2l+1} \right\} \left(\frac{n'}{n} \right)^3 \left\{ \frac{R_{nl}^{n', l+1}}{a_0} \right\} \quad (8.2-15)$$

where the required asymptotic expansions of the Gordon (1929) hydrogen dipole integrals $R_{nl}^{n', l+1}$ are

$$R_{nl}^{n', l-1} (n' \rightarrow \infty) \sim \frac{(-1)^{n'-l}}{4(2l-1)!} \left(\frac{(n'+l-1)!}{(n'-l)!} \right)^{1/2} x \quad (8.2-16a)$$

$$\begin{aligned} & \frac{(4n')^{l+2} e^{-2n'}}{n'^{3/2}} \left\{ F_C(-n'_r, 2l, -4n') \right. \\ & \left. + \left(\frac{n'-l}{l} \right) F_C(-n'_r+1, 2l+1, -4n') \right\} \end{aligned}$$

and

$$R_{n,l}^{n', l-1} (n' \rightarrow \infty) \sim \frac{(-1)^{n'-l}}{4(2l-1)!} \left(\frac{(n+l)!}{(n-l-1)!} \right)^{1/2} x \quad (8.2-16b)$$

$$\frac{(4n)^{l+1} e^{-2n}}{(n')^{3/2}} \left\{ F_C(-n'_r, 2l, -4n) - F_C(-n'_r-2, 2l, -4n) \right\}$$

In these formulas $F_c(\alpha, \beta; x)$ is the confluent hypergeometric function, and the radial quantum numbers n_r are defined by $n_r = n - \ell - 1$, $n_r' = n' - \ell$.

Figs. 8-4, 8-5, and 8-6 show the cross sections of Eq. (8.2-14) for hydrogen, viz., $\mu(\nu)/N_V P_T$ for $F^2 = 1$, for principal quantum numbers n from one through fifteen. They are shown as functions of photon energy $h\nu$ in eV; the solid curves are exact results due to McDowell (1964), and the dotted curves shown for $n = 1, 2$, and 3 have been obtained from Eq. (8.2-14) by taking the Gaunt factors as constant and equal to their threshold values. The cross sections given are shell-averaged values σ_n where the average is defined by:

$$\sigma_n = \sum_{\ell} \frac{2\ell+1}{n^2} \sigma_{n\ell} \quad (8.2-17)$$

Extensive tables of the exact hydrogen cross sections have been given by Burgess (1964).

8.2.2 Hydrogenic free-free absorption

The basic calculation of free-free cross sections has already been reviewed in Sec. 3.2.2.4; in this section we will merely discuss some of the formulas and results (in the hydrogenic approximation) that have been used in practice. Most opacity calculations have made use of the Kramers' (classical) formula for the free-free absorption coefficient suitably modified by a Gaunt factor g_{ff} :

$$\mu_{ff} = \frac{16\pi^3}{3\sqrt{3}} \alpha \frac{Z^2 e^4}{m^2 \omega^3 v_i} N_e N_i g_{ff} \quad (8.2-18)$$

(cf. Eq. 3.2-216). In this formula N_e and N_i are the number densities of free electrons and of ions, respectively, v_i is the initial free electron velocity, and α is the fine-structure constant. In practice one is usually interested in an average of the absorption coefficient (viz. g_{ff}/v_i) over a Maxwellian distribution. Since the Maxwell average of v^{-1} is given by

$$\overline{v^{-1}} = \frac{\int e^{-\frac{mv^2}{2kT}} v \, dv}{\int e^{-\frac{mv^2}{2kT}} v^2 \, dv} = \left(\frac{2m}{\pi kT} \right)^{1/2}$$

Eq. (8.2-18) can be written, upon averaging, as

$$\bar{\mu}_{ff} = \frac{16\pi^3}{3\sqrt{3}} \alpha \frac{Z^2 e^4 N_e N_i}{m^2 \omega^3 v_i} \bar{g}_{ff} \quad (8.2-19)$$

$$= \frac{16\pi^{5/2}}{3\sqrt{3/2}} \alpha \frac{Z^2 e^4 N_e N_i}{m^{3/2} \omega^3 (kT)^{1/2}} \bar{g}_{ff}$$

where

$$g_{ff} = \frac{\int \frac{g_{ff}}{v} f(v) v^2 dv}{\int \frac{f(v)}{v} v^2 dv} \quad (8.2-20)$$

and $f(v)$ is the Maxwellian distribution function.

A formula for g_{ff} given by Menzel and Pekeris (1935), Eq. (3.2-221), has frequently been used in opacity calculations (e.g., Mayer, 1948; Moszkowski and Meyerott, 1951). This formula becomes, when the Maxwell average (Eq. 8.2-20) is taken,

$$\bar{g}_{ff} \approx 1 + 0.1728 \left(\frac{1}{\beta Z^2} \right)^{1/3} u^{1/3} \left(1 + \frac{2}{u} \right), \quad (8.2-21)$$

where $u \equiv hv/kT$ and $\beta \equiv \text{Ryd}/kT$. (Note that this formula is given incorrectly by Mayer, 1948, and by Moszkowski and Meyerott, 1951.)

There are a large number of papers in the literature prior to the late 1950's which discuss and derive approximate Gaunt factors valid under very limited circumstances. We will not review these, as they are more or less superseded by the excellent reviews and discussions of Grant (1958), and of Brussard and Van de Hulst (1962), and exact numerical computations for hydrogen. The numerical computations beginning with Berger (1956) were culminated by the comprehensive calculation and tabulation of Karzas and Latter (1961). Grant (1958) gives the semi-classical (WKB) approximation (Eq. 3.2-224a):

$$g_{ff}^{s.c.} \sim 1 + 0.21775 |\xi|^{-2/3} - 0.01312 |\xi|^{-4/3} + \dots \quad (8.2-22)$$

valid when $|\xi| \gg 1$, where $\xi \equiv Z\alpha c \left| \frac{1}{v_f} - \frac{1}{v_i} \right|$. It is interesting to

note that this formula is more accurate than the Menzel-Pekeris formula. Grant also calls attention to the fact that Gauss-Laguerre numerical integration is very effective for obtaining the Maxwell averages needed. According to him, three terms are usually adequate to obtain 3-significant-figure accuracy, using the weighting factors and roots of Gauss-Laguerre integration, Grant obtains the 3-term formula for \bar{g} :

$$\bar{g} = 0.711 g(0.416) + 0.279 g(2.294) + 0.010 g(6.290) \quad (8.2-23)$$

where the argument of the Gaunt factor which is to have the values indicated in this equation is y , given by

$$y = \frac{mv_1^2}{2kT} - \frac{h\nu}{kT} \quad (8.2-24)$$

Grant's 3-term integration of the semi-classical formula (Eq. 8.2-22) and of the Born-approximation result (Eq. 3.2-222) compares favorably with Berger's (1956) numerical calculations, and are, of course, much simpler. However, he evidently overlooked a useful limiting form of the Born approximation result (apparently first given by Elwert -- see Brussard and Van de Hulst, 1962).

If, in addition to the validity requirement of the Born approximation:

$$\begin{aligned} \eta_i &\ll 1 \\ \eta_f &\ll 1 \end{aligned} \quad (8.2-25)$$

$$\left(\eta = \frac{Z\alpha c}{v} \right),$$

we require that

$$h\nu \ll kT, \quad (8.2-26)$$

we can write

$$\eta_f \approx \eta_i = \eta, \text{ say.} \quad (8.2-27)$$

This yields, when inserted into Eq. (3.2-222)

$$g_{ff}^{\text{Born}} \approx \frac{\sqrt{3}}{\pi} \ln \frac{2\eta}{\eta_f - \eta_i} \quad (8.2-28)$$

In view of our requirements (Eq. (8.2-27)) we can write

$$\eta_f - \eta_i \approx \frac{Z\alpha c}{v^2} \Delta v = \frac{Z\alpha c}{2\varepsilon} \frac{\Delta\varepsilon}{v} = \frac{\eta\Delta\varepsilon}{2\varepsilon} \quad (8.2-29)$$

where $\varepsilon = \frac{mv^2}{2}$ is the electron energy, and $\Delta\varepsilon = h\nu$ is the photon energy.

Thus, we obtain

$$g_{ff}^{\text{B}} \approx \frac{\sqrt{3}}{\pi} \ln \frac{4\varepsilon}{h\nu}. \quad (8.2-30)$$

Setting

$$u' \equiv \varepsilon/kT, \quad u \equiv h\nu/kT, \quad (8.2-31)$$

the Maxwell average, Eq. (8.2-20) yields

$$\begin{aligned} \overline{g_{ff}^B} &= \frac{\sqrt{3}}{\pi} \int e^{-u'} \ln \frac{4u'}{u} du' \\ &= \frac{\sqrt{3}}{\pi} \ln \frac{4}{\gamma u} \end{aligned} \tag{8.2-32}$$

where $\gamma = 1.78107$ is given by e^c where c is Euler's constant. Expressing this result numerically we obtain

$$\overline{g_{ff}^B} = 0.55131 \ln \frac{2.2458}{u} \tag{8.2-33}$$

For Grant's (1958) example 2, the conditions (Eq. 8.2-25) and (Eq. 8.2-26) are satisfied, and u (defined by our Eq. (8.2-31) has the value 0.0124. Eq. (8.2-33) yields, for this value of u , $\overline{g_{ff}^B} = 2.866$. This result is considerably closer to Berger's presumably more accurate value of 2.817 than is Grant's value of 2.979 obtained by 3-point Gauss-Laguerre integration. The Karzas-Latter (1961) result (from their Fig. 5) is 2.9, which, unfortunately, cannot be read to greater precision. This appears to dispute Grant's claim that the difference between his result and Berger's is due primarily to the inaccuracy of the Born approximation. As noted above, the Born-approximation validity conditions as well as the additional condition imposed by Eq. (8.2-26) are well satisfied at $u = 0.0124$ and $kT = 100$ eV, the conditions of this example. Thus, not much error should be expected from the Born approximation.

Eq. (8.2-33) should prove quite useful in a broad low-frequency, high-temperature region where free-free absorption tends to be most important.

8.2.3 Hydrogenic Bound-Bound Transitions and Oscillator Strengths

In the case of bound-bound transitions, there is now sufficient tabular data to provide exact values of the bound-bound oscillator strengths for practically all transitions of interest (Menzel and Pekeris, 1935; Karzas and Latter, 1961; Green, Rush, and Chandler, 1957). For large-scale calculations or for exploratory or approximate results a Kramers'-type value may nevertheless still be useful. By comparing Eq. 63-11 of Bethe and Salpeter (1957) and Eqs. 1.31 and 1.33 of Menzel and Pekeris (1935) we see that we can write the exact hydrogenic f -number for a transition from a lower state n to an upper state n' averaged over the shell of principal quantum number n (containing $2n^2$ states) as*

$$f_{nn'} = \frac{2^5}{3\sqrt{3}\pi n^5 (n')^3} \left(\frac{1}{n^2} - \frac{1}{n'^2} \right)^{-3} g_{nn'} \quad (8.2-34)$$

where $g_{nn'}$, the bound-bound Gaunt factor is given approximately by

$$g_{nn'} \approx 1 - 0.1728 \left(\frac{\nu}{RZ^2} \right)^{1/3} \left[\frac{2}{(n')^2} \left(\frac{RZ^2}{\nu} \right) - 1 \right]$$

or

$$g_{nn'} \approx 1 - 0.1728 \left(\frac{\nu}{RZ^2} \right)^{1/3} \left[\frac{2}{n^2} \left(\frac{RZ^2}{\nu} \right) + 1 \right]$$

(8.2-35)

where

$$\nu = R \left(\frac{1}{(n')^2} - \frac{1}{n^2} \right)$$

* This expression is not valid when $n = n'$.

and $R = 2\pi^2 e^4 m/h^3$ is the Rydberg frequency. If this line oscillator strength is "smeared" over the regions between the lines it can be seen that the effective oscillator strength per unit frequency interval $\frac{df}{d\nu}$, approximately has a ν^{-3} principal dependence just as in the bound-free and free-free cases. We can show this by converting the f -number sum over a finite number of lines to an integral by use of the Euler-Maclaurin theorem* (Franklin, 1940).

Summing of Hydrogenic Line f -numbers Near the Ionization Edge:

We recall that for hydrogen

$$h\nu_{mn} = \text{Ryd} \left(\frac{1}{n^2} - \frac{1}{m^2} \right). \quad (8.2-36)$$

$h\nu_{mn}$ is the energy absorbed or emitted in the transition from a state with principal quantum number n to a state with principal quantum number m . Ryd is 13.6 eV.

The ionization energy is ($m \rightarrow \infty$) $h\nu_0 = \frac{\text{Ryd}}{n^2}$, which enables us to write

$$m = n \left(\frac{\nu_0}{\nu_0 - \nu_m} \right)^{1/2}. \quad (8.2-37)$$

The asymptotic f -number per electron from Eq. (8.2-34) can also be written as ($\zeta = 2^5/3/3\pi$):

$$f_{mn} = \zeta n \left(\frac{m}{m^2 - n^2} \right)^3. \quad (8.2-38)$$

* From unpublished material by J.D. Weisner.

Consider

$$\sum_{m=M}^{\infty} f_{mn} = \zeta_n \sum_M \left(\frac{m}{m^2 - n^2} \right)^3 .$$

By use of the Euler-Maclaurin formula (Franklin, 1940):

$$\sum_M f(m) = \int_M^{\infty} f(x) dx + \frac{1}{2} f(M) - \frac{1}{12} f'(M) + \frac{1}{720} f'''(M) + \dots, \quad (8.2-39)$$

we obtain

$$\sum_M f_{mn} = \zeta_n \left\{ \frac{2M^2 - n^2}{4(M^2 - n^2)^2} + \frac{1}{2} \left(\frac{M}{M^2 - n^2} \right)^3 + \frac{1}{4} \frac{M^2(M^2 + n^2)}{(M^2 - n^2)^4} + \dots \right\} . \quad (8.2-40)$$

We will denote $\sum_M f_{mn}$ by simply \sum_O when convenient. If we rewrite Eq. (8.2-40) in terms of v_O and v_M , we obtain

$$\begin{aligned} \sum_O = \zeta_n \left\{ \frac{1}{4n^2} \left(\frac{v_O^2 - v_M^2}{v_M^2} \right) + \left(\frac{1}{2n^3} \right) \frac{v_O^{3/2} (v_O - v_M)^{3/2}}{v_M^3} + \right. \\ \left. + \frac{1}{4n^4} \frac{v_O (v_O - v_M)^2 (2v_O - v_M)}{v_M^4} + \dots \right\} . \end{aligned} \quad (8.2-41)$$

Neglecting the "overflow" of line strength below v_M or past v_O , this expression gives the total f-number between v_M and v_O . We wish to obtain a function $\frac{dF}{dv}$ such that

$$\int_{v_M}^{v_O} \frac{dF}{dv} dv = \sum_M f_{mn} . \quad (8.2-42)$$

This will be the continuation of the photoelectric f-number per unit frequency interval. By differentiating Eq. (8.2-42) (a function of ν_M), the following result is obtained:

$$\text{Let } \frac{d}{d\nu_M} \sum_0 = \frac{dF^{(0)}}{d\nu} \quad (8.2-43a)$$

$$\begin{aligned} \text{Then } \frac{dF^{(0)}}{d\nu} = \frac{c}{n} \left\{ \frac{1}{2} \frac{\nu_0^2}{\nu^3} + \frac{\nu_0^{3/2}}{2n} \left[\frac{3(\nu_0 - \nu)^{3/2}}{\nu^4} + \frac{3}{2} \frac{(\nu_0 - \nu)^{1/2}}{\nu^3} \right] + \right. \\ \left. + \frac{\nu_0}{4n^2} \frac{(\nu_0 - 2)(8\nu_0 - 7\nu\nu_0 + \nu^2)}{\nu^5} + \dots \right\} \quad (8.2-43b) \end{aligned}$$

or, in terms of $x = \nu/\nu_0 = 1 - n^2/m^2$,

$$\frac{dF^{(0)}}{dx} = \frac{c}{2n} \left\{ \frac{1}{x^3} + \frac{3}{2n} \frac{(1-x)^{1/2} (1-x/2)}{x^4} + \frac{1}{2n^2} \frac{(1-x)(8-7x+x^2)}{x^5} + \dots \right\} \quad (8.2-44)$$

This expression is an expansion around $x = 1$, in powers of $(1 - x)$; the second term is exceptional; the next term contains $(1 - x)^2$.

Convergence is, of course, most rapid for x close to 1, i.e., m large. Actually the series is asymptotic in $\frac{1}{m}$. The leading term is just the extension of the photoelectric formula (with Gaunt factor put equal to 1). The function (Eq. (8.2-44)) is plotted in Figs. 8-7, 8-8, and 8-9 for various values of n . The dotted lines correspond to the lowest order term of Eq. (8.2-44), and the solid line is the total.

The foregoing discussion, though overapproximate, provides much physical insight to the problem. Corrections may be added as follows. The deficiency arises in the fact that the bound-bound Gaunt factor which was set equal to 1 in Eq. (8.2-38) has terms in its asymptotic expansion which are of the same order in n as the first and subsequent correction terms which we have obtained to the leading term in Eq. (8.2-44). As will be seen in the following discussion, these act to cancel part of the higher term contribution of the expansion and, hence, cause $\frac{dF}{dv}$ to approach closer to the simple $\frac{1}{v^3}$ behavior of the first term of Eq. (8.2-44).

Summing of Hydrogenic Line f-numbers, Including the Gaunt Factor Correction:

If Eq. (8.2-36) is used to express $h\nu$ in terms of n and m , and g as given by Eq. (8.2-35) is multiplied into Eq. (8.2-38), the result is

$$f_{mn} = \frac{\zeta n m^3}{(m^2 - n^2)^3} \left[1 - 0.1728 z^{2/3} \left(\frac{2m^{4/3}}{(m^2 - n^2)^{2/3}} - \frac{(m^2 - n^2)^{1/3}}{m^{2/3} n^{2/3}} \right) \right]. \quad (8.2-45)$$

We now set

$$f(x) = \frac{x^{13/3}}{(x^2 - n^2)^{11/3}} ; \quad g(x) = \frac{x^{7/3}}{(x^2 - n^2)^{8/3}} . \quad (8.2-46)$$

Use can again be made of the Euler-Maclaurin formula if the integrals of $f(x)$ and $g(x)$ can be evaluated.

Consider the integral of $f(x)$:

$$\int_M^{\infty} \frac{x^{13/3} dx}{(x^2 - n^2)^{11/3}} = \frac{1}{n^2} \int_{M/n}^{\infty} \frac{y^{13/3} dy}{(y^2 - 1)^{11/3}} \quad (8.2-47)$$

where $y = x/n$.

Substitute $\frac{n}{x} = \frac{1}{y} = \cos \theta$, and

$$\int_M^{\infty} f(x) dx = \frac{1}{n^2} \int_{\theta_0}^{\pi/2} \frac{\cos \theta d\theta}{(\sin \theta)^{19/3}}$$

with the lower limit θ_0 given by $\cos \theta_0 = \frac{n}{M}$.

Integration yields

$$\int_M^{\infty} f(x) dx = \frac{3}{16} \frac{1}{n^2} \left[\left(\frac{M^2}{M^2 - n^2} \right)^{8/3} - 1 \right] \quad (8.2-48)$$

Further, by differentiating $f(x)$,

$$f'(x) = \frac{13}{3} \frac{x^{10/3}}{(x^2 - n^2)^{11/3}} - \frac{22}{3} \frac{x^{16/3}}{(x^2 - n^2)^{14/3}} \quad (8.2-49)$$

Similarly

$$\int_M^x g(x) dx = \frac{3}{10} \frac{1}{n^2} \left[\left(\frac{M^2}{M^2 - n^2} \right)^{5/3} - 1 \right], \quad (8.2-50)$$

and

$$g'(x) = \frac{7}{3} \frac{x^{4/3}}{(x^2 - n^2)^{8/3}} - \frac{16}{3} \frac{x^{10/3}}{(x^2 - n^2)^{11/3}}. \quad (8.2-51)$$

We now insert Eqs. (8.2-46), (8.2-48), (8.2-49), (8.2-50), and (8.2-51) into formula (Eq. (8.2-39)) (retaining thereby the terms up to and including the first derivative). The result is, after some simplification,

$$\begin{aligned} \Sigma - \Sigma_0 + 0.1728 z^{-2/3} n^{1/3} \zeta & \left[-\frac{3}{8n^2} \left(\frac{M^2}{M^2 - n^2} \right)^{8/3} + \right. \\ & + \frac{3}{40n^2} + \frac{7}{6} \frac{M^{10/3}}{(M^2 - n^2)^{11/3}} - \frac{M^{13/3}}{(M^2 - n^2)^{11/3}} - \frac{11}{9} \frac{M^{16/3}}{(M^2 - n^2)^{14/3}} + \\ & \left. + \frac{3}{10} \frac{1}{n^2} \frac{M^2}{M^2 - n^2}^{5/3} + \frac{1}{2} \frac{M^{7/3}}{(M^2 - n^2)^{8/3}} - \frac{7}{36} \frac{M^{4/3}}{(M^2 - n^2)^{8/3}} \right], \quad (8.2-52) \end{aligned}$$

where Σ_0 is given by Eq. (8.2-40). If we now make use of Eq. (8.2-37) and its variants:

$$\frac{M^2}{M^2 - n^2} = \frac{v_0}{v_M}; \quad M^2 - n^2 = n^2 \frac{v_M}{v_0 - v_M},$$

we obtain after some more algebra,

$$\begin{aligned} & \Sigma - \Sigma_0 + 0.1728 z^{-2/3} n^{1/3} \left[\frac{1}{n^2} \left(\frac{3}{40} - \frac{3}{8} \left\{ \frac{v_0}{v_M} \right\}^{8/3} + \frac{3}{10} \left\{ \frac{v_0}{v_M} \right\}^{5/3} \right) + \right. \\ & \left. + \frac{(v_0 - v_M)^{3/2}}{n^3} \left(\frac{v_0^{7/6}}{2v_M^{8/3}} - \frac{v_0^{13/6}}{v_M^{11/3}} \right) + \frac{(v_0 - v_M)^2}{n^4} \left(\frac{7}{6} \frac{v_0^{5/3}}{v_M^{11/3}} - \frac{11}{9} \frac{v_0^{8/3}}{v_M^{14/3}} - \frac{7}{36} \frac{v_0^{2/3}}{v_M^{8/3}} \right) \right]. \end{aligned} \quad (8.2-53)$$

Note that the first term is essentially (i.e., to within the factor $n^{1/3}$) of the same order as the first correction term in Eq. (8.2-41).

If we now differentiate Eq. (8.2-53) with respect to v_M , and set $\frac{v_M}{v_0} = x$ again, we obtain

$$\begin{aligned} \frac{dF}{dx} = \frac{dF^{(0)}}{dx} - 0.1728 n^{1/3} & \left[\frac{x^{1/3}}{n^2} \left(x^{-4} - \frac{1}{2} x^{-2} \right) + \right. \\ & \frac{1}{n^3} x^{1/3} (1-x)^{1/2} \left(\frac{7}{12} x^{-3} - \frac{7}{2} x^{-4} + \frac{11}{3} x^{-5} \right) \\ & \left. + \frac{1}{n^4} (1-x)x^{1/3} \left(-\frac{7}{54} x^{-3} + \frac{133}{54} x^{-4} - \frac{407}{54} x^{-5} + \frac{154}{27} x^{-6} \right) \right]. \end{aligned} \quad (8.2-54)$$

(The third derivative in the Euler-Maclaurin formula (Eq. (8.2-39)) will have as lowest terms those of order $1/n^6$).

Calling the term of order n^{-2} in the brackets $\frac{dF^{(2)}}{dx}$, that of order n^{-3} , $\frac{dF^{(3)}}{dx}$, etc., the numerical results of Table 8.6 are obtained for the case $n = 3$:

Table 8.6

x	$\frac{dF^{(0)}}{dx}$	$\frac{dF^{(2)}}{dx}$	$\frac{dF^{(3)}}{dx}$	$\frac{dF^{(4)}}{dx}$	$\frac{dF}{dx}$
1.0	0.33	-.0271	0	0	0.30
0.9	0.50	-.04728	-.0027	-.00085	0.45
0.8	0.77	-.0836	-.0091	-.0050	0.67
0.7	1.30	-.1512	-.0267	-.0131	1.11
0.6	2.40	-.2885	-.0788	-.0884	1.94
0.5	5.35	-.600	-.248	-.337	4.17

Line f-number sum per unit (reduced) frequency interval for principal quantum number $n = 3$. The reduced frequency x is given by ν/ν_0 where ν_0 is the ionization, or photoelectric edge frequency. The f-number sum is given by $F = \sum_{m=M(x)}^{\infty} f_{m3}$, and the superscripts appended to $\frac{dF}{dx}$ for the various columns give the terms of that order in powers of the quantum number n of the lower state (here $n = 3$). The last column is the sum of all the terms calculated.

8.2.4 Coherent scattering from bound systems

As has already been implied in our brief classical introduction (Eqs. 3.1-14, 3.1-15), when light scatters off an atom, the scattering is termed "Rayleigh scattering" if the photon frequency ν is below the atomic resonance (or "line") frequencies, and it is termed "Thomson scattering", or "Compton scattering from bound electrons" if the frequency ν is above the resonance frequencies and below the photoelectric thresholds. As one approaches the bound-bound resonances from either direction in frequency, the scattering processes pass continuously into the processes of simultaneous absorption and re-emission of a photon. This has been touched on qualitatively in Sec. 2.3 and is discussed by Heitler (1954) and Dirac (1947). Dirac (p. 206) shows explicitly by integration over a Lorentz profile that, "the total number of scattered particles in the neighborhood of an absorption line is equal to the total number absorbed." This supports the interpretation of resonance scattering as absorption followed by emission.

This has occasionally been overlooked in considering the problem (e.g., see Dalgarno, 1963; this oversight was corrected by Heddle, 1964). The basic formula for either coherent scattering process is the Kramers'-Heisenberg formula (Heitler, 1954):

$$\frac{d\sigma}{d\Omega} = r_0^2 \left[\frac{1}{m} \sum_i \left(\frac{\langle \vec{p} \cdot \vec{\epsilon}_0 \rangle_{n_i n_0} \langle \vec{p} \cdot \vec{\epsilon} \rangle_{n_0 n_i}}{E_0 - E_i + \hbar\omega_0} + \frac{\langle \vec{p} \cdot \vec{\epsilon}_0 \rangle_{n_0 n_i} \langle \vec{p} \cdot \vec{\epsilon} \rangle_{n_i n_0}}{E_0 - E_i - \hbar\omega_0} \right) + \vec{\epsilon}_0 \cdot \vec{\epsilon}_i \right]^2 \quad (8.2-55)$$

The photon polarization vectors before and after the collision have been denoted by $\vec{\epsilon}_0$ and $\vec{\epsilon}$, respectively, \vec{p}_0 is the electron momentum operator, E_i and E_0 are the energies of the intermediate and initial states, respectively. The photon energy is $\hbar\omega_0$, and the initial and intermediate states have been designated n_0 and n_i , respectively. r_0 is e^2/mc^2 , the classical electron radius. Because of the difficulties of evaluating this formula for real, many-electron atoms, and because of the relative smallness of the magnitude of the effect, it has been customary in opacity calculations to approximate the effect very severely. Mayer (1947) suggested merely assigning the Compton scattering cross section $\frac{8\pi}{3} r_0^2$ to all the bound electrons in the atom as an estimate of the total coherent scattering (this Compton cross section is the dimensional factor appearing in the Kramers-Heisenberg formula to within the angular factor $8\pi/3$). Mittleman and Wolf (1962) have shown that the Kramers-Heisenberg formula for the differential scattering cross section for hydrogen can be reduced to

$$\frac{d\sigma}{d\Omega} = r_0^2 (\vec{\epsilon}_0 \cdot \vec{\epsilon})^2 [1 - P(k) - P(-k)]^2 \quad (8.2-56)$$

where $P(k)$ is a function of the photon momentum magnitude k which can be computed numerically by means of a differential equation. They present a graph of $P(k)$, as well as a graph of $[1 - P(k) - P(-k)]^2$ from which the differential cross section can be immediately obtained from Eq. (8.2-56). For opacity calculations, one is usually interested in unpolarized light. In this event, we need the average of $\vec{\epsilon}_0^{(i)} \cdot \vec{\epsilon}^{(i)}$ over the two possible initial

polarization directions (i) , and the sum over the two final polarization directions (j) . This computation can be performed as follows. There is complete azimuthal symmetry in this problem; if we choose the +y axis as the direction of the incident light we can therefore rotate the z-axis to lie in the scattering plane as shown in Fig. 8.10.

The scattering angle has been designated θ ; we are free to choose any orientation of the orthogonal initial $\vec{\epsilon}$'s we wish, and accordingly select them (as shown in Fig. 8.10) to be along the +z-axis and along the -x axis. The final $\vec{\epsilon}$'s must then lie relative to the axis we have chosen, as shown in the figure. From this figure it is clear that

$$\begin{aligned} \frac{1}{2} \sum_{ij} \vec{\epsilon}^{(i)} \cdot \vec{\epsilon}^{(j)2} &= \frac{1}{2} \left[(\vec{\epsilon}_1 \cdot \vec{\epsilon}_1^{(j)})^2 + (\vec{\epsilon}_1 \cdot \vec{\epsilon}_2^{(j)})^2 + (\vec{\epsilon}_2 \cdot \vec{\epsilon}_1^{(j)})^2 + (\vec{\epsilon}_2 \cdot \vec{\epsilon}_2^{(j)})^2 \right] \\ &= \frac{1}{2} \left[\cos^2 \varphi \cos^2 \theta + \sin^2 \varphi \cos^2 \theta + \sin^2 \varphi + \cos^2 \varphi \right] \\ &= \frac{1}{2} \left[\cos^2 \theta + 1 \right] \end{aligned} \tag{8.2-57}$$

From this result, the polarization-averaged differential cross immediately follows, and the total scattering cross section is easily obtained by integration over solid angle. The integral of $\frac{1}{2} (\cos^2 \theta + 1)$ over solid angle yields $8\pi/3$, the factor which multiplies r_0^2 in the total Compton cross section, so that the Mittleman-Wolf formula yields for the total cross section

$$\sigma = \frac{8\pi}{3} \left[1 - P(k) - P(-k) \right]^2$$

The total Rayleigh scattering cross section can be written in terms of the polarizability α of a gas by means of the equation

$$\sigma_R = \frac{128 \pi^5}{3 \lambda^4} |\alpha|^2, \quad (8.2-58)$$

Equivalently, it can be written in terms of f-numbers as

$$\sigma_R = \frac{8\pi}{3} r_o^2 \left| \sum \frac{\nu^2}{(\nu_{ij}^2 - \nu^2)} f_{ij} \right|^2 \quad (8.2-59)$$

where the sum is taken over all the transitions $i-j$. Since approximate f-numbers are available for most of the transitions in nitrogen and oxygen, improved estimates of the scattering cross sections can be obtained by means of this equation (Stergis, 1966). Alternatively, one might attempt to scale the results for hydrogen as given by Mittleman and Wolf (1962).

With the more detailed and accurate line broadening theory now available, the importance of scattering in high-temperature plasmas appears still further reduced over what one might estimate a priori. The reason is, as pointed out by Baranger (1962) that a photon can be absorbed in the far wing of a line (at a point where one might be considering Rayleigh scattering) by a transfer of energy and momentum to a free electron. For very modest concentrations of free electrons the cross section for this process dominates that for scattering.

Let us consider some crude numerical comparisons of these effects. We restrict the discussion to the appropriate condition that $\nu_o - \nu \gg \gamma$,

where ν_0 is the resonance frequency at the center of a single isolated line and γ is its full half width. We can approximate the Baranger absorption cross section as

$$\sigma_B = \frac{hcr_f \gamma}{(\nu - \nu_0)^2}$$

by means of the Lorentz formula neglecting the half-width as stated above. The f-number of the line has been designated as simply f , and the half-width can be approximated as (Stewart and Pyatt, 1961)

$$\gamma = \frac{8\pi^2}{z^2} e^2 \alpha a_0^2 \left(\frac{mc^2}{2\pi kT} \right)^{1/2} n^4 \rho$$

where ρ is the density, α is the fine-structure constant and n is the principal quantum number of the upper level involved in the line transition. From Eq. (8.2-57) we obtain the Rayleigh scattering cross section as

$$\sigma_R = \frac{8\pi}{3} r_0^2 \frac{\nu^4}{(\nu_0^2 - \nu^2)^2} f^2$$

Now in order to observe Rayleigh scattering we must have

$$\sigma_R > \sigma_B$$

From the foregoing formulas for σ_R and σ_B , this yields an upper limit

$$\rho < \rho_c$$

to the density in order that Rayleigh scattering be observed. For a line with

$$n = 4, Z = 1,$$

$$\rho_c \sim 10^{11} \frac{\nu^4 f}{(\nu_0 + \nu)^2} (kT)^{1/2},$$

where ν_0 and kT are expressed in eV. If we assume an t -number $f = 0.1$, $kT = 1$ eV, a line position ν_0 at 5 eV, and a density $\rho = 10^9$, say, we find that below a frequency $\nu \sim 1$ eV on the line wing, only Baranger absorption will be observed, above this, Rayleigh scattering will be observable up to the point where it cannot be differentiated from absorption/re-emission, as shown in Fig. 8.11. On the other hand, by taking $\nu = \nu_0$ we find that for $\rho \sim 6 \times 10^{10} \text{ cm}^{-3}$, no Rayleigh scattering at all should be observable.

In low-temperature applications such as terrestrial atmospheric problems, where there is little or no free electron concentration, it has traditionally sufficed to simply use the classical formula, Eq. (3.1-15) for most problems.

8.2.5 Compton Scattering Cross Sections

Although Compton scattering is not really part of any hydrogenic model it is included in our discussion at this point for convenience and because of the fact that the accuracy of the results with which we concern ourselves is comparable to the accuracy of the hydrogenic model.

The simplest approximate method to treat scattering, and the method most commonly used in practice, is to set the absorption coefficient due to scattering equal to

$$\mu_s(\nu) = N_e \sigma_T \quad (8.2-60)$$

as mentioned in the previous section. We recall that $\sigma_T = \frac{8\pi}{3} r_0^2 = \frac{8\pi}{3} \left(\frac{e^2}{m_0 c^2} \right)^2$ is the total Thomson classical electron cross section, and is independent of frequency.

N_e is the number density of free electrons. This is a valid approximation to the correct Klein-Nishina (Heitler, 1954) quantum mechanical cross section as long as $h\nu$ and kT are small compared to mc^2 , which is the region of primary interest to us.

Eq. (8.2-60) correctly gives the absorption out of a beam due to scattering of radiation by free electrons, in the above approximation. In the transfer equation, one must, of course, include all terms which correspond to radiation being emitted back into the beam, as well as those which correspond to radiation taken out of the beam. For true absorption processes (bound-free, free-free, bound-bound) in LTE, the emission back into the beam is simply related to the absorption out of the beam (Kirchoff's law). One

part of the emission back into the beam is isotropic, and the other (induced) part is in the same direction as the incident beam, so that no angular integrations involving these terms need appear in the transfer equation to account for transfer back into the beam from other directions. For these and other reasons the transfer equation for true absorption processes reduces in the presence of LTE to a simplified form that can be expressed in terms of a modified or effective absorption coefficient $\mu'(\nu)$ given by

$$\mu'(\nu) = \mu(\nu) (1 - e^{-h\nu/kT}) \quad (8.2-61)$$

This situation does not prevail in the case of scattering (Mayer, 1947; see also Chapter 3). The scattering cross sections are not generally isotropic, so that the intensity scattered back into the beam in a given direction depends on the intensity of the beam in other than that given direction. Thus, the intensity scattered into the beam in a given direction must remain in integral form in the transfer equation, and there is no simple relation between scattering "emission" and scattering "absorption", viz., there is no Kirchoff's law for scattering. The intensity scattered out of the beam and the intensity scattered into the beam cannot be combined in a general way, as can the corresponding intensities for true emission and absorption, to yield a simple effective absorption coefficient of the form of Eq. (8.2-61). This is true regardless of the behavior of induced scattering as the simple modification $1 - e^{-h\nu/kT}$ expressed in Eq. (8.2-61) arises purely from terms linear in the intensity. That is to say for true absorption and emission, both the absorption and the induced emission are linear in the intensity. This is not the case for scattering; induced scattering

is quadratic in the intensity function. Therefore induced scattering into and out of the beam could not lead to a simple modification of the $1 - e^{-hv/kT}$ form. It turns out, fortunately enough, that at low frequencies where the Thomson cross section is valid, the induced scattering (in and out) terms exactly cancel. This was shown by Mayer (1947), who also showed that the proper form of the absorption coefficient to enter the Rosseland mean under conditions of LTE is

$$\mu(\nu) = \mu'(\nu)_{\text{abs}} + \mu(\nu)_{\text{scat}} \quad (8.2-62)$$

(cf our discussion of this topic in sections 2.3 and 3.2.2.4)
in the low-frequency Thomson limit.

More recently, Sampson (1959) has shown that for the Klein-Nishina formula, which must be used when $h\nu \sim mc^2$, this cancellation of induced scattering terms no longer occurs, and other terms appear as well, so that the effective $\mu_{\text{scat}}(\nu)$ that enters the Rosseland mean calculation is no longer $N_e \sigma_T$, nor is it in fact $N_e \sigma_T$ (Klein-Nishina), but is a complicated function of the Klein-Nishina differential cross section. He has performed numerical calculations of the Rosseland mean opacity for Compton scattering alone based on the effective absorption coefficient which he derives. We reproduce his graph in Fig. 8-12 of the Rosseland Opacity as a function of kT and $\frac{\rho Z}{M}$, where ρ is the density (gm/cm^3), Z is the atomic number, and M the atomic weight. He has assumed that the material is completely ionized, i.e., that

$$N_e = A \rho Z / M \quad (A = \text{Avogadro's number})$$

and has also included the effects of electron-positron pair formation.

Sampson has also made an interesting comparison of his results for the Rosseland mean opacity with the results one would obtain from a naive use of the Klein-Nishina formula. He recovers a "Rosseland mean cross section" $\bar{\sigma}_{RM}(T)$ from the computed value of the Rosseland mean opacity according to:

$$\bar{\sigma}_{RM}(T) = \frac{\rho \kappa_c(T)}{N} \quad , \quad (8.2-63)$$

where N is the number density of scattering electrons (and positrons). In units of σ_T , the Thomson cross section, this can be written

$$\frac{\bar{\sigma}_{RM}(T)}{\sigma_T} = \frac{\rho \kappa_c(T)}{N\sigma_T} \quad (8.2-64)$$

Sampson gives values of this ratio derived from opacities κ_c computed by naive use of the Klein-Nishina cross section, and by use of the effective Klein-Nishina cross section which he derives (as appropriate for the diffusion approximation). In Fig. 8-13 we plot his results as a function of temperature, T . His corrected values drop substantially lower towards high temperature than the values obtained by uncorrected use of the Klein-Nishina formula. Values of the Rosseland mean opacity for scattering alone can, of course, be recovered from the figure by inverting Eq. (8.2-64) and substituting values of $\frac{\bar{\sigma}_{RM}(T)}{\sigma_T}$ from the figure. Simple use of the Thomson formula, as discussed in the preceding section, would correspond to the value unity in the figure.

8.3 Analytic formulas and approximations to hydrogenic absorption coefficients

8.3.1 The Rosseland-Menzel-Pekeris Formula

Relatively simple analytic formulas can be obtained, from the hydrogenic approximation, for the total spectral absorption and also for the mean coefficients of atomic species which behave hydrogenically. This can be done by such techniques as approximating the sum over discrete states by integrals, by using the Saha equation (perhaps restricted to two states of ionization) to evaluate the occupation numbers, and noting the close relation between the expressions for the bound-free and free-free cross sections. Menzel and Pekeris (1935) derive the approximate formula for the combination of bound-free and free-free absorption coefficients:

$$\mu(\nu) = \frac{C_0 Z^2 N_e N_i}{\nu^3 (kT)^{1/2}} g' \quad (8.3-1)$$

where $C_0 = \frac{2^4 \pi^2 e^6}{3^3 ch (2\pi m)^{3/2}}$, N_e is the electron concentration in electrons/cm³, N_i is the number density of ions*. The effective Gaunt factor g' is given by

$$g' \approx 1 - 0.1728 \left(\frac{\nu}{RZ^2} \right)^{1/3} \left(1 - \frac{2kT}{h\nu} \right) \quad (8.3-2)$$

(Recall that $R = 2\pi^2 e^4 m/h^3$ is the Rydberg in frequency units.) This formula can be integrated to yield a Rosseland mean absorption coefficient

$$\bar{\mu}_R = \frac{C_0 h^3 Z^2 N_e N_i}{(kT)^{7/2}} \theta g_R' \quad (8.3-3)$$

* Recall that in the presence of single ionization only, the product $N_e N_i$ is proportional to N_0 , the neutral number density, through the Saha equation.

where θ is a complicated numerical function defined and evaluated by Menzel and Pekeris. Numerically, Eq. (8.3-3) is

$$\bar{\mu}_R = \frac{4.58 \times 10^{-23} Z^2 N_e N_1}{T^{7/2}} \left[1 - 0.1098 \left(\frac{T}{1.57 \times 10^5 Z^2} \right)^{1/3} \right] \text{ (cm}^{-1}\text{)} \quad (8.3-4)$$

with T in $^{\circ}\text{K}$. The bracketed expression is g_R' .

Except for the correction factor g_R' due to their use of Gaunt factors this formula is the same as an earlier one due to Rosseland. Their extensive discussion of the approximations involved indicates that under the proper circumstances, it is a very useful approximation. Expressions of this sort have been used more recently by various authors (see, e.g., Raizer, 1960; Pappert and Penner, 1961; Penner and Thomas, 1964; Stewart and Pyatt, 1961; Bond, Watson, and Welch, 1965, Sec. 11-4.2; Unsold, 1955, Sec. 47; Ashley, 1964) who show that they can be made to reproduce the gross features of the detailed monochromatic hydrogenic absorption coefficients rather well. However, they should be used with caution. Over such fine spectral regions as considered by Ashley (1964) for example, the resultant re-distribution of oscillator strength can be quite violent.

Stewart and Pyatt (1961) on the basis of such a method derive the result for the continuum Rosseland mean opacity, κ_R

$$\kappa_R \approx 1.15 \frac{\langle Z^2 \rangle}{M} \left[\frac{Ryd}{kT} \right]^2 \frac{h^3 N_e}{2(2\pi m kT)^{3/2}} \left\{ \frac{64\pi}{3} \frac{1}{137} \frac{a_0^2}{M_1} \right\} \quad (8.3-5)$$

In this formula, M is the atomic mass number, M_1 is the atomic mass unit, $\langle Z^2 \rangle$ the mean ionic charge, N_e the number density of free

electrons, and the bracketed $\{ \}$ quantity has the value $4.76 \times 10^6 \text{ cm}^2/\text{gm}$. They compared the values predicted by this formula (using accurate $\langle Z^2 \rangle$ values from their detailed occupation-number calculation) with the continuum Rosseland mean results of Armstrong (1959). At temperatures $kT = 5$ and 10 eV the two results agree to within 30% over the entire density range covered by the Armstrong calculations. At $kT = 2$ and 20 eV , the agreement deteriorates towards high densities but remains within an order of magnitude. Thus, as far as continuum means are concerned this equation provides a quick and simple order-of-magnitude estimate. Unfortunately when line absorption is included these methods break down; they also, of course, will break down whenever the hydrogenic approximation breaks down.

8.3.2 The Strömgen Function

Because of the ν^3 frequency dependence of the Kramers radiation absorption cross sections, Strömgen was able to devise a very convenient and quick method for computing Rosseland mean absorption coefficients. We present this method here as outlined by Mayer, including Mayer's table of the Strömgen function. We write the Rosseland expression from Chapter 2 (Eq. (2.5-6)), in terms of the mean free path $(\bar{\mu}_R)^{-1} = \Lambda_R$ as

$$\Lambda_R = \Lambda_0 \int_0^\alpha \frac{Z(u) du}{D(u)} \quad (8.3-6)$$

where we incorporate the ν^{-3} dependence of the cross sections into the weighting function Z and define the reduced absorption coefficient $D(u)$

as

$$D(u) = \Lambda_0 u^3 \mu_c(\nu) \quad (8.3-7)$$

where $\mu_c(\nu)$ is the continuous part of the usual absorption coefficient in cm^{-1} , $u = h\nu/kT$, and the universal length Λ_0 , given by

$$\Lambda_0^{-1} = \frac{2^4}{3^3} \frac{h^2}{mc} \frac{\rho_N}{kT} \quad (8.3-8)$$

has been defined in order to make the expressions simple and dimensionless.

In the definition Eq. (8.3-8), ρ_N is the total particle number density.

Numerically Λ_0 can be expressed as

$$\Lambda_0^{-1} = \left(\frac{64}{3^3} \cdot \frac{2}{hc} \cdot \pi e_0^2 \right) \left(\frac{\text{Ryd}}{kT} \right) \rho_N = 0.790 \times 10^{-17} \text{ cm}^2 \times \left(\frac{\text{Ryd}}{kT} \rho_N \right)$$

or

$$= 4.762 \times 10^6 \frac{\text{cm}^2}{\text{gm}} \times \left(\frac{\text{Ryd}}{kT} \right) (\rho_N M_Y) \quad (8.3-9)$$

The weighting function $Z(u)$ differs from the Rosseland weighting function $W(u)$ only by the factor u^3 ; viz.,

$$Z(u) = W(u) u^3 = \frac{15}{4\pi^4} u^7 e^{-2u} (e^u - 1)^{-3} \quad (8.3-10)$$

Since the function $W(u)$ is of considerable utility in opacity calculations, we give in Table 8-7, values of $W(u)$ for a wide range of the argument u .

Rough values of a Rosseland mean can often be obtained simply by inspection of the value of the absorption coefficient in the region of u where the function $W(u)$ has its maximum.

Table 8 - 7

The Rosseland Weighting Function $W(u) = \frac{15}{4\pi^4} \frac{u^4 e^{-2u}}{(e^u - 1)^3}$

u	W(u)	u	W(u)	u	W(u)
0.0	0.000000	4.3	1.660538-01	8.0	3.679122-02
0.1	4.642070-03	4.4	1.638407-01	8.7	3.675906-02
0.2	8.406623-03	4.5	1.613474-01	8.8	3.461513-02
0.3	1.326629-02	4.6	1.785958-01	8.9	3.295712-02
0.4	1.643641-02	4.7	1.756077-01	9.0	3.118264-02
0.5	2.595647-02	4.8	1.724051-01	9.1	2.948925-02
0.6	2.981178-02	4.9	1.690096-01	9.2	2.787444-02
0.7	3.597826-02	5.0	1.654428-01	9.3	2.633569-02
0.8	4.243062-02	5.1	1.617254-01	9.4	2.487645-02
0.9	4.913914-02	5.2	1.578779-01	9.5	2.347615-02
1.0	5.607090-02	5.3	1.539197-01	9.6	2.215025-02
1.1	6.319013-02	5.4	1.498700-01	9.7	2.089022-02
1.2	7.045058-02	5.5	1.457466-01	9.8	1.969352-02
1.3	7.783596-02	5.6	1.415669-01	9.9	1.855767-02
1.4	8.528045-02	5.7	1.373471-01	1.0	1.748023-02
1.5	9.274922-02	5.8	1.331026-01		
1.6	1.001989-01	5.9	1.288477-01		
1.7	1.075861-01	6.0	1.245958-01	10.2	1.549095-02
1.8	1.148679-01	6.1	1.203595-01	10.4	1.370702-02
1.9	1.220025-01	6.2	1.161501-01	10.6	1.211064-02
2.0	1.289495-01	6.3	1.119792-01	10.8	1.068499-02
2.1	1.356702-01	6.4	1.078534-01	11.0	9.414257-03
2.2	1.421284-01	6.5	1.037643-01	11.5	6.821045-03
2.3	1.482904-01	6.6	9.977668-02	12.0	4.904922-03
2.4	1.541254-01	6.7	9.584355-02	12.5	3.502651-03
2.5	1.596056-01	6.8	9.198502-02	13.0	2.485313-03
2.6	1.647666-01	6.9	8.820843-02	13.5	1.753050-03
2.7	1.694079-01	7.0	8.451643-02	14.0	1.229769-03
2.8	1.736917-01	7.1	8.091892-02	16.0	2.839236-04
2.9	1.775441-01	7.2	7.741316-02	18.0	6.154921-05
3.0	1.809550-01	7.3	7.400383-02	20.0	1.269590-05
3.1	1.839173-01	7.4	7.069300-02	22.0	2.515622-06
3.2	1.864277-01	7.5	6.748221-02	24.0	4.821816-07
3.3	1.884859-01	7.6	6.437253-02	26.0	8.988146-08
3.4	1.900946-01	7.7	6.136455-02	28.0	1.636138-08
3.5	1.912596-01	7.8	5.845648-02		
3.6	1.919891-01	7.9	5.565410-02		
3.7	1.922940-01	8.0	5.295090-02		
3.8	1.921873-01	8.1	5.034603-02		
3.9	1.916837-01	8.2	4.784436-02		
4.0	1.907999-01	8.3	4.543852-02		
4.1	1.895540-01	8.4	4.312693-02		
4.2	1.879653-01	8.5	4.091382-02		

With the definitions given in Eqs. (8.3-7) and (8.3-6), the Kramers' D-function becomes

$$D_{bf}(u) = \sum_n P_n \frac{I_n^2}{(kT)^2} \frac{g_{bf}^{(n)}(u)}{n} \quad (8.3-11)$$

where $P_n = \frac{N_n}{n}$ is the fractional occupation number of state n^* . We limit ourselves now to constant Gaunt factors $g_{bf}^{(n)}$ (taken, e.g., to be threshold values). With this limitation, and the further definition

$$D_{Rf}(u) = \sum_{u_1=0}^{u_j} D(u_1), \quad (8.3-12)$$

where

$$D(u_1) = P_1 \left(\frac{I_1}{kT} \right)^2 \frac{g_{bf}^{(1)}}{1} \quad \begin{array}{l} u \geq u_1 = I_1/kT \\ \\ = 0 \quad \quad \quad u < u_1 \end{array} \quad (8.3-13)$$

the Rosseland mean for bound-free absorption (only) becomes

$$\Lambda_R = \Lambda_0 \int_0^\infty \frac{Z(u) du}{\sum_{u_1=0}^u D(u_1)} \quad (8.3-14)$$

Each of the $D(u_1)$'s is a step function beginning at u_1 (and zero prior to u_1), and $D_{Rf}(u)$ is the sum of these step functions over the range 0 to u of u_1 . Therefore, between each step $D_{Rf}(u)$ is constant, and we can perform the integration of Eq. (8.3-14) step-by-step:

* And each term in the sum contributes only for $u_1 > \frac{I_u}{kT}$.

$$\Lambda_R = \Lambda_0 \sum_j \frac{1}{D(u_{j+})} \int_{u_j}^{u_{j+1}} Z(u) du$$

$$= \Lambda_0 \sum_j \frac{S(u_{j+1}) - S(u_j)}{D(u_{j+})} \quad (8.3-15)$$

where $S(u) = \int_0^u Z(u) du$ is the Strömgen function, and we have used the notation u_{j+} to indicate that the D function of argument u_{j+} is to be evaluated past the j^{th} -edge (i.e., larger u) for inclusion in the denominator when the Strömgen-function numeration is $S(u_{j+1}) - S(u_j)$.

Table 8-8 (taken from H. Mayer, 1947) lists values of S and Z as functions of u . The method outlined above is very useful for obtaining approximate results quickly, particularly if many of the absorption edges can be lumped together. For heuristic simplicity we have illustrated this method for the bound-free case only. It can, of course, be simply extended to include the Kramers free-free cross section, since the latter also varies as ν^{-3} . It cannot, however, be generalized to include bound-bound transitions (except for merged lines) without a radical departure from the use of the Strömgen function. Although the line f -number strength, as we have seen, approximates a ν^{-3} dependence when smeared over the region between the lines, unless they are completely merged together, the sum of the actual line profiles yields a frequency dependence of widely-varying ν dependence.

Table 8-8

The Function $Z(u) = \frac{15}{4\pi^4} \frac{u^7 e^{2u}}{(e^u - 1)^3}$ and its Integral

the Strömgen Function $S(u) = \int_0^u Z(u) du$ (from Mayer (1947)).

u	Z(u)	S(u)	u	Z(u)	S(u)
0.0	0	0	3.5	8.2003	6.2881
.1	4.042×10^{-6}	8.015×10^{-8}	3.5	8.9572	7.1469
.2	6.773×10^{-5}	2.669×10^{-6}	3.7	9.7404	8.0819
.3	3.582×10^{-4}	2.103×10^{-5}	3.8	10.546	9.0957
.4	1.180×10^{-3}	9.185×10^{-5}	3.9	11.371	10.1902
.5	2.995×10^{-3}	2.902×10^{-4}	4.0	12.211	11.3676
.6	6.440×10^{-3}	7.454×10^{-4}	4.1	13.064	12.6309
.7	.012339	1.660×10^{-3}	4.2	13.926	13.9808
.8	.021726	3.351×10^{-3}	4.3	14.793	15.4174
.9	.035822	6.170×10^{-3}	4.4	15.660	16.9409
1.0	.05607	1.071×10^{-2}	4.5	16.525	18.5793
1.1	.08410	1.765×10^{-2}	4.6	17.384	20.2478
1.2	.12175	2.787×10^{-2}	4.7	18.232	22.0290
1.3	.17101	4.214×10^{-2}	4.8	19.067	23.8940
1.4	.23401	6.257×10^{-2}	4.9	19.884	25.8403
1.5	.31303	8.981×10^{-2}	5.0	20.681	27.8664
1.6	.41042	.1258	5.1	21.453	29.9725
1.7	.52859	.1724	5.2	22.199	32.1510
1.8	.67064	.2313	5.3	22.915	34.4014
1.9	.83681	.3066	5.4	23.599	36.7225

Table 8-8 (continued)

u	Z(u)	S(u)	u	Z(u)	S(u)
2.0	1.0316	.3994	5.5	24.249	39.1128
2.1	1.2564	.5129	5.6	24.861	41.5698
2.2	1.5134	.6502	5.7	25.436	44.0895
2.3	1.7970	.8144	5.8	25.970	46.6656
2.4	2.1307	1.009	5.9	26.463	49.2917
2.5	2.4940	1.238	6.0	26.913	51.9633
2.6	2.8948	1.505	6.1	27.319	54.6755
2.7	3.3344	1.815	6.2	27.682	57.4249
2.8	3.8128	2.173	6.3	28.000	60.2082
2.9	4.3302	2.582	6.4	28.273	63.0213
3.0	4.8857	3.048	6.5	28.502	65.8637
3.1	5.4791	3.568	6.6	28.686	68.7225
3.2	6.1087	4.1483	6.7	28.826	71.5978
3.3	6.7735	4.7923	6.8	28.923	74.4853
3.4	7.4715	5.5041	6.9	28.977	77.3810
7.0	28.991	80.2800	10.2	17.027	157.1759
7.1	28.961	83.1773	10.4	16.163	160.3624
7.2	28.895	86.0698	10.6	15.053	163.3490
7.3	28.789	88.9546	10.8	13.815	166.1404
7.4	28.646	91.8283			
7.5	28.470	94.6856	11.0	12.530	168.7424
7.6	28.258	97.5219	11.5	10.787	174.4525
7.7	28.016	100.3346	12.0	8.4757	179.1535
7.8	27.742	103.1223	12.5	7.0717	182.9749
7.9	27.439	105.8825	13.0	5.4602	186.0382

Table 8-8 (continued)

u	Z(u)	S(u)	u	Z(u)	S(u)
8.0	27.110	108.6119	13.5	4.4377	188.4766
8.1	26.757	111.3053	14.0	3.3745	190.3846
8.2	26.379	113.9608	15.0	2.0121	193.0267
8.3	25.981	116.5797	16.0	1.1629	194.5800
8.4	25.562	119.1587	18.0	.35896	195.9583
8.5	25.126	121.6939	20.0	.10157	196.3685
8.6	24.673	124.1825	22.0	.028787	196.4813
8.7	24.206	126.6251	24.0	.0066659	196.5103
8.8	23.726	129.0210	26.0	.0015798	196.5174
8.9	23.234	131.3691	30.0	.000071419	196.5194
9.0	22.732	133.6682	∞	0	196.5194
9.1	22.222	135.9163			
9.2	21.706	138.1127			
9.3	21.183	140.2571			
9.4	20.658	142.3499			
9.5	20.127	144.3881			
9.6	19.596	146.3742			
9.7	19.066	148.3066			
9.8	18.535	150.1856			
9.9	18.007	152.0119			
10.0	17.480	153.7856			

8.3.3 High Temperature Limiting Values of the Opacity

At sufficiently high temperatures, all the atoms of any material will become completely ionized so that the only processes which absorb radiation will be free-free transitions, Compton scattering, and pair production.* The free-free absorption will be accurately hydrogenic (except for plasma screening effects; these can be approximately included in the Gaunt factors; see J.M. Green, 1958) so that we can use analytic formulae for it. In addition, Compton scattering is given approximately by

$$\mu_{\text{scat}} = N_e \sigma_T \quad (8.3-16)$$

where $\sigma_T = \frac{8\pi}{3} \left(\frac{e^2}{mc^2} \right)^2$ is the classical Thompson Cross Section. Unfortunately, this formula is more accurate at the lower than the higher temperatures which we wish to discuss now. However, as we will see in the next paragraph, it is still a useful order-of magnitude estimate, even in the region where the Klein-Nishina formula (Heitler, 1954) is required for accurate computation. Therefore, we proceed to use it and to neglect pair production before turning to a more accurate account, as the formulae obtained have been used in the Astrophysical literature and thus are of considerable heuristic value.

We follow closely the treatment of Mayer (1947). Now the scattering absorption is proportional to the number of free electrons per unit volume, whereas the free-free absorption is proportional to the square of the number of electrons. Therefore, scattering will dominate at low densities and free-free absorption will dominate at high densities. Let us consider the

* We neglect photon-photon scattering. On this point see Sampson (1959).

low-density scattering limit first.

Use of Eq. (8.3-11) in the formula for the Rosseland mean free path leads simply to

$$\Lambda_{\text{scat}} = \frac{1}{N_e \sigma_T} \int_0^\infty W(u) du = \frac{1}{N_e \sigma_T} \quad (8.3-17)$$

since $N_e \sigma_T$ is independent of frequency* we can also write in this limit

$$N_e = \bar{Z} \rho A / \bar{M}$$

where ρ is the density in gm/cm³, A is Avogadro's number, $\bar{Z} = \sum_Z Z \frac{N_Z}{N}$ is the average atomic number, and $\bar{M} = \sum_Z M_Z \frac{N_Z}{N}$ is the average molecular weight (N_Z is the number of nuclei of charge Z and N is the total number of nuclei). Using these definitions, we obtain for the mean opacity:

$$\kappa_{\text{scat}} = \frac{1}{\rho \Lambda_{\text{scat}}} = \frac{\bar{Z} A}{\bar{M}} \sigma_T \quad (8.3-18)$$

In this limit, the opacity is independent of density and temperature. Using the first-order (in $h\nu/mc^2$ and v/c) corrections to σ_T from the Klein-Nishina formula, Meyer (1947) has improved this result somewhat. He gives

$$\kappa_c \approx \frac{\bar{Z} A}{\bar{M}} \sigma_T \left[1 - 11 (kT/mc^2) \right] \quad (8.3-19)$$

* If the erroneous factor $1 - e^{-h\nu/kT}$ is included in μ_{scat} the result is $\Lambda_{\text{scat}} = \frac{1.055}{N_e \sigma_T}$.

which shows a mild temperature dependence. In the high-density, free-free limit, we can write

$$\Lambda_c = \Lambda_0 \int_0^{\infty} \frac{Z(u) du}{D_{ff}(u)} \quad (8.3-20)$$

in analogy to Eq. (8.3-6). The value of D_{ff} is derived by Mayer (1947), e.g., and by Stewart and Pyatt (1961).

We write it in the form (defined according to Eq. (8.3-7))

$$D_{ff}(u) = 4\pi^{3/2} \left(\frac{Ryd}{kT} \right)^{5/2} \langle Z^2 \rangle N_e a_0^3 g_{ff} \quad (8.3-21)$$

where $\langle Z^2 \rangle = \sum_Z \frac{N_Z Z^2}{N}$. (8.3-22)

Inserting this value into Eq. (8.3-20) yields

$$\Lambda_c = \Lambda_0 \frac{1}{4\pi^{3/2} \left(\frac{Ryd}{kT} \right)^{5/2} \langle Z^2 \rangle N_e a_0^3} \int_0^{\infty} \frac{Z(u) du}{g_{ff}} \quad (8.3-23)$$

If we set $g_{ff} = 1$ and use $S(\infty) = \int_0^{\infty} Z(u) du = 196.5$, we can write

$$\kappa_c = \frac{1}{\rho \Lambda_c} = \frac{1}{\rho \Lambda_0} \left(\frac{4\pi^{3/2} \left(\frac{Ryd}{kT} \right)^{5/2} \langle Z^2 \rangle N_e a_0^3}{196.5} \right) \quad (8.3-24)$$

Inserting Λ_0 from Eq. (8.3-9) we obtain

$$\kappa_c = 4.762 \times 10^6 \left(\frac{\text{Ryd}}{kT} \right)^{7/2} \frac{\langle Z^2 \rangle N_e a_0^3}{M (196.5)} \quad (4\pi^{3/2}) \quad (8.3-25)$$

Now $N_e = \frac{a_0^3}{M}$, so we obtain

$$\kappa_c = 5.4 \times 10^5 \rho \left(\frac{\text{Ryd}}{kT} \right)^{7/2} \frac{Z \langle Z^2 \rangle a_0^3}{(M)^2} \quad (8.3-26)$$

(This is equivalent to Eq. 28 of Stewart and Pyatt, 1961; if their Eq. 19 is substituted into their Eq. 28, the equation above results. Mayer, 1947, gives 4.815×10^4 as the coefficient in the above formula instead of 5.4×10^5 .) In the analysis given by Mayer (1947) he retains the approximate form of the free-free Gaunt factor:

$$g_{ff} \approx 1 + 0.1728 \left[\frac{kT}{\text{Ryd} (Z')^2} \right]^{1/3} u^{1/2} \left(1 + \frac{2}{u} \right) \quad (8.3-27)$$

rather than setting it equal to unity, and takes it out from under the integral in Eq. (8.3-23) by evaluating it at the point where $Z(u)$ has its maximum, that is, at $u \approx 7$. This provides a correction to κ_c which is

$$\bar{g}_{ff} \approx 1 + .588 \left(\frac{kT}{\text{Ryd} Z^2} \right)^{1/3}$$

This correction, however, is of dubious value, since no one form of the free-free Gaunt factor is valid over the complete frequency range of the integral in Eq. (8.3-23). For specific temperatures, one could evaluate the integral numerically from a tabulation of values of g_{ff} such as has been provided, e.g., by Karzas and Latter (1961).

In contrast to the scattering limit, Eq. (8.3-26) for the free-free opacity limit is proportional to the density and to the 7/2 power of the temperature. This temperature dependence has been used in astrophysical studies, but its limitations -- neglect of scattering, neglect of proper variation of Gaunt factor, and neglect of screening, should be borne in mind.

8.4 Non-hydrogenic absorption-coefficient calculations

8.4.1 Deficiencies of the Hydrogenic Approximation

Some of the more recent opacity calculations (cf. e.g., Armstrong, Johnston, and Kelly, 1965) have departed substantially from hydrogenic approximations, for reasons discussed below. First, in illustration of the type of difference between the hydrogenic result and more accurate results in the case of line transitions, consider Table 8-9 which presents a comparison of values of the radial dipole integral (squared):

$$\sigma^2 = \frac{1}{(4l > 2 - 1)} \left(\int R_i R_f r^3 dr \right)^2 \quad (8.4-1)$$

R_i and R_f are the initial and final state radial wave functions, and $l >$ is the greater of the angular momentum belonging to the two states. The results to which the hydrogenic values are compared have been computed according to the Hartree-Fock-Slater (HFS; Kelly, 1964b) method, and (where available), to the Hartree Fock (HF) analytic Hartree-Fock (AHF; Kelly, 1964a), or Coulomb approximation (CA) methods (Bates and Damgaard, 1949). In one case, an experimental value is quoted. The f -number and

Table 8-9

Species	Initial State	Final State	σ^2 (dipole length)		
			Hydrogenic **	HFS*	HF, CA, or Expt'l
Ni	$2s^2 2p^3 (^4S)$	$2s^2 2p^2 3s (^4P)$	0.294	0.243	0.131 (AHF)
		$4s (^4P)$	0.0488	0.024	0.0211 (HF)
		$3d (^4P)$	1.50	0.0138	0.0060 (AHF)
		$4d (^4P)$	0.195	0.0090	0.00317 (HF)
NiI	$2s^2 2p^2$	$2s^2 2p3d$	0.375	0.043	0.033 (HF)
		$2s^2 2p3s$	13.5	5.1	4.1 - 5.9 (Expt'l)
		$2s^2 2p3p$	1.69	1.2	1.3 - 1.5 (HF)
NV	$1s^2 2s (^2S)$	$1s^2 2p (^2P)$	0.360	0.318	0.323 (AHF)
		$1s^2 2p (^2P)$	0.0117	0.0335	0.0280 (CA)
		$1s^2 3d (^2D)$	0.060	0.0532	0.0595 (CA)
OI	$2s^2 2p^4 (^3P)$	$2s^2 2p^3 3s (^3S)$	0.294	0.151	0.0974 (AHF)
		$4s (^3S)$	0.0488	0.0171	0.0180 (HF)
		$3d (^3D)$	1.50	0.0055	0.0026 (AHF)
		$4d (^3D)$	0.195	0.0037	0.00147 (HF)

A comparison of the squared radial dipole integral $\sigma^2 = \frac{1}{(4l^2 - 1)} \left(\int R_1 R_2 r^3 dr \right)^2$ in the hydrogenic and Hartree-Fock-Slater (HFS) approximations with more accurate results where available. AHF denotes Analytic Hartree-Fock values, CA, Coulomb Approximation values, and HF, numerical Hartree-Fock values.

* The hydrogenic and HFS values are independent of the angular momentum coupling

** The residual charge seen by the active electron at large distances is used to define the hydrogenic approximation.

cross section, the quantities of physical interest, are proportional to this square of the dipole integral. As can be seen from the table, all the values tend to agree near a high degree of ionization (NV) -- this is to be expected due to the dominance of the Coulomb force. However, for neutral atoms, there is a wide scatter of values, the hydrogenic and more accurate values occasionally agreeing, but more often not.

The HFS approximation is an approximation to the HF scheme and as such is not as accurate. It is obtained if one replaces the exchange term in the HF equations by the exchange term appropriate for a free-electron gas. This simplifies the equations considerably and uncouples them. Although the results are not as accurate as HF results, they are in general considerably better than hydrogenic values and the calculations are sufficiently general, yet simple and economical, to be very appropriate to the air-radiation problem under discussion here. It is not yet possible to obtain HF results for more than a fraction of the transitions needed in this type of work.

It may be possible systematically to improve the hydrogenic approximation to bound-bound matrix elements to the point where their accuracy competes with that of the Hartree-Fock method. Attempts in this direction have been made by Varsevsky (1958), Naqvi (1964), and others, but the results are not yet sufficiently definitive nor general to afford adequate reliability. In addition, it would appear that the amount of labor and complication involved will probably exceed that of the HFS method and approach that of the Hartree-Fock method so that no advantage would be gained by this approach.

Another difference between a hydrogenic and non-hydrogenic model for line transitions occurs if one bases the approximation (as is usually done) on f -numbers rather than on dipole integrals. In terms of the f -number, the absorption cross section and absorption coefficient are given by

$$\sigma_{ij}(\epsilon) = \frac{h\nu_{ij}^2}{mc} f_{ij} b_{ij}(\epsilon) \quad (8.4-2)$$

and

$$\mu(\epsilon) = \frac{h\nu_{ij}^2}{mc} \sum_{i,j} N_i f_{ij} b_{ij}(\epsilon) \quad (8.4-3)$$

where $b_{ij}(\epsilon)$ is the line shape factor normalized to unity over the extent of the line:

$$\int b_{ij}(\epsilon) d\epsilon = 1 \quad (8.4-4)$$

In the independent-electron hydrogenic approximation, the electrons are uncoupled and we need only specify the orbital angular momentum and principal quantum number n . In terms of these quantities the f -number for a transition from state n, l ("i") to n', l' ("j") is given by (Chapter 3, Eq. (3.86))

$$f = \frac{1}{3} \cdot \frac{l > (4l >^2 - 1)}{(2l + 1)} \cdot \left(\frac{h\nu_{ij}}{\text{Ryd}} \right) \sigma_{ij}^2 \quad (8.4-5)$$

where $l >$ denotes the greater of the two quantum numbers l and l' , and σ_{ij} is the radial dipole integral in units of a_0 , as given in Eq. (8.4-1).

Now in the hydrogenic approximation, all the angular-momentum sub-levels

belonging to a given principal quantum number n (viz., levels for $l = 0, 1, 2 \dots n-1$) have the same energy. Thus, for transitions between these levels, the so-called "same-shell" transitions, between such states as $2s - 2p, 3s - 3p, 3p - 3d$, etc., the factor $h\nu_{ij}$ in the expression for f_{ij} is zero and therefore f_{ij} vanishes. In N and O (as in any many-electron atom), these levels are separated by a few volts so that $h\nu_{ij}$ is appreciably different from zero. The dipole integrals tend to be very large because of the substantial overlap of the wave functions. Consequently, the f -numbers or cross sections turn out to be usually moderately large for transitions among these states, and their omission leads to a serious discrepancy.

It would be possible, of course, to avoid this problem by using hydrogenic values for the σ_{ij} and experimental or calculated values of the $h\nu_{ij}$. This could be done through Eq. (8.4-5), neglecting the angular momentum coupling and L-S term splitting of the actual many-electron (light) atom, or through the more correct relation

$$f_{ij} = \frac{1}{3} \left(\frac{h\nu_{ij}}{\text{Ryd}} \right) \frac{S(M) S(L) \sigma_{ij}^2}{g_i} \quad (8.4-6)$$

appropriate to L-S coupling and separable wave functions for the individual electrons. In this formula, the factors $S(L)$ and $S(M)$ are called relative line strengths and relative multiplet strengths, respectively. The statistical weight of the initial state is called g_i . This formula will sum back to Eq. (8.4-5) (except for a factor amounting to the number of available electrons), if the σ_{ij} and $h\nu_{ij}$ are assumed to be the same for all the terms (viz., if hydrogenic degeneracy is assumed) and the equation

is summed over all the terms of a transition array. In other words, a "hydrogenic" model could be based on Eq. (8.4-6) which would account for all the multiplet structure of the atom and the correct energy differences $h\nu_{ij}$. The only difference between this "hydrogenic" and a non-hydrogenic model would reside in the radial integrals σ_{ij} . This intermediate type of approximation was used by Armstrong, Johnston and Kelly (1965) for high levels and large angular momenta. For the more important low-lying levels, the more accurate radial integrals of the HFS theory were used.

It is also interesting to note the difference between hydrogenic and non-hydrogenic results in the case of photoelectric transitions. There are a number of possible differences between a strictly hydrogenic approximation and a more detailed description such as the HF scheme which takes into account the electron interactions and coupling.

Take OI as an example. The configuration is $1s^2 2s^2 2p^4$. In a strictly hydrogenic (independent-electron) approximation there would be just one state for this configuration and one photoelectric edge for photoejection of a 2p-electron. In actuality, the electron angular momenta can couple in several different ways, each of which leads to a different interaction energy. The result is that this configuration of OI has three terms, or states (ignoring the fine structure) rather than just one: 3P , 1D , 1S where this notation designates the total angular momentum and spin in the usual spectroscopic notation.

The 3P is the lowest level with the $^1D \sim 2$ eV above it, and the $^1S \sim 4$ eV above it, as illustrated in Fig. 8-14.

The configuration which results from the $2s^2 2p^4$ upon photoejection of a 2p-electron, viz., $2s^2 2p^3$, likewise has three terms $^4S, ^2D, ^2P$, separated by similar amounts. Photoejection of a 2p electron from the 3P ground term leaves the ion in a linear combination of the $^4S, ^2D$, and 2P "parent" terms so that three photoelectric edges are observed as shown in Fig. 8-15 rather than the one edge that a strictly hydrogenic approximation would entail. The 1D term yields two edges and the 1S , one, so that a total of 6 edges results from photoejection of a 2p electron from the $2s^2 2p^4$ configuration. For temperatures $kT \leq \Delta E$ where ΔE is this "term splitting" of the configuration, the differences in the spectral absorption features of the hydrogenic and non-hydrogenic models are likely to be of considerable importance.

In addition to the splitting of the photoelectric edges due to electron interactions, the actual magnitudes of the cross sections are, of course, also different in the hydrogenic approximation and in a more exact theory. Fig. 8-16 illustrates this difference for the lowest edge of the ground term of OI. The cross section for the transition $OI 2s^2 2p^4 (^3P) \rightarrow 2s^2 2p^3 (^4S)_\epsilon$ is shown in the figure with threshold or edge at 13.6 eV where ϵ denotes the energy of the photoejected electron and the contributions of both the p - s and p - d branches of the transition are included. The dashed curve is the IIF result from a computer code due to Dalgarno, Henry, and Stewart (1964) in the dipole-length form. The dotted curve represents the same approximation but in the dipole-velocity form. The difference between these is a crude measure of the uncertainty in the result. The solid line is the result of a calculation of Armstrong, Johnston, and Kelly (1965) which is more amenable

to large-scale machine computations, while at the same time no less accurate than the HF results. It employs an approximation at low energies due to Burgess and Seaton (1960) and at high energies one due to Johnston (1964). These are discussed below. The two dash-dot curves are hydrogenic-approximation results, one with the correct Gaunt factor^{*}, one with this factor set equal to unity. The difference between the hydrogenic and the more accurate non-hydrogenic results are quite striking: factors of two to four at threshold increasing to more than an order of magnitude at high energies. The ionization potential appearing in the hydrogenic photoelectric cross section formula has been taken as the appropriate oxygen experimental value, and the Gaunt factor has been made consistent with this choice of ionization potential. This is tantamount to employing a screened effective nuclear charge. From such calculations as this it appears that the hydrogenic result lies consistently below the Hartree-Fock photoelectric results for O and N, but with agreement improving as one passes to states with higher and higher degree of ionization. Thus, as one might expect, the hydrogenic approximation is most suitable at high temperatures and low densities.

8.4.2 The Methods used by Armstrong, Johnston, and Kelly (1965)

8.4.2.1 The Low-Energy Theory.

Recently, Burgess and Seaton (1960) presented an approximation to the radial matrix elements in terms of the asymptotically-correct wave functions. This approximation derives from the observation of Bates and Damgaard (1949) that the major contribution to the radial integral for bound-bound transitions usually comes from values

* The Gaunt factor is the ratio of the quantum-mechanical cross section to the classical Kramers value discussed previously.

of r sufficiently large that the effective potential is a Coulomb potential. Replacing the actual one-electron wave function by its asymptotic form - (a linear combination of the regular and irregular Coulomb wave functions for the observed value of the energy, modified for small r to ensure convergence of the radial integrals) Bates and Damgaard evaluated the radial matrix elements $R_{n\ell}^{n'\ell'}$ and presented their results in tabular form.

Burgess and Seaton applied similar considerations to the evaluation of the radial matrix elements $R_{n\ell}^{e\ell'}$ for bound-free transitions. Whereas the asymptotic behavior of the bound-state wave function is determined by the physically-observed energy of the bound state, the large-radius behavior of the free-electron wave function, at a given energy, is determined by a phase shift $\delta_{\ell'}(L', \epsilon)$. In the approximation of asymptotically-correct wave functions, Burgess and Seaton numerically evaluated the radial matrix elements, parameterized the resulting photo-ionization cross sections, and tabulated their results. The basic variable of the theory is the effective quantum number ν defined by

$$(\epsilon_{n'\ell} - I_e) = -1/\nu_{n'\ell}^2 \quad (8.4-7)$$

where I_e is the ionization limit of the $\epsilon_{n'\ell}$ series, and the effective quantum number and the quantum defect satisfy $\nu_{n'\ell} = n' - \mu_{n'\ell}$.

In order to use the Burgess-Seaton theory one assumes that the quantum defect or phase shift which are related at the series limit by

$$\delta_{\ell'}(\epsilon, L') = \pi\mu_{\ell'}(\epsilon, L') \quad (8.4-8)$$

can be extrapolated to small positive energies. Thus, a knowledge of the bound states of the line series connected with a given photoelectric edge is needed. Although this experimental information is available for many of the most important photoelectric edges, it is not for all. When it is lacking, cruder approximations must be made, the crudest of which would be to set the phase shift equal to zero where no experimental information is available (this is the situation with, for example, most states involving double excitation beyond the $n = 2$ shell).

A low-energy expansion of the Burgess-Seaton cross section for integer ν agrees with a corresponding expansion of the exact hydrogenic results to first order in ϵ . Thus the Burgess-Seaton theory is to be considered a valid approximation when the electron kinetic energy is much less than Z^2 Rydbergs. Furthermore, when sufficient information regarding the physical bound states is available, the result of Burgess and Seaton is probably more reliable than continuum Hartree-Fock calculations (Dalgarno, Henry, and Stewart, 1964) as some effects due to exchange and polarization of the core are reflected in the physical energies of the states with large principal quantum number used in the extrapolation for the phase shift.

Thus we conclude that the Burgess-Seaton approximation is a reasonably valid and useful approximation near the photoionization threshold, with the exception of the inner-shell transitions in the presence of an excited outer electron. The simplicity of the resulting expression for the photoionization cross section renders it particularly suitable for evaluation of the large number of initial states present in the usual opacity problem.

8.4.2.2 The High-Energy Theory.

For energies of the final-state free electron much greater than zero the Burgess-Seaton approximation is inapplicable. An approximation of frequent utility in high-energy scattering calculations is the Born approximation. A straightforward application of the Born approximation to calculation of the photoionization cross section, however, leads to an incorrect result. It can be shown (Johnston, 1964) that a use of the acceleration form of the matrix element in a high-energy Born approximation gains one iterate of the Born series over the use of the dipole-velocity form. The second Born approximation to the velocity matrix element contains a term with the same high-energy behavior as the first Born approximation (thus guaranteeing an incorrect high-energy result when using the first Born approximation alone) whereas the first Born approximation to the acceleration matrix element gives the correct high-energy behavior. Accordingly, the dipole-acceleration Born approximation (or better) should be used for high electron energy.

When the angular integrations and polarization averages are performed on the acceleration form of the matrix element the result obtained is:

$$\sigma_{ij}(\epsilon) = \frac{16\pi^3 Z^2 e^6}{3m^2 \omega^3 c} F_p \left[\left(\frac{l}{2l+1} \right) \left(R_{nl}^{\epsilon, l-1} \right)^2 + \left(\frac{l+1}{2l+1} \right) \left(R_{nl}^{\epsilon, l+1} \right)^2 \right] \quad (8.4-9)$$

with

$$R_{nl}^{\epsilon l'} = \int_0^\infty R_{\epsilon l'}(r) \frac{1}{r^2} R_{nl}(r) r^2 dr \quad (8.4-10)$$

where, in the first Born approximation, the properly normalized free-electron wave function is a plane wave.

In the Armstrong, Johnston, and Kelly (1965) calculation, through use of a generalization of the HFS code of Hermann and Skillman (1963) wave functions were generated for the many bound atomic states present in the gas. The resulting numerical bound-state wave functions were fitted with analytic functions and from these, the matrix elements of Eq. (8.4-10) and the cross sections were computed. The HFS line f-numbers were used for the low-lying states ($l \leq 3, n < 6$) and quasi-hydrogenic (as described above) or hydrogenic values were used for the remainder. No attempt was made to compute a non-hydrogenic free-free contribution; the results of an earlier calculation (Armstrong, Holland, and Meyerott, 1958) were used for this part. The atomic core configurations included in this calculation (along with the relevant ionization potentials) are tabulated in Table 8-10.

Table 8-10 Table of Atomic Core Configurations and Ionization Potentials

Species	State	Core Designation	Ioniz. Potentials	
			O	N
O-I	$1s^2 2s^2 2p^3 ({}^4S) nL ({}^{2S+1}L)$	$\gamma = 1$	13.617	
	$({}^2D)$	2	16.942	
	$({}^2P)$	3	18.631	
	$2s 2p^4 ({}^4P)$	4	28.42	
	$({}^2D)$	5	34.19	
	$({}^2S)$	6	37.88	
	$({}^2P)$	7	39.99	
	$2p^5 ({}^2P)$	8	52.11	

* The ionization potentials given are from the lowest state of each stage of ionization, to the ionized state with core coupling as stated.

Table 8-10 (cont'd)

Species	State	Core Designation	Ioniz. Potentials*	
			O	N
O-II, N-I	$1s^2 2s^2 2p^2 (^3P) nL^{2S+1}L$	$\gamma = 1$	35.154	14.543
	(^1D)	2	37.659	16.447
	(^1S)	3	40.50	18.601
	$2s 2p^3 (^5S)$	4	42.623	20.400
	(^3D)	5	50.028	25.989
	(^3P)	6	52.799	28.094
	(^1D)	7	58.336	32.430
	(^3S)	8	59.580	33.787
	(^1P)	9	61.238	35.230
	$2p^4 (^3P)$	10	70.339	42.3
	(^1D)	11	72.127	43.1
	(^1S)	12	77.708	47.4
O-III, N-II	$1s^2 2s^2 2p (^2P) nL^{2S+1}L$	$\gamma = 1$	54.946	29.617
	$2s 2p^2 (^4P)$	2	63.758	36.703
	(^2D)	3	70.671	42.145
	(^2S)	4	75.312	45.861
	(^2P)	5	77.309	47.716
	$2p^3 (^4S)$	6	83.607	52.781
	(^2D)	7	86.568	54.799
	(^2P)	8	90.642	58.188
O-IV, N-III	$1s^2 2s^2 (^1S) nL^{2S+1}L$	$\gamma = 1$	77.411	47.426
	$2s 2p (^3P)$	2	87.575	55.757
	(^1P)	3	97.081	63.629
	$2p^2 (^3P)$	4	103.881	69.189
	(^1D)	5	106.122	70.843
	(^1S)	6	113.088	76.606
O-V, N-IV	$1s^2 2s (^2S) nL^{2S+1}L$	$\gamma = 1$	113.898	77.450
	$2p (^2P)$	2	125.821	87.442
O-VI, N-V	$1s^2 (^1S) nL^{2S+1}L$	$\gamma = 1$	138.110	97.863

* The ionization potentials given are from the lowest state of each stage of ionization, to the ionized state with core coupling as stated.

8.5 Review of Major Calculations Made to Date

The first documented calculation of the opacity of air including the high-temperature regime appears to be that of Hirschfelder and Magee (1945; 1958/1947). In the original (1945) calculation, the opacity due to photo- and free-free absorption was calculated between $20,000^{\circ}\text{K}$ and 10^6°K . The formulas employed were those of Morse (1940) which, in turn, were based on the methods of Stromgren (1932, 1933). Since these methods utilize a severe hydrogenic model, the principal effort in this type of calculation centers about the obtaining of Eddington's (1926) "guillotine factor" which contains the combined effect of the photoelectric edge positions and the occupation numbers of the atomic states involved. They neglected the excited states of the various ionic species, and assumed all such species to be in their ground states. Pressure ionization was also neglected, and the effective nuclear charge was computed from Slater screening constants. Below $20,000^{\circ}\text{K}$, they computed the free-free and photoabsorption by O^- and N^- , and the absorption by NO_2 . They found the free-free absorption of O^- and N^- to be the dominant effect down to about $3,000^{\circ}\text{K}$. For the calculation of this effect, they used the partial wave free-free formula of Wheeler and Wildt (1942), including s- and p-states, and made a numerical computation of the free electron functions involved. Later on (see Magee and Hirschfelder, 1947/1958) they included the effect of O_2^- , and used the Bates and Massey (1943) cross section for O^- . In this later report, they also give the details of the NO_2 calculation and consider the Planck mean absorption coefficient defined to permit the radiation and matter to exist at different temperatures.

The atomic calculation of Hirschfelder and Magee was later refined and extended downward in temperature by Kivel and Mayer (1965/1954), using Mayer's (1947) more detailed methods including some consideration of the effect of lines. A comparison of the Kivel-Mayer, and the Hirschfelder-Magee results is given in Fig. 7 of Kivel and Mayer (1965).

In 1955, a brief report by F.R. Gilmore and A.L. Latter appeared (Gilmore and Latter, 1955), in which they give values of the continuous absorption coefficient of air and the Rosseland mean free path between 2 and 600 eV temperature. The density range covered is from 10^{-4} to 10 times normal density. They assumed that the air molecules are completely dissociated into atoms, and that all atoms are identical and have the average atomic number 7.262. Mayer's (1947) equations were used, first to calculate the average electronic occupation and ionization energy of the K, L, and M shells and then to calculate the continuous absorption coefficient and the Rosseland mean free path. The effects of fluctuations (from the average atom), of line absorption and of scattering (in the spectral coefficient) are omitted, and the Gaunt factors are taken to be unity. This preliminary work was subsequently refined and extended by Gilmore, and although the results have not been published, they have been made available to other workers in the field by private communication.

The work of Kivel and Mayer (1965/1954) referred to above in which use is made of a simplified atomic model (energies from screening constants, a limited number of excited states, neglect of configuration splitting) which is not accurate for low stages of ionization left the important temperature range

from 2 to 20 eV in doubt. This was pointed out in the extensive and elegant analysis of atomic opacity calculations carried out by Plass, et al. (1957). Immediately thereafter, a calculation in this region was undertaken by Armstrong, Holland, and Meyerott (1958). The limitations of the ionic method which concerned Plass, et al. (1957; see, e.g., p ix) were circumvented by employing empirical energy-level values, and by extensive use of digital computers. This use of computers enabled Armstrong, Holland, and Meyerott to incorporate much more atomic structure detail into an opacity calculation than had previously been practical.

In this calculation, the photoelectric, free-free and Compton scattering contributions to the absorption coefficient of nitrogen, oxygen and air, were computed over the temperature range 2 to 20 eV as mentioned and over the density range from about 10^{-5} times normal density to normal density. The photon energy range covered was 1 eV to 1 keV*. The occupation numbers of the ionic states were computed with the ion-sphere/grand canonical ensemble statistical methods introduced by H. Mayer (1947) (and developed somewhat further by Brachman and Meyerott, 1953). Individual LS coupling terms were included for levels of principal quantum numbers 2 and 3 with energies obtained from experiment where known. Where empirical energy-level information was lacking, estimates of the energies were made by isoelectronic interpolation, or by the Bacher-Goudsmit (Bacher and Goudsmit, 1934) method. In the cases where insufficient experimental information was available to yield results by the foregoing methods,

* The K-shell contribution which appears explicitly in Figs. 4-1 to 4-30 of AFSWC TR 58-36 are too small by a factor of 2 and should be corrected accordingly.

the Bohr formula was used with a constant quantum defect assigned by obtaining a value from a related configuration. For principal quantum number $n \geq 4$, the quantum defect formula was used for all levels, although angular momentum sub-levels were treated individually for $l = 0, 1, 2$ and 3 up to $n = 9$. (Levels for $l \geq 4$ were lumped.) Multiple excitations were partially included by using one-electron levels of ionic cores for all core-coupling possibilities of the $n = 2$ shell. Screened Kramers' hydrogenic cross sections were used with Gaunt factors taken as constant and equal to their values at the photoelectric edges. Fractional parentage coefficients were included in the cross section formulas in order to account properly for transitions from equivalent electron states.

The calculations of Armstrong, Holland, and Meyerott (1958) were of spectral absorption coefficients (and air compositions) only; these results were subsequently integrated over the appropriate weighting functions in frequency to form Planck and Rosseland mean coefficients by Armstrong (1959a). Some of the results of the earlier calculation which had not been included in the Armstrong, Holland, and Meyerott (1958) report (*viz.*, separate absorption coefficients for N and O) were also included in this subsequent report. Very shortly after this Lockheed work was done, the first of the reports issued by the General Atomic Opacity group appeared (Bernstein and Dyson, 1959). This latter work, although undertaken without knowledge of the Lockheed work, was quite similar to it. A larger variety of elements (from hydrogen to fluorine) was considered, rather than just oxygen and nitrogen as in the Armstrong, Holland, and Meyerott work. However, in compensation, less atomic detail was included. Quantitatively, the greatest difference in the two sets of results

is caused by the fact that Bernstein and Dyson used, in effect, ideal gas occupation numbers, and did not lower the continuum edge ("pressure ionization") to account for bound electron-free electron interactions. This effect is moderately significant towards the low temperature end of these calculations. The first "opacity bound" theorem appeared in the Bernstein-Dyson report. (For a discussion of such theorems see Chapter 6.)

The opacity calculation program at General Atomic (as well as the one at Lockheed) was continued, with the result that in September of 1961, the comprehensive report of Stewart and Pyatt (1961) appeared. This was probably the most significant improvement in opacity calculation methods since the war-time work of Mayer. For the first time, full advantage of modern computers (IBM 7090) could be taken. This fact along with use of the line broadening theory developed in the interim by Baranger and others (Baranger, 1962), permitted a detailed, realistic inclusion of line effects for the first time. Stewart and Pyatt calculated atomic photon absorption coefficients and mean opacities for hydrogen, beryllium, carbon, nitrogen, aluminum, and silicon over the temperature range from 1.5 to 34 eV, and the density range from roughly 0.10 gm/cm^3 downward to values around 10^{-12} and 10^{-13} gm/cm^3 . The calculation included the usual contributions from free-free, bound-free, and Compton scattering processes, as well as the line effect. They used Kramers formulas with unit Gaunt factors for their bound-free and free-free cross sections. For the line effect they used an ("oscillating") Elsasser-band formula which analytically sums the line profiles over an entire line series; this profile formula is multiplied by a line-strength to line-spacing ratio. They take this ratio to be the same function ($\propto \nu^{-3}$) as for the photoelectric and free-free contributions.

The atomic energy levels which Stewart and Pyatt employed were computed internally by their code by isoelectronic interpolation, using the nuclear charge expansion-screening theory developed by Layzer (1959) and by Varsavsky (1958) which permits use of empirical data for the zero-order (in nuclear charge Z) contribution to the energy. Corrections to the zero-order energy are then made by perturbation theory; it is only at this level that (empirically evaluated) screening constants are used, so that the results are considerably more accurate than energies obtained by Slater-type screening constants. Stewart and Pyatt tabulate some thermodynamic functions (pressure and internal energy) as well as opacities, and they make use of a considerably improved pressure ionization (or bound-free electron interaction) theory compared to previous work. The effect of line absorption is quite dramatic; their results show that lines increase the Rosseland mean by a factor which is as much as ten (for hydrogen at 2.25 eV and high density) but which is more typically about two for nitrogen at moderate densities. Omission of same-shell transitions for the non-hydrogenic atoms impairs the accuracy of their Planck mean results at the lower temperatures which they consider (Armstrong and Aroeste, 1964). This is not so serious an effect in the case of the Rosseland mean.

Stewart and Pyatt did not actually give results for air, per se, but their work was continued by Freeman who performed calculations for air (Freeman, 1963) by use of the Stewart-Pyatt codes. Shortly after the appearance of the Stewart-Pyatt work, more accurate values of the Planck mean were computed by Armstrong, et al. at Lockheed (Armstrong, Buttrey, Sartori, Siegert, and Weisner, 1961)

who for the first time departed from the traditional hydrogenic matrix element approximations. No comprehensive results were forthcoming from this group however, until 1965. At this time, the work of Armstrong, Johnston, and Kelly (1965a) appeared (see also Johnston, Armstrong and Platas, 1965; Armstrong, Johnston, and Kelly, 1965b). These authors carried out a comprehensive opacity calculation using the old occupation numbers of the Armstrong, Holland, and Meyerott (1958) work, but with non-hydrogenic photoelectric and bound-bound matrix elements. They also utilized the Stewart and Pyatt (1960) prescriptions for line widths and shapes. Since a brief description of the theory involved has been given above (section 8.4.2), and a detailed description has now been published (Armstrong, Johnston, Kelly, DeWitt, and Brush, 1966) it is not necessary to comment further on this work here. It should be noted, however, the paper by Armstrong, Johnston, Kelly, DeWitt, and Brush (1966) also contains a relevant discussion of the statistical mechanics of plasmas and an extensive bibliography of the literature relating to the lowering of the ionization potential in a plasma.

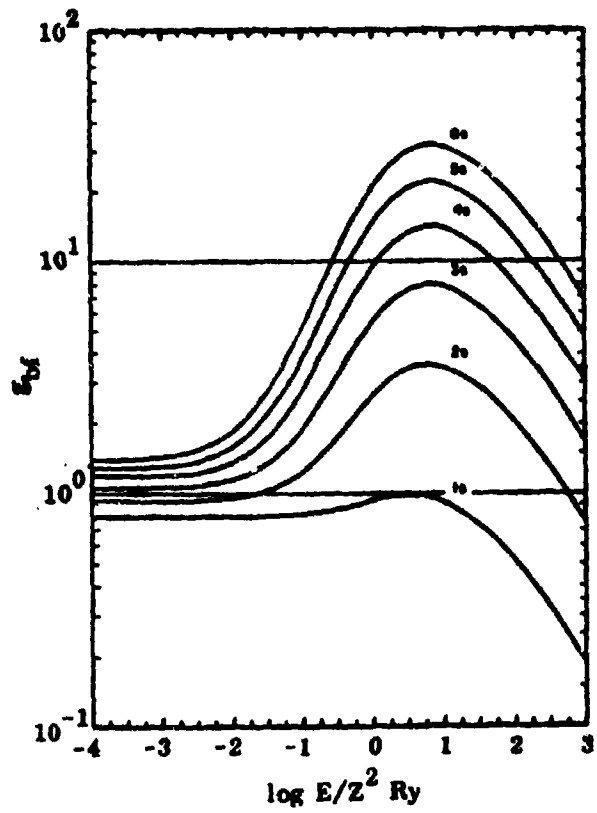


FIG. 8-1 BOUND-FREE GAUNT FACTOR VERSUS
FREE ELECTRON ENERGY FOR $l = 0$,
 $n = 1-6$.

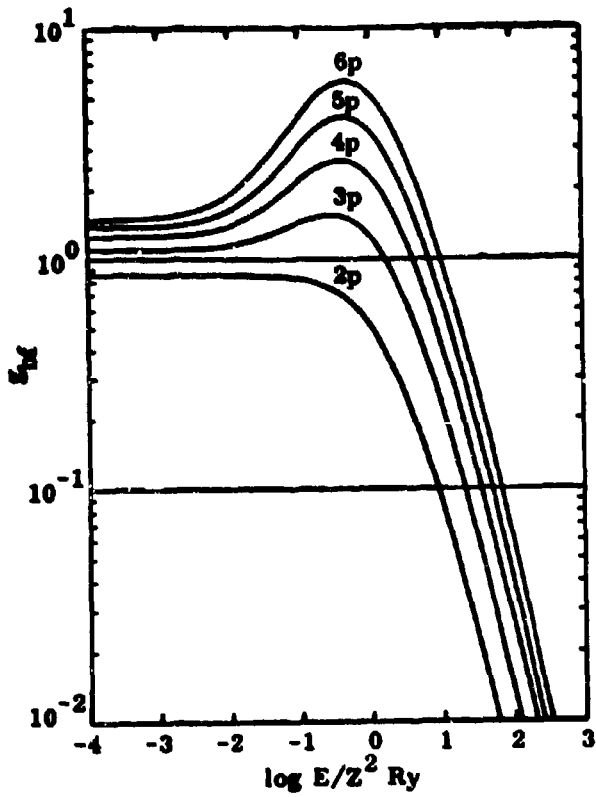


FIG. 8-2 BOUND FREE GAUNT FACTOR VERSUS FREE ELECTRON ENERGY FOR $l = 1$, $n = 2-6$.

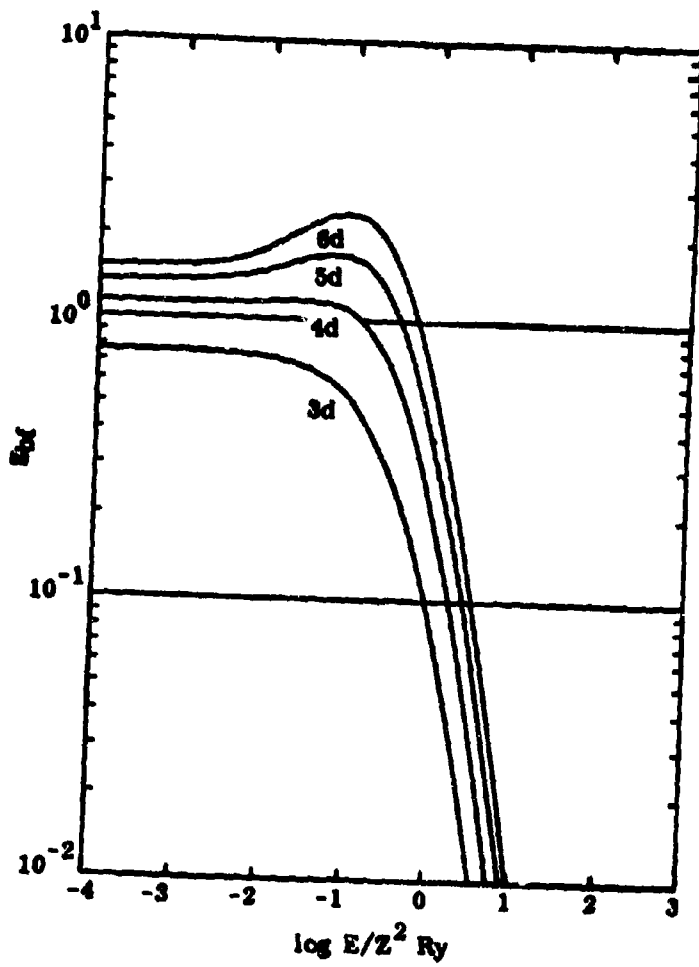


FIG. 8-3 BOUND-FREE GAUNT FACTOR VERSUS
 FREE ELECTRON ENERGY FOR $l = 2$,
 $n = 3-6$.

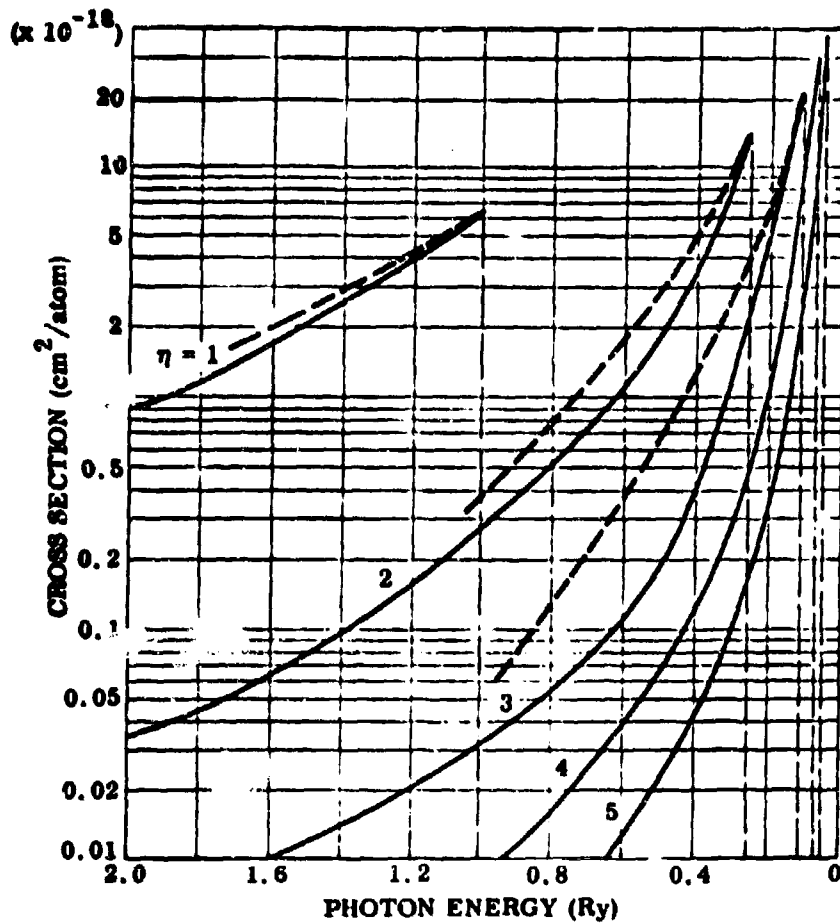


FIG. 8-4 CROSS SECTIONS FOR THE PHOTOIONIZATION OF ATOMIC HYDROGEN FOR PRINCIPLE QUANTUM NUMBERS (n) 1 THROUGH 5. THE SOLID CURVES ARE THE EXACT RESULTS OF McDOWELL (1964), AND THE DASHED CURVES REPRESENT THE CONSTANT GAUNT FACTOR APPROXIMATION.

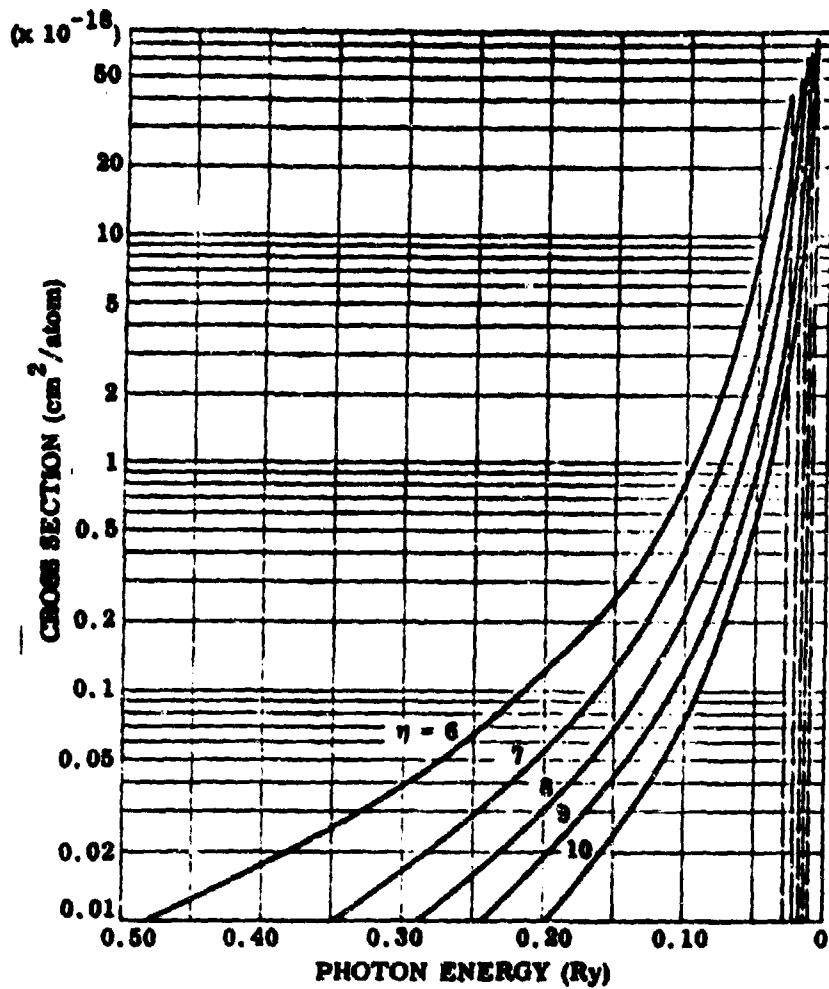


FIG. 8-5 CROSS SECTIONS FOR THE PHOTOIONIZATION OF ATOMIC HYDROGEN FOR PRINCIPLE QUANTUM NUMBERS (n) 6 THROUGH 10. (McDOWELL, 1964.)

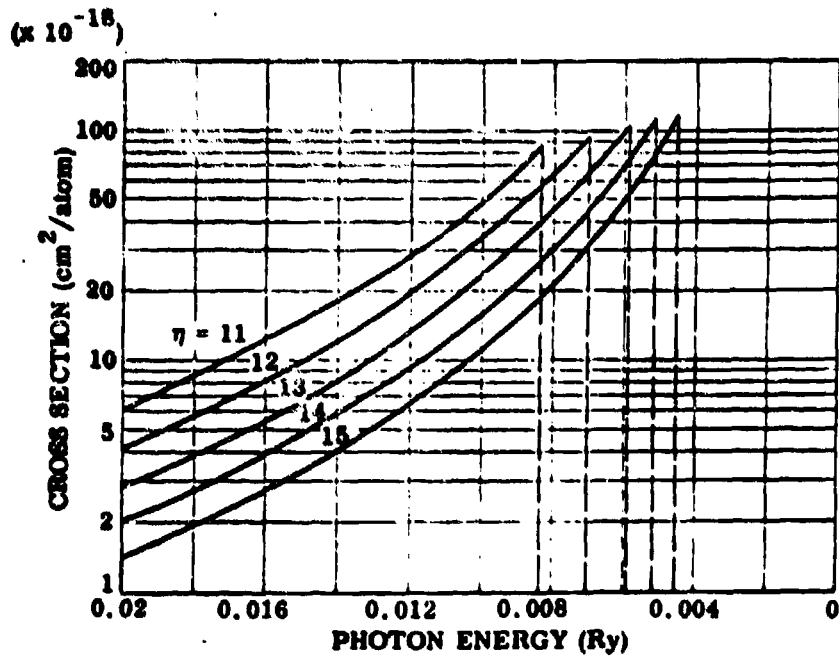


FIG. 8-6 CROSS SECTIONS FOR THE PHOTOIONIZATION OF ATOMIC HYDROGEN FOR PRINCIPLE QUANTUM NUMBERS (n) 11 THROUGH 15. (McDOWELL, 1964.)

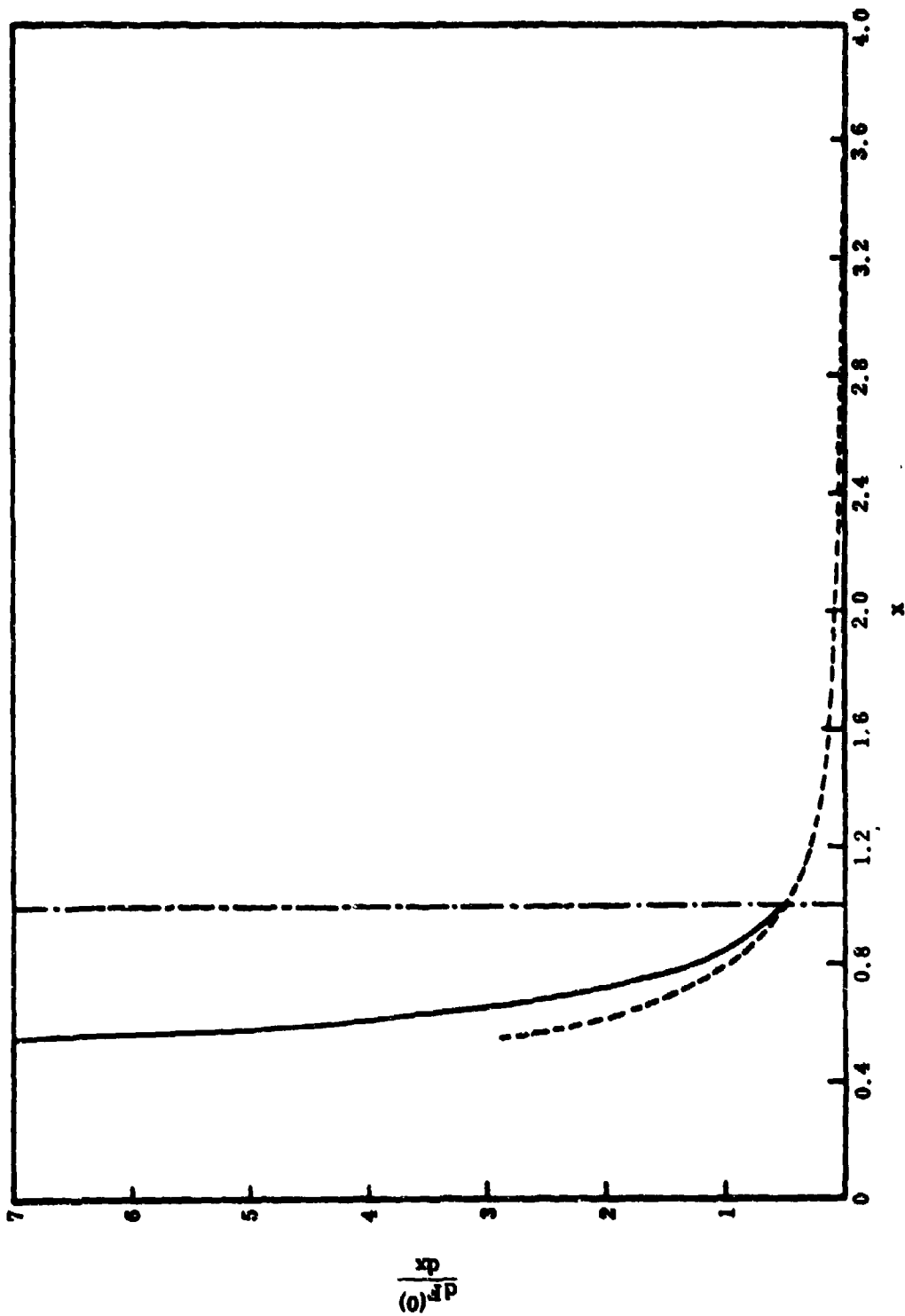


FIG. 8-7 f-NUMBER PER UNIT FREQUENCY INTERVAL FOR SMEARED LINES NEAR THE PHOTOELECTRIC EDGE. INITIAL STATE $n = 2$.

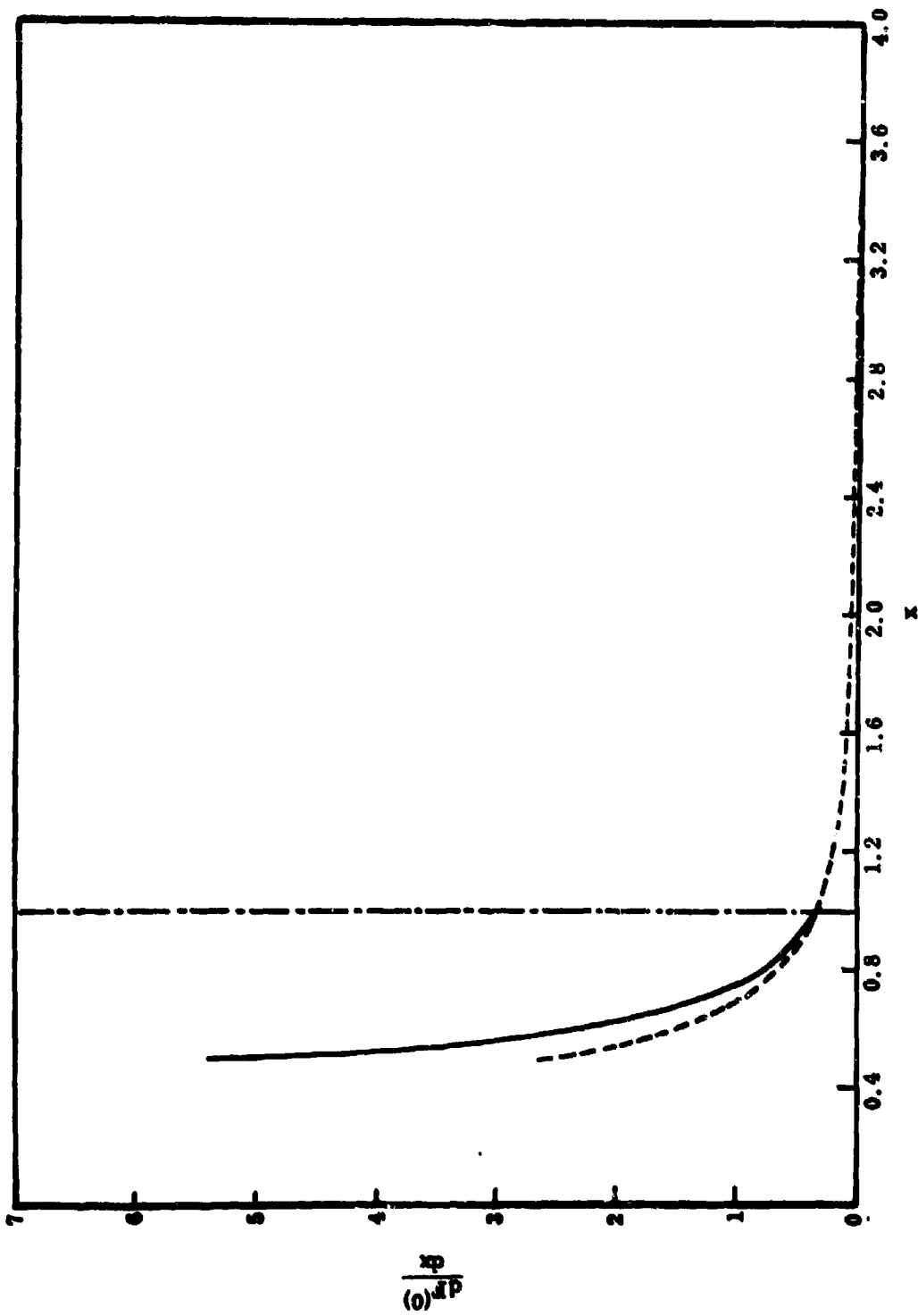


FIG. 8-8 i -NUMBER PER UNIT FREQUENCY INTERVAL FOR SMEARED LINES NEAR THE PHOTOELECTRIC EDGE. INITIAL STATE $n = 3$.

$P_i(x)$

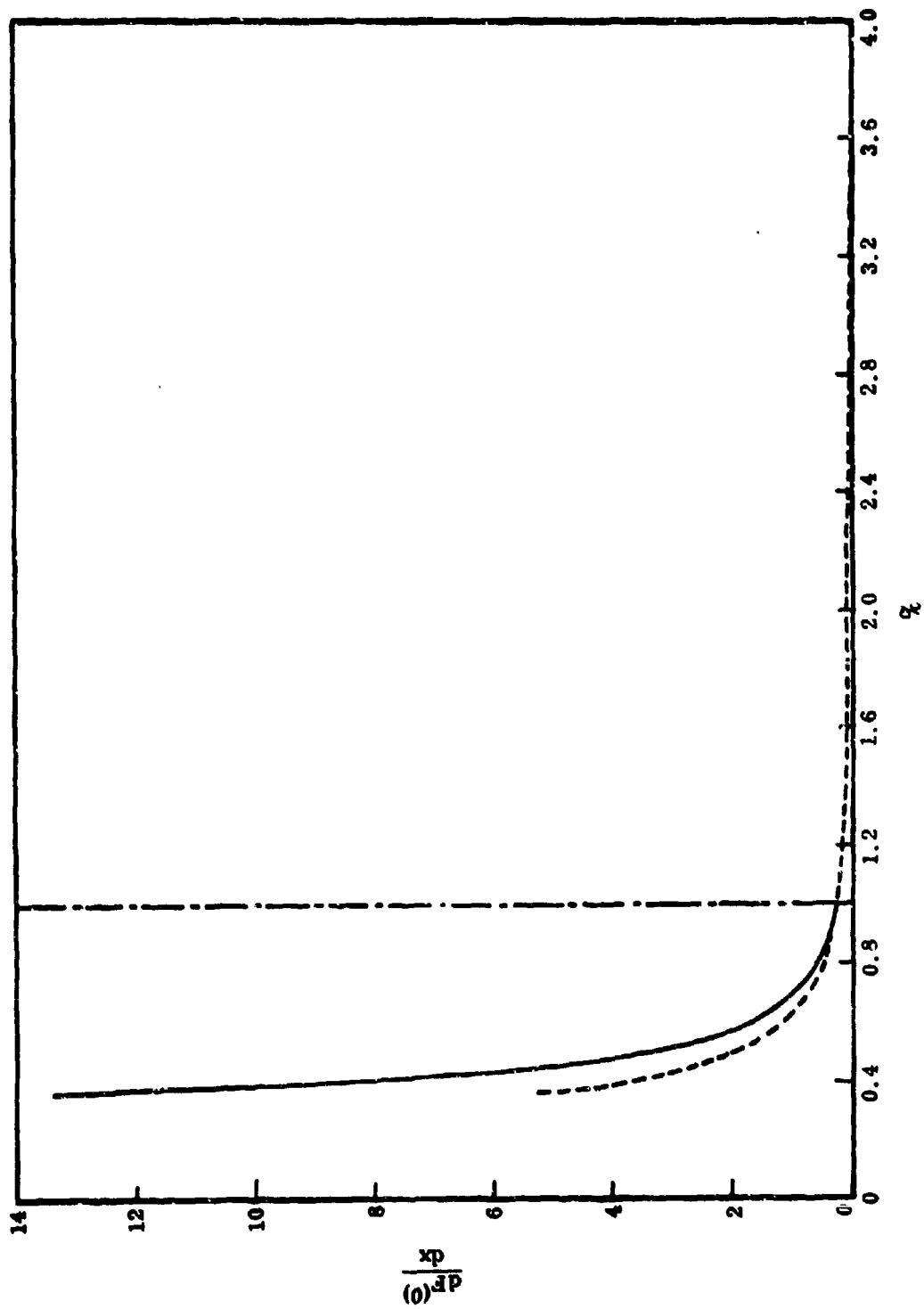


FIG. 8-9 f -NUMBER PER UNIT FREQUENCY INTERVAL FOR SMEARED LINES NEAR THE PHOTOELECTRIC EDGE. INITIAL STATE $n = 4$.

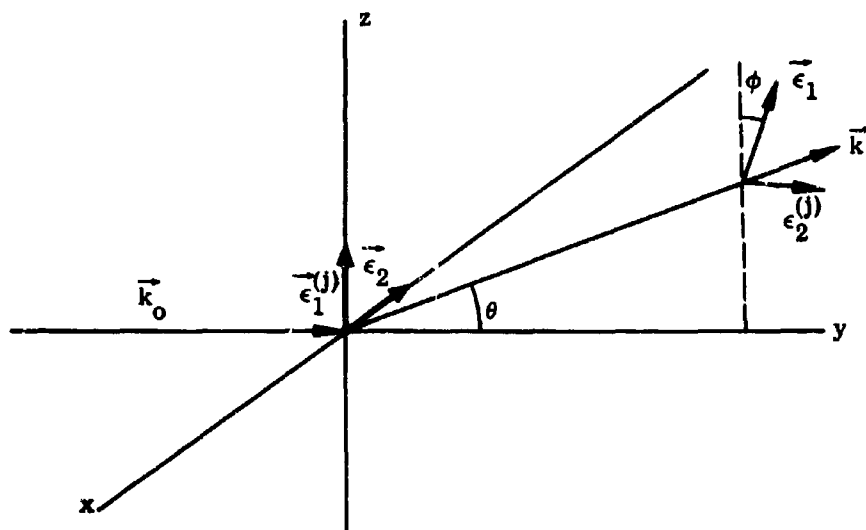


FIG. 8-10 POLARIZATION VECTORS AND SCATTERING ANGLE FOR COHERENT SCATTERING

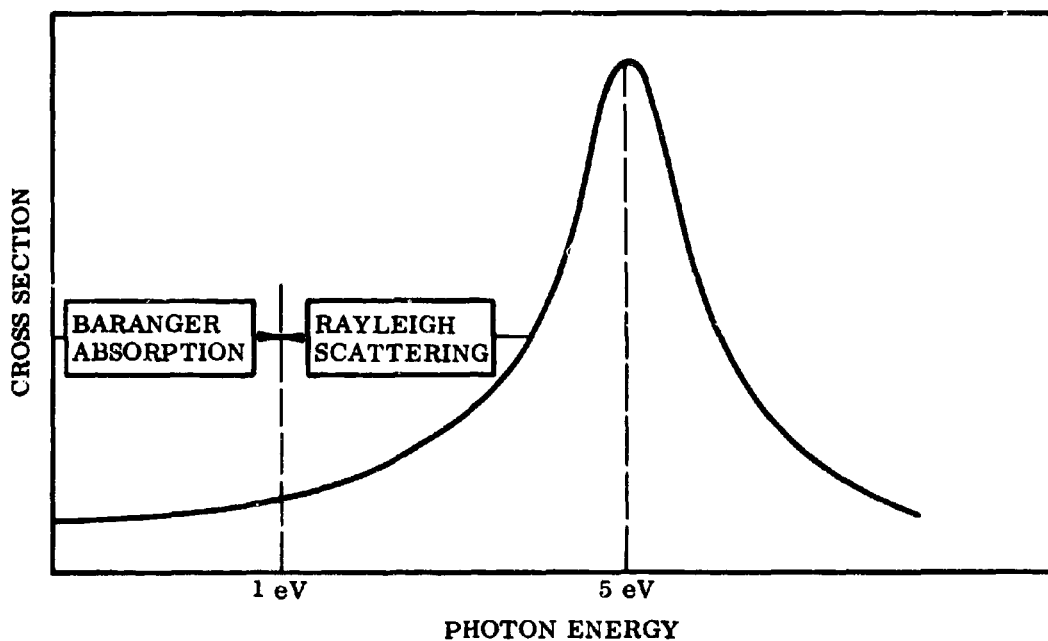


FIG. 8-11 A ROUGH COMPARISON OF REGIONS OF IMPORTANCE FOR RAYLEIGH SCATTERING VERSUS PHOTON ABSORPTION PERMITTED BY ENERGY TRANSFER TO AMBIENT FREE ELECTRONS (TERMED BARANGER ABSORPTION). CONDITIONS: ELECTRON DENSITY = 10^9 cm^{-3} , $kT = 1 \text{ eV}$, FOR A LINE WITH f NUMBER ~ 0.1 AND UPPER PRINCIPAL QUANTUM NUMBER OF 4.

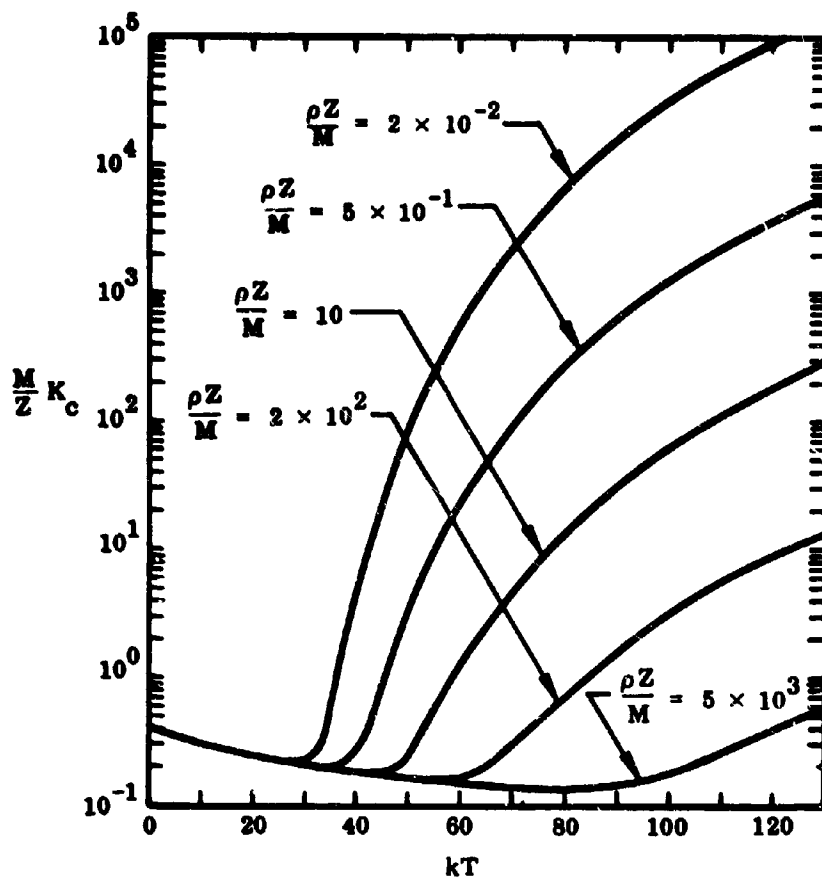


FIG. 8-12 $\frac{M}{Z} \times$ THE COMPTON OPACITY, κ_c , AS A FUNCTION OF TEMPERATURE kT FOR VARIOUS VALUES OF $\frac{\rho Z}{M}$. THE UNITS OF κ_c ARE $\text{cm}^2 \text{gm}^{-1}$; kT IS IN KeV, AND $\frac{\rho Z}{M}$ IS IN MOLES cm^{-3} . (Sampson, 1959.)

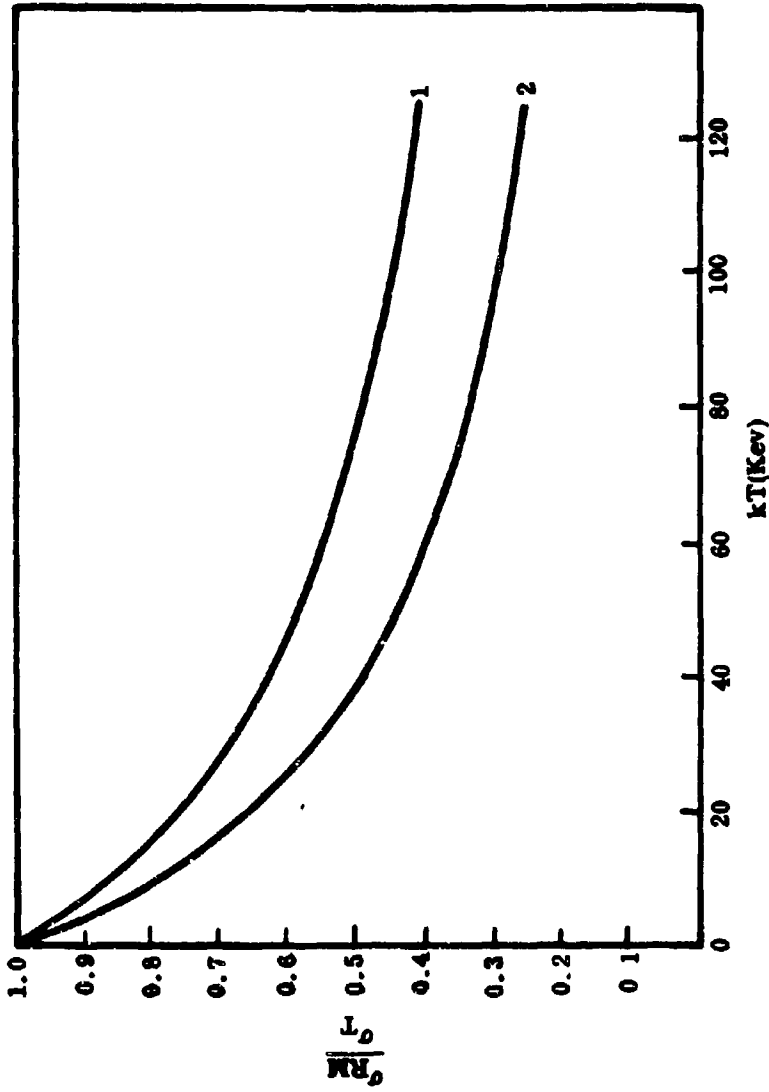


FIG. 8-13 RELATIVE "ROSSELAND MEAN COMPTON SCATTERING CROSS SECTIONS" AS A FUNCTION OF TEMPERATURE.
 (CURVE 1: ROSSELAND MEAN OF THE KLEIN-NISHINA CROSS SECTION)
 (CURVE 2: ROSSELAND MEAN OF THE EFFECTIVE KLEIN-NISHINA CROSS SECTION DERIVED BY SAMPSON)

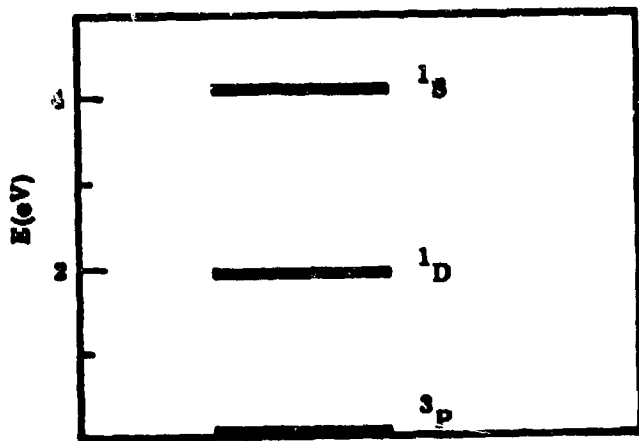


FIG. 8-14 ENERGY-LEVEL DIAGRAM OF THE TERMS OF THE OI $2s^2 2p^4$ CONFIGURATION.

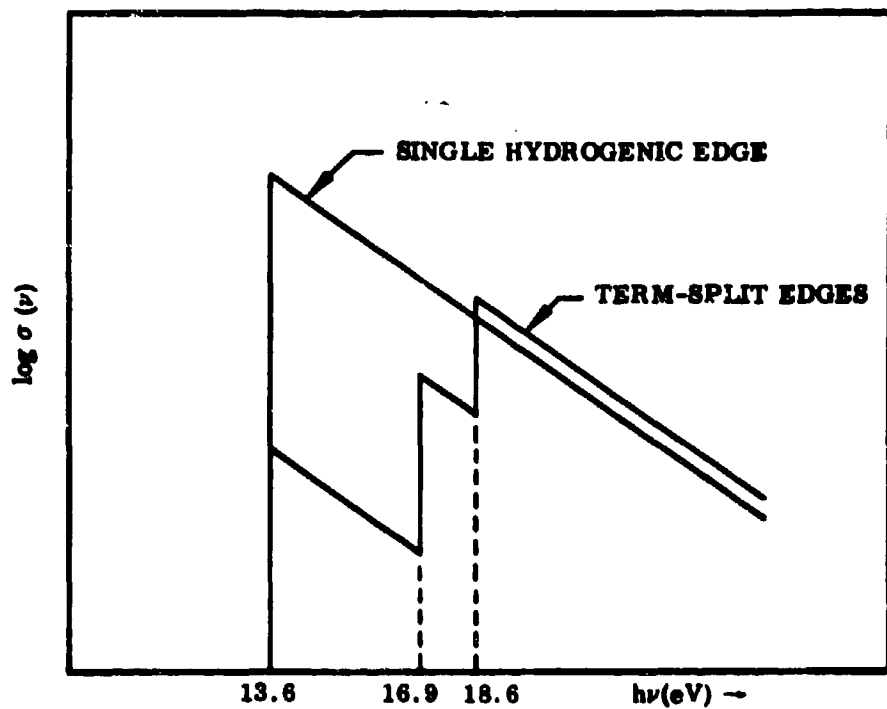


FIG. 8-15 TERM SPLITTING OF THE OI $2s^2 2p^4(3P)$ PHOTOELECTRIC EDGES.

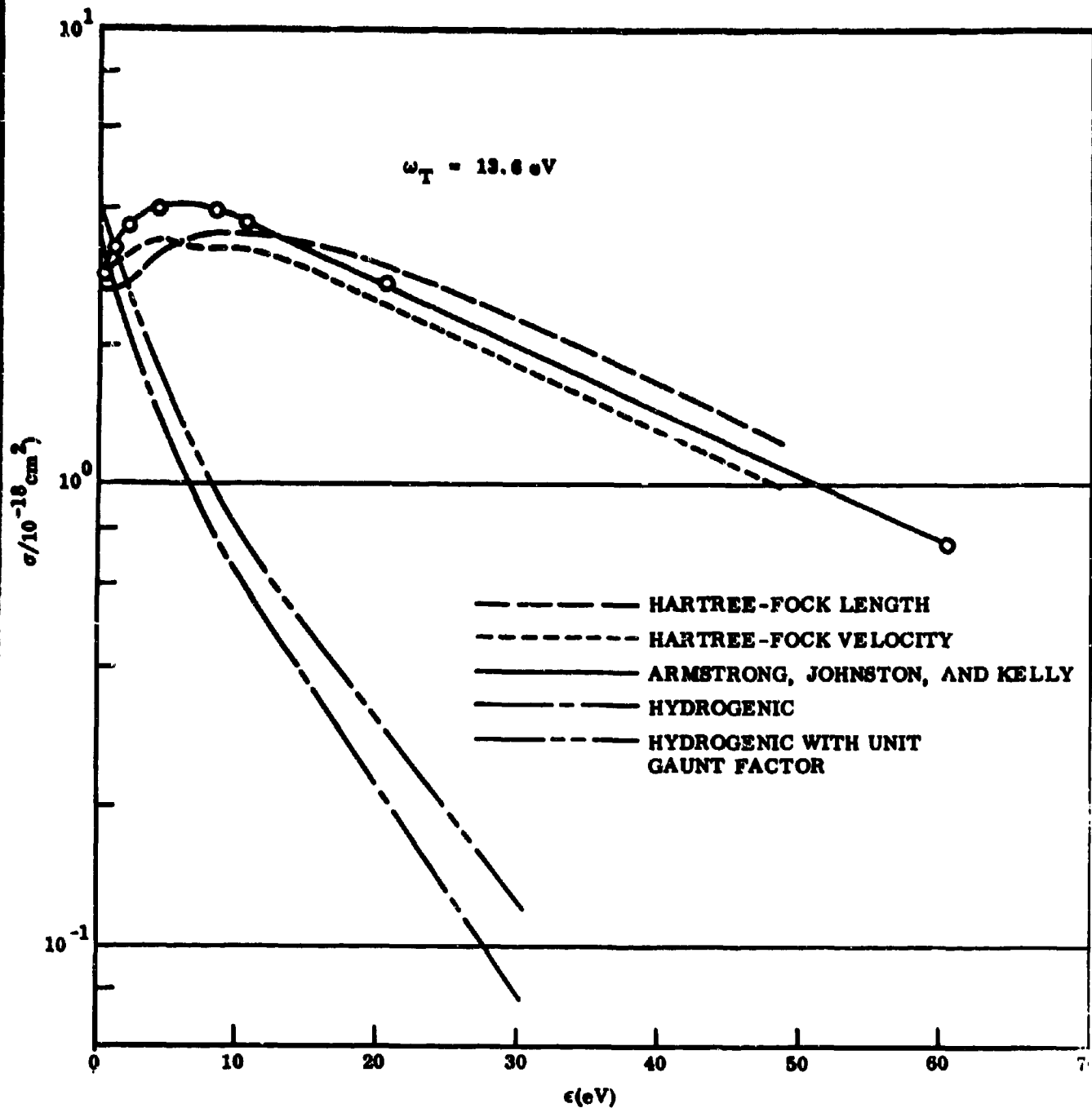


FIG. 8-16 A COMPARISON OF SEVERAL CALCULATIONS OF THE PHOTOIONIZATION CROSS SECTION FOR $\text{OI } 2s^2 2p^4(^3P) \rightarrow 2s^2 2p^3(^4S)\epsilon$ WHERE ϵ IS THE ENERGY OF THE PHOTOEJECTED ELECTRON.

References

- Aiken, H.H., Harvard Problem Report 27, Computation of the Intensities of Vibrational Spectra of Electronic Bands in Diatomic Molecules (AF Problem 56, Harvard Computation Laboratory), 1951.
- Alder, K., A. Bohr, T. Huus, B. Mottelson, and A. Winther, *Revs. Modern Phys.* 28, 432, 1956.
- Allen, C.W., Astrophysical Quantities, (The Athlone Press, London), 2nd Edition, 1963.
- Allen, R., B. Kivel, R. Taylor, and A. Textoris, Opacity of Low-Temperature Air, Air Force Weapons Laboratory Report, AFWL-TR 65-144, Feb., 1966.
- Aller, L. H., Astrophysics, The Atmospheres of the Sun and Stars, (Ronald Press Co., New York), 2nd Edition, 1963.
- Altick, P.L. and A.E. Glassgold, *Phys. Rev.* 133, A632, 1964.
- Altick, P.L. in Excited State Wave Functions, Air Force Weapons Laboratory Report, WL TR-64-172, by Kelly, Sokoloff and Armstrong, 1965.
- Armstrong, B.H., D.H. Holland, and R.E. Meyerott, Absorption Coefficients of Air from 22,000° to 220,000°, Air Force Special Weapons Center Report, AFSWC-TR-58-36, 1958.
- Armstrong, B.H. and H.P. Kelly, *J. Opt. Soc. Am.* 49, 949, 1959.
- Armstrong, B.H., Mean Absorption Coefficients of Air, Nitrogen and Oxygen from 22,000° to 220,000°, Lockheed Missiles and Space Company Report, LMSC 49759, 1959a.
- Armstrong, B.H., *Proc. Phys. Soc. (London)* 74, 136, 1959b.
- Armstrong, B.H., J. Sokoloff, R.W. Nicholls, D.H. Holland, and R.E. Meyerott, *J. Quant. Spectry. Radiative Transfer* 1, 143, 1961.
- Armstrong, B.H., D.E. Buttrey, L. Sartori, A.J.F. Siegert, and J.D. Weisner, Radiative Properties of High Temperature Gases, Air Force Special Weapons Center Report, AFSWC-TR-61-72, 1961.
- Armstrong, B.H. and H. Aroeste, *J. Quant. Spectry. Radiative Transfer* 4, 829, 1964a.
- Armstrong, B.H., *J. Quant. Spectry. Radiative Transfer* 4, 207, 1964b.
- Armstrong, B.H., R.R. Johnston, and P.S. Kelly, Opacity of High-Temperature Air, Air Force Weapons Laboratory Report, TR 65-17, 1965a.

- Armstrong, B.H., R.R. Johnston, and P.S. Kelly. *J. Quant. Spectry. Radiative Transfer* 5, 55, 1965b.
- Armstrong, B.H., *Astrophys. J.* 136, 309, 1962; *J. Quant. Spectry. Radiative Transfer* 5, 55, 1965c.
- Armstrong, B.H., R.R. Johnston, P.S. Kelly, H.E. DeWitt, and S.G. Brush, Opacity of High-Temperature Air, in Progress in High Temperature Physics and Chemistry, Vol. I, Ed. by Carl Rouse, Pergamon Press, Oxford, in press, 1966.
- Ashkin, M., *Phys. Rev.* 141, 41, 1966.
- Ashley, E.N., Jr., EG&G Report B-2782, DASA 1506, 1964.
- Bacher, R.F., and S. Goudsmit, *Phys. Rev.* 46, 948, 1934.
- Baranger, M., Spectral Line Broadening in Plasmas, in Atomic and Molecular Processes, Ed. by D.R. Bates, (Academic Press, New York) 1962.
- Barnes, J.F. and R.D. Cowan, *Phys. Rev.* 132, 236, 1963.
- Bates, D.R., R.A. Buckingham, H.S.W. Massey, and J.J. Unwin, *Proc. Roy. Soc. (London)* A170, 322, 1939.
- Bates, D.R. and H.S.W. Massey, *Phil. Trans. Roy. Soc. (London)* A239, 269-304, 1943.
- Bates, D.R. *Monthly Notice Roy. Astron. Soc.* 106, 432, 1946a; 106, 423, 1946b.
- Bates, D.R. and M.J. Seaton, *Monthly Notice Roy. Astron. Soc.* 109, 698, 1949.
- Bates, D.R., *Proc. Roy. Soc. (London)* A196, 217, 1949.
- Bates, D.R., and A. Damgaard, *Phil. Trans. Roy. Soc. (London)*, A242, 101, 1949.
- Bates, D.R., *Monthly Notice Roy. Astron. Soc.* 112, 614, 1952.
- Bennett, R.G. and F.W. Dalby, *J. Chem. Phys.* 31, 434, 1959.
- Bennett, R.G. and F.W. Dalby, *J. Chem. Phys.* 32, 1111, 1960a.
- Bennett, R.G. and F.W. Dalby, *J. Chem. Phys.* 32, 1716, 1960b.
- Berger, J.M., *Astrophys. J.* 124, 550, 1956.
- Bernstein, J. and F.J. Dyson, The Continuous Opacity and Equations of State of Light Elements at Low Densities, General Atomic Report, GA-848, 1959.

- Bethe, H.A., Quantenmechanik der Ein- und Zwei-Elektronenprobleme, Handbuch der Physik, Bd 24/1, (Springer, Berlin) 1933.
- Bethe, H., The Specific Heat of Air to 25,000°C, OSRP Report 369, 1942.
- Bethe, H.A., and E.E. Salpeter, Quantum Mechanics of One- and Two-Electron Systems, (Academic Press, New York) 1957.
- Bethke, G.W., J. Chem. Phys. 31, 669, 1959a.
- Bethke, G.W., J. Chem. Phys. 31, 662, 1959b.
- Biberman, L.M. and G.E. Norman, Optics and Spectroscopy 8, 230, 1960.
- Biberman, L.M., G.E. Norman and Ul'ianov, Optics and Spectroscopy 10, 297, 1961.
- Biberman, L.M., G.E. Norman and Ul'ianov, Astronom. Zh. 39, 107, 1962, English transl: Soviet Astron. -AJ 6, 77, 1962.
- Biberman, L.M. V.S. Borob'ev, and G.E. Norman, Optics and Spectroscopy 14, 176, 1963.
- Biberman, L.M. and G.E. Norman, J. Quant. Spectry, Radiative Transfer 3, 221, 1963.
- Biedenharn, L., Phys. Rev. 102, 262, 1956.
- Biedenharn, L.C. and H. Van Dam, Quantum Theory of Angular Momentum, (Academic Press, New York) 1965.
- Boldt, G., Z. Phys. 154, 319, 330, 1959.
- Bond, J.W., Jr., K.M. Watson and J.A. Welch, Jr., Atomic Theory of Gas Dynamics (Addison-Wesley, Reading, Mass.), 1965.
- Born, M. and J.R. Oppenheimer, Annalen der Physik 84, 457, 1927.
- Brachman, M.K. and R.E. Meyerott, Electronic Distribution Functions and Thermodynamic Properties at High Temperatures, Argonne National Lab., Report ANL 4986, May, 1953.
- Brandt, W. and S. Lundqvist, Phys. Rev. 132, 2135, 1963.
- Brannen, E., F.R. Hunt, R.H. Adington and R.W. Nicholls, Nature 175, 810, 1955.
- Branscomb, L.M. and S. Smith, Phys. Rev. 98, 1127, 1955.
- Breene, R.G., J. Chem. Phys. 29, 512, 1958.

- Breene, R.G., Jr., and M.C. Nardone, *J. Opt. Soc. Am.* 50, 1111-1114, 1960; 51, 692, 1961; 53, 924-928, 1963.
- Breene, R.G., Jr., *Phys. Rev.* 128, 2190, 1962.
- Breene, R.G. and M.C. Nardone, *J. Quant Spectry, Radiative Transfer* 2, 273, 1962.
- Brewer, L., C.G. James, R.G. Brewer, F.E. Stafford, R.H. Berg, and G.M. Rosen, *Rev. Sci. Instr.* 33, 1450, 1962.
- Brinkley, S.R., J.G. Kirkwood, and J.M. Richardson, Tables of the Properties of Air Along a Hugoniot Curve and the Adiabatic Terminating in the Hugoniot, OSRD Report 3350, 1944.
- Brussaard, P.J., and H.C. Van de Hulst, *Rev. Modern Phys.* 34, 507, 1962.
- Budo, A., *Z. Physik* 96, 219, 1935; 98, 437, 1936; 105, 579, 1937.
- Burgess, A., *Monthly Notice Roy. Astron. Soc.* 118, 477, 1958.
- Burgess, A. and M.J. Seaton, *Monthly Notice Roy. Astron. Soc.* 120, 121, 1960.
- Burgess, A., *Memoirs of the Roy. Astron. Soc.* 69, Part I, 1964.
- Burke, P.G. and K. Smith, *Rev. Modern Phys.* 34, 458, 1962.
- Cashion, J.K., *J. Chem. Phys.* 39, 1872, 1963.
- Chamberlain, J.W., *Astrophys. J.* 128, 713, 1958.
- Chamberlain, J.W., Physics of the Aurora and the Airglow (Academic Press, New York), 1961.
- Chandrasekhar, S., An Introduction to the Study of Stellar Structure (Univ. of Chicago Press), 1939.
- Chandrasekhar, S., *Astrophys. J.* 102, 223, 1945a; 102, 395, 1945b.
- Chandrasekhar, S. and F. Breen, *Astrophys. J.* 104, 430, 1946.
- Chandrasekhar, S., Radiative Transfer (Oxford Univ. Press), 1950.
- Churchill, D.R., S.A. Hagstrom and R.K.M. Landshoff, The Calculation of the Spectral Absorption Coefficient of Heated Air, Lockheed Report 3-27-63-4, DASA Report 1465, 1963.
- Churchill, D.R., and S.A. Hagstrom, Infrared Absorption in Heated Air from Vibration-Rotation Bands of Nitric Oxide, Lockheed Report 2112-64-2, 1964.

- Churchill, D.R., S.A. Hagstrom, and R.K.M. Landshoff, *J. Quant. Spectry. Radiative Transfer* 4, 291, 1964.
- Churchill, D.R. and R.E. Meyerott, *J. Quant. Spectry. Radiative Transfer* 5, 69, 1965.
- Churchill, D.R., B.H. Armstrong and K.G. Mueller, Absorption Coefficients of Heated Air: A Compilation to 24,000°, Lockheed Report 4-77-65-1, 1965.
- Compton, A.H., X-Rays and Electrons (D. Van Nostrand Co., New York), 1926.
- Condon, E.U., *Phys. Rev.* 28, 1182, 1926.
- Condon, E.U., *Phys. Rev.* 32, 858, 1928.
- Condon, E.U. and G.H. Shortley, The Theory of Atomic Spectra (Cambridge Univ. Press, Reprinted (1957)), 1935.
- Condon, E.U., *Am. J. Phys.* 15, 365, 1947.
- Cooley, J.W., *Mathematics of Computation* 15, 363, 1961a.
- Cooley, J.W., AEC Report No. NYO-9490, 1 May, 1961h.
- Coolidge, A.S., H.M. James and R.D. Present. *J. Chem. Phys.* 4, 193, 1936.
- Cooper, J.W., *Phys. Rev.* 128, 681, 1962.
- Cooper, John W. and J.B. Martin, *Phys. Rev.* 126, 1482, 1962.
- Cowan, R.D. and J. Ashkin, *Phys. Rev.* 105, 144, 1957.
- Cox, A.N., *J. Quant. Spectry, Radiative Transfer* 4, 737, 1964.
- Cox, A.N., *Astrophys. J. Supplement* 95, 1965.
- Craggs, J.D. and H.S.W. Massey, The Collision of Electrons with Molecules, *Handbuch der Physik* 37/1, 314, Ed. S. Flügge (Springer, Berlin), 1959.
- Dalby, F.W., Transition Probabilities of Molecular Spectra, *Handbuch der Physik* 27, 464, Ed. S. Flügge (Springer, Berlin), 1964.
- Dalgarno, A., and D. Parkinson, *J. Atmos. and Terr. Phys.* 18, 335, 1960.
- Dalgarno, A., *J. Opt. Soc. Am.* 53, 1223, 1963.
- Dalgarno, A., R.J.W. Henry, and A.L. Stewart, *Planetary and Space Science* 12, 235, 1964.
- Dalgarno, A. and N. Lane, *Astrophys. J.* 145, 623, 1966.

- Davidson, N., Statistical Mechanics (McGraw-Hill, New York), 1962.
- Davis, H.J., Thermal Radiation from High-Temperature Air, Harry Diamond Laboratories Technical Report TR-1225, May, 1964.
- Demtroder, W., Z. Physik 166, 42, 1962.
- Dennison, D.M., Phys. Rev. 28, 318, 1926.
- DeVore, R.V., Phys. Rev. 136, A666, 1964; with errata Phys. Rev. 140, AB3, 1965.
- Ditchburn, R.W. and D.W.O. Heddle, Proc. Roy. Soc. (London) A220, 61, 1953.
- Ditchburn, R.W. and D.W.O. Heddle, Proc. Roy. Soc. (London) A226, 509, 1954.
- Ditchburn, R.W. and P.A. Young, J. Atmos. and Terr. Phys. 24, 127, 1962.
- Ditchburn, R.W. and U. Öpik, Photoionization Processes in Atomic and Molecular Processes, Ed. by D.R. Bates (Academic Press, New York and London), 1962.
- Dirac, P.A.M., The Principles of Quantum Mechanics, (Clarendon Press, Oxford), 3rd Ed., 1947.
- Dixon, R.N. and R.W. Nicholls, Can. J. Phys. 36, 127, 1958.
- Dunham, J.L., Phys. Rev. 41, 713, 721, 1932.
- Earls, L.T., Phys. Rev. 48, 423, 1935.
- Eddington, A.S., The Internal Constitution of the Stars (Cambridge Univ. Press, 1926, Dover Ed.), 1959.
- Edmonds, A.R., Angular Momentum in Quantum Mechanics, (Princeton Univ. Press), 1957.
- Elsasser, W.M., Phys. Rev. 54, 126, 1938.
- Elsasser, W., Heat Transfer by Infrared Radiation in the Atmosphere (Harvard Meteorological Studies No. 6, Harvard Univ. Press), 1942.
- Elwert, G., Ann. Physik 34, 178, 1939.
- Fermi, E., Z. Physik 26, 54, 1924.
- Fermi, E., Nuclear Physics, Notes compiled by Orear, J., Rosenfeld, A.H., and Schluter, R.A. (Univ. of Chicago Press, Chicago), 1950.
- Feynman, R.P., Metropolis, and E. Teller, Phys. Rev. 75, 1561, 1949.

- Feynman, R.P., Quantum Electrodynamics (W.A. Benjamin, Inc., New York, Second Printing with corrections. First printing, Dec., 1961), 1962.
- Firsov, O.B. and M.I. Chibisov, Soviet Physics JETP 12, 1235, 1961.
- Fowler, R.H., Statistical Mechanics (Cambridge Univ. Press) 2nd Edition, 1936.
- Franck, J., Transactions of the Faraday Society 21, 536, 1925.
- Franklin, Philip, A Treatise on Advanced Calculus (John Wiley and Sons, Inc., New York), 1940.
- Fraser, P.A. and W.R. Jarman, Proc. Phys. Soc. (London) A66, 1145, 1953.
- Fraser, P.A., W.R. Jarman and R.W. Nicholls, Astrophys. J. 119, 286, 1954.
- Fraser, P.A., Can. J. Phys. 32, 515, 1954a.
- Fraser, P.A., Proc. Phys. Soc. (London) A67, 939, 1954b.
- Fraser, P.A., Scientific Report No. 6, Contract AF 19(604)-1718, University of Western Ontario, 1958.
- Freeman, B.E., Opacity and Absorption Coefficients for Ionic Air, General Atomic Report, GAMD-4566, 1963.
- Froese, C., Can. J. Phys. 41, 1895, 1963.
- Gaunt, J.A., Trans. Roy. Soc. (London) A228, 195, 1928.
- Gaunt, J.A., Proc. Roy. Soc. A126, 654; Phil. Trans. Roy. Soc. (London) A229, 163, 1930.
- Gaydon, A.G., and R.W.B. Pearse, Proc. Roy. Soc. (London) A173, 37, 1939.
- Gaydon, A.G., Dissociation Energies (Chapman and Hall), 2nd Ed., 1953.
- Gibson, Mrs. J., M.S. Thesis, Stanford University, 1962.
- Gilmore, F.R., Equilibrium Composition and Thermodynamic Properties of Air to 24,000°K, Rand Memorandum No. 1543, 1955.
- Gilmore, F.R. and A.L. Latter, Approximate Values for the Continuous Absorption Coefficient of Air Between 2 and 600 Volts, RM-1551, 1955.
- Gilmore, F.R., J. Quant. Spectry. Radiative Transfer 5, 125, 1965a.
- Gilmore, F.R., J. Quant. Spectry. Radiative Transfer 5, 369, 1965b.

- Goldberg, L., W.H. Parkinson and E.M. Reeves, *Astrophys. J.*, 1965.
- Goldberger, M.L. and K.M. Watson, Collision Theory (John Wiley), 1964.
- Golden, S.A. and R.V. Miller, Approximate Calculations of Spectral Absorption Coefficients of Diatomic Molecules I, Rocketdyne Report R-5393, 1963.
- Gombás, P., *Revs. Modern Phys.* 35, 512, 1963.
- Goody, R.M., *Quant. J. Roy. Met. Soc.* 78, 165, 1952.
- Goody, R.M., Atmospheric Radiation, Theoretical Basis (Oxford Univ. Press), 1964.
- Gordon, W., *Ann. Physik* (5) 2, 1031, 1929.
- Granmontagne, R., J. D'Incan and J. Janin, *J. de Physique et la Radium* 20, 598, 1959.
- Grant, I.P., *Monthly Notice Roy. Astron. Soc.* 118, 241, 1958.
- Green, L.C., P. Rush, and C. Chandler, *Astrophys. J. Suppl.* 3, 37, 1957.
- Green, J.M., The Free-Free Gaunt Factor in an Ionized Medium, Rand Research Memorandum RM-2223-AEC, July, 1958.
- Griem, H.R., Plasma Spectroscopy (McGraw-Hill Book Co., New York), 1964.
- Hagan, L., Ph.D. Thesis, University of California, UCRL 19620, 1963.
- Hall, H., *Revs. Modern Phys.* 8, 358, 1936.
- Halman, M. and I. Laulicht, *J. Chem. Phys.* 42, 137, 1965.
- Hartree, D.R., *Repts. Progr. Phys.* 11, 113, 1948.
- Hartree, D.R., The Calculation of Atomic Structures (John Wiley and Sons, Inc., New York), 1957.
- Haycock, Miss S., Line Intensities in Diatomic Electronic Spectra. The Effect of Vibration-Rotation Interaction, M.Sc. Thesis, University of Western Ontario, 1963.
- Hedde, D.W.O., *J. Opt. Soc. Am.* 54, 264, 1964.
- Heitler, W., The Quantum Theory of Radiation (Clarendon Press, Oxford), 3rd Edition, 1954.

- Herman, F. and S. Skillman, Atomic Structure Calculations (Prentice-Hall, Inc., Englewood Cliffs, New Jersey), 1963.
- Herman, R.C. and R. Rubin, *Astrophys. J.* 121, 2, 1955.
- Herman, R.C., R. Rothery and R. Rubin, *J. Mol. Spectroscopy* 2, 369, 1958.
- Heron, S., R.W.P. McWhirter, E.H. Roderick, *Nature* 174, 564, 1954.
- Heron, S., R.W.P. McWhirter, E.H. Roderick, *Proc. Roy. Soc. (London)* A234, 565, 1956.
- Herzberg, G., Molecular Spectra and Molecular Structure, I. Spectra of Diatomic Molecules (D. Van Nostrand, Princeton, New Jersey), 1950.
- Hesser, J.E. and K. Dressler, *Astrophys. J.* 142, 389, 1965.
- Hillendahl, R.W., Approximation Techniques for Radiation-Hydrodynamics Computations, Lockheed Missiles and Space Co., Report LMSC 3-27-64-1, Feb., 1964. See also
- Carter, D.S., Methods for the Approximate Determination of Radiative Energy Transfer in the Case of Spherical Symmetry, Lockheed Missiles and Space Division Report 2-57-61-1, June, 1961.
- Hirschfelder, J.O. and J.L. Magee, Opacity and Thermodynamic Properties of Air at High Temperatures, Los Alamos Report 296, 1945.
- Hirschfelder, J.O., and J.L. Magee, Blast Wave, LA 2000, 1958, (report written, 1947).
- Holstein, T., Westinghouse Scientific Paper, 65-1E2-GASES-P2, 1965m (unpublished).
- Hönl, H. and F. London, *Z. Physik* 33, 803, 1925.
- Howell, K.M., Revised Tables of ϵ -j Symbols, Research Report 59-1, University of Southampton, 1959.
- Huebner, W.F., *J. Quant. Spectry. Radiative Transfer* 4, 753-760, 1964.
- Hummer, , *Memoirs of the Royal Astronomical Society*, 1966.
- Hundley, R.O. Bremsstrahlung During the Collision of Low-Energy Electrons with Neutral Atoms and Molecules, Rand Research Memorandum RM-3334-ARPA, Oct., 1962.
- Hurley, A.C., *J. Chem. Phys.* 36, 1117, 1962.

- James, T.C., J. Chem. Phys. 32, 1770, 1960.
- James, T.C., J. Chem. Phys. 35, 767, 1961.
- Janin, J. and J. d'Incan, Comptes Rendus (Paris) 246, 3436, 1958.
- Jarmain, W.R. and P.A. Fraser, Proc. Phys. Soc. (London) A66, 1153, 1953.
- Jarmain, W.R., P.A. Fraser and R.W. Nicholls, Astrophys. J. 118, 228, 1953.
- Jarmain, W.R. and R.W. Nicholls, Can. J. Phys. 32, 201, 1954.
- Jarmain, W.R., P.A. Fraser and R.W. Nicholls, Astrophys. J. 122, 55, 1955.
- Jarmain, W.R., J. Chem. Phys. 31, 1137, 1959.
- Jarmain, W.R., Can. J. Phys. 38, 217, 1960.
- Jarmain, W.R., Numerical Solution of the Schroedinger Equation, Scientific Report 6, Contract AF 19(604)-4560, 1961.
- Jarmain, W.R., Can. J. Phys. 41, 414, 1963a.
- Jarmain, W.R., Can. J. Phys. 41, 1926, 1963b.
- Jarmain, W.R. and R.W. Nicholls, Proc. Phys. Soc. (London) 84, 417, 1964.
- Jarmain, W.R. and R.W. Nicholls, Proc. Phys. Soc. (London) (in press), 1966.
- Jeunehomme, M., J. Chem. Phys. 42, 4086, 1965.
- Jevons, W., Band Spectra of Diatomic Molecules (The Physical Society, London), 1932.
- John, T.L., Monthly Notice Roy. Astron. Soc. 128, 93, 1964; 131, 315, 1966.
- Johnson, R.C., An Introduction to Molecular Spectra (Methuen, London), 1949.
- Johnston, R.R., Phys. Rev. 136, A958, 1964.
- Johnston, R.R., B.H. Armstrong, and O.R. Platas, J. Quant. Spectry. Radiative Transfer 5, 49, 1965.
- Kahn, F.D., Astrophys. J. 129, 205, 1959.
- Karzas, W.J. and R. Latter, Astrophys. J. Suppl. 6, 167, 1961.
- Keck, J.C., J.C. Camm, B. Kivel, and J. Wentink, Jr., Annals of Physics (New York) 7, 1, 1959.

- Keck, J.C., R.A. Allen and R.L. Taylor, *J. Quant. Spectry. Radiative Transfer* 3, 335, 1963.
- Keller, G. and R.E. Meyerott, The Ionization of Gas Mixtures in Stellar Interiors, ANL-4771, 1952 (1952a).
- Keller, G. and R.E. Meyerott, The Ionization of Gas Mixtures in Stellar Interiors. II The Average Number of Electrons Occupying Various Shells, ANL-4856, 1952 (1952b).
- Kelner, G. and R.E. Meyerott, *Astrophys. J.* 122, 32, 1955.
- Kelly, H.P., *Phys. Rev.* 131, 685, 1963.
- Kelly, P.S., Techniques for Calculation of F.P.C. and Nuclear Matrix Elements, Technical Report, Dept. of Physics, U.C.L.A., 1959.
- Kelly, P.S. and B.H. Armstrong, *Astrophys. J.* 129, 786, 1959.
- Kelly, P.S., *Astrophys. J.* 140, 1247, 1964a.
- Kelly, P.S., *J. Quant. Spectry. Radiative Transfer* 4, 117, 1964b.
- Kelly, P.S. in Excited-State Wave Functions by Kelly, Sokoloff, and Armstrong, Air Force Weapons Laboratory Report WL TR-64-172, 1965.
- Kennard, E.H., Kinetic Theory of Gases (McGraw-Hill Book Co., inc., New York), 1938.
- Khare, S. and M. Rudge, *Proc. Phys. Soc. (London)* 86, 355, 1965.
- King, R.B., *Astrophys. J.* 108, 87, 1948.
- Kivel, B. and H. Mayer, *J. Quant. Spectry. Radiative Transfer* 5, 13, 1965 (1965/1954).
- Kivel, B., H. Mayer and H. Bethe, *Annals of Physics (New York)* 2, 57, 1957.
- Kivel, B., Neutral Atom Bremsstrahlung, AVCO Research Report 247, June, 1966.
- Klein, O., *Z. Physik* 76, 221, 1932.
- Kolganoff, V., Basic Methods in Transfer Problems (Oxford Univ. Press), 1952.
- Kovacs, I., *Can. J. Phys.* 38, 955, 1960.
- Kramers, H.A., *Phil. Mag.* 46, 836, 1923.
- Kronig, R.L. and I.I. Rabi, *Phys. Rev.* 29, 262, 1927.

- Ladenburg, R., and F. Reiche, Ann. Phys. 42, 181, 1913.
- Landau, L.D. and E.M. Lifshitz, Quantum Mechanics (Pergamon Press, London), 1959.
- Landau, L. and E. Lifshitz, The Classical Theory of Fields (Addison-Wesley, Reading, Mass.) 2nd Ed., Section 70, 1962.
- Latter, R., Phys. Rev. 99, 510, 1955a.
- Latter, R., Phys. Rev. 99, 1814, 1955b.
- Lawrence, G.M., J. Quant. Spectry. Radiative Transfer 5, 359, 1965.
- Layzer, David, Ann. Phys. 8, 271 (New York), 1959.
- Learner, R.C.M., Ph.D. Thesis, University of London, 1961;
Proc. Roy. Soc. (London), 1962.
- Levinson, I.B., and A.A. Niketin, Handbook for Theoretical Computation of Line Intensities in Atomic Spectra, (Russian Translation by Israel Program for Scientific Translations, Daniel Davey and Co., Inc., 257 Park Ave. South, New York), 1965.
- Liberman, D., Upper Limits on the Rosseland Mean Opacity, Los Alamos Report LA-2700, 1962.
- Lippincott, E.R., J. Chem. Phys. 21, 2070, 1953; 23, 603, 1955.
- Lofthus, A., The Molecular Spectrum of Nitrogen, Spectroscopic Report 2, Department of Physics, University of Oslo, 1960.
- Low, F.E., Phys. Rev. 110, 974, 1958.
- Magee, J.L. and J.O. Hirschfelder, Thermal Radiation Phenomena, LA-1020 Chapter IV (unclassified) Reproduced in LA-2000 (1947/1958) Blast Wave, H.A. Bethe, K. Fuchs, J.O. Hirschfelder, J.L. Magee, R.E. Pierls and J. von Neumann.
- Main, R.P. and E. Bauer, Opacity of Carbon-Air Mixtures at Temperatures from 3000° to 10,000°, Publication U-3046, Aeronutronic Division of Philco Corporation, 1965.
- Manneback, C., Physica 17, 1001, 1951.
- March, N.H., Advances in Physics 6, 21, 1957.
- Marmo, F.F., J. Opt. Soc. Am. 47, 1186, 1953.
- Marr, G.V., Proc. Phys. Soc. (London) 83, 293, 1964a.

- Marr, G.V., *Can. J. Phys.* 42, 282, 1964b.
- Marshak and Bethe, *Astrophys. J.* 91, 239, 1940.
- Massey, H.S.W. and R. Smith, *Proc. Roy. Soc. (London)* A155, 472, 1936.
- Maue, A., *Ann. Phys.* 13, 161, 1932.
- Mayer, H., Methods of Opacity Calculations, Los Alamos Scientific Laboratory Report LA 647, unpublished, 1947.
- Mayer, H., *J. Quant. Spectry. Radiative Transfer* 4, 585 (1st Opacity Conf. Issue), 1964.
- McDowell, M.R.C., As quoted by C.F. Barnett, J.A. Ray, and J.C. Thompson in Atomic and Molecular Collision Cross Sections of Interest in Controlled Thermonuclear Research, Oak Ridge National Lab. Report ORNL-3113, Revised, August, 1964.
- Mentall, J. and R.W. Nicholls, *Proc. Phys. Soc. (London)* 86, 873, 1965.
- Menzel, D. and C. Pekeris, *Monthly Notice Roy. Astron. Soc.* 96, 77, 1935.
- Menzel, D.H. and L. Goldberg, *Astrophys. J.* 84, 1, 1936.
- Meyerott, R.E., *Phys. Rev.* 95, 72, 1954.
- Meyerott, R.E., Absorption Coefficients of Air from 6000° to 18,000°K, Rand Memorandum, RM-1554, 1955.
- Meyerott, R.E., The Threshold of Space, Ed. M. Zelikoff (Pergamon, New York), p. 259, 1956.
- Meyerott, R.E., Radiant Heat Transfer to Hypersonic Vehicles, Combustion and Propulsion, Third Agard Colloquium (Pergamon, New York) p. 431, 1958.
- Meyerott, R.E., J. Sokoloff and R.W. Nicholls, Absorption Coefficients of Air, Geophysical Research Paper No. 68, Geophysical Research Directorate, Air Force Cambridge Research Laboratories, TR 60-277, 1960.
- Miescher, E., *J. Quant. Spectry. Radiative Transfer* 2, 421, 1962.
- Milne, E.A., *Phil. Mag.* 47, 209, 1924.
- Milne, E.A., Thermodynamics of the Stars, in *Handbuch der Astrophysik*, Band III. Erste Halfte, Herausgeben von G. Eberhard, A. Kohlschutter, and H. Ludendorff (Springer Verlag, Berlin), 1930.

- Mitchell, A.C.G. and M.W. Zemansky, Resonance Radiation and Excited Atoms (Cambridge Univ. Press), 1934.
- Mittleman, M.H. and F.A. Wolf, Phys. Rev. 128, 2686, 1962.
- Moiseiwitsch, B., Proc. Phys. Soc. (London) 81, 35, 1963.
- Moore, C.E., Atomic Energy Levels, Circular of the National Bur. Stand. 467, Washington, Vol. I, 1949, Vol. II, 1952, Vol. III, 1958.
- Morse, P.M., Phys. Rev. 34, 57, 1929.
- Morse, P.M. Astrophys. J. 92, 27, 1940.
- Morse, P.M. and H. Feshbach, Methods of Theoretical Physics (McGraw-Hill Book Co., Inc., New York), 1953.
- Moszkowski, S.A. and R.E. Meyerott, Opacity Calculations for Light Elements and Mixtures, Argonne Nat. Lab. Report ANL 4743, 1951.
- Moszkowski, S.A., Rand Report RM-2610-AEC, 1960; Prog. Theor. Phys. 28, 1, 1962.
- Mott, N.F. and A.S.W. Massey, The Theory of Atomic Collisions, (Clarendon Press, Oxford), 2nd Ed., 1949.
- Mueller, K.G., The Absorption Coefficient of NO₂, Lockheed Report 2-27-63-1, DASA Report 1416, 1963.
- Mulliken, R.S., Revs. Modern Phys. 3, 89, 1931.
- Murty, M., Condon Lock of Diatomic Molecular Spectra, M.Sc. Thesis, University of Western Ontario (in preparation for publication), 1964.
- Murty, M. and R.W. Nicholls, Nature (in press), 1966.
- Naqvi, A., J. Quant. Spectry. Radiative Transfer 4, 597, 1964.
- Nicholls, R.W. and W.R. Jarman, J. Chem. Phys. 23, 1561, 1955.
- Nicholls, R.W. and W.R. Jarman. Proc. Phys. Soc. (London) A69, 253, 1956.
- Nicholls, R.W., W.H. Parkinson, D. Robinson and W.R. Jarman, Proc. Phys. Soc. (London) A69, 713, 1956.
- Nicholls, R.W., Phys. Rev. 77, 44, 1950.

- Nicholls, R.W., Proc. Phys. Soc. (London) 74, 133, 1959.
- Nicholls, R.W., P.A. Fraser and W.R. Jarman, Combustion and Flame 3, 13, 1959.
- Nicholls, R.W., Can. J. Phys. 38, 1705, 1960.
- Nicholls, R.W., P.A. Fraser, W.R. Jarman, and R.P. McEachran, Astrophys. J. 131, 399, 1960.
- Nicholls, R.W., J. Res. Nat. Bur. Standards 65A, 451, 1961.
- Nicholls, R.W. and A. Stewart, Allowed Transitions, Chapter 2, Atomic and Molecular Processes, Ed. D.R. Bates (Academic Press), 1962.
- Nicholls, R.W., J. Quant. Spectry. Radiative Transfer 2, 433, 1962a.
- Nicholls, R.W., Can. J. Phys. 40, 523, 1962b.
- Nicholls, R.W., Can. J. Phys. 40, 1772, 1962c.
- Nicholls, R.W., J. Res. Nat. Bur. Standards 66A, 227, 1962d.
- Nicholls, R.W., Nature 193, 966, 1962e.
- Nicholls, R.W., J. Chem. Phys. 38, 1029, 1963a.
- Nicholls, R.W., Nature 199, 794, 1963b.
- Nicholls, R.W., J. Res. Nat. Bur. Standards 68A, 75, 1964a.
- Nicholls, R.W., J. Res. Nat. Bur. Standards 68A, 535, 1964b.
- Nicholls, R.W., Nature 204, 373, 1964c.
- Nicholls, R.W., Annales de Geophysique 20, 144, 1964d.
- Nicholls, R.W., J. Chem. Phys. 42, 804, 1965a.
- Nicholls, R.W., Astrophys. J. 141, 819, 1965b.
- Nicholls, R.W., J. Res. Nat. Bur. Standards 69A, 369, 1965c.
- Nicholls, R.W., J. Res. Nat. Bur. Standards 69A, 397, 1965d.
- Nicholls, R.W., in preparation for publication, 1965e.
- Nicholls, R.W., J. Quant. Spectry. Radiative Transfer 5, 647, 1965f.
- Nicholls, R.W., Proc. Phys. Soc. (London) 85, 159, 1965g .

- Nicholls, R.W., *Laboratory Astrophysics and Combustion Spectroscopy*, p. 413, *Supersonic Flow, Chemical Processes and Radiative Transfer AGARDOGRAPH* (ed. B. Olfe, Pergamon, New York), 1964b.
- Nicholls, R.W. *Proc. Phys. Soc. (London)* (in press), 1966.
- Norman, G.E. *Optics and Spectroscopy* 12, 183, 1962.
- Norman, G.E., *Optics and Spectroscopy* 14, 277, 1963.
- Norman, G.E., *Optics and Spectroscopy* 14, 315, 1963.
- Numerov, B., *Pub. Obs. Cont. Astrophys. Russ.* 2, 188, 1933.
- Ohmura, H. and T. Ohmura, *Astrophys. J.* 131, 8, 1960;
Phys. Rev. 121, 513, 1961.
- Ohmura, T., *Astrophys. J.* 140, 282, 1964.
- O'Malley, T., L. Spruch, and L. Rosenberg, *J. Math. Phys.* 2, 491, 1961.
- Oppenheimer, J.A., *Z. Physik* 55, 725, 1929; *Phys. Rev.* 31, 349, 1928.
- Ory, H.A., *Astrophys. J.* 139, 346, 1964a.
- Ory, H.A., *Astrophys. J.* 139, 557, 1964b.
- Pappert and S.S. Penner, *J. Quant. Spectry. Radiative Transfer* 1, 258, 1961.
- Patch, R.W., W.L. Shackelford and S.S. Penner. *J. Quant. Spectry. Radiative Transfer* 2, 263, 1962.
- Peach, G., *Monthly Notice Roy. Astron. Soc.* 124, 371, 1965.
- Peach, G., *Monthly Notice Roy. Astron. Soc.* 130, 361-377, 1965.
- Pearse, R.W.B. and A.G. Gaydon, *The Identification of Molecular Spectra*, (Chapman and Hall, London) 3rd Ed., 1963.
- Pekeris, C.L., *Phys. Rev.* 45, 98, 1934.
- Penner, S.S. and D. Weber, *J. Chem. Phys.* 21, 649, 1953.
- Penner, S.S., *Quantitative Molecular Spectroscopy and Gas Emissivities*, (Addison-Wesley, Reading, Mass), 1959.
- Penner, S.S. and M. Thomas, *Journal AIAA* 2, 1572, 1964.
- Phillips, J.G., *Proceedings of The Royal Society of Liege*, 1954.

- Phillips, J.G., *Astrophys. J.*, 1957.
- Phillips, J.G., The Spectrum of CN (University of California Press, Berkeley), 1963.
- Pillow, M.E., *Proc. Phys. Soc. (London)* A62, 237, 1949.
- Plass, G.N., H.L. Mayer, R.S. Wright, J.W. Rosengren, S.I. Schlesinger, L. Sashkin, and E.J. Browne, Methods for Calculating Thermodynamic and Optical Properties of Air, AFSWC-TR-57-34, 1957.
- Power, E.A., Introductory Quantum Electrodynamics (Longmans, Green, and Co., Ltd., London), 1964.
- Racah, G., *Phys. Rev.* 61, 186; 62, 438, 1942; 63, 367, 1943; 76, 1352, 1949.
- Raizer, Y.P., *Soviet Phys. JETP* 10, 769, 1960.
- Rees, A.L.G., *Proc. Phys. Soc. (London)* 59, 998, 1946.
- Reiche, F. and H. Rademacher, *Z. Physik* 39, 444, 1926; 41, 453, 1927.
- Rohrlich, F., *Astrophys. J.* 129, 441, 449, 1949.
- Roothaan, C.C.J. and P.S. Bagus, in Methods in Computational Physics, Vol. II, (Academic Press, Inc., New York), 1963.
- Roothaan, C.C.J. and P.S. Kelly, *Phys. Rev.* 131, 1177, 1963.
- Rose, M.E., Elementary Theory of Angular Momentum (John Wiley and Sons, New York), 1957.
- Rosseland, S., *Monthly Notices* 84, 525, 1924.
- Rotenberg, Manuel, et al., The 3-j and 6-j Symbols, (Cambridge Tech. Press), 1959.
- Rydberg, R., *Z. Physik* 73, 376, 1931.
- Rydberg, R., *Z. Physik* 80, 514, 1933.
- Salpeter, *Phys. Rev.* 120, 1528, 1960.
- Sampson, D.H., *Astrophys. J.* 129, 734, 1959.
- Schadee, A., *Bulletin Astronomisches, Nederland* 17, 341, 1964.
- Schiff, L.I., *Quantum Mechanics* (McGraw-Hill Book Co., Inc., New York) footnote, p. 256, 1949.

- Schiff, L.I., Quantum Mechanics (McGraw-Hill Book Co., Inc., New York), 2nd Ed., 1955.
- Schlapp, R., Phys. Rev. 39, 806, 1932.
- Schurin, B. and S.A. Clough, J. Chem. Phys. 38, 1855, 1963.
- Schwarzschild, K., Göttinger Nachrichten, p. 41, 1906.
- Schwenker, R.P., J. Chem. Phys. 42, 1895, 1965.
- Seaton, M.J., Proc. Roy. Soc. (London) A208, 408, 1951.
- Seaton, M.J., Monthly Notice Roy. Astron. Soc. 118, 504, 1958.
- Seaton, M.J., Revs. Modern Phys. 30, 979, 1958.
- Shore, B.W. and D.H. Menzel, Astrophys. J. Supplement Series, Vol. 12, No. 106, 187, 1965.
- Simon, A., J.H. Vander Sluis, L.C. Biedenharn, Tables of the Racah Coefficients, ORNL 1679, 1954.
- Slater, J.C. and H.M. Krutter, Phys. Rev. 47, 559, 1935.
- Slater, J.C., Quantum Theory of Atomic Structure (McGraw-Hill Book Co., Inc., New York), 1960.
- Sommerfeld, A., Atombau und Spektrallinien, 2 Aufl. Bd. 2, (Vieweg und Sohn, Braunschweig) 1939 and 1951.
- Spindler, R.J., J. Quant. Spectry. Radiative Transfer 5, 165, 1965.
- Steele, D., E.R. Lippincott, J.T. Vanderslice, Revs. Modern Phys. 34, 239, 1962.
- Stergis, C.G., Journal Atm. and Terr. Phys. 28, 273, 1966.
- Stewart, J.C. and K.D. Pyatt, Jr., Theoretical Studies of Optical Properties, Air Force Special Weapons Center Report, AFSWC-TR-61-71, 1961.
- Stewart, J.C. and M. Rotenberg, Phys. Rev. 140, A1508, 1965.
- Stobbe, M., Ann. d. Physik 7, 661, 1930.
- Stone, J., Radiation and Optics (McGraw-Hill), 1963.
- Strack, S., A.R.S. Journal 32, 1404, 1962.
- Strömngren, B., Zs. f. Astrophys. 4, 118, 1932; 7, 222, 1933.
- Sziklas, E.A., United Aircraft Report M-1688-1, 1961.

- Tanaka, Y., T. Namioka, A.S. Jursa, *Can. J. Phys.* 39, 1138, 1961.
- Tatum, J.B., *Astrophys. J. Supplement* (in press) 1966.
- Taylor, R., *J. Chem. Phys.* 39, 2354, 1963.
- Tolman, R.C., *The Principles of Statistical Mechanics* (Clarendon Press, Oxford), 1938
- Treanor, C.E. and W.H. Wurster, *J. Chem. Phys.* 32, 758, 1960.
- Tyte, D.C. and R.W. Nicholls, *Identification Atlas of Molecular Spectra 1: AlO* 1964a; *Identification Atlas of Molecular Spectra 1: Blue-Green System*, 1964b; *Identification Atlas of Molecular Spectra 2: N₂, Second Positive System*, 1964c; *Identification Atlas of Molecular Spectra 2: N₂⁺ First Negative System*, 1965, York University, Department of Physics.
- Unsold, A., *Physik der Sternatmosphären*, (Springer-Verlag, Berlin) 2nd Ed., 1955.
- Urey, H.C., *Astrophys. J.* 59, 1, 1924.
- Van de Hulst, H.C., *Light Scattering by Small Particles* (John Wiley, New York), 1957.
- Vanderslice, J.T., E.A. Mason, W.G. Maisch and E.R. Lippincott, *J. Mol. Spectroscopy* 3, 17, 1959.
- Vanderslice, J.T., E.A. Mason, W.G. Maisch and E.R. Lippincott, *J. Mol. Spectroscopy* 5, 83, 1960.
- Varsavsky, C.M., *The Calculation of Absolute Line Strengths in Atomic Spectra*, Thesis, Harvard University, 1958.
- Varsavsky, C.M., *Astrophys. J. Suppl. Ser.* 6, No. 53, 75, 1961.
- Voigt (see Van der Hulst and Reesnick) *Astrophys. J.* 106, 121, 1947.
- Vorobyov, V.S. and G.E. Norman, *Optics and Spectroscopy* 17, 96, 1964.
- Wacks, M.E. and M. Kraus, *J. Chem. Phys.* 35, 1902, 1961.
- Wacks, M.E., *J. Chem. Phys.* 41, 930, 1964.
- Wallace, L.V., *Astrophys. J. Supplement* 6, 455, 1962a; 7, 165, 1962b.
- Weber, D. and S.S. Penner, *J. Chem. Phys.* 26, 860, 1957.
- Weissler, G.L., In *Handbuch der Physik* 21, Ed. S. Flügge (Springer, Berlin), p. 304, 1956.

- Wentinck, T., L. Isaacson and J. Morreal, *J. Chem. Phys.* 41, 278, 1964.
- Wheeler, J. and R. Wildt, *Astrophys. J.* 95, 281, 1942.
- Whittaker, E.T. and G.N. Watson, *A Course of Modern Analysis* (Cambridge Univ. Press), 1952.
- Wiese, W.L., M.W. Smith, and B.M. Glennon, *Atomic Transition Probabilities*, U.S. Dept. of Commerce, National Bureau of Standards, Wash. D.C., May 1966 (NSRDS-NBS4, Vol. I).
- Wildt, R., *Astrophys. J.* 89, 295, 1939.
- Wilkinson, P.G., *J. Mol. Spectroscopy* 6, 1, 1961.
- Winans, J.G. and E.C.G. Stueckelberg, *Proceedings of the National Academy of America* 14, 867, 1928.
- Wray, K.L. and J.D. Teare, *J. Chem. Phys.* 36, 2582, 1962.
- Wu, T.Y., *Proc. Phys. Soc. (London)* A65, 965-972, 1952.
- Zare, R.N., E.O. Larson, R.A. Berg, *J. Mol. Spectroscopy*, 1965.

Appendix A

SPECTROSCOPIC PROPERTIES OF SIX IMPORTANT BAND SYSTEMS WHICH CONTRIBUTE TO THE OPACITY OF HEATED AIR

It was pointed out in Chapter 7 that the following six band systems

O_2 ($B^3\Sigma_u^- - X^3\Sigma_g^-$) Schumann-Runge

N_2 ($B^3\Pi_g - A^3\Sigma_u^+$) First Positive

N_2 ($C^3\Pi_u - B^3\Pi_g$) Second Positive

N_2^+ ($B^2\Sigma_u^+ - X^2\Sigma_g^+$) First Negative

NO ($B^2\Pi - X^2\Pi$) Beta

NO ($A^2\Sigma - X^2\Pi$) Gamma

make important contributions to the spectral absorption coefficient of heated air. Basic energy level diagrams which incorporate these transitions are displayed in Figs. 7-1, 7-2, 7-3, and 7-4.

It was also pointed out in section 7.3.3 describing the use of the SACHA code, which takes account of the contribution to the absorption coefficient of the line structure of molecular bands, that the absorption coefficient in the region of a line could be written

$$\mu_\nu = \left[\frac{N_{\text{total}}}{L_0 Q_{\text{vib-rot}}} P_{n''} \right] H_{n''\nu''J''}^{n'\nu'J'} \exp\left(-E_{\nu''J''}/T\right) \pi b(\nu) \quad (\text{A-1})$$

where

$$H_{n''v''J''}^{n'v'J'} = \frac{8\pi^2 L_0}{3hc} \frac{\omega_I}{(2S+1) \omega_\Lambda Q_{\text{nuclear}}} \nu_{n''v''J''}^{n'v'J'} R_e^2 (\bar{F}_{v'v''}) q_{v'v''} S_{J''\Lambda}^{J'\Lambda'} \quad (\text{A-2})$$

$$E_{v''J''} = \frac{hc}{k} [G_0(v'') + F_{v''}(J'')] \quad (\text{A-3})$$

and

$$\nu_{n''v''J''}^{n'v'J'} = \nu_{00} + F'(J') - F''(J'') + G'(v') - G''(v'') \quad (\text{A-4})$$

Further

$$F_v(J) = B_v J(J+1) - D_v J^2(J+1)^2 + \dots \quad (\text{A-5})$$

and

$$G(v) = \omega_e(v+1/2) - \omega_e x_e(v+1/2)^2 + \dots \quad (\text{A-6})$$

The quantities $\nu_{n''v''J''}^{n'v'J'}$ (line frequency), $E_{v''J''}$ (lower level energy), $S_{J''\Lambda}^{J'\Lambda'}$ (Hönl-London factor) depend entirely upon the type and structure of the molecular transition considered. In this appendix therefore, a detailed discussion is given of the form of $H_{n''v''J''}^{n'v'J'}$ for each of the above band systems, taking its properties into account. Much of the material which follows is based upon the report by Churchill, Hagstrom, and Landshoff (1963) on the SACHA code which has been discussed by Churchill and Meyerott (1965).

The symbols in the above formulae are standard (Herzberg, 1950) and values of molecular constants are taken either from papers cited below or from Herzberg's compilation in application of the formulae.

The O_2 ($B^3\Sigma_u^- - X^3\Sigma_g^-$) Schumann-Runge System

The allowed rotational transitions of a Schumann-Runge band are illustrated in Fig. A-1 which shows typical rotational energy levels, and the quantum numbers and symmetry properties associated with each. Each band has six strong branches: P_1 , P_2 , P_3 , R_1 , R_2 , R_3 for each of which ΔJ and ΔK is ± 1 . (The Q branch is forbidden in a $\Sigma - \Sigma$ transition.) The separation of these lines is such that the three R lines are so close together as are the P lines that the six lines often appear as one unresolved P and one unresolved R line. Six weak satellite branches of the form R_P , R_Q , P_R and P_Q for which $\Delta J \neq \Delta K$ are also illustrated in Fig. A-1. Alternate triplets in the P and R branches are missing since the oxygen atoms have zero nuclear spin. Even K rotational levels are missing in the X state and odd K rotational levels are missing in the B state. The SACHA calculations merged the three R-lines into one line and the three P-lines into another line by addition of the appropriate Hönl-London factors as Schumann-Runge lines do appear as singlets except at very high resolution.

The values of the Hönl-London factors were thus $3K''$ for P-lines and $3(K''+1)$ for R-lines. For each of the states, Eq. (A-5) is rewritten

$$F_v(K) = B_v K(K+1) - D_v K^2(K+1)^2 \quad (A-7)$$

The B_v and D_v values for the $X^3\Sigma$ state were calculated from the constants given by Herzberg (1950) and the values for the $B^3\Sigma$ state were taken from the work of Brix and Herzberg (1954). Thus the H-function of Eqs. (A-1 and A-2) for the Schumann-Runge system is

$$\begin{aligned}
 H_{n''v''J''}^{n'v'J'} &= H_{K'K''} = \frac{8\pi^2 L_0}{3hc} \frac{1}{3} \left(\frac{\omega_I}{Q_{\text{nuclear}}} \right) \nu_{K'K''} R_e^2 (r_{v'v''}) q_{v'v''} S_{K'K''} \\
 &= \frac{16\pi^2 L_0}{3hc} \nu_{K'K''} R_e^2 (r_{v'v''}) q_{v'v''} \begin{cases} K''+1 & \text{if } K' = K''+1 \\ K'' & \text{if } K' = K''-1 \end{cases} \quad (\text{A-8})
 \end{aligned}$$

for $K'' = 1, 3, 5 \dots$

The N_2 ($B^3\Pi_g - A^3\Sigma_u^+$) First Positive System

As is seen in Fig. A-2, which illustrates the branch structure of bands of the N_2 First Positive system, a $^3\Pi - ^3\Sigma$ band is very complicated, exhibiting as it does 27 possible branches, distributed between three sub-bands $^3\Pi_0 - ^3\Sigma^+$, $^3\Pi_1 - ^3\Sigma^+$, $^3\Pi_2 - ^3\Sigma^+$. Each sub-band has nine possible branches. For any band the nine principal branches $P_1, P_2, P_3, Q_1, Q_2, Q_3, R_1, R_2, R_3$ which obey all the selection rules are strongest, the ten P-form and Q-form satellite branches are somewhat weaker and the eight 'forbidden' N-form, O-form, S-form and T-form satellite branches (shown dotted in Fig. A-2) are extremely weak and neglected here. The remaining nineteen branches are included in the calculations.

Formulae for the levels of a $^3\Sigma$ state have been provided by Schlapp (1937). The spin splitting of the $A^3\Sigma$ state is known to be small and only approximately known at that. The $A^3\Sigma$ state was thus treated as an effective $^1\Sigma$ state as for the Schumann-Runge system described above. Eq. (A-7) was again used and the B_v and D_v constants calculated from the work of Naudé (1932). The triplet splitting of the $^3\Pi$ state was however taken into account using the formulae of Budo (1935) for any degree of uncoupling

$$F_{v1}(J) = B_v \left[J(J+1) - \sqrt{Z_1} - 2Z_2/3Z_1 \right] - D_v(J-1/2)^4 \quad (\text{A-9})$$

$$F_{v2}(J) = B_v \left[J(J+1) + 4Z_2/3Z_1 \right] - D_v(J+1/2)^4 \quad (\text{A-10})$$

$$F_{v3}(J) = B_v \left[J(J+1) + \sqrt{Z_1} - 2Z_2/3Z_1 \right] - D_v(J+3/2)^4 \quad (\text{A-11})$$

where

$$Z_1 = Y_v(Y_v-4) + \frac{4}{3} + 4J(J+1) \quad (\text{A-12})$$

$$Z_2 = Y_v(Y_v-1) - \frac{4}{9} + 2J(J+1) \quad (\text{A-13})$$

and $Y_v = A_v/B_v$ is a measure of the degree of coupling of the spin to the internuclear axis.

At high J numbers with $J = K+1$, K and $K-1$ respectively, F_{v1} , F_{v2} and F_{v3} are representative of the case 'b' coupling model of Hund. At low J numbers case 'a' holds. Further $F_{v2}(0)$, $F_{v3}(0)$ and $F_{v3}(1)$ are undefined because of the case 'a' requirement that $J \approx \Omega = |\Lambda + \Sigma|$. The B_v , D_v and Y_v values for each vibrational level were taken from the work of Budo (1935) and because Λ -doubling is small except at large K it is neglected here.

The H-function for the First Positive system of N_2 then becomes

$$H_{n''v''J''}^{n'v'J'} = H_{K'K''} = \frac{8}{9} \frac{\pi^2 L_0}{hc} \nu_{K'K''} R_e^2 (\bar{r}_{v'v''}) q_{v'v''} \times \begin{pmatrix} \frac{2}{3} & \text{for } K'' \text{ even} \\ \frac{4}{3} & \text{for } K'' \text{ odd} \end{pmatrix} S_{K''} \quad (\text{A-14})$$

where

$$3S_{K''} = S_{J''} = S_J ;$$

S_J taken for each respective branch and line from the tables of Budo (1937) as follows

<u>Line and branch</u>	<u>$S_J (J=J'')$</u>
$P_1(J+1)$	$\frac{J[J(J+2) u_1 + (J+2)(Y-2) + 2(J-1)(J+1)^2]^2}{(J+1)(2J+3) C_1(J)}$
$Q_1(J)$	$\frac{[(J^2+J-1) u_1 + (Y-2) + 2J(J^2-1)]^2}{J C_1(J)}$
$R_1(J-1)$	$\frac{(J^2-1) [(J+1) u_1 - Y + 2J^2]^2}{(2J-1) C_1(J)}$

Line and branch

$S_1(J=J'')$

$P_2(J+1)$

$$\frac{8 J^3 (J+2)}{(J+1) C_2(J)}$$

$Q_2(J)$

$$\frac{8(2J+1) (J^2+J-1)^2}{J(J+1) C_2(J)}$$

$R_2(J-1)$

$$\frac{8 (J-1) (J+1)^3}{J C_2(J)}$$

$P_3(J+1)$

$$\frac{J(J+2) [J u_3 - (Y-2) + 2J(J+2)]^2}{(2J+3) C_3(J)}$$

$Q_3(J)$

$$\frac{[(J^2+J-1) u_3 - (Y-2) + 2J(J+1) (J+2)]^2}{(J+1) C_3(J)}$$

$R_3(J-1)$

$$\frac{(J+1) [(J^2-1) u_3 + (J-1) (Y-2) + 2J^2(J+2)]^2}{J(2J-1) C_3(J)}$$

$P_{Q_{12}}(J)$

$$\frac{(2J+1) [(J^2+J-1) (Y-2) + u_1]^2}{J(J+1) C_1(J)}$$

$P_{R_{13}}(J-1)$

$$\frac{(J-1)^2 (J+1) [(J+1) u_1 - (Y-2) - 2J(J+1)]^2}{J(2J-1) C_1(J)}$$

$Q_{R_{12}}(J-1)$

$$\frac{(J^2-1) [(J+1) (Y-2) - u_1]^2}{J C_1(J)}$$

Line and branch

$S_J(J=J'')$

$P_{Q_{23}}(J)$

$$\frac{2[(J+1)Y - 2J]^2}{(J+1)C_2(J)}$$

$Q_{P_{21}}(J+1)$

$$\frac{2J[(J+1)Y - 2(2J+3)]^2}{(J+1)(2J+3)C_2(J)}$$

$Q_{R_{23}}$

$$\frac{2(J+1)[J(Y-4) + 2]^2}{J(2J-1)C_2(J)}$$

$R_{Q_{21}}(J)$

$$\frac{2[J(Y-2) - 2]^2}{JC_2(J)}$$

$Q_{P_{32}}(J+1)$

$$\frac{J(J+2)[J(Y-2) - u_3]^2}{(J+1)C_3(J)}$$

$R_{Q_{32}}(J)$

$$\frac{(2J+1)[(J^2+J-1)(Y-2) - u_3]^2}{J(J+1)C_3(J)}$$

$R_{P_{31}}(J+1)$

$$\frac{J(J+2)^2 [Ju_3 - (Y-2) - 2J(J+1)]^2}{(J+1)(2J+3)C_3(J)}$$

where

$$u_1 = (Y(Y-4) + 4J^2)^{1/2}$$

$$u_3 = (Y(Y-4) + 4(J+1)^2)^{1/2}$$

$$C_1(J) = J(J+1) Y(Y-4) + 2(2J+1) (J-1) (J+1)J$$

$$C_2(J) = Y(Y-4) + 4J(J+1)$$

$$C_3(J) = (J-1) (J+2) Y(Y-4) + 2(2J+1) J(J+1) (J+2)$$

N_2 ($C^3\Pi_u - P^3\Pi_g$) Second Positive System

The six main branches of an N_2 Second Positive band are shown in Fig. A-3. The band structure is simple if both states behave according to Hund's case 'a' or both behave according to Hund's case 'b'. Both $^3\Pi$ states of the N_2 Second Positive system are represented by case 'a' at low K-values and to case 'b' at high K-values. Three sub-bands $^3\Pi_0 - ^3\Pi_0$, $^3\Pi_1 - ^3\Pi_1$, $^3\Pi_2 - ^3\Pi_2$ are present in each case and each sub-band has strong R and P branches and (except for $^3\Pi_0 - ^3\Pi_0$) a weak Q branch. For all K values in case 'a' and for high K values in case 'b' the three P branches are close together and the three R branches are close together which gives rise to a characteristic triplet structure. Nitrogen nuclei follow Bose statistics ($I=1$) and thus the symmetrical levels(s) will have the higher statistical weight $w_I(s) = (2I+1) (I+1)$ and the antisymmetrical levels(a) will have the lower statistical weight $w_I(a) = (2I+1)$. For example $w_I(s) = 6$; $w_I(a) = 3$. Thus the total weight for the doublet is 9 which is $1/2$ the maximum weight $w_Q(2I+1)^2$ one would expect for a heteronuclear system of the same type and for which both nuclei have $I_a = I_b = 1$.

The Q_2 and Q_3 branches have line intensities which fall off as $1/J$ ". Their contribution is thus small and neglected in this work.

Formulae for the rotational terms are as follows:

Let

$$\nu_{v''v'} = \nu_{00} + G'(v') - G''(v'') \quad (\text{A-15})$$

then

$$\nu_{J''}^R = \nu_{v'',v',J''(J''+1)} = \nu_{v''v'} + F_n'(J''+1) - F_n'(J'') \quad (\text{A-16a})$$

$$\nu_{J''}^P = \nu_{v'',v',J''(J''-1)} = \nu_{v''v'} + F_n'(J''-1) - F_n'(J'') \quad (\text{A-16b})$$

for

$$n = 1, 2, 3$$

The two line components of a Λ -doublet have identical frequency except for the influence of ω_I . The symmetrical component has $\omega_I = 6$ while the unsymmetrical component has $\omega_I = 3$. The H-function for the whole doublet is then constructed from the sum of the two contributions as follows

$$H_{n'',v'',J''}^{n',v',J'} = H_{J'J''} = \frac{8\pi^2 L_O}{3hc} \frac{1}{2 \cdot 3} \nu_{J'J''} R_e^2 (\bar{r}_{v',v''}) q_{v',v''} S_{J''} \left(\frac{3}{9/2} + \frac{6}{9/2} \right) \quad (\text{A-17a})$$

$$= \frac{8\pi^2 L_O}{9hc} \nu_{J'J''} R_e^2 (\bar{r}_{v',v''}) q_{v',v''} S_{J''} \quad (\text{A-17b})$$

where

$$Q_{\text{nuclear}} = 9/2$$

Budo (1937) has given Hönl-London factors for various coupling cases. In this work, and because of the compact structure of the sub-bands they were treated as a ${}^1\Pi - {}^1\Pi$ transition for which

$$S_{J''}^R = J''+1 \quad (\text{A-18a})$$

$$S_{J''}^P = J'' \quad (\text{A-18b})$$

The final for the H-functions are then

$$H_{J''}^R = \frac{8\pi^2 L_O}{9hc} \nu_{J''}^R R_e^2 (\bar{r}_{v'v''}) q_{v'v''} [J''+1] \quad (\text{A-19a})$$

(R branch)

$$H_{J''}^P = \frac{8\pi^2 L_O}{9hc} \nu_{J''}^P R_e^2 (\bar{r}_{v'v''}) q_{v'v''} J'' \quad (\text{A-19b})$$

for

$$n = 1, 2, 3$$

Values of B_v , D_v , and Y_v for the $C^3\Pi_u$ and $B^3\Pi_g$ states of N_2 were taken from the work of Budo (1935; 1936).

N_2^+ ($B^2\Sigma_u^+ - X^2\Sigma_g^+$) First Negative System

The branch structure of N_2^+ bands is illustrated in Fig. A-4). The situation is rather simple as only P and R branches occur and the doublet structure is not well resolved in many cases. Thus the band system can be treated as a ${}^1\Sigma - {}^1\Sigma$ transition. Case 'b' coupling applies strictly. The energy and

frequency behavior are well represented by Eqs. (A-3 and A-4). The molecular constants B_v , D_v and $G_0(v)$ were taken from the work of Douglas (1952). The H-function for this system then becomes

$$H_{n''v''J''}^{n'v'J'} = H_{K''K'} = -\frac{16\pi^2 L_0}{3hc} \nu_{K'K''} R_e^2 (\bar{r}_{v'v''}) q_{v'v''} S_{K''} X \begin{cases} \frac{2}{3} & \text{if } K'' \text{ even} \\ \frac{1}{3} & \text{if } K'' \text{ odd} \end{cases} \quad (\text{A-20})$$

where

$$S_{K''}^R = K''+1 \quad (\text{R branch}) \quad (\text{A-21a})$$

$$S_{K''}^P = K'' \quad (\text{P branch}) \quad (\text{A-21b})$$

The alternative factors depending on evenness or oddness of K'' arise from symmetry properties of ${}^2\Sigma^+ - {}^2\Sigma^+$ transition of homonuclear molecules. Even K'' levels are symmetric ($\nu_1(s) = 6$) and odd levels are antisymmetric ($\nu_1(s) = 3$).

The ($B {}^2\Pi - X {}^2\Pi$) Beta System of NO

The branch structure of NO Beta bands is illustrated in Fig. A-5. It is relatively simple as both ${}^2\Pi$ states pass from case 'a' to case 'b' coupling together with increasing internuclear separation. There are thus two sub-bands for each band, one for each of the ${}^2\Pi_{1/2} - {}^2\Pi_{1/2}$ and ${}^2\Pi_{3/2} - {}^2\Pi_{3/2}$ transition. The strong P and R branches are solely taken into account here as the Q-branch contribution is small and decreases as J^{-1} .

The B and X states are each intermediate between case 'a' and case 'b'. Hill and Van Vleck (1928) have analyzed the term structure for such a case. It is represented by the expression

$$T_n(\nu, J) = T_e + G_n(\nu) + B_v \left[(J+1/2)^2 - 1 + (-1)^n \mu(J) \right] - D_v \begin{cases} J^4 & \text{if } (n=1) \\ (J+1)^4 & \text{if } (n=2) \end{cases} \quad (\text{A-22})$$

where

$$\mu(J) = \left[(J+1/2)^2 - Y_v + Y_v^2/4 \right]^{1/2}; \quad Y_v = A/B_v \quad (\text{A-23})$$

$n = 1$ stands for ${}^2\Pi_{1/2}$ and $n = 2$ stands for ${}^2\Pi_{3/2}$. Frequencies of lines in the various branches of a band are then

$$R_1(J) = \nu_e + \nu_v^{(1)} + F_1'(J''+1) - F_1''(J'') \quad (\text{A-24a})$$

$$R_2(J) = \nu_e + \nu_v^{(2)} + F_2'(J''+1) - F_2''(J'') \quad (\text{A-24b})$$

$$P_1(J) = \nu_e + \nu_v^{(1)} + F_1'(J''-1) + F_1''(J'') \quad (\text{A-24c})$$

$$P_2(J) = \nu_e + \nu_v^{(2)} + F_2'(J''-1) + F_2''(J'') \quad (\text{A-24d})$$

where

$$\nu_e = T_e' - T_e'' \quad (\text{A-24e})$$

$$v_{\nu}^{(n)} = v_{\nu'\nu''}^{(n)} = G_n'(v') - G_n''(v''); \quad n = 1, 2 \quad (\text{A-24f})$$

and

$$F_n(J) = F_n(v, J) = B_{\nu} \left\{ (J+1/2)^2 - 1 + (-1)^n [(J+1/2)^2 - Y_{\nu} + Y_{\nu}^2/4]^{1/2} \right\} - D_{\nu} \begin{cases} J^4 & \text{if } n=1 \\ (J+1)^4 & \text{if } n=2 \end{cases} \quad (\text{A-24g})$$

B_{ν} and D_{ν} were calculated from the work of Gillette and Eyster (1939).

As the $^2\Pi$ states approach case 'b' behavior the selection rule $\Delta K = 0 \pm 1$ increasingly applies and satellite branches are very weak. Disregarding Λ doubling and neglecting the weak Q and satellite branches the band structure is quite similar to that of a $^2\Sigma - ^2\Sigma$ transition, i.e., it has four strong branches. If the satellite lines are merged into the composite line but Q branch contributions completely neglected the Hönl-London factors are sufficiently accurately given by

$$\frac{R_2}{S_{J''}} = \frac{R_1}{S_{J''}} = J''+1 \quad (\text{A-25a})$$

$$\frac{P_2}{S_{J''}} = \frac{P_1}{S_{J''}} = J'' \quad (\text{A-25b})$$

and the H-function becomes

$$H_{n''\nu''J''}^{n'\nu'J'} = H_{J'J''} = \frac{4\pi^2 L_0}{3hc} R_e^2 (f_{\nu'\nu''}) v_{J'J''} q_{\nu'\nu''} S_{J''} \quad (\text{A-26})$$

The NO ($A^2\Sigma - X^2\Pi$) Gamma System

The rotational transitions of an NO Gamma band are illustrated in Fig. A-6. The transition is quite complex because while $A^2\Sigma$ behaves strictly according to case 'b', the $X^2\Pi$ state moves from case 'a' to case 'b' behavior with increasing rotation. The doublet splitting of the X state gives rise to two sub bands, six strong branches ($P_1, Q_1, R_1, P_2, Q_2, R_2$) four weaker satellite branches (${}^P Q_{12}, {}^Q R_{12}, {}^Q P_{21}, {}^R Q_{21}$) and two very weak forbidden satellite branches (${}^O P_{12}$ and ${}^S R_{21}$). The effect of the last two was neglected and the remaining ten branches merged as follows $P_1, R_2, (R_1 + {}^R Q_{21}), (Q_1 + {}^Q P_{21}), (Q_2 + {}^Q R_{12}), (P_2 + {}^P Q_{12})$. Term values for the $X^2\Pi$ state follow Eq.(A-22). Term values for the $A^2\Sigma$ state follow Eq.(A-5). The constants in these equations were taken from the experimental work of Barrow and Miescher (1957), and Deezsi (1959). Hönl-London factors for the complete transition have been given by Earls (1935) apart from an arbitrary constant. They were normalized in this work to obey the sum rule (Eq. 4.1-16a). The Hönl-London factors for the lines combined in the above way are

<u>Transition and Branch</u>	$\frac{S_1}{8J}$
$P_1(J)$	$\frac{(2J+1)^2 + (2J+1)u(4J^2 + 4J+1 - 2Y)}{8J}$
$R_2(J)$	$\frac{(2J+1)^2 + (2J+1)u(4J^2 + 4J+1 - 2Y)}{8(J+1)}$
$R_1(J) + {}^R Q_{21}(J)$	$\frac{(2J+1)}{8J} \{6J-1 - u(4J^2 + 4J+1 - 2Y)\}$
$Q_1(J) + {}^Q P_{21}(J)$	$\frac{(2J+1)}{8(J+1)} \{6J+7 + u(4J^2 + 4J+1 - 2Y)\}$
$Q_2(J) + {}^Q R_{12}(J)$	$\frac{2J+1}{8J} \{6J-1 + u(4J^2 + 4J+1 - 2Y)\}$
$P_2(J) + {}^P Q_{12}(J)$	$\frac{2J+1}{8(J+1)} \{6J+7 - u(4J^2 + 4J+1 - 2Y)\}$

where

$$u = [Y^2 - 4Y + (2J+1)^2]^{-1/2} \quad (\text{A-27})$$

Thus the H-function for lines of this system is

$$H_{n''v''J''}^{n'v'J'} = H_{J''J'} = \frac{2\pi^2 L_0}{3hc} \nu_{J''J'} R_e^2 (r_{v'v''}) q_{v'v''} S_{J''J'}^* \quad (\text{A-28})$$

where the $S_{J''J'}^*$ values are listed in the above table.

References

- Barrow, R.F. and E. Miescher, Proc. Phys. Soc. A7, 219, 1957.
- Budo, A., Zeits fur Physik 96, 219, 1935; 98, 437, 1937; 105, 579, 1937.
- Brix, P. and G. Herzberg, Can. J. Phys. 32, 110, 1954.
- Deezsi, I., Acta Physica 9, 125, 1959.
- Douglas, A.E., Can. J. Phys. 30, 302, 1952.
- Earls, L.T., Phys. Rev. 48, 423, 1935.
- Gillette, R.H. and E.H. Eyster, Phys. Rev. 56, 1113, 1939.
- Hill, E. and J.H. Van Vleck, Phys. Rev. 32, 250, 1928.
- Naudé, S.M., Proc. Roy. Soc. A136, 114, 1932.
- Schlapp, R., Phys. Rev. 51, 342, 1937.